

THESIS ON CIVIL ENGINEERING F46

**Sediment Transport Patterns
Along the Eastern Coasts of the Baltic Sea**

MAIJA VIŠKA

TUT
PRESS

TALLINN UNIVERSITY OF TECHNOLOGY
Institute of Cybernetics
Laboratory of Wave Engineering

The thesis was accepted for the defence of the degree of Doctor of Philosophy in Engineering on 06 August 2014

Supervisor: Prof. Dr. Tarmo Soomere
Institute of Cybernetics, Tallinn University of Technology, Estonia

Opponents: Prof. Dr. Jan Harff
Institute of Marine and Coastal Sciences, University of Szczecin,
Poland
Leibniz-Institute for Baltic Sea Research, Warnemünde, Germany

Dr. Albertas Bitinas
Marine Science and Technology Center
Department of Geophysical Sciences, Faculty of Natural Sciences
and Mathematics, Klaipėda University, Lithuania

Defence of the thesis: 22 September 2014

Declaration:

Hereby I declare that this doctoral thesis, my original investigation and achievement, submitted for the doctoral degree at Tallinn University of Technology, has not been submitted for a doctoral or an equivalent academic degree.



/Maija Viška/

Copyright: Maija Viška, 2014
ISSN 1406-4766
ISBN 978-9949-23-638-1 (publication)
ISBN 978-9949-23-639-8 (PDF)

EHITUS F46

**Settetranspordi mustrid Läänemere
idarannikul**

MAIJA VIŠKA

Contents

List of publications constituting the thesis	6
List of figures	6
Introduction	9
Sedimentary coasts of the eastern Baltic Sea	11
Modelling of the evolution of southern and eastern Baltic Sea coasts	13
The objectives and outline of the thesis	15
Approbation of the results	16
1. Quantification of the role of waves in the Baltic Sea	17
1.1. Modelling waves in the Baltic Sea	17
1.2. Dean's equilibrium beach profile and the concept of closure depth ...	19
1.3. Closure depth for the eastern Baltic Sea coasts	21
1.4. Express method for estimation of the closure depth in the Baltic Sea	24
2. Simulated sediment transport	26
2.1. Sediment transport along the eastern Baltic Sea coast	27
2.2. Coastal Engineering Research Centre approach	28
2.3. Resolving joint impact of shoaling and refraction	30
2.4. Simulated net and bulk transport	32
3. Variations in simulated sediment transport	39
3.1. Interannual variability	39
3.2. Large-scale spatial variations	42
3.3. Reversals of counter-clockwise transport	44
3.4. Divergence and convergence of alongshore sediment flux	46
4. Future projections and ground truth	49
4.1. Functioning of the Curonian Spit	49
4.2. Stability of the Curonian Spit under rotating wave climate	51
4.3. The match of nearshore geology and sediment flux	54
Conclusions	59
Summary of the results	59
Main conclusions proposed to defend	61
Recommendations for further work	62
Bibliography	63
Acknowledgements	72
Abstract	73
Resümee	74
Appendix A: Curriculum Vitae	75
Appendix B: Elulookirjeldus	78

List of publications constituting the thesis

The thesis is based on five academic publications which are referred to in the text as Paper I, Paper II, Paper III, Paper IV and Paper V. Papers III and IV are indexed by the ISI Web of Science and other papers by the SCOPUS database:

- Paper I Soomere T., **Viška M.**, Lapinskis J., Räämet A. 2011. Linking wave loads with the intensity of erosion along the coasts of Latvia. *Estonian Journal of Engineering*, 17(4), 359–374.
- Paper II Soomere T., **Viška M.**, Eelsalu M. 2013. Spatial variations of wave loads and closure depths along the coast of the eastern Baltic Sea. *Estonian Journal of Engineering*, 19(2), 93–109.
- Paper III Soomere T., **Viška M.** 2014. Simulated wave-driven sediment transport along the eastern coast of the Baltic Sea. *Journal of Marine Systems*, 129, 96–105.
- Paper IV **Viška M.**, Soomere T. 2013. Simulated and observed reversals of wave-driven alongshore sediment transport at the eastern Baltic Sea coast. *Baltica*, 26(2), 145–156.
- Paper V **Viška M.**, Soomere T. 2012. Hindcast of sediment flow along the Curonian Spit under different wave climates. In: *IEEE/OES Baltic 2012 International Symposium*, 8–11 May 2012, Klaipėda, Lithuania; Proceedings. IEEE, 7 pp.

List of figures

- Figure 1.** The Baltic Sea and the research area.....10
- Figure 2.** Closure depths along the eastern Baltic Sea coast and in the Gulf of Riga evaluated using Eq. (3). The quantity $H_{0.137}$ was calculated over the entire time interval of wave simulations for 1970–2007 (Paper II) adjusted by M. Eelsalu.22
- Figure 3.** Spatial variation in the threshold for the highest 0.137% significant wave height (red), the closure depth calculated from Eq. (2) (blue) and from Eq. (3) with $q_2 = 6.75$ (green), and the erosion (negative values) and accumulation (positive values) rate along the eastern Baltic Sea (purple) from 20°E, 55°N on the Sambian Peninsula up to Pärnu Bay with a step of about 3 nautical miles (5.5 km). Short dashed lines reflect the mean slope of the alongshore variation in the highest 0.137% of waves (Paper I).23
- Figure 4.** The estimates of the closure depth along the coasts of the Baltic Proper, the Gulf of Finland and the Gulf of Riga calculated using Eq. (3) with $q_1 = 1.5$ (green), Eq. (4) (red), Eq. (1) (black) and Eq. (2) (blue). The quantity $H_{0.137}$ was calculated over the entire time interval of wave simulations for 1970–2007 (Paper II).....24

Figure 5. Scheme of calculation points of the wave model and corresponding coastal sections along the study area (Paper III).26

Figure 6. A. Numerically simulated potential bulk transport in the study area for $d_{50} = 0.17$, using significant wave height as input for the CERC formula and a simple representation of the shoaling. Green: single years, blue: average for 1970–2007; red: moving average of the blue line over three subsequent coastal sections. B. Same as A but using the full solution of Eq. (14) and root mean square wave height as the input for the CERC formula (Paper III).33

Figure 7. A. Numerically simulated potential net transport in the study area for $d_{50} = 0.17$, using significant wave height as input for the CERC formula and a simple representation of the shoaling. Green: single years; blue: average for 1970–2007; red: moving average of the blue line over three subsequent coastal sections (Paper III). B. Same as A but using the full solution of Eq. (14) and root mean square wave height as the input for the CERC formula (Paper IV).35

Figure 8. The ratio of net to bulk potential transport at the eastern Baltic Sea coast in single years (green line) and on average over 1970–2007 (red line). The black line indicates the ratio for 1984 when transport to the north predominated in the entire study area. The calculations used the significant wave height as input for the CERC formula and a simple representation of shoaling (Paper III).....36

Figure 9. Simulated potential bulk transport (A) and net transport (B). All lines indicate the moving average over three subsequent coastal sections, calculated as an average over 1970–2007. Blue: $d_{50} = 0.17$ mm, simplified representation of shoaling, significant wave height as input for the CERC formula (Paper III). Other colours correspond to the use of solutions of Eq. (14). Red lines: significant wave height as input for the CERC formula; dotted line (upper): $d_{50} = 0.063$ mm, solid line (middle): $d_{50} = 0.17$ mm, dashed line (lower): $d_{50} = 1.0$ mm. Green: $d_{50} = 0.17$ mm; root mean square wave height as input for the wave energy but group velocity at the breaker line estimated based on the significant wave height. Cyan: $d_{50} = 0.17$ mm, root mean square wave height as input for the CERC formula (Paper IV).37

Figure 10. Location scheme of the Curonian Spit. Boxes represent the 15 grid cells used in the calculations of sediment flux and the associated coastal sections (Paper V).40

Figure 11. Annual mean bulk sediment transport along the entire Curonian Spit (red), its five-year average (blue) and linear trend (black line) for 1970–2000 (Paper V).41

Figure 12. Annual mean net sediment transport along the entire Curonian Spit (red), its five-year average (blue) and trendlines for 1970–1993 and 1993–2007 (Paper V).41

Figure 13. Bulk sediment transport integrated over three sections of the eastern Baltic Sea coast: red – from the Sambian Peninsula to Cape Akmenrags (the southern compartment); cyan – from Cape Akmenrags to Cape Kolka (the northern compartment), green – from Cape Kolka to Pärnu Bay. All values are smoothed over three subsequent years. The yellow line shows half of the transport over the entire eastern Baltic Sea coast (Viška and Soomere, 2013).	42
Figure 14. Net sediment transport integrated over three sections of the eastern Baltic Sea coast. Notations are the same as for Figure 13 (Viška and Soomere, 2013).....	43
Figure 15. Location of the most persistent reversals (magnitude in red) and zero-crossing points of annual net sediment transport (divergence points – red circles; convergence points – green circles; see explanation in Section 3.4) in different years. Direction (arrows) and magnitude (numbers at arrows, in 1000 m ³) indicate the net sediment transport calculated using $d_{50} = 0.17$ mm, Eq. (14) and root mean square wave height as the input to the CERC formula. Modified from Paper III. ..	45
Figure 16. The relationship between the intensity (green line) and direction (horizontal arrows) of alongshore net sediment transport and areas of likely erosion and accumulation.....	46
Figure 17. Numerically simulated location of zero-crossing points in the net sediment transport along the study area in 1970–2007: circles – convergence points; squares – divergence points (Paper III).	47
Figure 18. Wave propagation directions at different sections of the Curonian Spit. The bars correspond to the southernmost part of the spit. The distributions for subsequent sections along the spit from south to north are vertically shifted by 0.1 units of the vertical axis (Paper V).	50
Figure 19. Relocation of the zero-crossing point of convergence of net sediment flux (red rhombi) and its three-year average (blue line) along the Curonian Spit in 1970–2007. The green dashed horizontal lines indicate the location of the western (Zelenogradsk) and northern (Klaipėda) ends of the spit and the position of Nida on the spit. Modified from Paper III and Gilbert (2008).	51
Figure 20. Annual mean bulk and net transport per a single coastal section of the Curonian Spit for rotated wave climates (Paper V).	53
Figure 21. Annual net transport for single years (green) and long-term average (blue, red) for the Curonian Spit for clockwise (left panel) and counter-clockwise (right panel) rotation of the wave climate by 10° (Paper V).....	54
Figure 22. Geological composition of the nearshore study area (Paper IV).....	56

Introduction

The Baltic Sea is a unique water body in many aspects. Owing to its brackish water, location at high latitudes, extremely sensitive ecosystem and strong anthropogenic pressure the International Maritime Organization has ascribed it, among other decisions, a status of a particularly sensitive sea area (Leppäranta and Myrberg, 2009; Harff et al., 2011). Its dynamics often combines features of a large lake with those characteristic of a large estuary or even a small ocean (BACC Author Team, 2008). Understanding the complexity of its driving forces and the intricacy of its reaction to various drivers has been a challenge for several generations of scientists (Leppäranta and Myrberg, 2009).

In spite of the relatively small size of the Baltic Sea, its coasts exhibit extensive variability. Moreover, the pool of its coasts represents a substantial part of various coastal types of the World Ocean (van Rijn, 1998; Woodroffe, 2002; Knauss, 2005; Holton and Hakim, 2012). As the amplitude of tides is very small in the Baltic Sea, the development of its coasts is mainly controlled by waves and to a lesser extent by the local water level. The impact of these hydrodynamic drivers is at times modulated by winds (aeolian transport) and (the presence or absence of) sea ice, in a few occasions also by a direct effect of ice on sediment or vegetation. In this thesis I focus on the quantification of the wind wave impact on coastal processes.

The vulnerability of different sections of the Baltic Sea coasts to various drivers and especially to wind waves is radically different. These coasts can be divided into two large categories. Bedrock-based shores are characteristic of its western and northern parts. Such coasts, frequently of so-called skären type (Harff et al., 2011), start from south-eastern Sweden, spread over the entire Sea of Bothnia and Gulf of Bothnia, extend until the north-eastern Gulf of Finland and are at certain locations complemented by limestone cliffs at Estonian coasts and along the islands of Gotland and Åland. These coasts are extremely steady with respect to any driving forces. Sedimentary segments of this coastline are usually short, often pocket beaches in bayheads that are almost sheltered from wave action. These beaches are not considered in this thesis.

The presented studies focus on the core features of alongshore sediment transport and their potential impact on the evolution of long interconnected segments of sedimentary coasts of the Baltic Sea. Such coasts predominate along the southern and eastern margins of this water body, from the southern tip of Sweden over Denmark, Germany, Poland and the Baltic states. While most of the coasts of the southern and south-eastern Baltic Sea are relatively straight (Eberhards, 2003; Zhamoida et al., 2009; Zhang et al., 2010; Pranzini and Williams, 2013), the shores of Estonia are heavily fragmented. Numerous islands, peninsulas and bays deeply cut into the mainland restrain alongshore sediment transport into small and almost disconnected compartments (Soomere and Healy, 2011), each of which can be considered independently of the others.

The evolution of sedimentary coasts of Denmark, Germany and Poland has been extensively described in scientific literature (e.g., Clemmensen et al., 2001; Meyer et al., 2008; Reimann et al., 2011). The southern Baltic Sea coasts are exposed to erosion due to climate conditions (BACC Author Team, 2008) and specific geological structure, sediment accumulation can occur only in some shorter sections, mostly in bayheads and along some spits (Pranzini and Williams, 2013).

However, very limited information is available about the key features of the functioning of the longest connected domain of the Baltic Sea sedimentary coasts. This domain stretches from the Sambian (Samland) Peninsula over the Kurzeme (Courland) Peninsula up to the eastern coast of the Gulf of Riga (Figure 1). It develops under the largest intensity of wind waves in the Baltic Sea (Schmager et al., 2008; Soomere and Räämet, 2011). Almost all its sections suffer from overall sediment deficit (Eberhards and Lapinskis, 2008; Žaromskis and Gulbinskas, 2010; Kartau et al., 2011; Pranzini and Williams, 2013).

The length of erosion-dominated areas considerably exceeds the length of accumulation sections in this domain (Eberhards, 2003; Eberhards et al., 2009; Kelpšaitė et al., 2011). Weak uplift of the Earth's crust in a part of this domain (Ekman, 2009) is superimposed with climatically controlled sea level rise (Harff

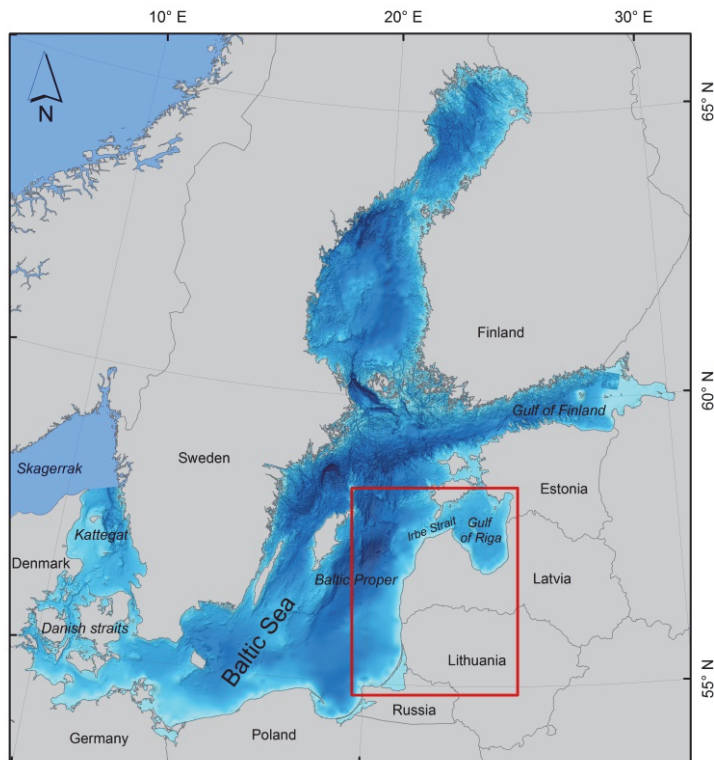


Figure 1. The Baltic Sea and the research area.

and Meyer, 2011). The accelerating sea level rise is leading to gradually increasing relative sea level in the southern part of this domain already today (Dailidienė et al., 2004; Rosentau et al., 2007) but it is likely that the relative coast downlift will spread to the north in the near future (Johansson et al., 2014; Zhang et al., 2014).

The domain in question is thus very sensitive to any changes in the hydrodynamic loads (Eberhards et al., 2006) and potential impacts of anthropogenic interference. It is particularly susceptible to climate change, especially to sea level rise. Even its relatively healthy sections (in terms of sediment budget) or landforms that usually show accumulation (e.g., the Curonian Spit) may be heavily damaged in certain storms (Žaromskis and Gulbinskas, 2010). For example, large parts of the Latvian coast are estimated in terms of risk of erosion as either “very vulnerable” or “vulnerable”. Such risk of erosion is most common along both the Baltic Proper coast (69%) and the coast of the Gulf of Riga (66%) (Eberhards, 2003; Eberhards et al., 2006).

Sedimentary coasts of the eastern Baltic Sea

Most of the Baltic Sea coasts are inherited from the Quaternary period. The coasts of the study area and the Polish and partly German shorelines have largely been shaped by the Scandinavian ice sheet and during its retreat. The seabed in the coastal zone generally consists of sand, shingle and gravel (Pranzini and Williams, 2013). Sedimentary coasts of the eastern Baltic Sea stretch from the Sambian Peninsula over the shores of Lithuania and Latvia to the eastern coast of the Gulf of Riga (Figure 1). During the last millennia, this domain has undergone remarkable changes. For example, the Curonian Spit has apparently been formed from sediment eroded from the Sambian Peninsula (Žaromskis and Gulbinskas, 2010). The coasts to the north of the Curonian Spit have been distinctly straightened under the impact of various hydrometeorological drivers (Knaps, 1966; Gudelis, 1967; Ulsts, 1998; Eberhards, 2003; Eberhards et al., 2006). Similar changes (albeit less radical) have occurred in the Gulf of Riga and Pärnu Bay (Kartau et al., 2011). These processes have formed the two main types of coasts in this domain. The erosional coasts often host a characteristic scarp or bluff, usually in relatively soft cliffs. The depositional coasts have typically a gently sloping profile (Gudelis, 1967; Eberhards, 2003; Eberhards et al., 2006).

This extensive system of coastal areas with various properties is usually interpreted as a highly interconnected and more or less continuous sedimentary system (Žaromskis and Gulbinskas, 2010). An idealised view, developed more than half a century ago, is that the general movement of sediment is counter-clockwise along the entire south-eastern coast of the Baltic Proper (Knaps, 1966; Gudelis et al., 1977) and further along the southern and eastern margins of the Gulf of Riga. This motion has an obvious discontinuity and a partial disruption at Cape Kolka (Žaromskis and Gulbinskas, 2010). At times and/or in places this long-term pattern is not completely continuous and may contain sections with oppositely directed

littoral flow¹ (Knaps, 1982). Variations in the nature of the coast add complexity to the evolution of the entire system. For example, large parts of the underwater slope along the Latvian shores are covered with boulders, pebbles and coarse sand. Only a few places (the Curonian Spit, southern part of the Gulf of Riga and a short coastal section to the south-east of Cape Kolka) host substantial amounts of fine sediment (Ulsts, 1998).

Among the multitude of ways of sediment transport in the marine environment, wave-driven alongshore drift is usually thought to be the predominant one in the coastal environment (Carter, 2002). This drift includes the direct wave-driven relocation of sediment grains and the impact of strong currents created when waves break in the surf zone. These two mechanisms are often decisive for the sediment transport and morphological development at the coast (Fredsoe and Deigaard, 1992). Waves evidently play an even larger role in such processes in the almost tideless Baltic Sea.

The Baltic Sea is a practically closed system for wind waves. It receives very limited wave energy through the Danish straits (Figure 1). Differently from many open ocean areas, the proportion of intense swells is very low (Soomere, 2008) and almost all wave energy is supplied to the coasts of this basin by relatively short and steep windseas. The wave climate in the Baltic Sea is still very complicated and has high temporal and spatial variability. As the fetch length in the Baltic Sea is relatively small, both the reaction and decay time of wave fields are quite small (Soomere, 2005). The duration of severe wave storms is usually below 8 h (Broman et al., 2006).

The major contributor to the complexity of the wave climate and to the specific features of wave-driven transport is the highly anisotropic angular distribution of moderate and strong winds in the Baltic Sea area. This distribution has two distinct peaks in a large part of the Baltic Proper. The most frequent wind direction is from the south-west but north-northwestern (NNW) winds may be even stronger (Soomere and Keevallik, 2001).

The described directional structure of the Baltic Sea winds gives rise to the anisotropic wave climate in this basin. This becomes evident in two aspects. Firstly, the distribution of wave approach directions has also two clear peaks (Räämet et al., 2010) (Paper V). Secondly, the combination of the predominant wind pattern and the geometry of the Baltic Sea suggests that the fetch length for strong winds is the longest in the eastern part of the Baltic Proper. Consequently, the highest and longest waves occur along Polish coasts, the Latvian Baltic Proper coast, coasts of Saaremaa and Hiiumaa and at the entrance to the Gulf of Finland (Räämet, 2010). This conjecture means that changes in strong wind directions (Soomere and Räämet, 2014) may result in very large changes in littoral flow, comparable to or even exceeding those caused by an alteration of the wave height.

¹ The process whereby beach material is gradually shifted laterally as a result of currents and waves meeting the shore at an oblique angle; also called littoral drift. Following Carter (2002), the terms “alongshore transport” and “alongshore flux” are used to denote the wave-driven movement of material in the surf and swash zones.

As the Baltic Sea is relatively small and the wave fields are here totally created by local winds, even a change in the trajectories of cyclones crossing the sea (Sepp et al., 2005) may lead to great changes in the wave approach direction. The potential results of such a change are analysed in Paper V.

The impact of waves may be substantially modulated by variations in water level. These modulations have different nature in different parts of the Baltic Sea. While along the Swedish eastern coasts high waves usually occur during low water levels, in the study area high waves are often accompanied by a high water level. The largest variations in the water level along the eastern Baltic Sea coast are caused by storm surges (Suursaar and Sooäär, 2007). The severest surges in this area are created by cyclones coming from the North Atlantic and propagating from west to east. Such cyclones support strong westerly winds over the entire Baltic Sea region and in many cases push large amounts of water from the North Sea into the Baltic Sea (Leppäranta and Myrberg, 2009). The highest storm surges at the eastern coast of the sea (Eberhards, 2003) develop when a strong storm approaches after a sequence of previous events that have already increased the volume of water in the Baltic Sea (Johansson et al., 2001). The joint impact of storm waves and high water levels is crucial in morphological models (Deng et al., 2014) and in predictions of the coastal flooding risk (Soomere et al., 2013) but immaterial from the viewpoint of studies presented in this thesis.

Modelling of the evolution of southern and eastern Baltic Sea coasts

A relatively large pool of studies exists about the evolution and modelling of the southern Baltic Sea coasts. As discussed above, the major factors that influence the coasts in this region are severe storms possibly accompanied with a high water level (Zeidler et al., 1995), unfortunate combinations of which may lead to catastrophic erosion events (Furmańczyk et al., 2012). The majority of winds come from the south-west but they have limited impact on the shoreline because of relatively short fetch and the exposure of the coast mostly to the northerly directions. This feature means that severe storms from the north-west and north-east are the major events that shape this coast (Furmańczyk and Dudzińska-Novak, 2009). The actual changes in the shoreline and dune erosion are governed by a multitude of factors, including the sea-level, its rise, coastal depositional morphology (Hoffmann and Lampe, 2007), total storm energy and duration. In some cases wave direction is the most important variable along with the significant wave height and sea level during the storm (Furmańczyk et al., 2011).

Most of the Polish coastline is classified as stable as it has revealed only minor changes during the last 100 years. The total length of erosion-prone areas is, however, longer than the length of accumulation areas (Pranzini and Williams, 2013). These processes are asymmetric: after severe storms the beach area is gradually restored but the natural process of rebuilding functions approximately five times slower than the erosion (Pranzini and Williams, 2013). Part of the coastline is protected or stabilised by various coastal protection structures but these

may enhance erosion in the neighbouring areas. This effect is often avoided by applying soft protection measures (like beach nourishment) that have become popular in German and Polish coastal areas (Hanson et al., 2002; Pranzini and Williams, 2013).

Modelling efforts for the southern Baltic Sea coasts involve calculations of the closure depth. It has been estimated for the Pomeranian Bight with methods similar to those employed in this thesis. Theoretical estimates of the closure depth were amended using empirical data and applied as a first approximation in the analysis of coastal evolution (Schwarzer et al., 2003). Several calculations of alongshore sediment transport using different methods have also been made for the southern Baltic Sea. A coupled model with different approaches and empirical formulas was used to calculate the total alongshore sediment transport of the wave dominated coasts of the Pomeranian Bight (Zhang et al., 2013). The outcome of efforts towards analysing and predicting the long-term impact of beaching waves on the evolution of coastal morphology are presented in (Zhang et al., 2010; Deng et al., 2014) for several sections of the southern Baltic Sea.

The existing observational evidence about the properties of alongshore sediment flux in the study area (Ulsts, 1998; Eberhards, 2003; Eberhards and Lapinskis, 2008) is complemented by very few theoretical estimates of the wave properties and current-driven sediment transport. The direction of the nearshore current in the surf zone driven by the release of momentum of waves (Longuet-Higgins and Stewart, 1964) usually coincides with the average direction of the wave energy flux. As wave directions normally match the course of strong winds in the Baltic Sea basin, the predominant direction of wave-driven alongshore sediment transport in the surf and swash zones can be estimated based on the similar direction of local wind-driven nearshore currents. The strongest currents among these, for example, near the Latvian Baltic Proper coast are excited by (south-)westerly and northerly winds (Eberhards, 2003). As the predominant wind directions near Ventspils in 1980–2000 were from the south-west, west and south, Eberhards (2003) concluded that the associated wave fields supported littoral flow to the north. Similarly, calculations of wave-driven transport for a few locations along the Latvian Baltic Proper coast using the Coastal Engineering Research Council method (see Chapter 2) suggested that littoral drift is mostly to the north (Ulsts, 1998).

The transport may be, however, reversed at certain locations. For example, at the Lithuanian–Latvian border the simulated net alongshore sediment flow was mostly directed to the south (Ulsts, 1998). These results did not match the outcome of observations that mostly signified sediment transport to the north (Ulsts, 1998). A set of calculations with a better resolution (about 25 points from the Sambian Peninsula to Cape Kolka) showed more realistic properties of littoral flow (Eberhards, 2003). However, these calculations had also too low resolution for making definite conclusions about details of alongshore transport. Several attempts to model the properties of sediment transport have been undertaken for shorter coastal segments (Zemlys et al., 2007). A few studies have tried to link wave properties (or their changes) with the associated changes in coastal processes,

usually for limited coastal sections (Hanson and Larson, 2008; Kelpšaitė et al., 2009, 2011; Tönisson et al., 2011).

The objectives and outline of the thesis

Many properties of single coastal segments of the Baltic Sea have been studied in detail (see Harff et al., 2011; Pranzini and Williams, 2013 and references therein). Still, the functioning of single segments of its sedimentary coasts, the division of longer segments into almost disconnected structural units, interconnections of the neighbouring units via littoral flow, the reaction of the entire system of sedimentary coasts to climate variability and climatic changes are almost unknown.

The studies presented in this thesis target the longest interconnected system of sedimentary coasts of the eastern Baltic Sea (from the Sambian Peninsula to Pärnu Bay) from its functional and structural perspectives. The particular objectives are as follows:

- to quantify the magnitude of wave-driven impact on this sedimentary coastal stretch in terms of the approaching wave energy and associated parameters of equilibrium coasts;
- to establish the key structural features of the entire domain such as the major divergence and convergence areas, associated reversals of alongshore sediment flux and almost disconnected regions in terms of sediment flux;
- to identify possible major changes in the course of coastal processes owing to changing forcing in this domain and to develop a rough estimate of structural stability of the major landform in this area, the Curonian Spit.

To fulfil the objectives, it is first necessary to quantify the impact of the major driver of alongshore sediment transport in this domain, the two-peak wave system, in terms that can be used in the analysis of coastal processes. For this purpose I employ high-resolution time series of nearshore wave properties calculated by Dr. A. Räämet using the WAM model and adjusted geostrophic winds for 1970–2007. The necessary quantification is performed via the evaluation of the time series, average and extreme levels of the energy flux brought to the coast by wind waves and via further calculation of the basic properties of idealised coastal systems such as the closure depth and its variations along the coast (Paper I, Paper II described in Chapter 1).

This work is followed by the construction of a more detailed picture about the magnitude of and alongshore variations in the wave-driven bulk and net sediment flux. Particularly interesting are zero-crossing points of the alongshore variations in the net sediment flux (Paper III). Finally, I address the match of the established structural features of alongshore sediment transport (Paper IV) and analyse their sensitivity to different methods for their calculation and to the possible rotation of the wave climate (Paper V). I only analyse wave-driven alongshore transport in this thesis and leave out the possible effects of cross-shore transport.

Approbation of the results

The basic results described in this thesis have been presented by the author at the following international conferences:

Viška M., Soomere T., Nikolkina I., Räämet A. 2014. Variations of wave-driven sediment flux along the eastern Baltic Sea reflecting the choice of wind data. Oral presentation at the *6th IEEE/OES Baltic International Symposium* (26–29 May 2014, Tallinn, Estonia).

Viška M., Soomere T. 2014. On sensitivity of wave-driven alongshore sediment transport patterns with respect to model setup and sediment properties. Poster presentation at the *2nd International Conference on Climate Change – The environmental and socio-economic response in the Southern Baltic region* (12–15 May 2014, Szczecin, Poland).

Viška M., Soomere T. 2013. Spatio-temporal variations in the wave-driven alongshore sediment transport along the eastern Baltic Sea coast. Poster presentation at the *9th Baltic Sea Science Congress* (26–30 August 2013, Klaipėda, Lithuania).

Eelsalu M., Soomere T., **Viška, M.** 2013. Closure depth along the north-eastern coast of the Baltic Sea. Poster presentation at the *9th Baltic Sea Science Congress* (26–30 August 2013, Klaipėda, Lithuania).

Viška M., Soomere T. 2013. Long-term variations of simulated sediment transport along the eastern Baltic Sea coast as a possible indicator of climate change. Oral presentation at the *7th Study Conference on BALTEX* (10–14 June 2013, Borgholm, Island of Öland, Sweden).

Viška M., Soomere T. 2012. Decadal variations of simulated sediment transport patterns along the eastern coast of the Baltic Sea. Oral presentation at the *11th Colloquium on Baltic Sea Marine Geology* (19–21 September 2012, Helsinki, Finland).

Viška M., Soomere T. 2012. Hindcast of sediment flow along the Curonian Spit under different wave climates. Oral presentation at the *5th IEEE/OES Baltic International Symposium* (08–11 May 2012, Klaipėda, Lithuania).

Viška M., Soomere T., Kartau K., Räämet A. 2011. Patterns of sediment transport along the Latvian and Estonian coasts along the Baltic Proper and the Gulf of Riga. Oral presentation at the *8th Baltic Sea Science Congress* (22–26 August 2011, St. Petersburg, Russian Federation).

1. Quantification of the role of waves in the Baltic Sea

Reaching the objectives of this thesis requires extensive and detailed information about several wave properties (wave height, period and propagation direction) along the entire eastern coast of the Baltic Sea. A number of recent studies have focused on the basic properties of the Baltic Sea wave climate for various open sea and nearshore areas. They have employed instrumental measurements (Broman et al., 2006; Soomere et al., 2012), visual wave observations (Zaitseva-Pärnaste et al., 2009, 2011) and numerical simulations (Suursaar et al., 2008; Suursaar, 2010; Soomere and Räämet, 2011; Tuomi et al., 2011). Unfortunately no long-term instrumental wave measurements have been carried out in the vicinity of the eastern coast of the Baltic Sea (Soomere and Räämet, 2011; Tuomi et al., 2011). The required information cannot be extracted from historical visual wave observations (Soomere, 2013), first of all because of their low resolution in both space and time.

For the listed reasons the analysis below is largely based on the outcome of numerical simulations of the entire Baltic Sea wave fields. I use the results of simulations performed for 1970–2007 and shortly presented in Section 1.1. The data set of time series of nearshore wave properties extracted from these simulations is extensively used in Papers I–V.

Section 1.2 gives a short overview of the concept of equilibrium beach profile. Section 1.3 depicts its governing parameters and methods used for express estimates of their values from certain properties of the wave climate. Section 1.4 describes a potential link of the alongshore changes in the overall wave intensity with the major erosion and accumulation regions (Paper I). Paper II illustrates spatial variations in the closure depth of equilibrium profiles along the eastern Baltic Sea, shows that a common express method for the estimates of the closure depth often fails in the Baltic Sea and presents a modified express method that is suitable for the open Baltic Sea coasts.

1.1. Modelling waves in the Baltic Sea

Simulations of the intensity of wave impact, characteristics of equilibrium beach profiles and properties of alongshore sediment transport presented in this thesis rely on time series of wave properties calculated using the third-generation spectral wave model WAM Cycle 4 (Komen et al., 1994). The simulations performed by Räämet (2010) are extensively discussed in scientific literature (see Soomere and Räämet, 2011, 2014 and references therein) and I only shortly depict here their basic features.

The wave model WAM was originally constructed for calculations of wave properties in open ocean conditions but with appropriate wind information and spatial resolution it gives equally good results also in coastal areas (Roland and Ardhuin, 2014). Its applications in the Baltic Sea (Soomere et al., 2008; Räämet,

2010; Weisse and von Storch, 2010; Tuomi et al., 2011) lead to acceptable results at much smaller depths than in the coastal ocean basically because the typical wave periods are smaller in the Baltic Sea than in the ocean.

The model was run for the entire Baltic Sea basin with a spatial resolution of 3' along latitude and 6' along longitude (about 3×3 nautical miles) and directional resolution of 15° (24 equally spaced directions for wave propagation) for 38 years (1970–2007) in idealised ice-free conditions (Räämet and Soomere, 2010). Ignoring sea ice is generally acceptable for the southern part of the Baltic Proper but might overestimate the wave loads in the northern Baltic Proper and particularly in the Gulf of Finland and Gulf of Riga. It is, though, likely that this approximation is still adequate for the estimation of the closure depth and wave loads along the eastern coast of the Baltic Sea (Paper I, Paper II) as well as for the evaluation of alongshore sediment flux in Papers III–V because the strongest storms usually occur before the ice cover is formed.

While this spatial and directional resolution is relatively high for the Baltic Proper (Tuomi et al., 2011), it might not be fine enough for smaller sub-basins like the Gulf of Riga or the Gulf of Bothnia (Soomere and Räämet, 2014; Tuomi et al., 2014). As the basic properties of reconstructed wave fields reasonably match the observed ones in the Gulf of Finland and in the Darss Sill area (Soomere et al., 2010, 2012; Suursaar, 2010), it is apparently acceptable to use them also in the Gulf of Riga.

The wind information for the wave model was constructed from the Swedish Meteorological and Hydrological Institute (SMHI) geostrophic wind database with a spatial resolution of $1 \times 1^\circ$ and temporal resolution of 3 h (6 h before September 1977). The properties of geostrophic wind are determined by the balance of the pressure gradient force and Coriolis effect and thus express large-scale motions in the upper atmosphere. On the one hand, even in the adjusted form they almost always differ from true wind properties since no other forces (like friction) are taken into account (Holton and Hakim, 2012). On the other hand, geostrophic winds represent global wind patterns and are thought to replicate well the changes in the entire climate system, including long-term variations in synoptic-scale storminess (Alexandersson et al., 2000) that largely governs the Baltic Sea wave properties. Consequently, their use makes it possible to identify the basic trends and decadal changes in wave properties (Soomere and Räämet, 2014) that may otherwise be masked by uncertainties and inconsistencies in higher-resolution modelled wind fields (Keevallik and Soomere, 2010). It is not unusual that wind information available from coastal measurement sites does not properly represent actual properties of marine winds and that researchers substitute the true marine wind by properly adjusted geostrophic winds (Myrberg et al., 2010; Lehmann et al., 2014).

The reliability and accuracy of these wave calculations are discussed in several papers (e.g., Räämet et al., 2009; Soomere and Räämet, 2011). In general, the simulated wave properties acceptably replicate the time series of measured wave data (Räämet et al., 2009) and mimic the statistical properties of the wave fields at

several observation sites quite well (Soomere and Räämet, 2011). For calculations of alongshore potential sediment transport and closure depth I used time series of hourly significant wave height², peak period³ and mean wave direction at the closest grid cells to the coastline.

1.2. Dean's equilibrium beach profile and the concept of closure depth

A coastal engineer frequently needs to obtain a rough estimate of potential impact of waves upon a coastal section or to quickly assess the sediment budget of a coastal segment. For this purpose normally long-term measurements of waves or equally long monitoring of sediment transport are required. The problem can be greatly reduced for beaches that are close to an equilibrium state, in other words, for beaches that only reveal small-scale and temporary changes in their cross-section. It was recognised in the 1980s that a specific shape of many open ocean beaches is constantly maintained by ocean waves. This shape is called the equilibrium beach profile (Dean, 1991). It was further established that cross-sections (profiles) of many sedimentary coasts are qualitatively similar although they are exposed to radically different wave conditions and have different sediment properties (Dean and Dalrymple, 2002). This similarity extends to semi-sheltered basins: most of the Estonian beaches have the same qualitative features (Didenkulova et al., 2013) and belong to the class of almost equilibrium beaches (Soomere and Healy, 2011)

The most important simplification for coastal engineering is that both the instantaneous properties and features of long-term evolution of such beaches are largely governed by a small number of parameters. The most common equilibrium beach profile can be described as $h(y) = Ay^b$, where $h(y)$ is the water depth along the profile at a distance of y from the waterline. The profile scale factor A depends on the grain size of bottom sediments. The exponent b can vary over quite a large range (Dean, 1991; Komar and William, 1994; Kit and Pelinovsky, 1998; Didenkulova et al., 2013). The most widely used value $b = 2/3$ corresponds to so-called Dean's equilibrium beach profile and reflects constant wave energy dissipation per unit water volume in the surf zone (Dean and Dalrymple, 2002).

The concept of the equilibrium profile has a large number of applications. For example, the core assumption of Bruun's Rule is the existence of such a persistent shape of the beach profile (Bruun, 1962). This rule explains how small changes in the mean sea level can result in relatively large changes in the location of the waterline. Although it is only conditionally applicable in areas with extensive

² Significant wave height was defined in the past as the average height of the highest one-third of waves that occurred in a given time period. In contemporary wave models it is calculated as the fourfold standard deviation of the surface elevation (Massel, 1989).

³ The peak period represents the period of waves that correspond to the largest values of the directionally averaged wave spectrum; in other words, the wave components with the highest energy.

sediment transit such as the Curonian Spit (Jarmalavičius et al., 2013), it serves as a conceptual basis for many morphological models applied to the sedimentary Baltic Sea coast (Deng et al., 2014). An inverse Bruun's Rule can be used to determine the amount of sediment, eroded or accreted from the shore using waterline position changes (Kask et al., 2009; Kartau et al., 2011).

Dean's equilibrium profile is defined by two quantities: the profile scale factor A and the depth h^* down to which the profile extends. This depth, called the closure depth, indicates the water depth until which storm waves substantially and regularly affect the shape of the coastal profile. It is an important and widely used concept in coastal engineering and a fundamental variable in the modelling of coastal evolution due to sea-level change and alongshore sediment transport (Dean and Dalrymple, 2002; Robertson et al., 2008). It is generally defined as the depth where repeated survey profiles pinch out to a common line (Kraus, 1992). Dean (2002) observed that closure depth is more a concept than an unambiguously defined quantity, but it helps to calculate equilibrated beach widths and to plan beach nourishment.

The concept of closure depth has been developed for beaches that are composed of relatively fine movable and non-coherent sediment (sand, gravel, shingle) so that waves can freely reshape the nearshore profile. Beaches that have part of their bottom composed of hard ground (e.g., limestone beaches in some sections of the northern coast of Estonia) cannot be described in terms of the theory of equilibrium beaches. The parts of the bottom consisting of hard ground (e.g., solid rock) are not only resistant to wave action but can also influence sediment movement in other parts of the beach by changing wave shoaling, refraction and dissipation patterns or directly restricting sediment movement (Robertson et al., 2008).

The closure depth, in essence, characterises the wave regime in a particular coastal section. Its possible variation as a function of sediment grain size is often considered as immaterial. Defined as the maximum depth at which the waves effectively shape the coastal profile, it basically depends on the roughest wave conditions that persist for a reasonable time at a given site (Hallermeier, 1981). Seawards from the closure depth, waves may still at times affect sediment movement but are not able to maintain a specific profile (Dean and Dalrymple, 2002). Therefore, the closure depth is mostly a function of the local wave climate. This feature makes it possible to replace repeated profiling of the beach by estimates derived from wave measurements or numerical modelling of the wave climate.

Hallermeier (1977, 1981) derived an empirical relationship for the closure depth as a function of wave properties assuming that it is related to sediment resuspension energetics. He also assumed that there is an unlimited amount of loose sand along the beach profile and wave energy is the main hydrodynamic factor driving the sand movement (Hallermeier, 1977). A convenient measure of the wave climate was the significant wave height $H_{0,137}$ that was exceeded during 12 h in a year, that is, with a probability of 0.137% (Hallermeier, 1981). The

relevant approximation of the closure depth in terms of a quadratic function of this quantity is

$$h^* = 2.28H_{0.137} - 68.5 \left(\frac{H_{0.137}^2}{gT_s^2} \right), \quad (1)$$

where $g = 9.81 \text{ m/s}^2$ is acceleration due to gravity and T_s is the typical peak period that corresponds to the largest significant wave height that occurs for 12 h/yr. The original version of this approximation (Hallermeier, 1981; USACE, 2002) to some extent overestimates the closure depth because the response of beach profiles is usually relatively slow and the duration of the highest waves is sometimes too short for the formation of the equilibrium profile down to the closure depth (Robertson et al., 2008). This approximation is often used in coastal engineering as a conservative estimate in the design of beach refill under the assumption of unlimited availability of sand. To reach a more exact match with the field data, Birkemeier (1985) modified Hallermeier's equation (1) to:

$$h^* = 1.75H_{0.137} - 57.9 \left(\frac{H_{0.137}^2}{gT_s^2} \right). \quad (2)$$

This expression is used in Papers I and II.

1.3. Closure depth for the eastern Baltic Sea coasts

Papers I and II address the methods for the determination of typical values of the closure depth for the sections of the eastern Baltic Sea coast, which are exposed to predominant waves. This depth serves as a key property of each single beach profile as well as of longer coastal segments. It not only directly characterises the overall intensity of wave impact for a particular coastal section (and thereby the potential for coastal erosion) but also portrays the range of alongshore variations in the relevant wave loads.

For the analysis of the closure depth I employed wave time series calculated using the wave model WAM (see Section 1.1) for a selection of nearshore cells, each of which corresponds to an about 5.5–6 km long coastal section. These cells were chosen in the immediate vicinity of the waterline in Paper I and at water depth ranging from 7 to 48 m (18 m on average) in Paper II (Figure 2). While in Paper I the goal was to quantify the alongshore changes in the wave properties and associated parameters of the equilibrium beach profile and to avoid the potential distortion of wave fields in nearshore areas with complex geometry, Paper II aimed at the development of a proper express formula for the closure depth for engineering applications in the Baltic Sea. Therefore several grid cells in Paper II differ from the cells that are used in Paper I. Doing so results in minor differences of the numerical values of the closure depth along the Lithuanian coast and the

Baltic Proper coast of Latvia but in more substantial deviations along the eastern part of the Gulf of Riga.

I used two different approaches to calculate the closure depth in Paper I and Paper II based on Eq. (3) (see Section 1.4). Firstly, the values of $H_{0,137}$, the corresponding typical wave periods and the annual values of the closure depth for each section were evaluated separately for every year in the time interval 1970–2007. The long-term closure depth was estimated as an average of the annual values. Secondly, the (long-term) closure depth was evaluated directly from the entire dataset comprising 333 096 hourly values of the wave height and period at the selected grid cells. The difference between the results was notably small. For single sections it was less than 4% and as low as about 2.5% on average. The modest difference suggests that the overall storminess level during the simulation period remained fairly constant.

As expected, the closure depth is largest (almost 7 m) in regions that are fully open to the predominant south-westerly winds and where the overall wave intensity is largest in the Baltic Proper (Figure 2). These areas occur along the north-western (NW) coast of the Courland Peninsula. The Gulf of Riga coast (except for a few locations) has a closure depth well below 5 m. This reflects a somewhat milder

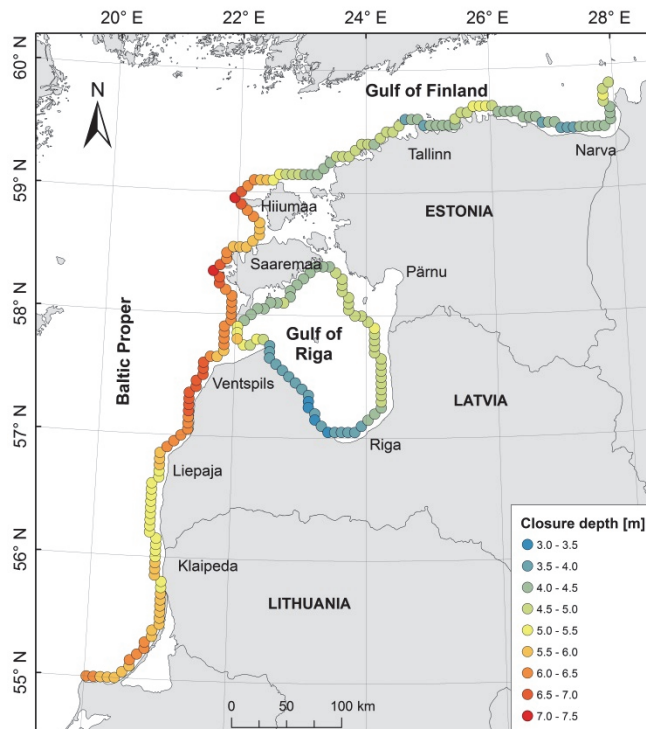


Figure 2. Closure depths along the eastern Baltic Sea coast and in the Gulf of Riga evaluated using Eq. (3). The quantity $H_{0,137}$ was calculated over the entire time interval of wave simulations for 1970–2007 (Paper II) adjusted by M. Eelsalu.

wave climate in the Gulf of Riga compared to that in the Baltic Proper (Eelsalu et al., 2014).

The values of the closure depth were compared in Paper I with long-term accumulation and erosion rates from the data set obtained by state monitoring of geological processes in Latvia (Figure 3). These data exist starting from the year 1993 or 1994, depending on the particular location. The largest accumulation and erosion rates in Figure 3 reflect the impact of large harbours of Liepaja and Ventspils. Their jetties and breakwaters block the natural littoral drift and cause rapid accumulation to the south and erosion to the north of these harbours.

Not unexpectedly, the major natural accumulation and erosion domains coincide with areas of the largest wave heights and closure depths (Paper I). This relationship between wave activity and the development of the coast is, however, not statistically significant. Much more interesting relationship became evident between the alongshore variations in the closure depth and the presence of accumulation or erosion. Only one mostly naturally developing longer coastal section exists in the study area between the harbours of Liepaja and Ventspils where erosion predominates (Figure 3). Only one longer section where accumulation predominates is also known along the NW coast of the Courland Peninsula between Ventspils and Kolka. These sections host the largest average alongshore gradients for both the wave height and the closure depth along the coast of the Baltic Proper (Paper I).

The estimates presented in Papers I and II are based exclusively on simulated wave heights and periods and ignore the dependence of alongshore sediment flux

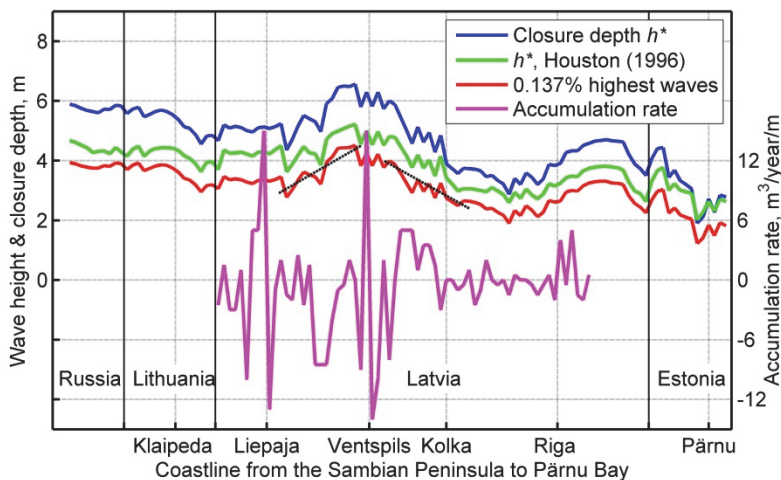


Figure 3. Spatial variation in the threshold for the highest 0.137% significant wave height (red), the closure depth calculated from Eq. (2) (blue) and from Eq. (3) with $q_2 = 6.75$ (green), and the erosion (negative values) and accumulation (positive values) rate along the eastern Baltic Sea (purple) from 20°E , 55°N on the Sambian Peninsula up to Pärnu Bay with a step of about 3 nautical miles (5.5 km). Short dashed lines reflect the mean slope of the alongshore variation in the highest 0.137% of waves (Paper I).

on the wave approach direction. The results suggest that the alongshore variations in the wave height, combined with the basic information about the direction of littoral flow, may still be used for the approximate identification of the major accumulation and erosion domains. Namely, these coastal sections that host the largest alongshore increase in the wave height (or closure depth, Figure 4) in the direction of littoral flow should reveal erosion features. Contrariwise, accumulation is expected to occur in sections where the wave height decreases along the coast in this direction. In other words, the location of extensive domains of accumulation and erosion can be extracted already from the analysis of wave heights, provided the predominant wave approach direction is known.

1.4. Express method for estimation of the closure depth in the Baltic Sea

The estimates of the properties of the highest waves often contain extensive uncertainties (e.g., Soomere et al., 2012). These properties may also largely vary along the coast. It is thus desirable to develop simple express estimates of the closure depth based on commonly used average wave parameters. The simplest approximation for the closure depth is a linear function of certain wave properties. The closure depth is usually expressed using either the annual mean significant wave height H_{mean} or $H_{0.137}$:

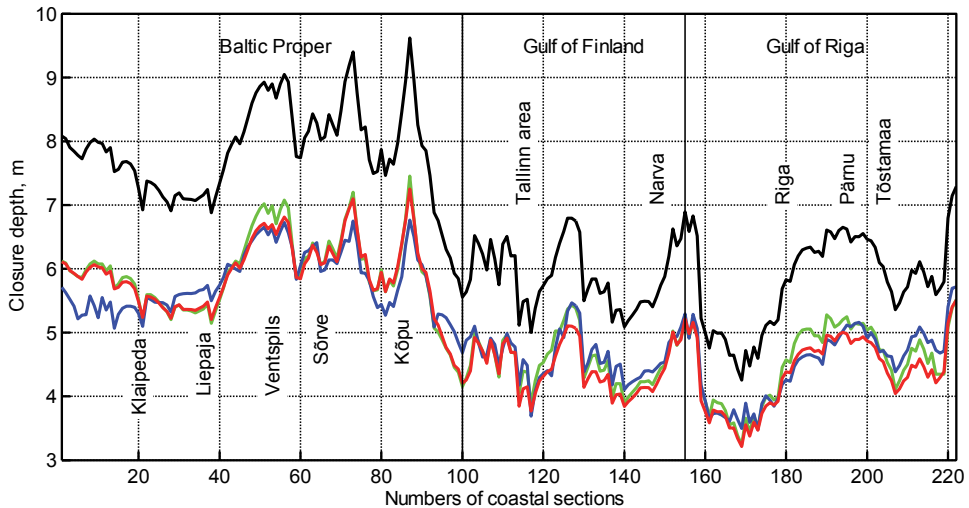


Figure 4. The estimates of the closure depth along the coasts of the Baltic Proper, the Gulf of Finland and the Gulf of Riga calculated using Eq. (3) with $q_1 = 1.5$ (green), Eq. (4) (red), Eq. (1) (black) and Eq. (2) (blue). The quantity $H_{0.137}$ was calculated over the entire time interval of wave simulations for 1970–2007 (Paper II).

$$h_c \cong q_1 H_{0.137} \cong q_2 H_{mean}. \quad (3)$$

The commonly used values are $q_1 = 1.5$ (Birkemeier, 1985) and $q_1 = 1.57$ (Hallermeier, 1981; USACE, 2002).

Houston (1996) extended Eq. (3) towards the use of long-term significant wave height H_{mean} and $q_2 = 6.75$. This extension is very convenient to use but not necessarily correct for areas with a specific wave climate. Equation (3) with $q_2 = 6.75$ is valid only for short relatively sheltered sections of the Baltic Sea coast located in bayheads and has to be adjusted for the open sea coasts (Paper II). The use of $q_2 = 6.75$ implicitly assumes a constant ratio $H_{0.137}/H_{mean} \cong 4.5$ of the extreme to average wave heights. This ratio has been established for wave fields with a Pierson-Moskowitz spectrum that are common for the observed wave statistics along the US coasts (Houston, 1996). But in semi-enclosed seas like the Baltic Sea, where swells are almost absent and the wave height is mainly governed by local storms, this ratio may be different. One specific feature of the Baltic Sea wave climate is that the average wave conditions are relatively mild but very rough seas may occur episodically in long-lasting severe storms (Soomere, 2005; Broman et al., 2006; Soomere et al., 2012). Waves in such storms are much higher than expected from the mean wave conditions. The main reason is the complicated geometry of the Baltic Sea.

The described difference leads to a marked difference between the factor q_2 used in Eq. (3) for the open ocean coasts and its analogue for the Baltic Sea. The typical ratio of extreme wave heights to average wave heights along the eastern Baltic Sea coast is $H_{0.137}/H_{mean} \cong 5.5$ (Paper II). This result suggests that an appropriate express formula for the closure depth in the Baltic Sea conditions is

$$h_c^B \cong 1.5 H_{0.137} \cong 8.25 H_{mean}. \quad (4)$$

This modified expression gives more realistic results for semi-sheltered domains of the Baltic Sea (Soomere et al., 2008; Kartau et al., 2011) (Figure 4).

Equations (1) and (4) were used for calculating the closure depth in Paper II and Eqs. (2) and (3) were used in both Paper I and Paper II. As expected, the calculations with Eq. (1) gave fairly larger values than Eq. (2) (Figure 4). Equation (3) is acceptable for bayheads of deeply indented bays where the wave field contains an appreciable amount of remote swells (Paper II).

2. Simulated sediment transport

As discussed above, wave-driven sediment transport is the predominant mode of sediment motion along the eastern Baltic Sea coast and the leading constituent of the evolution of sedimentary coasts in this domain. Based on this perception, the calculations in this and the following chapter rely on the assumption that sediment flow near the waterline is driven exclusively by waves. The properties of this transport are evaluated using the most popular, worldwide used Coastal Engineering Research Council (CERC) method (USACE, 2002). This method is based on the assumption that wave-driven alongshore sediment transport is proportional to the wave energy flux (equivalently, wave power) per unit of length of the coastline. The calculations implicitly include two main modes of transport – bed load and suspended load.

Section 2.1 gives a brief overview of the simulation area (Figure 5) and the basics of the existing evidence of sediment movements derived from theoretical

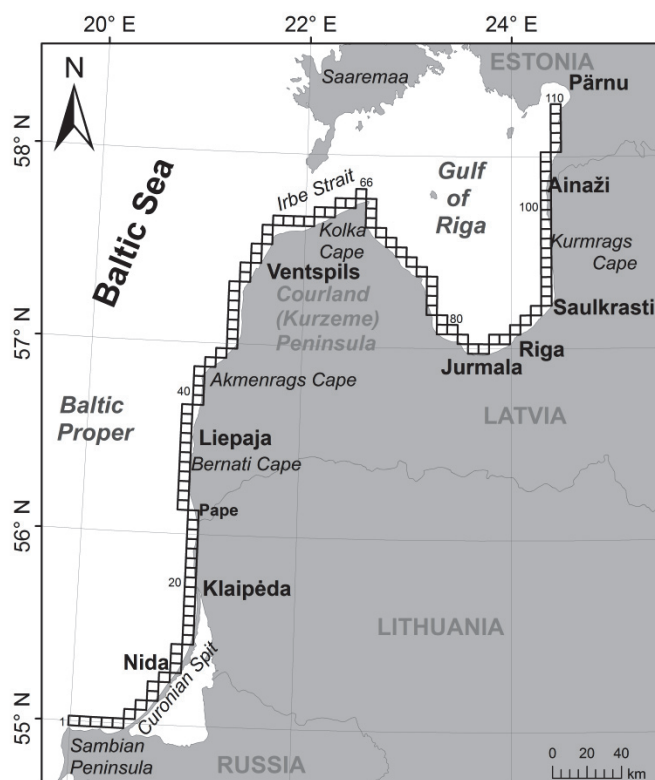


Figure 5. Scheme of calculation points of the wave model and corresponding coastal sections along the study area (Paper III).

estimates and historical observations. Section 2.2 introduces the CERC method that is used in sediment transport calculations in Papers III–V. Section 2.3 presents an upgrade of this approach that makes it possible to fully account for the joint impact of shoaling and refraction of waves in the nearshore. This upgrade (Paper IV) is crucial for the Baltic Sea region where waves often approach the coast under large angles. Results of sediment transport calculations are described in Section 2.4. The alongshore transport is characterised by the annual net and bulk transport rates and varies considerably depending on the particular implementation of the CERC approach. Paper IV identifies the reasons for the discrepancy between the outcome of simulations and the observed magnitude of sediment flow.

2.1. Sediment transport along the eastern Baltic Sea coast

The presented simulations cover an about 700 km long coastal stretch from the Sambian Peninsula in Kaliningrad District (Russia) to Pärnu Bay (Estonia) (Figure 5). This stretch consists of several partially connected sedimentary compartments (Knaps, 1966; Eberhards, 2003). The sediment is predominantly transported counter-clockwise (Knaps, 1966; Gudelis et al., 1977; Eberhards et al., 2009). For single sediment grains moving in this direction it is a more or less continuous sedimentary system (Žaromskis and Gulbinskas, 2010) in which some grains may be transported along the entire stretch. The basic process is the straightening of the coastline (Knaps, 1966; Gudelis, 1967; Ulsts, 1998; Eberhards, 2003), while extensive spit formation has occurred in its southern part in the past. The associated issues of erosion and accumulation along the study area have been widely discussed in the scientific literature (e.g., Gudelis et al., 1977; Eberhards and Lapinskis, 2008; Eberhards et al., 2009; Kartau et al., 2011).

The overall appearance of the alongshore sediment flow along the south-eastern margin of the Baltic Sea is well known. Its direction is inherited from the Littorina Sea period (Ulsts, 1998). The first known theoretical estimates of the properties of the wave-driven alongshore transport in this area were obtained using an improved Munch-Petersen formula (Munch-Petersen, 1936; Knaps, 1938, 1966). These estimates have later been substantially upgraded (Ulsts, 1998; Lapinskis, 2010). Both theoretical considerations and observational evidence confirm that the long-term net sediment transport is generally counter-clockwise. Littoral drift starts from the Sambian Peninsula and continues until Cape Kolka in Latvia. Its capacity (net transport up to 1×10^6 m³/yr in selected sections) was portrayed by Knaps (1966) already half a century ago (see Eberhards, 2003 for a historical overview).

Later studies have added many details to this picture. The nature and typical grain size of sediments vary markedly between different sections of the coast (Ulsts, 1998; Kalniņa et al., 2000; Saks et al., 2007). The Curonian Spit is entirely sandy, while gravel with pebbles and boulders often dominates the western Courland coasts. The coasts of the Gulf of Riga usually consist of mixed sediments and have much finer-grained sand than the Lithuanian shores.

Consistently with the alongshore variation in wave intensity and closure depth (Chapter I), sediment transport, coastal processes in general and erosion in particular are usually more intense along the open Baltic Sea coast than in the Gulf of Riga. Local deviations of littoral flow from the general pattern have been analysed using both observational (Gilbert, 2008; Eberhards et al., 2009; Zhamoïda et al., 2009) and numerically simulated data sets (Ulsts, 1998; Zemlyš et al., 2007). The direction of the alongshore net transport may be variable, at least within single years. There is some evidence about occasional clockwise sediment transport in an area to the south of Cape Akmenrags (Stone Cape in some sources) and near Klaipėda (U. Bethers, pers. comm. 2013). The segments that host clockwise net transport are called reversals below.

Eberhards (2003) suggests that several eminent headlands like Cape Akmenrags, Cape Ovisrags or Cape Kolka may serve as natural barriers for the alongshore sediment flow. These headlands often contain bedrock or Quaternary rocks in the nearshore or along the coast, which are more resistant to erosion (Eberhards, 2003). The combination of the geometry of the coast and the predominant wave direction in the Baltic Proper suggests that Cape Kolka serves as the end station of much of the transport and serves as a one-way transit gateway for part of it into the Gulf of Riga. Part of the sediment may be deposited in the vicinity of Cape Kolka or transported away from the coast at this cape and in the vicinity of the above-mentioned headlands (Eberhards, 2003).

2.2. Coastal Engineering Research Centre approach

The intensity of wave-driven alongshore sediment transport is commonly expressed in terms of its potential rate Q_t (USACE, 2002). This rate expresses the volume of sediment (such as cubic metres) carried through a coastal section per unit of time. An equivalent of the potential alongshore transport rate is the potential immersed weight transport rate I_t (USACE, 2002)

$$I_t = (\rho_s - \rho)g(1 - p)Q_t, \quad (5)$$

where ρ_s and ρ are the densities of sediment particles and sea water, respectively, and p is the porosity coefficient. It is often convenient to use the quantity I_t that combines the effect of sediment porosity and specific weight of sediment components. The CERC method is based on the assumption that the potential alongshore sediment transport is proportional to the alongshore wave energy flux (wave power) per unit of length of the coastline P_t :

$$I_t = KP_t, \quad (6)$$

where K is a nondimensional (CERC) coefficient. In essence, this coefficient expresses the efficiency of wave-driven transport in a particular coastal section. It indicates the proportion of the approaching wave power that is used to suspend and relocate the sediment under the particular beach slope and sediment grain size. The

grain size is taken into account through the fall velocity of the grains (Dean and Dalrymple, 2002). There is no consensus as to whether K is a constant or possibly varies with sand grain size, shape or density, fall velocity, the beach profile, water temperature and wave incidence angle (Dean and Dalrymple, 2002). Various implementations of this method use numerical values of the coefficient K that vary almost by an order of magnitude (USACE, 2002).

The implementations of the CERC method commonly use either the significant wave height H_b or the root mean square wave height H_{brms} at the breaker line. As the wave energy flux is a vector, only its alongshore component contributes to alongshore transport. The transport rate is proportional to the beaching rate of this component. If the wave propagation direction makes an angle α with the normal to the coast, the alongshore component of the energy flux is $P_t = Ec_g \sin \alpha$ (E is the wave energy and c_g is the group speed) and the rate of its beaching per unit of the coastline is

$$P_t = Ec_g \sin \alpha \cos \alpha . \quad (7)$$

Since the majority of wave-driven sediment transport occurs in the surf zone, both energy and group velocity in Eq. (7) are usually chosen to characterise the wave properties at the seaward border of the surf zone. At this location waves can be reasonably well described as long waves, thus,

$$E_b = \frac{\rho g H_b^2}{8}, \quad c_{gb} = \sqrt{gd_b} = \sqrt{\frac{gH_b}{\gamma_b}}, \quad (8)$$

$$Q_t = \frac{Kp\sqrt{g}}{16(\rho_s - \rho)(1-p)\sqrt{\gamma_b}} H_b^2 \sqrt{H_b} \sin 2\alpha_b, \quad (9)$$

where the subscript b represents wave properties at the breaking line, $\gamma_b = H_b/d_b$ is the breaking index, d_b is the water depth at the breaking line (breaking depth) and α_b is the angle between the wave crests and the isobaths at breaking. As the dependence of the potential transport rate on the variations in the coastal sediment texture is insignificant for the Baltic Sea conditions (Soomere et al., 2008), these variations are ignored in our calculations. The value $d_{50} = 0.17$ for the median size d_{50} of sediment particles is used for the entire coast in Paper III and several different values are applied in Paper IV. The dependence of the coefficient K on the wave properties is taken into account using the following empirical expression (USACE, 2002):

$$K = 0.05 + 2.6 \sin^2 2\alpha_b + 0.007 u_{mb} / w_f, \quad (10)$$

where $u_{mb} = \gamma_b \sqrt{gd_b} / 2$ is the maximum orbital velocity in breaking waves within the linear wave theory and $w_f = 1.6 \sqrt{gd_{50}(\rho_s - \rho)} / \rho$ is an approximation of the fall velocity in the surf zone.

2.3. Resolving joint impact of shoaling and refraction

The wave properties are hindcast by the WAM model (Section 1.1) at hourly intervals at the closest grid point to the shore, while Eqs. (7)–(10) rely on the wave properties at the seaward border of the surf zone. The evaluation of the breaking wave properties from the model output is a complicated problem in the context of the Baltic Sea where waves may approach the coastline under quite large angles (Kelpšaitė et al., 2011; Ryabchuk et al., 2011). This feature means that approaches based on the common assumption that the breaking waves are almost incident (Dean and Dalrymple, 1991) is not valid at the Baltic Sea coasts. The orientation of the coastline also determines the direction and intensity of alongshore sediment transport (Lapinskis, 2010). The changes in the approach angle have direct impact on the sediment transport patterns and vulnerable areas along the coast. Usually sediment transport driven by waves tends to straighten the coastline. Strictly speaking, this is true only when waves approach the coast under a small angle. If the predominant wave approach angle (e.g., between the wave crests and the coastline) is larger than 45° , the coastline may become unstable (Ashton et al., 2001). The predominance of high-angle waves can create large spits and sand ridges. The growth of such structures has recently been observed in the eastern part of the Gulf of Finland (Ryabchuk et al., 2011).

I have used two methods to evaluate the properties of waves at the breaker line based on the properties of modelled waves. First, I took only refraction into account under the assumption that shoaling is balanced by other processes (Paper III). In the other method both shoaling and refraction were taken into account (Paper IV). In both methods the modifications to the wave properties are estimated based upon the linear wave theory and the assumption that the wave energy is concentrated in monochromatic plane waves with the period equal to the peak period and the direction of propagation equal to the mean propagation direction. Given the uncertainties in the wind data and wave hindcast (Räämet et al., 2009), more exact calculations of transport properties based on the full wave spectrum or estimates of wave energy loss owing to wave-bottom interactions were not reasonable.

In Paper III only refraction was fully considered in the description of the phenomena occurring during the wave propagation from the model point to the surf zone. The impact of wave shoaling was included in a simplified manner by choosing the breaking index $\gamma_b = 1$. In this approximation, $d_b = H_b$ and the breaking wave height is simply equal to the modelled wave height. The change in the wave propagation direction is calculated from Snell's law $\sin\theta/c_f = \text{const}$, where θ is the local angle between the wave crests and the isobaths and c_f is the wave celerity (phase velocity). An application of this law requires an approximate solution to the dispersion relation at the model grid points. This relation is a transcendental equation for the wave number $k = 2\pi/L$ or the wave length L :

$$c_f = \frac{\omega}{k} = \frac{\sqrt{gk \tan(kd)}}{k} = \sqrt{\frac{g \tan(2\pi d/L)}{2\pi/L}}. \quad (11)$$

A solution with an error not exceeding 1.7% (Dean and Dalrymple, 2002) was employed in Paper III:

$$L = L_0 \left\{ \tanh \left[\left(2\pi \sqrt{\frac{d}{gT^2}} \right)^{3/2} \right] \right\}^{2/3}. \quad (12)$$

The results of calculations using this approach are compared with the outcome of simulations that account for both refraction and shoaling in Paper IV and Chapter 3.

Alongshore transport was calculated in Paper IV by using the CERC approach and taken fully into account the joint impact of shoaling and refraction of waves from the wave model grid cell to the breaker line. This approach has been used in the Baltic Sea context only in Soomere et al. (2013) and Deng (2013). These sources contain no information about its use in other studies.

The common assumption in addressing the problem of refraction is that the depth isolines are straight and parallel to the average orientation of the coastline within each coastal section. If wave reflection, whitecapping, interactions with the seabed and nonlinear interactions within the wave field are ignored, the wave height at the breaker line H_b is (Dean and Dalrymple, 1991)

$$H_b = H_0 \left(\frac{c_{g0} \cos \theta_0}{c_{gb} \cos \theta_b} \right)^{1/2}, \quad (13)$$

where the subscripts b and 0 represent wave properties at the model grid cell and at the breaking line, respectively.

Refraction of the waves can be estimated from Snell's law as above. The phase and group speed in a model grid cell are found from the finite-depth dispersion relation (11). The breaking wave height H_b is defined using the concept of breaking index $\gamma_b = H_b/d_b$. As the coasts are mostly sedimentary and with gently sloping profiles, the use of a constant value $\gamma_b = 0.8$ is justified (Dean and Dalrymple, 1991; Dean and Dalrymple, 2002; USACE, 2002).

As the breaking waves are long waves, their group velocity and phase speed are equal $c_{gb} = \sqrt{gd_b} = \sqrt{gH_b/\gamma_b}$. Substituting these expressions into Eq. (13) leads to the following algebraic equation of 6th order for the breaking wave height H_b (Soomere et al., 2013):

$$F(H_b) = H_b^6 \frac{g^2 \sin^2 \theta_0}{\gamma_b^2 c_{f0}^2} - H_b^5 \frac{g}{\gamma_b} + H_0^4 c_{g0}^2 (1 - \sin^2 \theta_0) = 0. \quad (14)$$

The leading term of Eq. (14) vanishes for incident waves with $\theta_0 = 0$. Such waves only experience shoaling and their breaking height is $H_b = (H_0^4 c_{g0}^2 \gamma_b / g)^{1/5}$ (Komar and Gaughan, 1972; Dean and Dalrymple, 1991). This expression is often used for almost incident waves for which $\cos\theta_b \approx 1$ and $\sin^2\theta_b \approx 0$ (Dalrymple et al., 1977; Dean and Dalrymple, 1991).

The calculations in Paper IV use an exact solution of Eq. (14). The polynomial at its left-hand side has only three non-zero coefficients. Its leading term and the constant term have the same sign, whereas the coefficient at H_b^5 has the opposite sign. Therefore, this equation has generally two positive solutions (Paper IV). Previous attempts to use this equation rely on certain solvers of the algebraic equations (Deng, 2013) or just declare that an estimate of the breaking-wave height is given by its smaller solution (Soomere et al., 2013). Paper IV provides a simple proof that the smaller solution is the correct one. The solution that represents the breaking height can be identified by considering the case $\theta_0 \rightarrow 90^\circ$. For such angles, the constant term of Eq. (14) is very small, the smaller real solution tends to zero and the larger real solution approaches a constant value $\hat{H} = \gamma_b c_{f0}^2 / g$. For typical Baltic Sea wave fields, this value substantially exceeds the possible wave heights. Thus, the smaller real solution represents the breaking height.

A comparison of the two approaches demonstrates that taking only refraction into account overestimates both the breaking wave height and approach angle of high-angle waves at the breaker line. The transport driven by waves approaching the coast under angles $>30^\circ$ was significantly overestimated and sediment transport by waves with an approach angle less than 30° was usually slightly underestimated in Paper III. Implementation of the full representation of shoaling and refraction gives a more realistic sediment flux (Paper IV).

2.4. Simulated net and bulk transport

For the calculations in this and following chapters the study area is divided into 110 approximately 3 nautical miles (about 5.5 km) long sectors (Figure 5). The sectors match the location of the wave model grid points closest to the shoreline. The coastline within each sector is approximated by a straight line (equivalently, the actual coastline is replaced by a piecewise straight line). The intensity of wave-driven alongshore sediment transport is assumed to be constant in each sector.

The calculations are made for 1 h long time intervals according to the resolution of simulated wave data (Section 1.1). An estimate of net transport (residual sediment motion or the amount of sediment that has been finally moved by waves over some time interval $[t_0, t_1]$) is obtained by integrating Q_t in Eq. (9) over $[t_0, t_1]$. The direction from the left to the right hand of the person looking to the sea (counter-clockwise for the study area) is regarded as positive. A measure of bulk transport (the total amount of sediment moved back and forth) is obtained by integrating $|Q_t|$ over the same time interval $[t_0, t_1]$. To compensate for systematic underestimation of the modelled wave height (Räämet and Soomere, 2010), significant wave height is used as the input wave information in Paper III. Doing so

led to an overestimation of the magnitudes of the alongshore transport rates but evidently did not impact their qualitative features.

The largest simulated rates of bulk transport occur along the NW part of Latvia, Courland Peninsula and near the Sambian Peninsula (Figure 6). They reach $6 \times 10^6 \text{ m}^3/\text{yr}$ on average and $10 \times 10^6 \text{ m}^3/\text{yr}$ in single years (Paper III). The intensity of transport is considerably lower in the Gulf of Riga (around $10^6 \text{ m}^3/\text{yr}$), whereas slightly larger values are found along the eastern part of the gulf (up to $2 \times 10^6 \text{ m}^3/\text{yr}$). As discussed above, these values are clearly overestimated but the

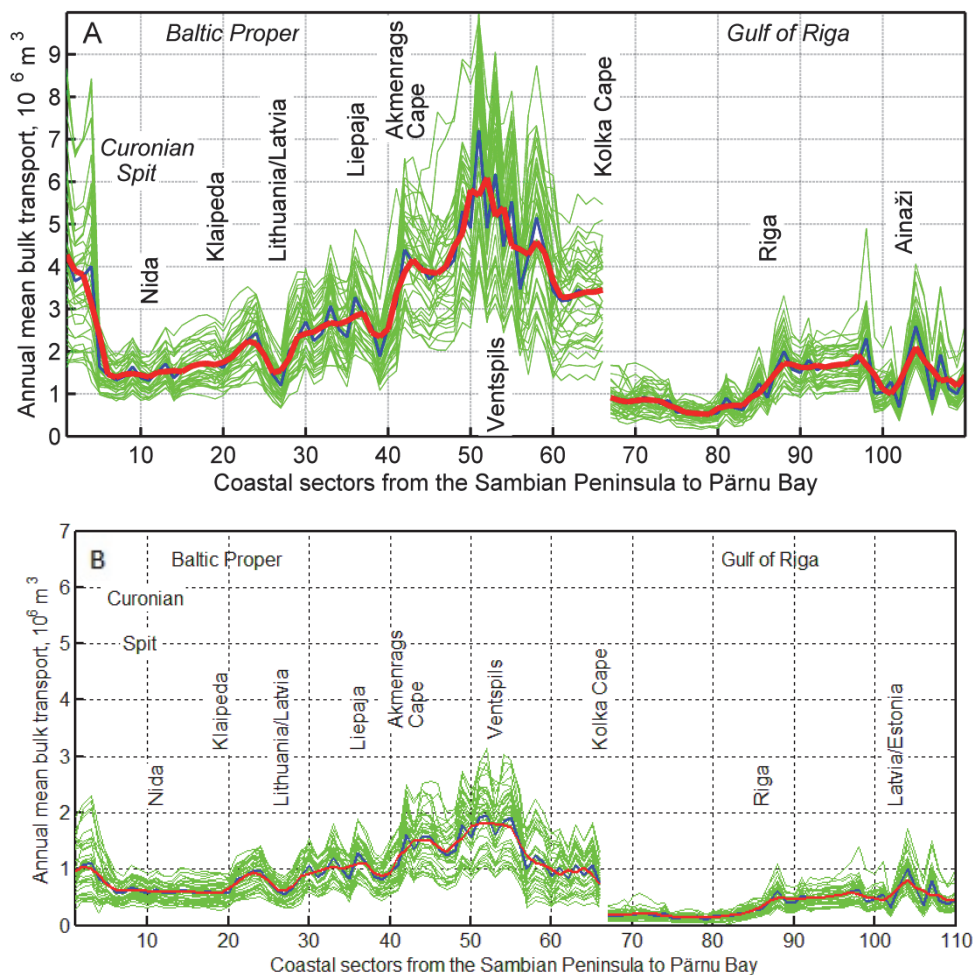


Figure 6. A. Numerically simulated potential bulk transport in the study area for $d_{50} = 0.17$, using significant wave height as input for the CERC formula and a simple representation of the shoaling. Green: single years, blue: average for 1970–2007; red: moving average of the blue line over three subsequent coastal sections. B. Same as A but using the full solution of Eq. (14) and root mean square wave height as the input for the CERC formula (Paper III).

qualitative features of their alongshore variations are adequate. More realistic transport volumes were reached in Paper IV. The long-term average bulk transport (obtained by using a proper representation of the wave height and taking full account of refraction and shoaling) is about 10^6 m³/yr in some parts of the Baltic Proper and close to 400×10^3 m³/yr in the Gulf of Riga (Figure 6).

The shores of the Sambian Peninsula and the NW coast of Latvia host clearly higher intensity of coastal processes than other segments of the study area. The largest local variations in bulk transport occur in the westernmost part of the Curonian Spit and around Cape Akmenrags, to the north of which the transport rate increases rapidly.

The alongshore variations in the long-term wave height along the Baltic Proper coastline are much smaller than similar variations in bulk transport intensity (Räämet and Soomere, 2010). Part of this difference stems from the fact that the transport rate is proportional to $H^{2.5}$. Another reason for large alongshore variations in bulk transport is the gradual change in the wave approach angle along some segments of the shore. This mainly reflects the geometry of the study area: the orientation of the coastline changes more than 60° from the Latvian–Lithuanian border to Ventspils.

Areas with a more or less constant rate of the bulk transport are the Curonian Spit, the western coast of the Gulf of Riga and the Latvian section of the eastern coast of this gulf. The difference between the typical values of the bulk transport at the western and eastern coasts of the Gulf of Riga largely reflects the anisotropy of the wave climate of this gulf: most frequent winds blow from the south-west and the associated waves propagate offshore from the western coast of the gulf.

The overall appearance of the simulated net potential alongshore transport confirms the well-known predominance of sediment drift to the east, north-east or north along the coasts of the Baltic Proper and a counter-clockwise littoral flow along the western, southern and eastern coasts of the Gulf of Riga (Pruszek, 2004; Eberhardts et al., 2009; Žaromskis and Gulbinskas, 2010).

Variations in the annual mean values of the net transport are much larger than similar variations in bulk transport. These values (calculated using the significant wave height as input for the CERC formula) vary from close to zero up to about 3×10^6 m³/yr for the long-term average and to 8×10^6 m³/yr for single years (Paper III). As discussed in Paper IV, these values are considerably overestimated. Realistic maximum values obtained using a proper representation of the wave height are up to 700 000 m³/yr in the Baltic Proper and 400 000 m³/yr in the Gulf of Riga (Figure 7). The locations of the most intense net sediment transport coincide with similar locations of bulk sediment transport – the Sambian Peninsula and an area to the north-east of Cape Akmenrags.

The net transport direction is highly variable along the Baltic Proper coast. Several sections host annual average transport to the north over the entire 38-year period. These areas are the Sambian Peninsula and a short section of the NW coast of Latvia, which have also high bulk sediment transport. The net sediment flux is mostly counter-clockwise along the south-western coast of the Gulf of Riga as

described also in Eberhards et al. (2009). Several sections of the eastern coast of the Gulf of Riga host exclusively transport to the north, whereas in some other sections the direction of net transport is variable.

The ratio of bulk to net transport (Figure 8) additionally confirms the presence of almost unidirectional transport direction in several sections of the study area (Paper III) such as around Cape Akmenrags or the NW coast of the Courland Peninsula. On the contrary, net transport along the Curonian Spit and from the Lithuanian–Latvian border to Ventspils is highly variable. Interestingly, in some

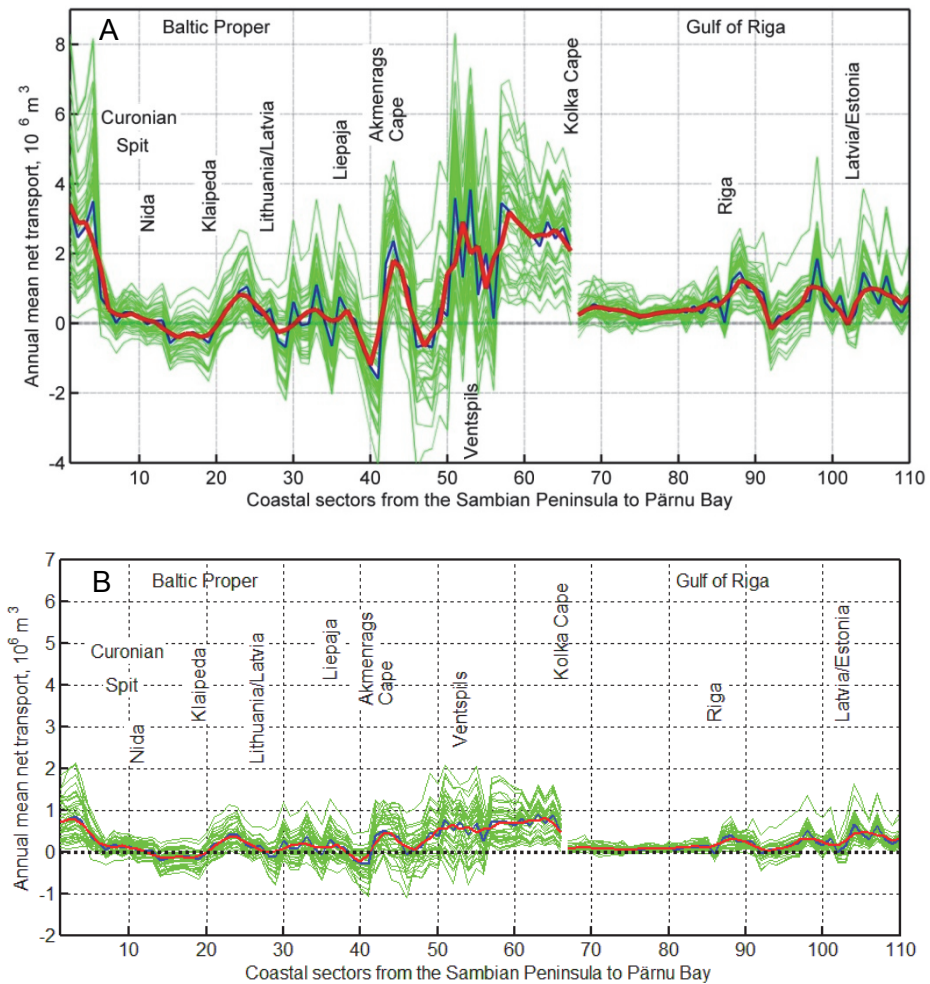


Figure 7. A. Numerically simulated potential net transport in the study area for $d_{50} = 0.17$, using significant wave height as input for the CERC formula and a simple representation of the shoaling. Green: single years; blue: average for 1970–2007; red: moving average of the blue line over three subsequent coastal sections (Paper III). B. Same as A but using the full solution of Eq. (14) and root mean square wave height as the input for the CERC formula (Paper IV).

years the transport may be completely unidirectional. One of these exceptional years was 1984 when about 50% of the entire sediment volume brought into motion was carried to the north along the coasts of both the Baltic Proper and the Gulf of Riga. Bulk sediment transport was at a long-term average level but net transport was almost three times as large as the average.

The results of calculations of wave-driven sediment transport and efforts to replicate the evolution of sedimentary coasts are very sensitive to input parameters like sediment properties, sinks and sources as well as driving forces like wave data and water level information (Deng et al., 2014). The proper value of the CERC coefficient can also vary several times for different beaches (Chapter III-2-3 in USACE, 2002). The existing implementations of the CERC formula for calculating sediment transport in the Baltic Sea area tend to indicate larger values compared to observations. Part of the bias can be associated with the low quality of wave information (Zemlys et al., 2007; Mėžinė et al., 2013). A substantial part of the bias may stem from different interpretations of the wave height in the CERC formula (Paper IV). Simplified handling of refraction and shoaling (e.g., when it is assumed that $\sin^2 \theta_b \approx 0$) also leads to an overestimation of the breaking wave height and the approach angle at breaking, consequently, to a large bias of the resulting transport rates for waves approaching under angles $>30^\circ$.

The sensitivity of numerically simulated potential sediment transport patterns and magnitudes to the model properties and input data was analysed in Paper IV by (i) including full shoaling and refraction into the model, (ii) adjusting the details of wave transformation in the nearshore, (iii) changing the typical grain size and (iv)

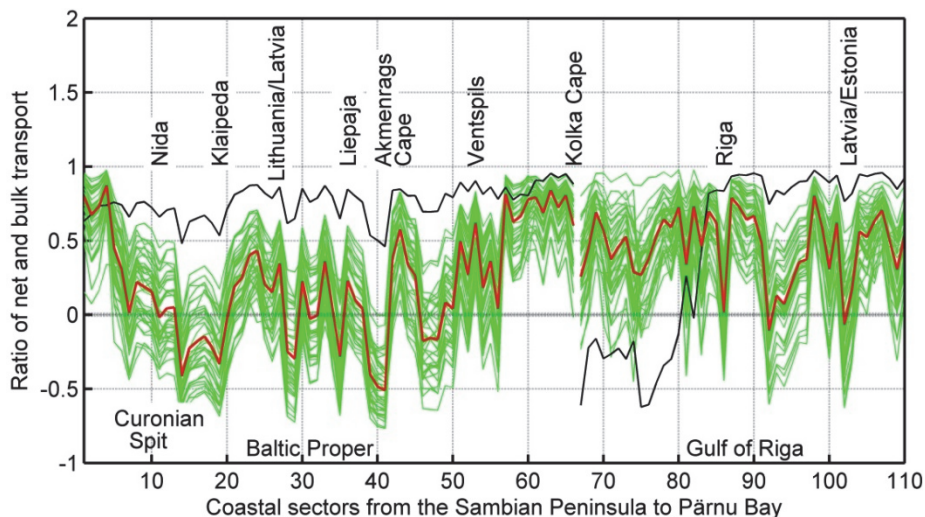


Figure 8. The ratio of net to bulk potential transport at the eastern Baltic Sea coast in single years (green line) and on average over 1970–2007 (red line). The black line indicates the ratio for 1984 when transport to the north predominated in the entire study area. The calculations used the significant wave height as input for the CERC formula and a simple representation of shoaling (Paper III).

employing different interpretations of the input wave height in different parts of the CERC formula (9).

The use of the method described in Section 2.3 for resolving the joint effect of shoaling and refraction (Paper IV) led to more than 30% decrease in both the bulk and net transport along the Sambian Peninsula and at the NW coast of the Courland Peninsula compared to the use of only refraction in Paper III. In these areas a significant amount of waves approach the coast under large angles and taking account of both shoaling and refraction is obviously necessary. Similar differences

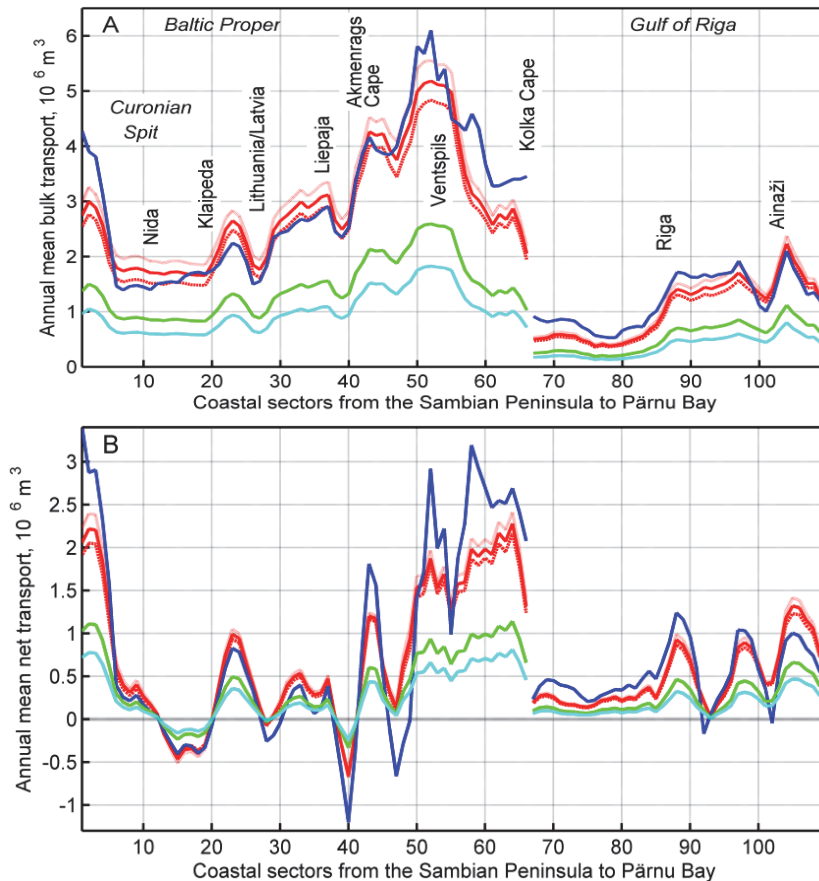


Figure 9. Simulated potential bulk transport (A) and net transport (B). All lines indicate the moving average over three subsequent coastal sections, calculated as an average over 1970–2007. Blue: $d_{50} = 0.17$ mm, simplified representation of shoaling, significant wave height as input for the CERC formula (Paper III). Other colours correspond to the use of solutions of Eq. (14). Red lines: significant wave height as input for the CERC formula; dotted line (upper): $d_{50} = 0.063$ mm, solid line (middle): $d_{50} = 0.17$ mm, dashed line (lower): $d_{50} = 1.0$ mm. Green: $d_{50} = 0.17$ mm; root mean square wave height as input for the wave energy but group velocity at the breaker line estimated based on the significant wave height. Cyan: $d_{50} = 0.17$ mm, root mean square wave height as input for the CERC formula (Paper IV).

are rather small, usually below 10%, in other areas. Considerable variations in the mean grain size (from 0.063 to 1.0 mm) led to very small changes in the transport rates. Importantly, the qualitative patterns of bulk and net transport did not change when different calculation methods were used (Figure 9).

Not unexpectedly, the magnitude of both net and bulk transport exhibited strong dependence on the particular interpretation of the wave height. As mentioned above, the use of the significant wave height in the entire CERC formula in Paper III led to severe overestimation of the magnitude of transport. The use of the root mean square wave height led to considerable underestimation of the transport rates (Paper IV). A solution was proposed in Paper IV to revert back to Eq. (7) and make use of different physical meanings of the wave height in Eq. (9). The two meanings are evident in Eq. (7) that expresses the wave energy flux as the product of wave energy and group speed. The latter is expressed via the breaking wave height using the concept of breaking depth and assumption that waves are long.

It is natural that the wave energy at the breaking line is expressed via the root mean square wave height if the CERC coefficient K is designed for this measure. The dependence of the rate of supply of wave energy (group speed) on the particular definition of the wave height is not obvious. For remote swells (that supply substantial part of wave energy at the open ocean coasts) all definitions of the wave height are almost equivalent. However, the largest storm waves start breaking at much larger depths than predicted by the concept of breaking index and the root mean square wave height. Following this observation, as an alternative, in Paper IV the transport rates were calculated by employing different definitions of the wave height in different components of Eq. (9). Namely, the root mean square wave height was used to evaluate the wave energy at the breaker line but the group speed was calculated from the significant wave height. Although such an approach is not fully justified, it led to realistic magnitudes of simulated net transport (Paper IV).

3. Variations in simulated sediment transport

The results presented in Chapter 2 indicate that wave-driven alongshore sediment transport varies considerably both in time and space. The variations in simulated bulk sediment transport show the existence of several sections of different transport properties. The maxima of sediment transport coincide with the locations where the closure depth is largest – around the western coast of the Courland Peninsula and the Western Estonian archipelago. This similarity is expected as the basic characteristics of coastal processes in this approximation are simply functions of the wave energy flux that reaches a particular coastal section during a selected time interval (Dean and Dalrymple, 2002).

The largest variations in alongshore sediment transport along the coastline are due to spatially changing wave patterns and joint impact of the coastline orientation and wave approach direction. Several sharp local variations could be associated with a particular choice of the local geometry and coastline representation and may not reflect the real situation. Most of the variations depicted in Section 2.4 are of particular value for coastal engineering and management as they reflect the divergence and convergence areas of sediment flux and thus can be associated with the locations of systematic erosion and accumulation.

From the viewpoint of establishing the basic patterns of sediment transport, the alongshore variations in bulk transport and in the direction of net transport are often more important than the magnitude of sediment transport. This viewpoint is employed in Papers III and V that focus on qualitative features of alongshore sediment transport in the study area, while Paper IV makes an attempt to develop realistic magnitudes of the transport. This Chapter explores variations in different kinds of simulated sediment transport. Section 3.1 presents the key features of long-term and interannual variations in the net and bulk transport integrated over the entire Curonian Spit (Paper V). Section 3.2 discusses similar variations for three large compartments of the study area. The location and persistence of reversals of the overall counter-clockwise pattern are discussed in Section 3.3. The areas of convergence and divergence are considered in Section 3.4.

3.1. Interannual variability

The nature of long-term changes and the level of interannual variability of wave-driven alongshore transport are exemplified by analysing these aspects for the Curonian Spit (Paper V). This is a narrow (about 98 km long but only 0.4–4 km wide) sandy peninsula that has been formed during a few millennia through intense sand drift from the Sambian Peninsula (Žaromskis and Gulbinskas, 2010). It stretches from the Sambian Peninsula to Klaipėda and separates the Curonian Lagoon from the Baltic Proper. This exceptionally fragile structure is under continuous impact of natural forces, predominantly of wind and waves, and virtually all its sections (even those that usually show accumulation features) may be heavily damaged in certain storms (Žaromskis and Gulbinskas, 2010).

Bulk sediment transport patterns integrated over all 15 grid cells used to represent the spit (Figure 10) show relatively large short-term variability apparently reflecting the difference in storminess through the years. The annual values of bulk transport exhibit extensive interannual variability. Its extreme pointwise values are roughly twice as large as the long-term mean, while the minimum levels are about a half of the long-term ones. The level of interannual variability along the coasts of the Baltic Proper and the Gulf of Riga is roughly the same (Paper III).

There are two interesting features in the variations of the annual bulk transport. Firstly, bulk transport increases by about 20% during the simulated time interval (Figure 11). This trend, however, is not statistically significant. Secondly, its course reveals clear, almost periodical cycles with a typical time scale of about 8–10 years and amplitudes close to about 1/4 of the long-term average. This increasing trend matches a similar increase in the wind speed over the northern Baltic Proper (Räämet and Soomere, 2011). However, long-term variations in the annual mean wind speed do not show any clear cyclic course. Therefore, cyclic decadal variations in the overall bulk transport are probably associated with changes in wind and wave propagation directions.

The total net transport integrated over the entire Curonian Spit fluctuates around zero. It exhibits very small absolute values, usually a few per cent of the bulk transport for each particular year (Figure 12). Therefore, in the existing wave climate the long-term net sediment transport has no preferred direction. The relative variability of the overall net transport is much larger than the similar variability of bulk transport. In single years net transport forms up to 50% of bulk



Figure 10. Location scheme of the Curonian Spit. Boxes represent the 15 grid cells used in the calculations of sediment flux and the associated coastal sections (Paper V).

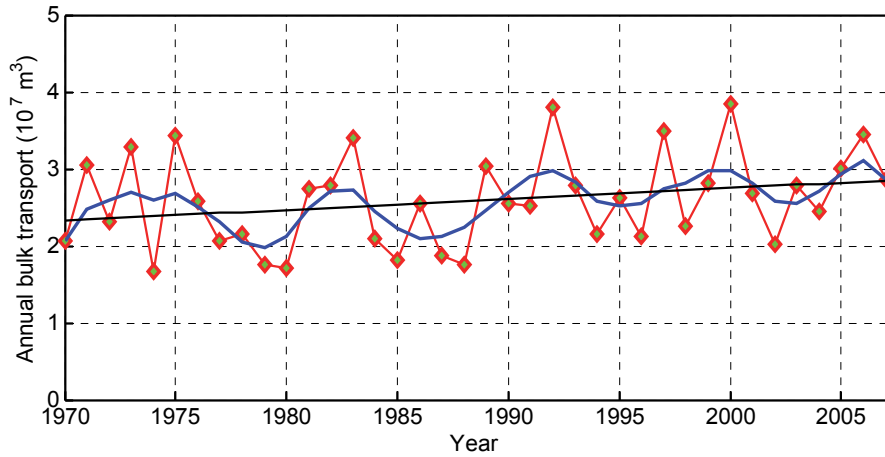


Figure 11. Annual mean bulk sediment transport along the entire Curonian Spit (red), its five-year average (blue) and linear trend (black line) for 1970–2000 (Paper V).

transport. The temporal course of net transport also shows a cyclic signal with a typical scale of about 10 years.

Importantly, the long-term course of net transport does not follow the increasing trend of bulk transport. Net transport increased in the 1970s and 1980s and decreased at the same rate from the mid-1990s onwards (Figure 12). This course is in phase with the evidence of changes in the annual mean wave height in the northern Baltic Proper (Broman et al., 2006; Soomere and Zaitseva, 2007) and in anti-phase with similar variations at the Lithuanian coasts (Zaitseva-Pärnaste et al., 2011). Therefore, a likely reason for such a behaviour of net sediment transport is a systematic change in wave direction. Similar changes (but much more gradual)

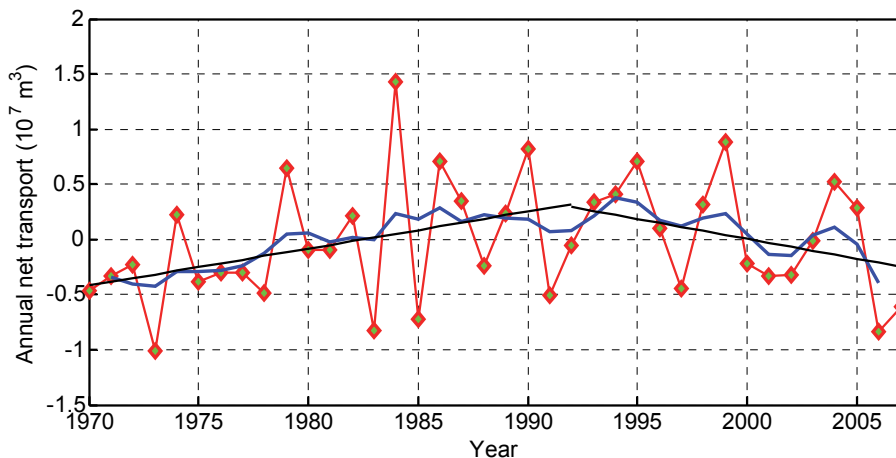


Figure 12. Annual mean net sediment transport along the entire Curonian Spit (red), its five-year average (blue) and trendlines for 1970–1993 and 1993–2007 (Paper V).

have been reported for wind direction over the Estonian mainland (Jaagus, 2009; Jaagus and Kull, 2011) and for the predominant wave approach direction in the south-eastern Gulf of Finland (Räämet et al., 2010). A possible reason for the change in the sign of the net transport trend could be a major shift in the geostrophic air flow by more than 30° from its usual eastward direction to almost south-east in the southern Baltic Sea at the end of the 1980s (Soomere and Räämet, 2014). It may reflect a relocation of the typical positions of cyclones to the east over the last decades (Lehmann et al., 2011).

3.2. Large-scale spatial variations

Spatial patterns of variations in bulk and net sediment transport can be to some extent revealed by analysing these quantities separately in three key parts of the study area. As will be shown in Section 3.3, Cape Akmenrags divides the sedimentary system of the eastern Baltic Proper coast into two almost independent compartments. Furthermore, Cape Kolka separates the sediment at the open Baltic Sea coast from sediment volumes of the Gulf of Riga. It is thus natural to look separately at the bulk and net transport in three large compartments: (i) from the Sambian Peninsula to Cape Akmenrags; (ii) from this cape to the Cape Kolka; (iii) sedimentary coasts of the Gulf of Riga.

As expected, the bulk sediment transport in both compartments of the Baltic Proper substantially exceeds similar transport along the entire Gulf of Riga (Figure 13). The interannual and decadal variability in the two Baltic Proper coastal compartments are almost identical in terms of a slightly increasing trend,

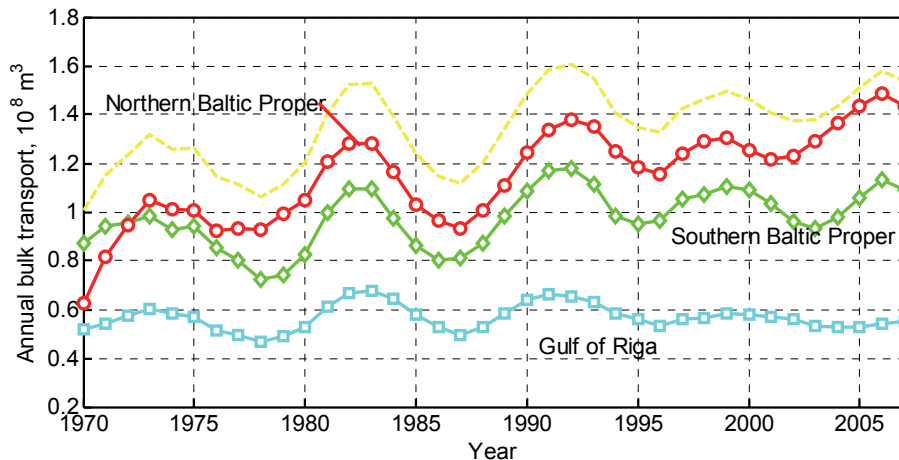


Figure 13. Bulk sediment transport integrated over three sections of the eastern Baltic Sea coast: red – from the Sambian Peninsula to Cape Akmenrags (the southern compartment); cyan – from Cape Akmenrags to Cape Kolka (the northern compartment), green – from Cape Kolka to Pärnu Bay. All values are smoothed over three subsequent years. The yellow line shows half of the transport over the entire eastern Baltic Sea coast (Viška and Soomere, 2013).

typical time scales, amplitudes and timing of the higher and lower intensities of coastal processes. Interestingly, the bulk transport rate in the Gulf of Riga practically does not change over the simulated time interval. Its decadal variations in the Gulf of Riga match similar variations in the other two areas until the mid-1990s and then behave in a different way.

The described property suggests that the storm impact on different coastal sections may have varied to a certain degree. Storm waves in the 1970s and the 1980s impacted the coasts of the Baltic Proper and the Gulf of Riga in a similar way, but the situation has changed afterwards – storms that impacted the Baltic Proper coasts had less impact on the Gulf of Riga and *vice versa*.

The net sediment transport integrated over these compartments also shows some interesting features. Most of this transport occurs in the section from Cape Akmenrags to Cape Kolka and forms about half of the net transport in the entire study area (Figure 14). The total net transport in the Gulf of Riga is larger than in the southern Baltic Proper.

The temporal course of the net transport in the Gulf of Riga qualitatively differs from that along the coasts of the Baltic Proper. A certain similarity between the courses of net transport in all three areas is evident until the end of the 1980s. Later on the temporal changes in the net transport in the Gulf of Riga have no correlation with those in the Baltic Proper. This loss of correlation may also reflect a large-scale change in the atmospheric conditions that have disconnected the impact of storms in the sub-basins of the Baltic Sea from those along the coast of the Baltic Proper.

The relatively large values of the net transport in the Gulf of Riga may be interpreted as follows. The coasts of the southern Baltic Proper partly consist of relatively soft sediment and have been developing under comparatively harsh wave conditions for several millennia. This has been favourable for the creation of a coastal shape that is almost in equilibrium with the local wind climate. The coasts

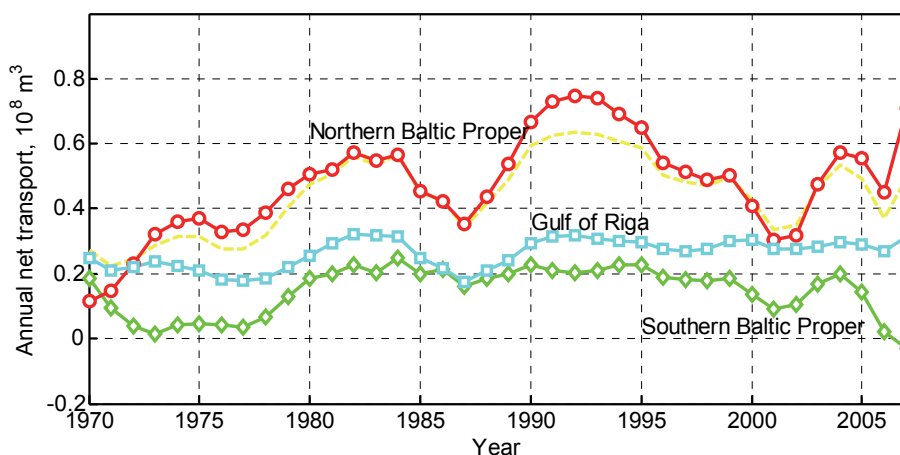


Figure 14. Net sediment transport integrated over three sections of the eastern Baltic Sea coast. Notations are the same as for Figure 13 (Viška and Soomere, 2013).

of the Gulf of Riga develop under much lower wave activity that is concentrated in clearly shorter waves (Eelsalu et al., 2014) and therefore provide substantially less wave energy to shape the coasts. Thus, the coasts of the Gulf of Riga apparently are still far from equilibrium and may host higher net transport even under relatively low waves.

3.3. Reversals of counter-clockwise transport

The littoral flow along the study area evidently contains several deviations from the overall counter-clockwise pattern. As mentioned before, several eminent headlands like Cape Akmenrags, Cape Ovisrags or Cape Kolka may serve as natural barriers for alongshore sediment flow (Eberhards, 2003). Part of the sediment brought into motion by waves may be transported away from the coast at these capes and headlands (Eberhards, 2003). Moreover, the direction of alongshore net transport may be variable within single years (Figures 7 and 8). In other words, several coastal segments may host clockwise net transport (reversals). Their presence is implicitly evident in historical studies by R. Knaps, the outcome of which has been presented in (Ulsts, 1998) (Paper IV).

The presence of a reversal for a single year means that the annual average alongshore net transport is negative along a certain coastal segment. This observation reduces the problem of identification of reversals to the determination of zero-crossings of the annual net transport (Papers III and IV).

Four such zero-crossings (at the Curonian Spit, near Klaipėda, at Cape Akmenrags and to the north of Liepaja) appear at almost the same location in all versions of calculations (Figure 9) and for almost all years (Figure 7). Several less persistent (possibly short-term) zero-crossings and associated reversals are represented in Figure 7 as segments that have almost zero long-term net transport. While most of such reversals correspond to local minima of bulk transport (Figure 6), one reversal to the north of Riga hosts intense bulk transport.

A relatively short but persistent reversal is located between Liepaja and Cape Akmenrags. Its length varies considerably in time, from about 15 to 50 km as its southern border substantially moves in different years (Figure 15). The most interesting feature is the highly persistent zero-crossing at Cape Akmenrags. Its location varies by only about ± 5 km from its average position. It is evident during all the simulated years except for the quite unusual year 1984 (Paper IV).

The zero-crossing points and the related reversals are much less persistent in the Gulf of Riga. No such areas seem to exist at its western coast except possibly in a few single years. Long-term sediment flux almost vanishes or is reversed at two locations at the eastern coast of the gulf – near Saulkrasti and at the border between Latvia and Estonia (Figure 15). The simulated net sediment transport shows quite frequently occurring short reversals at both sites. In selected years, the reversal near Saulkrasti may extend to several tens of kilometres. This matches the results of Knaps (1966) where this reversal covers more than 30 km. It occasionally starts from Cape Kurmrags and extends to almost Saulkrasti.

Another relatively persistent zero-crossing point is often located near Ainaži. The associated reversal is quite short, normally <15 km. Knaps (1965) suggested that the long-term average sediment flow is to the north. Eberhardts (2003) provided evidence about an oppositely directed sediment motion based on a set of underwater sandbars that are visible to the south of Ainaži on orthophotos made in 1982 and 2007. Therefore, the data simulated in Paper III for this region for 1970–2007 likely reflect the correct average direction of sediment flow to the south. The role of a persistent area in the northern part of the Curonian Spit is discussed in Section 4.1.

The described pattern of the overall counter-clockwise net transport and of its reversals seems to be generally stable. It may, however, undergo substantial changes in single years. For example, in 1984 the annual average transport was directed to the north (Figure 8). While this direction was usual for the coast of the

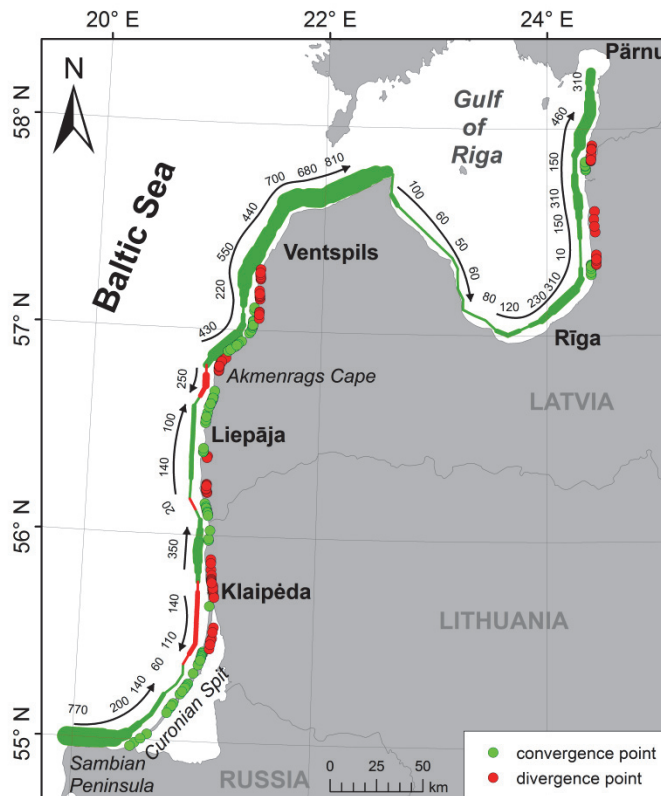


Figure 15. Location of the most persistent reversals (magnitude in red) and zero-crossing points of annual net sediment transport (divergence points – red circles; convergence points – green circles; see explanation in Section 3.4) in different years. Direction (arrows) and magnitude (numbers at arrows, in 1000 m³) indicate the net sediment transport calculated using $d_{50} = 0.17$ mm, Eq. (14) and root mean square wave height as the input to the CERC formula. Modified from Paper III.

Baltic Proper, it was exceptional along the south-western coast of the Gulf of Riga (Paper III). This hindcast matches the observational evidence about northward transport of large sediment volumes in that year (Ulsts, 1998).

3.4. Divergence and convergence of alongshore sediment flux

The physical meaning of zero-crossings, reversals and large alongshore gradients of sediment flux in the functioning of the overall counter-clockwise net sediment transport as well as their consequences for coastal engineering and management become evident from the analysis of the nature of alongshore variations in net sediment transport (Figure 16). These variations reflect typical areas of erosion and accumulation.

If sediment flux is constant along a certain coastal segment, this segment hosts pure transit in the context of the presented analysis and its sediment volume is constant. Sediment flux is convergent if net sediment transport decreases along some segment. In this case waves bring to each part of the beach more sediment than is carried further downdrift and such a beach experiences accumulation. Contrariwise, sediment flux is divergent if net sediment transport increases along a certain segment. The beach then experiences sediment deficit and eventually erosion (Hanson and Larson, 2008). Differently from the analysis in Paper I (where alongshore variations in the closure depth were not really associated with the direction of littoral flow), the divergence and convergence of sediment flux are intrinsically related to the direction of net transport.

The most probable and systematic (but not necessarily the most intense)

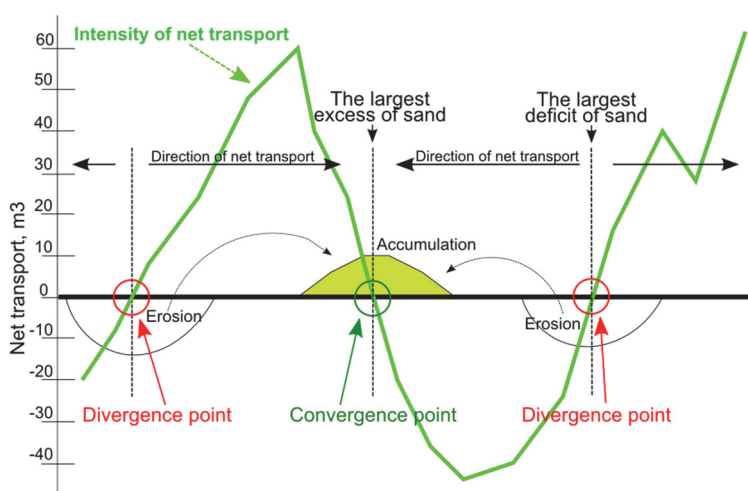


Figure 16. The relationship between the intensity (green line) and direction (horizontal arrows) of alongshore net sediment transport and areas of likely erosion and accumulation.

accumulation and erosion areas are the above-discussed zero-crossing points of the net sediment transport. Two types of such points are possible. The zero-downcrossing points in Figure 16 indicate the convergence (accumulation) areas of sediment flux (that are regularly filled by sediment) and zero-upcrossing points – the divergence (likely erosion) areas that are often stripped of sediment. Most of such points are located in the Baltic Proper. Only some points occur in the Gulf of Riga and are evident just in certain years (Figure 15). Particularly interesting aspects for applications are: (i) the range of changes in the locations of such points (which defines the spatial extent of reversals, Figure 15) and (ii) variations in these locations in different years (which defines how often reversals occur). The relevant intervals cover the areas where an intense accumulation or erosion may take place in the existing wind climate and for the existing configuration of the coastline.

The locations of zero-crossings of the net transport may vary considerably in different years (Figure 17). Some zero-crossing points keep their location over many years, while other similar points exert large shifts along the coast (Paper III). There exist two pairs of persistent (albeit moving in space) zero-crossing points in the study area. The convergence point with the largest amplitude of relocation over years is located in the Curonian Spit region. Its functioning, role and stability will

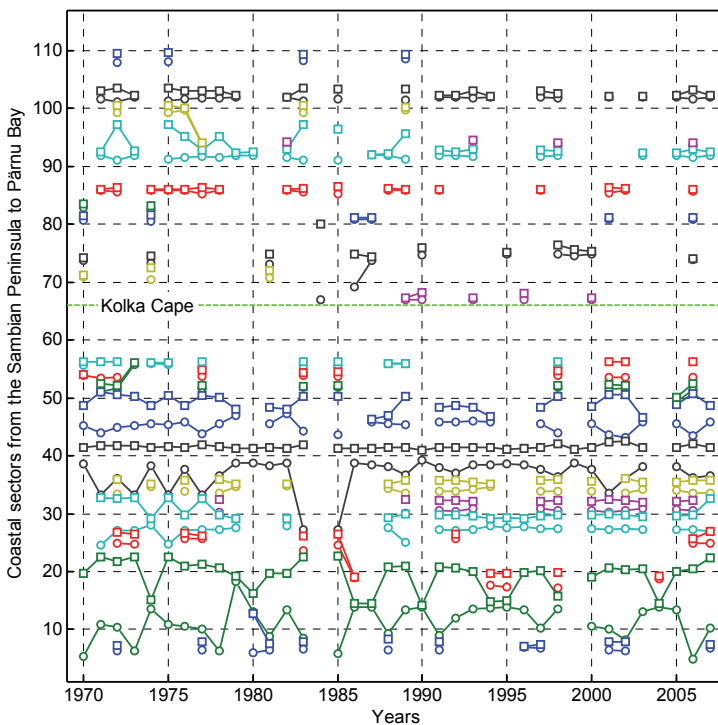


Figure 17. Numerically simulated location of zero-crossing points in the net sediment transport along the study area in 1970–2007: circles – convergence points; squares – divergence points (Paper III).

be analysed in detail in Sections 4.1 and 4.2. An associated divergence point is located in the vicinity of Klaipėda. The presence of one convergence and one divergence point between Klaipėda and Liepaja (both have a limited range of relocation) apparently reflects local changes in the coastline orientation. As they are evident only in selected years, their role in the large-scale sediment transport pattern is obviously minor. A point of divergence near Cape Akmenrags is extremely stable. Two other zero-crossing points to the north of this cape are present in selected years.

The zero-crossing points at the coasts of the Gulf of Riga are only evident in a few years. They were more frequent in the 1970s. This tendency may indicate certain changes in the wave climate in this region (Eelsalu et al., 2014).

The net transport around zero-crossing points of divergence is, on average, directed away from such points. Consequently, sediment is normally not carried through such points and they serve as a sort of invisible barrier for sediment transport (although some sediment may pass through such areas in single storms). The almost permanent presence of a zero-crossing point of divergence of the sediment flux near Cape Akmenrags suggests that barely any sediment is transported around this cape. This point is evident almost every year except in 1984 (Figure 8) when none of the zero-crossing points were registered and in 2004 when only some points were present. In essence, it divides the eastern coast of the Baltic Proper into two almost separated sedimentary compartments. This conjecture is true for the current wave climate and may change in other wind and wave climates.

The ratio of net to bulk transport also characterises the intensity of transit of sediments through each sector compared to the back-and-forth motions (Figure 8). Similarly to the above, it highlights four divergence and convergence areas that are regularly present. These are two divergence points near Klaipėda and Cape Akmenrags and two convergence areas at the Curonian Spit and to the north of Liepaja. These areas are almost insensitive to the particular implementation of the CERC approach (Paper IV).

4. Future projections and ground truth

The results presented in Chapters 2 and 3 show that the overall counter-clockwise pattern of net sediment transport along the eastern Baltic Sea coast and in the Gulf of Riga is modulated by several persistent reversals. As demonstrated in Section 2.4 and Paper IV, the four most persistent zero-crossing points of net sediment transport and the associated reversals are almost insensitive to various implementations of the CERC model and the input data. It is thus likely that these features have an important role in the functioning of the entire sedimentary system in question.

The role of these zero-crossing points and likely consequences of potential changes in their driving forces are analysed on the example of the Curonian Spit (Paper V). This landform hosts an interesting convergence area of sediment flux that has shifted along the spit through the years. Its presence is evidently connected with the long-term stability of this spit and its loss (under possible changes in the wind and wave climate) can lead to instability of the entire spit. Sections 4.1 and 4.2 present an analysis of the likely reasons for the stability of the Curonian Spit and its possible changes considering probable future climate changes.

The invariance of the overall transport pattern and its reversals with respect to many factors suggest that this pattern has been present for a long time. Most probably, it has exerted a certain impact on the sediment structure in the adjacent nearshore. The comparison of major features of the nearshore geological composition of the study area and simulated sediment transport is given in Section 4.3.

4.1. Functioning of the Curonian Spit

Further evolution of vulnerable sections of the southern and eastern Baltic Sea coasts eventually occurs in the changing climate, in particular, under gradual water level rise (Dailidienė et al., 2006), apparent increase in storminess (Alexandersson et al., 2000) and shortening of the duration of the ice cover (Sooäär and Jaagus, 2007). The consequences of combinations of these factors are of great concern for the coastal nations (Zeidler, 1997; Eberhards et al., 2006). Orviku et al. (2003) expressed the opinion that the gradually increasing pressure may already have overridden the mostly stable development of the eastern Baltic Sea coasts. Sandy coastal landforms that develop under direct impact of waves eventually exhibit the fastest changes. In this respect it is most interesting and important to understand processes that shape the Curonian Spit, the most unique and fascinating coastal landform of the eastern Baltic Sea.

The wave climate in the nearshore of the Curonian Spit is somewhat milder than in the Courland Peninsula. The long-term significant wave height is approximately 0.9–1 m in the open sea (Räämet and Soomere, 2010) and 0.7 m in the nearshore (Kelpšaitė et al., 2008, 2011; Zaitseva-Pärnaste et al., 2011). Wave fields in this

area as well as in other parts of the Baltic Sea show strong seasonal and interannual variability. The waves are, on average, the highest from September till January and the lowest in May. Similarly to the rest of the eastern Baltic Sea, the empirical distribution of wave propagation directions has two peaks for each sector of the Curonian Spit (Figure 18, Paper V). The exact direction and height of these peaks varies to some extent along its coast. In the northern part of the spit waves mostly approach from the west-southwest and slightly less from the NNW. These peaks have almost equal heights at the southernmost part of the spit but correspond to somewhat different directions. The nearshore of the south-eastern sections of the spit is to some extent sheltered by the Sambian Peninsula.

This complicated system of approaching waves, changing along the spit (and likely also in time), gives rise to an interesting phenomenon – a sort of dynamical equilibrium for the spit. The analysis in Sections 3.3 and 3.4 shows that most of the spit occasionally constitutes a reversal area of sediment transport. This reversal is usually located in the northern part of the spit between Nida and Klaipėda. Its borders vary considerably in different years (Figure 19). Only in single years it may be replaced by northward sediment flux. Differently from Cape Akmenrags, its northern border (a zero-crossing point of divergence next to Klaipėda) probably does not serve as a robust barrier for sediment motion. Such an “intermittent” transport regime seems to be an intrinsic part of the dynamical equilibrium of the spit. The overall appearance of the reversal indicates that in the long-term perspective the divergence area around Klaipėda suffers from sediment deficit.

The most interesting feature is the cyclic movement of the southern border of the reversal – a zero-crossing point of convergence – along the Curonian Spit (Figure 19). The location of this point varies in different years from the western

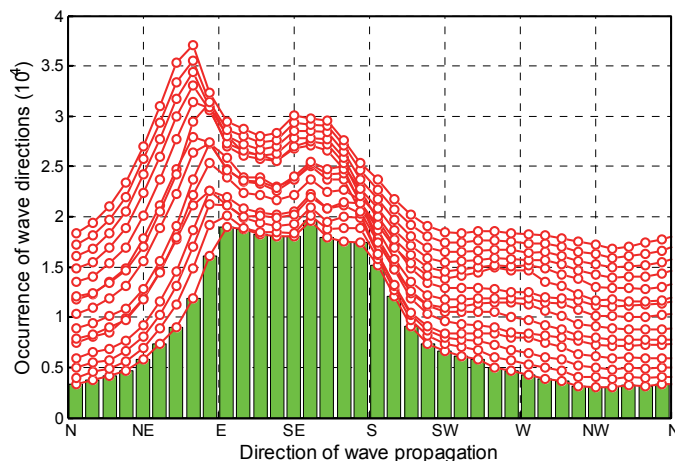


Figure 18. Wave propagation directions at different sections of the Curonian Spit. The bars correspond to the southernmost part of the spit. The distributions for subsequent sections along the spit from south to north are vertically shifted by 0.1 units of the vertical axis (Paper V).

end of the spit at Zelenogradsk up to the Klaipėda strait. The range of the locations covers the entire length of the Curonian Spit, whereas this point moves along the spit cyclically every three to five years.

The associated convergence area of sediment flux literally brings sediment to nearly all parts of the spit over the years, ensuring systematic sand refill of almost the entire spit. This movement is evident in all simulations with different choices of parameters in the CERC formula, showing that the spit regularly receives sediment along its entire length. These results suggest that the Curonian Spit is evidently in an almost equilibrium state under the simulated wave climate even if some of its parts might at times suffer from erosion (Gilbert, 2008; Zhamoida et al., 2009). The simulations, however, do not fully reveal the situation in the northern part of the spit, which is occasionally affected by a frequent zero-crossing point of divergence located near Klaipėda. This point is still mostly stable and its vicinity often experiences accumulation (Žaromskis and Gulbinskas, 2010). Regular erosion that has been observed at and to the north of Klaipėda (Gilbert, 2008) is consistent with the relocation range of this zero-crossing point of divergence.

4.2. Stability of the Curonian Spit under rotating wave climate

The analysis in Section 3.1 and Paper V has shown that the long-term average (averaged over the years 1970–2007) net transport over the entire Curonian Spit is very small, about a few per cent of the similar average of the bulk transport. This

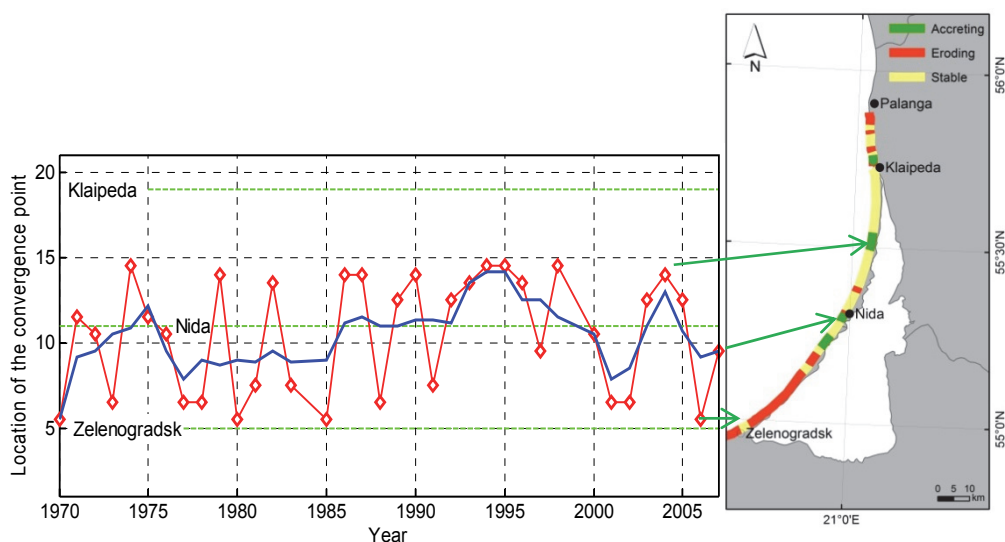


Figure 19. Relocation of the zero-crossing point of convergence of net sediment flux (red rhombi) and its three-year average (blue line) along the Curonian Spit in 1970–2007. The green dashed horizontal lines indicate the location of the western (Zelenogradsk) and northern (Klaipėda) ends of the spit and the position of Nida on the spit. Modified from Paper III and Gilbert (2008).

feature also suggests that under the existing wave climate the Curonian Spit as a whole is in an almost equilibrium state. The equilibrium is a natural consequence of the development of this landform. Such spits often develop in areas where long-term sediment drift moves large amounts of sand and the coastline suddenly changes its direction (Gudelis, 1967; Eberhards, 2003; Žaromskis and Gulbinskas, 2010). The resulting landform develops a characteristic curved shape. As discussed above, almost all sections of the eastern Baltic Sea coast are mostly shaped by waves and suffer from sediment deficit. A landform that is under such a strong wave impact can only develop in a stable manner if wave action keeps it in an almost equilibrium state. Slowly developing landforms like the Curonian Spit therefore generally have a shape that is almost in equilibrium with the amount of supplied sediment and the local contemporary wave climate, although some of its beaches may be damaged in extreme wave storms (Zhamoida et al. 2009; Žaromskis and Gulbinskas, 2010).

The total net sediment transport integrated over the entire Curonian Spit fluctuates around zero (Figure 12). Its absolute values are just a few per cent of bulk transport. This means that the long-term net sediment transport has no preferred direction in the simulated wave climate of today. The particularly small ratio of the overall rates of net and bulk transport suggests that this equilibrium is almost perfect in the existing wave climate. The same feature, however, signals that even a minor change in the wind properties may lead to a substantial imbalance in sediment transport and potentially to loss of the stability of the entire landform.

The existing research of the Baltic Sea wave climate (Soomere, 2013; Soomere and Räämet, 2014 and references therein) suggests that the wave heights may exhibit extensive decadal variations but no major long-term trend. Changes in the wave approach direction have an equally large potential to modify even the qualitative appearance of coastal processes (Furmańczyk et al., 2011) like the direction of littoral flow, rotation of short beaches (Ranasinghe et al., 2004) or entire sandy islands following seasonal variations in the predominant wind direction (Kench et al., 2009). As mentioned above, in some locations of the southern Baltic Sea they may be the major driver of changes (Furmańczyk et al., 2012). Substantial changes in the most frequent wave approach directions have been documented in the Gulf of Finland (Räämet et al., 2010) and a major rotation of the geostrophic winds has been identified for the south-western Baltic Sea (Soomere and Räämet, 2014). Wind directions may change in the Baltic Sea, for example, due to a shift in the trajectories of cyclones (Lehmann et al., 2011; Sepp and Jaagus, 2011). Moreover, a systematic change in wind directions has been identified for the Estonian mainland (Jaagus and Kull, 2011). As a large part of waves approach the nearshore of the Curonian Spit under a relatively high angle, possible changes in wave directions may strongly impact the functioning of the spit. These considerations suggest that the stability of the Curonian Spit may be first affected if the wave approach direction changes.

The stability of the Curonian Spit was examined by rotating all wave approach directions provided by the WAM model. Relatively small rotations of the approach angle did not affect bulk transport significantly. Bulk transport reached its minimum when the wave climate was rotated by 5° clockwise. This rotation mimics the case when the cyclones would be shifted to the north.

Net transport changes almost linearly with the rotation of wave approach directions (Figure 20). The current wave climate corresponds almost exactly to the zero level of net sediment transport. This feature confirms that the Curonian Spit has an almost perfect match with the existing wave climate and any considerable change in the wave approach directions may accelerate coastal processes in this domain. As the ratio of net to bulk transport is almost zero in the existing wave climate, even a small wave direction rotation by about 2–3° would lead to quite strong residual sediment transport.

Rotation of the wave climate would also have marked influence on the behaviour and even the presence of the zero-crossing point of convergence along the spit. As discussed above, in the modelled wave climate for the 38 year period of 1970–2007 such a point of convergence has always been located somewhere along the spit so that a certain sector of the spit is filled by sand each year. It is natural to assume that if the wave climate would only slightly rotate, the spit might be somewhat reshaped to match the new climate but would not lose large amounts of sediment.

The limits of stability can be to some extent quantified by analysing the behaviour of the zero-crossing point of convergence (Paper V). If this point is present at least in a substantial portion of years, the spit would eventually be stable. Such limits appear to be surprisingly small. If wave direction was rotated clockwise, the long-term average location of the zero-crossing point of convergence would move to the eastern end of the spit already for a rotation by 5°. This zero-crossing would disappear for most of the years if the directions were rotated by more than 10° (Figure 21). Such a rotation would eventually cause

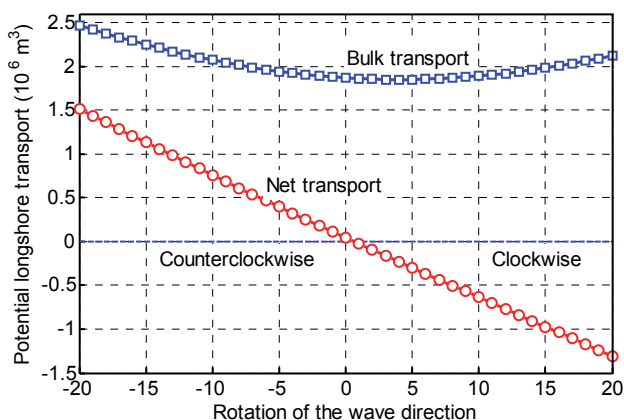


Figure 20. Annual mean bulk and net transport per a single coastal section of the Curonian Spit for rotated wave climates (Paper V).

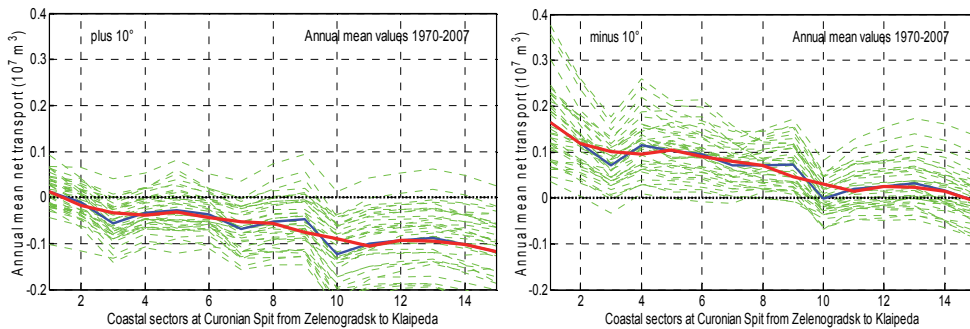


Figure 21. Annual net transport for single years (green) and long-term average (blue, red) for the Curonian Spit for clockwise (left panel) and counter-clockwise (right panel) rotation of the wave climate by 10° (Paper V).

strong net sediment flux (about 1/3 of bulk transport, that is, at least 15 000–30 000 m^3/yr , Figure 17, Paper IV) to the east in most years. This transport would finally result in rapid erosion in some parts of the beach because there would be no compensating sediment flux across the Klaipėda strait.

For counter-clockwise rotation exceeding 10° the zero-crossing point of convergence would move to the northern end of the spit and reach the Klaipėda region. Differently from the clockwise rotation, strong transport to the north would dominate in almost all years in the entire eastern section of the spit. In this scenario the net sediment deficit could be compensated with the material eroded from the Sambian Peninsula.

The shape of the spit and its exceptional stability in the existing wave climate suggests that the wave climate has been very much the same over a longer time interval in the past. An important message from Paper V is that even a small rotation in the wave approach direction (caused, e.g., by a temporal shift in the trajectories of the cyclones) may strongly impact the future development of the Curonian Spit. Substantial damages are likely for a clockwise rotation as virtually no sediment enters the system from the north.

4.3. The match of nearshore geology and sediment flux

It is natural to expect that the possibly long-term presence of the overall pattern of the simulated alongshore sediment transport in the study area becomes evident not only in the nature of the coast (distribution of erosion and accumulation areas) but also in the geological composition of the nearshore seabed. Comparisons of the results of simulations with the reality presented in this thesis are not straightforward because of the relatively low spatial resolution of calculations and the presence of major human interventions such as large harbours, beach refill activities (Tönisson et al., 2013), or historical efforts to immobilise sand along the Curonian Spit.

Some comparisons of simulated results and observed changes have been performed near harbours and coastal engineering structures. The volumes of material dredged from fairways or harbour basins are compared with sand movements along the coastline (Eberhards, 2003; Eberhards et al., 2009). However, these comparisons are not straightforward. The material removed may consist of former sand masses or reflect morphological structures like tombolos or salients that are formed owing to certain local features.

To minimise the impact of such local features, the comparisons have to reflect the impact of long-term processes in areas that are not directly impacted by human interventions. Early rough comparisons of the intensity of coastal processes with reality have shown at least qualitative match. For example, alongshore variations in the closure depth showed some connection with geological processes along the coast (Paper I). The increase in the closure depth showed also clear increase in the variability of the accumulation and erosion rates (Paper I).

The net sediment transport pattern along the eastern Baltic Sea coast was compared with the geological composition of the study area in Paper IV. Geological information was obtained and combined into Figure 22 from various nearshore bottom sediment maps (Bottom sediments ..., 1996; Bitinas et al., 2004; Ulsts and Bulgakova, 1998). Note that sediment classes in each country are slightly different and do not fully overlap over the research area.

A narrow strip of fine-grained, usually sandy sediment is mostly present at the waterline along the entire Courland coast starting from the Lithuanian–Latvian border until the Irbe strait. This strip simply reflects the tendency for sand to gather at the waterline even if there is a general deficit of finer sediment. Thus, the presence of this strip, often with very limited sand volume, cannot be associated with the specific patterns of alongshore transport. For this reason, Paper IV focuses on the geological composition of a wider underwater area.

The sea bottom of the eastern nearshore of the Baltic Proper is mostly composed of gravel with pebbles and boulders, or of sand and gravel with pebbles (Figure 22). The coasts of the Gulf of Riga are somewhat different: they are composed of more mixed sediment and fine-grained sand than the open coast. This difference apparently reflects a difference in the overall activity of sediment transport in these basins.

The nearshore bottom sediments vary from very fine sand and silt to coarse sand, gravel and boulders in the research area. The Curonian Spit consists entirely of fine sand and also its nearshore area is covered with fine sand. This composition has evidently a historical background but could still be linked to the almost permanent presence of a zero-crossing point of convergence in this area.

To the north of Klaipėda the underwater slope is mostly covered by till. The above-mentioned sandy strip widens starting from Palanga. Notably, the area of till roughly (albeit not perfectly) coincides with the region of frequent presence of sediment flux divergence. The neighbouring sandy area (to the north of Palanga) matches the location of a similar convergence area.

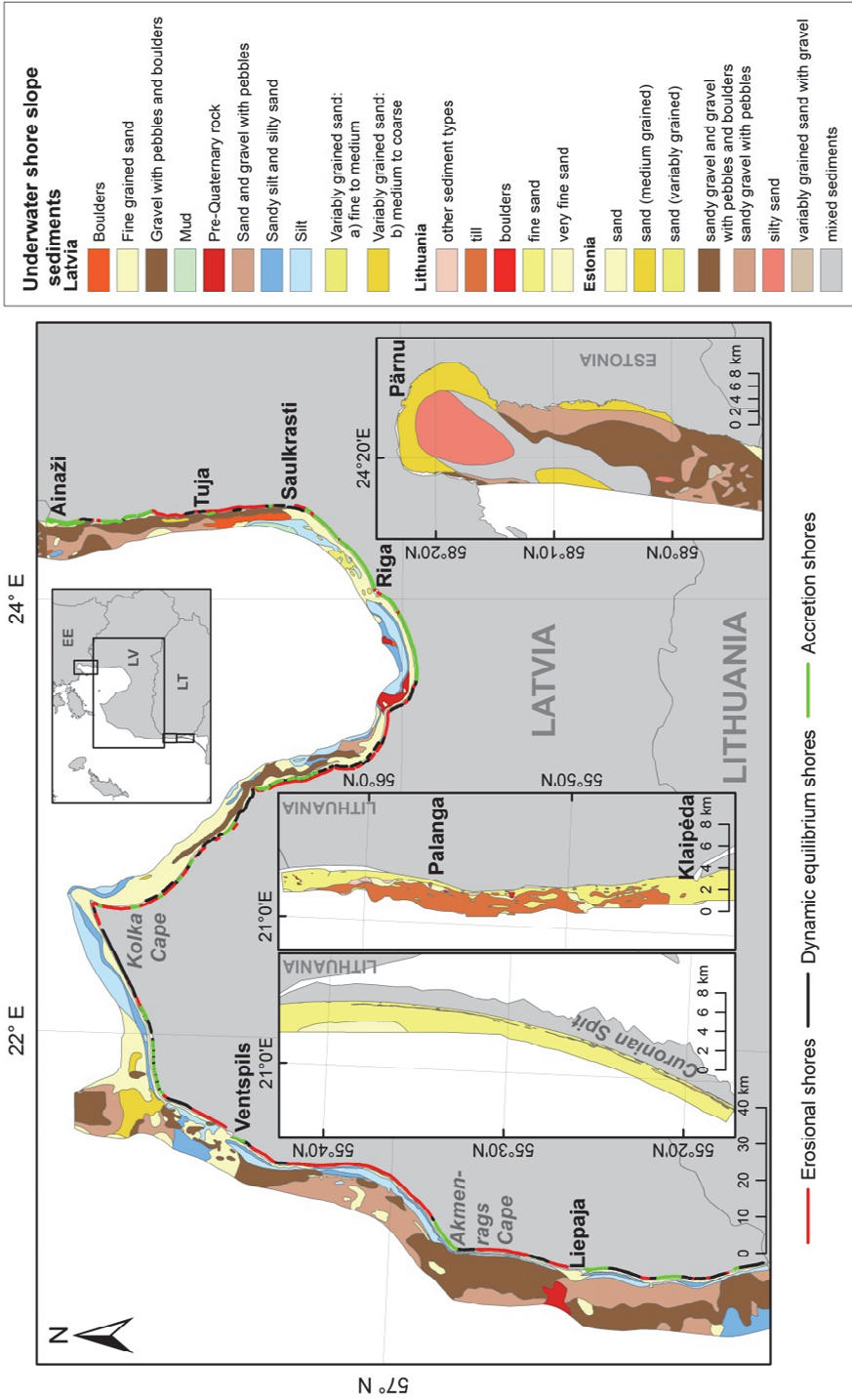


Figure 22. Geological composition of the nearshore study area (Paper IV).

Net sediment transport is often reversed to the north of the Latvian–Lithuanian border (Ulsts, 1998). In this segment gravel with pebbles and boulders covers the nearshore almost until the waterline. A frequent divergence area is located more to the north of this section. There is thus no perfect match of this divergence area with the geological composition of the nearshore.

A frequent divergence area occurs near Cape Bernati, to the south of Liepaja, where mostly gently sloping, low sedimentary coasts predominate. This area started to suffer from erosion in the middle of the 20th century. The mean retreat was about 1.4–3.8 m/yr until the end of the 20th century (Eberhards, 2003). The retreat was particularly intense, up to 13 m in three years (1991–1993). The length of the eroding section reached about 3 km (Ulsts, 1998). During strong storms like in the years 1993 and 1999 the retreat reached 40–50 m in a 1.1 km long section (Eberhards, 2003). Future predictions for this area suggest the development of a 5–12 m high scarp during the next 50 years (Eberhards, 2003). A likely reason for the increase in the sediment transport rate is the change in the predominant wave approach direction (Eberhards, 2003). This conjecture matches a major change in air-flow direction starting from 1988 in the north-eastern part of the Baltic Sea (Soomere and Räämet, 2014).

An occasional convergence area is located in the vicinity of Liepaja (Figure 15). Consistently with this observation, an area of fine-grained sand occurs at this city (Figure 22). It is, though, occasionally discontinuous to the north of Liepaja. The mismatch of the results of simulations (that suggest the presence of finer sediment in this area) is evidently because Liepaja Harbour disrupts the natural sediment transport. This major structure causes sediment deficit to the north of Liepaja where mostly gravel with pebbles and boulders occur on the seabed and fortifications built in the 1800s behind the dune crests are already falling into the sea (Tõnisson et al., 2013).

The vicinity of Cape Akmenrags (located between Liepaja and Ventspils) hosts a persistent area of divergence. Consistently with this result, the nearshore zone contains almost no fine sediment (although the beach is sandy and with growing foredunes). Simulations indicate a frequent convergence area to the north of the cape. This outcome also matches the presence of a wide sandy or silty strip in this region.

The simulations suggest intense and almost unidirectional (with no clearly distinguishable convergence or divergence areas) net sediment transport to the north-east of Ventspils until Cape Kolka, where the nearshore seabed mostly consists of sand or silt. A fine-grained sandy strip in the nearshore widens starting from the entrance to the Irbe strait and reaches a maximum width near Cape Kolka (Figure 22). This intense sediment flow along the Courland Peninsula provides sediment to Cape Kolka and causes extensive growth of the cape (Ulsts, 1998; Eberhards, 2003).

Part of this sediment is transported further into the Gulf of Riga where sediment transport is generally much less intense than at the coasts of the Baltic Proper. The flux of sand in the vicinity of Cape Kolka is relatively weak but almost

unidirectional (except for the unusual year 1984). The intensity of net transport increases in the southern part of the gulf near Jurmala. The nearshore sandy strip becomes narrower to the north of Riga but continues until Saulkrasti. An appreciably persistent convergence area exists near Saulkrasti. In general, it is not clear how precisely the simulations represent the joint impact of the two predominant wave systems (caused by south-western and NNW winds) in the southernmost part of the Gulf of Riga. Most probably, they drive intense back and forth transport between Jurmala and Saulkrasti, with no clearly dominating net movement (Ulsts, 1998). Also the Daugava River strongly affects the sediment budget in this area.

Another occasional reversal and a pair of zero-crossing points of divergence and convergence appear near Cape Kurmragi and Ainaži. It is likely that at least in some years there exists clockwise sediment movement between this cape and Ainaži. Sediment movement to the south in this area was also observed by Eberhards (2003).

In conclusion, there is an acceptable (albeit far from perfect) match between the major areas of convergence and divergence and the nearshore geological structure (Paper IV).

Conclusions

Summary of the results

The presented studies address the system of sedimentary coasts along the eastern Baltic Sea from the Sambian (Samland) Peninsula to Pärnu Bay from a functional and structural perspective. This coastal area mostly consists of easy erodible sediments that are vulnerable to strong waves and high water levels. The central objectives were: (i) to quantify the wave-driven impact on this coastal stretch, (ii) to establish the key structural features of the entire domain, (iii) to identify the major changes in the course of coastal processes in this domain and (iv) to develop a rough estimate of the structural stability of the major landforms.

Based on a high-resolution long-term wind wave hindcast for 1970–2007 driven by adjusted geostrophic winds, spatial variations in the closure depth have been established for the entire eastern Baltic Sea coast. The largest closure depths (almost 7 m) occur along the north-western coast of the Courland Peninsula and the Western Estonian archipelago that are fully open to the predominant south-westerly winds. The closure depth is much smaller (below 5 m and down to 2 m in sheltered areas) in the Gulf of Riga. Alongshore variations in this depth in naturally developing regions are linked to the major areas of predominant erosion.

It is shown that the typical ratio of extreme (occurring during 12 h/yr) and mean wave heights along the Baltic Sea coasts (5.5) considerably exceeds the similar ratio along the open ocean coasts (4.5). An upgrade of the widely used express formula for the evaluation of the closure depth based on the annual mean significant wave height and accounting for this difference is developed for the open Baltic Sea coasts. The traditional formula can be used in semi-sheltered bayheads where swells form an essential part of total wave intensity.

The Baltic Sea waves often approach the coast under relatively large angles. A method is developed to properly account for the joint impact of refraction and shoaling of such waves in the evaluation of wave-driven impact. Implementation of the full representation of shoaling and refraction gives considerably improved estimates of sediment flux by waves approaching the coast under angles $>30^\circ$.

Alongshore variations in sediment transport along the eastern Baltic Sea coast are analysed using the above wave hindcast and the Coastal Engineering Research Centre (CERC) wave energy flux model. The long-term average net transport is the largest (up to 700 000 m³/yr) along a short section of the Sambian Peninsula and along the north-western Latvian (Courland) coast, and much less in the Gulf of Riga. Consistently with the existing knowledge, net transport is mostly counter-clockwise in the entire study area and unidirectional in its several sections. About half of the net transport in the entire study area occurs in the section from Cape Akmenrags to Cape Kolka. The total net transport in the Gulf of Riga is larger than in the section from the Sambian Peninsula to Cape Akmenrags. While the long-term course of the bulk transport in the Gulf of Riga matches the similar course in

the Baltic Proper, the temporal courses of net transport qualitatively differ in these coastal stretches.

The simulations indicate the presence of a number of several divergence and convergence areas, associated local and/or temporary reversals of net transport and almost disconnected regions in terms of sediment flux. The system contains two pairs of persistent zero-crossing points of net sediment transport. They correspond to convergence (accumulation) and divergence (erosion) areas. An extremely stable divergence point near Cape Akmenrags serves as a natural barrier for sediment transport and apparently divides the sedimentary system of the eastern coast of the Baltic Proper into two almost completely independent sedimentary compartments. Single years with usual levels of wind speed may host totally different patterns of sediment transport. The zero-crossing points at the coasts of the Gulf of Riga are evident in only a few years. They have been more frequent in the 1970s.

Cyclic relocation of a highly persistent convergence point over the Curonian Spit and an almost zero level of the long-term net sediment transport suggest that this landform is in an almost perfect dynamical equilibrium in the contemporary wave climate. The total bulk sediment transport along this spit increased about 20% during the simulated time interval. Its course reveals almost periodical cycles with a typical time scale of about 8–10 years and amplitudes close to about 1/4 of its long-term average. The overall net sediment transport increased considerably in the 1970s and 1980s but decreased at the same rate from the mid-1990s onwards. This feature suggests that a systematic change in wave direction may have occurred in the nearshore of this spit.

To analyse the sensitivity of sediment flux to various model implementations and different choices of input data, the simulations were repeated with different versions of the implementation of the refraction and shoaling impact, interpretation of the wave height as the input data for the CERC model and for a range of typical grain sizes. It was shown that the qualitative transport patterns and major divergence and convergence areas are invariant with respect to the choice of the model, interpretation of the wave data and reasonable variations in grain size.

The analysis of the stability of the Curonian Spit with respect to potential rotation of the predominant wave approach direction shows that a rotation exceeding 5° clockwise or 10° counter-clockwise may result in complete disappearance of the above-discussed convergence area and thus may render the current stable evolution of this landform into an unstable regime.

The established main structural properties of alongshore sediment transport for the eastern Baltic Sea are verified against the relevant historical evidence. The nearshore geological composition shows evident similarities with the variability of simulated sediment transport and its spatial variations. There is an acceptable match between the location of major convergence areas and the geological structure of the seabed to a distance of a few kilometres from the waterline. The match is less evident for divergence areas.

Main conclusions proposed to defend

1. Spatial variations in the closure depth were established for the eastern Baltic Sea coast and linked to the areas of predominant erosion and accumulation. The largest closure depths (~7 m) occur along the NW coast of Latvia and coasts of the Western Estonian archipelago.
2. An upgrade of the express formula for the evaluation of the closure depth based on the annual mean significant wave height was developed for the Baltic Sea coasts. The traditional formula can be used in semi-sheltered bayheads where swells form an essential part of total wave intensity.
3. A method has been developed for systematically accounting for the joint impact of wave refraction and shoaling of waves approaching the coast under large angles in the evaluation of alongshore sediment transport. This method essentially improves the estimate for the impact waves that approach the coast under angles $>30^\circ$.
4. Alongshore variations in bulk and net sediment transport and the main structural properties of this transport along the eastern Baltic Sea coast were analysed using the Coastal Engineering Research Centre approach. Simulated net and bulk transport rates are the largest along the eastern Baltic Proper.
5. The overall counter-clockwise pattern of net transport along the eastern Baltic Sea coast contains several persistent divergence and convergence areas, associated local and/or temporary reversals of transport direction. A persistent divergence point at Cape Akmenrags (Courland) divides the study area into two almost independent compartments.
6. The qualitative transport patterns (incl. major divergence and convergence areas) are invariant with respect to the choice of the model, interpretation of the wave data and reasonable variations in grain size. The best match with historical estimates is obtained when the root mean square wave height is used to characterise the wave energy at breaking and the significant wave height is used to evaluate the group speed at breaking.
7. The Curonian Spit is in an almost perfect equilibrium shape under the existing wave climate. A rotation of the wave approach direction leads to an almost linear increase in net transport from its present almost zero value. A rotation $>10^\circ$ results in complete disappearance of convergence points of sediment transport along the spit and apparently in substantial coastal damage.
8. The established main structural properties of alongshore sediment transport for the eastern Baltic Sea were verified against the relevant historical evidence. The nearshore geological composition shows evident similarities with the variability of simulated sediment transport and its spatial variations. An acceptable match was found between the location of major convergence areas and the geological structure of the seabed to a distance of a few kilometres from the waterline. The match is less evident for divergence areas.

Recommendations for further work

The presented material suggests that many core features of coastal evolution can be revealed from spatial variations in wave-driven alongshore transport. This encourages performing similar analysis of the structural features of alongshore sediment transport for the entire pool of sedimentary coasts of the Baltic Sea. In the light of the presented results it is natural to evaluate the properties of wave-driven coastal processes based on directional wave information. Doing so allows establishing in a straightforward manner the divergence and convergence points of sediment flux. These points reflect the most intense erosion and accumulation areas and are crucial for coastal management. It is important to identify for each substantial sedimentary compartment the long-term patterns and variations in these points, sub-compartments and reversals of sediment flux.

It is natural to perform a first approximation of such an analysis based on the assumption implicitly employed in this thesis, namely, that the coastal evolution is largely governed by multivariate statistics of wave properties for each coastal segment. This assertion is not necessarily true for coastal segments that are sensitive to the sequence of different wave events. Also, variations in water level may substantially contribute to the coastal evolution. It is thus advisable to link the temporal course of wave properties with the time series of water level for more realistic calculations of the functioning and vulnerability of the Baltic Sea coasts. Similar simulations should be performed with an improved spatial resolution (~1 nautical mile) for more exact identification of the relocation range of the most persistent points of divergence and convergence and associated reversals. Higher-resolution simulations might be performed for the Gulf of Riga, with a side goal of establishing potential changes in the predominant wind directions and the reasons for the mismatch of the temporal course of net transport in the Gulf of Riga and in the Baltic Proper.

A further research subject is to resolve the discussed problems for the main scenarios for the future wind climates; to make sure whether some convergence or divergence points may be lost in some future scenarios, equivalently, whether some coastal segments may become unstable, with serious management implications. A key goal of the structural stability analysis of the coasts in likely future climates is establishing the limits of climate change that still keep the existing major patterns of alongshore transport. Another important challenge is to detect strongly unstable coastal sections where a large part of wave energy arrives at an angle $>45^\circ$ with respect to the coastline and where rapid excitation of sand spits is possible. The long-term course of the overall bulk and net transport along the entire eastern Baltic Sea coast should be analysed in the context of possible changes in wave approach directions. It is probably necessary to create an ensemble of simulations of alongshore transport using different wave data in the contemporary wave climate as the existing wave data are highly controversial (Nikolkina et al., 2014). Finally, a core challenge is the conversion of the outcome of this thesis into supporting material for decision-making in coastal management.

Bibliography

- Alexandersson H., Tuomenvirta H., Schmith T., Iden K. 2000. Trends of storms in NW Europe derived from an updated pressure data set. *Climate Research*, 14, 71–73.
- Ashton A., Murray A., Arnault O. 2001. Formation of coastline features by large-scale instabilities induced by high-angle waves. *Nature*, 414(6861), 296–300.
- BACC Author Team. 2008. *Assessment of Climate Change for the Baltic Sea Basin*. Heidelberg et al.: Springer, 473 pp.
- Birkemeier W. A. 1985. Field data on seaward limit of profile change. *Journal of Waterway, Port, Coastal and Ocean Engineering*, 111, 598–602.
- Bitinas A., Aleksa P., Damušytė A., Gulbinskas S., Jarmalavičius D., Kuzavinis M., Minkevičius V., Pupienis D., Trimonis E., Šečkus R., Žaromskis R., Žilinskas G. 2004. *Geological Atlas of Lithuanian Baltic Sea Coast*. Vilnius: Lithuanian Geological Survey, 94 pp.
- Bottom Sediments of the Gulf of Riga*. 1996. Riga: Geological Survey of Latvia, 53 pp.
- Broman B., Hammarklint T., Rannat K., Soomere T., Valdmann A. 2006. Trends and extremes of wave fields in the north-eastern part of the Baltic Proper. *Oceanologia*, 48(S), 165–184.
- Bruun P. 1962. Sea level rise as a cause of erosion. *Journal of the Waterways and Harbors Division–ASCE*, 88, 117–133.
- Carter R. W. G. 2002. *Coastal Environments*. 8th ed., Amsterdam: Academic Press, 617 pp.
- Clemmensen L., Pye K., Murray A., Heinemeier J. 2001. Sedimentology, stratigraphy and landscape evolution of a Holocene coastal dune system, Lodbjerg, NW Jutland, Denmark. *Sedimentology*, 48, 3–27.
- Dailidienė I., Davulienė L., Stankevičius A., Myrberg K. 2006. Sea level variability at the Lithuanian coast of the Baltic Sea. *Boreal Environment Research*, 11, 109–121.
- Dailidienė I., Tilickis B., Stankevicius A. 2004. General peculiarities of long-term fluctuations of the Baltic Sea and the Curonian Lagoon water level in the region of Lithuania. *Environmental Research, Engineering and Management*, 4(30), 3–10.
- Dalrymple R. A., Eubanks R. A., Birkemeier W. A. 1977. Wave-induced circulation in shallow basins. *Journal of the Waterways, Ports, Coastal and Ocean Division–ASCE* 103, 117–135.
- Dean R. G. 1991. Equilibrium beach profiles: characteristics and applications. *Journal of Coastal Research*, 7, 53–84.
- Dean R. G., Dalrymple R. A. 1991. *Water Wave Mechanics for Engineers and Scientists*. Portland: World Scientific, 368 pp.
- Dean R., Dalrymple R. 2002. *Coastal Processes with Engineering Applications*. Cambridge: Cambridge University Press, 475 pp.

- Deng J. 2013. *Modelling of Coastal Morphogenesis – Past and Future Projection (Examples from the Southern Baltic Sea)*. PhD thesis. Szczecin: University of Szczecin, 180 pp.
- Deng J., Zhang W., Harff J., Schneider R., Dudzińska-Nowak J., Terefenko P., Giza A., Furmańczyk K. 2014. A numerical approach for approximating the historical morphology of wave-dominated coasts – A case study of the the Pomeranian Bight, southern Baltic Sea. *Geomorphology*, 204(1), 425–443.
- Didenkulova I., Soomere T., Pindsoo K., Suuroja S. 2013. On the occurrence of non-reflecting cross-shore profiles along Estonian coasts of the Baltic Sea. *Estonian Journal of Engineering*, 19(2), 110–123.
- Eberhards G. 2003. *The Sea Coast of Latvia (Morphology. Structure. Coastal Processes. Risk Zones. Forecast. Coastal Protection and Monitoring)*. Riga: University of Latvia, 292 pp. (in Latvian).
- Eberhards G., Lapinskis J. 2008. *Processes on the Latvian Coast of the Baltic Sea. Atlas*. Riga: University of Latvia, 64 pp.
- Eberhards G., Grīne I., Lapinskis J., Purgalis I., Saltupe B., Torklere A. 2009. Changes in Latvia's seacoast (1935–2007). *Baltica*, 22(1), 11–22.
- Eberhards G., Lapinskis J., Saltupe B. 2006. Hurricane Erwin 2005 coastal erosion in Latvia. *Baltica* 19(1), 10–19.
- Eelsalu M., Org M., Soomere T. 2014. Visually observed wave climate in the Gulf of Riga. In *6th IEEE/OES Baltic Symposium Measuring and Modeling of Multi-Scale Interactions in the Marine Environment*, 26–29 May 2014, Tallinn, Estonia; IEEE Conference Publications.
- Ekman M. 2009. *The Changing Level of the Baltic Sea During 300 Years: A Clue to Understanding the Earth*. Åland Islands: Summer Institute for Historical Geophysics, 155 pp.
- Fredsøe J., Deigaard R. 1992. *Mechanics of Coastal Sediment Transport*. Advanced Series on Ocean Engineering: Volume 3. World Scientific, 392 pp.
- Furmańczyk K. K., Dudzińska-Nowak J. 2009. Effects of extreme storm on coastline changes: a South Baltic example. *Journal of Coastal Research*, Special Issue 56, 1637–1640.
- Furmańczyk K. K., Dudzińska-Nowak J., Furmańczyk K. A., Paplińska-Swerpel B., Brzezowska N. 2011. Dune erosion as a result of the significant storms at the western Polish coast (Dziwnow Spit example). *Journal of Coastal Research*, Special Issue 64, 756–759.
- Furmańczyk K. K., Dudzińska-Nowak J., Furmańczyk K. A., Paplińska-Swerpel B., Brzezowska N. 2012. Critical storm thresholds for the generation of significant dune erosion at Dziwnow Spit, Poland. *Geomorphology*, 143–144, 62–68.
- Gilbert C. (ed.) 2008. *State of the Coast of the South-East Baltic: an Indicators-Based Approach to Evaluating Sustainable Development in the Coastal Zone of the South East Baltic Sea*. Gdansk: Drukarnia WL, 160 pp.

- Gudelis V. 1967. The morphogenetic types of Baltic Sea coasts. *Baltica*, 3, 123–145 (in Russian).
- Gudelis V., Kirlyš V., Močiekienė S. 1977. Littoral drift regime and dynamics along the eastern coast of the Baltic Sea in the off-shore zone of the Curonian Spit according to the data of 1956–1974. *Transactions of the Lithuanian Academy of Sciences*, B 4(101), 123–128 (in Russian).
- Hallermeier R. J. 1977. *Calculating a Yearly Limit Depth to the Active Beach Profile*. Vicksburg: U.S. Army Engineer Waterways Experiment Station, Coastal Engineering Research Center. Technical Paper TP 77–9.
- Hallermeier R. J. 1981. A profile zonation for seasonal sand beaches from wave climate. *Coastal Engineering*, 4, 253–277.
- Hanson H., Larson M. 2008. Implications of extreme waves and water levels in the southern Baltic Sea. *Journal of Hydraulic Research*, 46(2), 292–302.
- Hanson H., Brampton A., Capobianco M., Dette H., Hamm L., Laustrup C., Lechuga A., Spanhoff R. 2002. Beach nourishment projects, practices, and objectives – a European overview. *Coastal Engineering*, 47, 81–111.
- Harff J., Meyer M. 2011. Coastlines of the Baltic Sea – zones of competition between geological processes and a changing climate: Examples from the southern Baltic. In J. Harff, S. Björck, P. Hoth, eds., *The Baltic Sea Basin*. Berlin, Heidelberg: Springer, 149–164.
- Harff J., Björck S., Hoth P. (eds.) 2011. *The Baltic Sea Basin*. Berlin, Heidelberg: Springer, 449 pp.
- Hoffmann G., Lampe R. 2007. Sediment budget calculation to estimate Holocene coastal changes on the southwest Baltic Sea (Germany). *Marine Geology*, 243, 143–156.
- Holton J. R., Hakim G. J. 2012. *An Introduction to Dynamic Meteorology*, 5th ed., Academic Press, 552 pp.
- Houston J. R. 1996. Simplified Dean's method for beach-fill design. *Journal of Waterway, Port, Coastal and Ocean Engineering–ASCE*, 122, 143–146.
- Jaagus J. 2009. Long-term changes in frequencies of wind directions on the western coast of Estonia. In A. Kont, H. Tõnisson, eds., *Climate Change Impact on Estonian Coasts*. Tallinn: Institute of Ecology, Tallinn University, 11–24 (in Estonian).
- Jaagus J., Kull A. 2011. Changes in surface wind directions in Estonia during 1966–2008 and their relationships with large-scale atmospheric circulation. *Estonian Journal of Earth Sciences*, 60, 220–231.
- Jarmalavičius D., Žilinskas G., Pupienis D. 2013. Observation on the interplay of sea level rise and the coastal dynamics of the Curonian Spit, Lithuania. *Geologija*, 55(2), 50–61.
- Johansson M., Boman H., Kahma K., Launiainen J. 2001. Trends in sea level variability in the Baltic Sea. *Boreal Environment Research*, 6, 159–179.
- Johansson M., Pellikka H., Kahma K., Ruosteenoja K. 2014. Global sea level rise scenarios adapted to the Finnish coast. *Journal of Marine Systems*, 129, 35–46.

- Kalniņa L., Dreimanis A., Mūrniece S. 2000. Palynology and lithostratigraphy of Late Elsterian to Early Saalian aquatic sediments in the Ziemeļu–Jūrkalne area, western Latvia. *Quaternary International*, 68–71, 87–109.
- Kartau K., Soomere T., Tõnisson H. 2011. Quantification of sediment loss from semi-sheltered beaches: a case study for Valgerand Beach, Pärnu Bay, the Baltic Sea. *Journal of Coastal Research*, Special Issue 64, 100–104.
- Kask A., Soomere T., Healy T. R., Delpeche N. 2009. Rapid estimates of sediment loss for “almost equilibrium” beaches. *Journal of Coastal Research*, Special Issue 56, 971–975.
- Keevallik S., Soomere T. 2010. Towards quantifying variations in wind parameters across the Gulf of Finland. *Estonian Journal of Earth Sciences*, 59(4), 288–297.
- Kelpšaitē L., Dailidienē I., Soomere T. 2011. Changes in wave dynamics at the south-eastern coast of the Baltic Proper during 1993–2008. *Boreal Environment Research*, 16, 220–232.
- Kelpšaitē L., Herrmann H., Soomere T. 2008. Wave regime differences along the eastern coast of the Baltic Proper. *Proceedings of the Estonian Academy of Sciences*, 57, 225–231.
- Kelpšaitē L., Parnell K. E., Soomere T. 2009. Energy pollution: the relative influence of wind-wave and vessel-wake energy in Tallinn Bay, the Baltic Sea. *Journal of Coastal Research*, Special Issue 56, 812–816.
- Kench P. S., Parnell K. E., Brander R. W. 2009. Monsoonally influenced circulation around coral reef islands and seasonal dynamics of reef island shorelines. *Marine Geology*, 266(1–4), 91–108.
- Kit E., Pelinovsky E. 1998. Dynamical models for cross-shore transport and equilibrium bottom profiles. *Journal of Waterway, Port, Coastal, and Ocean Engineering–ASCE*, 124, 138–146.
- Knaps R. 1938. Prüfung der Formel von prof. Munch-Petersen über Materialwanderung an der lettischen Küste. In *VI Baltische Hydrologische Konferenz, Bericht*. Berlin, 60–103 (in German).
- Knaps R. 1966. Sediment transport near the coasts of the Eastern Baltic. In *Development of Sea Shores Under the Conditions of Oscillations of the Earth's Crust*. Tallinn: Valgus, 21–29 (in Russian).
- Knaps R. 1982. Effects of shoreline unevenness on sediment drift along the shore. *Baltica*, 7, 195–202 (in Russian).
- Knauss J. 2005. *Introduction to Physical Oceanography*. Long Grove: Waveland Press, 320 pp.
- Komar P. D., Gaughan M. K. 1972. Airy wave theory and breaker wave height prediction. In *Proceedings of the 13th Conference on Coastal Engineering*, 10–14 July 1972, Vancouver. New York: ASCE, 405–418.
- Komar P. D., William G. 1994. The analysis of exponential beach profiles. *Journal of Coastal Research*, 10, 59–69.

- Komen G., Cavaleri L., Donelan M., Hasselmann K., Hasselmann S., Janssen P. A. E. M. 1994. *Dynamics and Modelling of Ocean Waves*. Cambridge: Cambridge University Press, 556 pp.
- Kraus N. C. 1992. Engineering approaches to cross-shore sediment processes. In *(Proc. Short Course On) Design and Reliability of Coastal Structures* (Lamberti A., ed.), *Attached to 23rd International Conference on Coastal Engineering*. Venice, 175–209.
- Lapinskis J. 2010. *Dynamics of the Kurzeme Coast of the Baltic Proper*. PhD thesis. Riga: University of Latvia, 111 pp. (in Latvian).
- Lehmann A., Getzlaff K., Harlaß J. 2011. Detailed assessment of climate variability in the Baltic Sea area for the period 1958 to 2009. *Climate Research*, 46, 185–196.
- Lehmann A., Hinrichsen H.-H., Getzlaff K. 2014. Identifying potentially high risk areas for environmental pollution in the Baltic Sea. *Boreal Environment Research*, 19, 140–152.
- Leppäranta M., Myrberg K. 2009. *Physical Oceanography of the Baltic Sea*. Chichester: Praxis Publishing, 378 pp.
- Longuet-Higgins M. S., Stewart R. W. 1964. Radiation stresses in water waves: a physical discussion with applications. *Deep-Sea Research*, 11, 529–562.
- Massel S. R. 1989. *Hydrodynamics of Coastal Zones*. Amsterdam: Elsevier, 336 pp.
- Meyer M., Harff J., Gogina M., Barthel A. 2008. Coastline changes of the Darss-Zingst Peninsula – A modelling approach. *Journal of Marine Systems*, 74, S147–S154.
- Mėžinė J., Zemlys P., Gulbinskas S. 2013. A coupled model of wave-driven erosion for the Palanga Beach, Lithuania. *Baltica*, 26(2), 169–176.
- Munch-Petersen T. 1936. Über Materialwanderung an Meeresküsten. In *V Hydrologische Konferenz der Baltischen Staaten*. Helsinki, 67 (in German).
- Myrberg K., Ryabchenko V., Isaev A., Vankevich R., Andrejev O., Bendtsen J., Erichsen A., Funkquist L., Inkala A., Neelov I., Rasmus K., Medina R. M., Raudsepp U., Passenko J., Söderkvist J., Sokolov A., Kuosa H., Anderson T. R., Lehmann A., Skogen M. D. 2010. Validation of threedimensional hydrodynamic models in the Gulf of Finland based on a statistical analysis of a six-model ensemble. *Boreal Environment Research*, 15, 453–479.
- Nikolkina I., Soomere T., Räämet A. 2014. Multidecadal ensemble hindcast of wave fields in the Baltic Sea. In *6th IEEE/OES Baltic Symposium Measuring and Modeling of Multi-Scale Interactions in the Marine Environment, May 26–29, Tallinn Estonia*; IEEE Conference Publications.
- Orviku K., Jaagus J., Kont A., Ratas U., Rivis R. 2003. Increasing activity of coastal processes associated with climate change in Estonia. *Journal of Coastal Research*, 19, 364–375.

- Pranzini E., Williams A. 2013. *Coastal Erosion and Protection in Europe*. Abingdon-New York: Routledge, Taylor and Francis, 457 pp.
- Pruszek Z. 2004. Polish coast – two cases of human impact. *Baltica*, 17(1), 34–40.
- Räämet A. 2010. *Spatio-Temporal Variability of the Baltic Sea Wave Fields*. PhD thesis. Tallinn: TUT Press, 169 pp.
- Räämet A., Soomere T. 2010. The wave climate and its seasonal variability in the northeastern Baltic Sea. *Estonian Journal of Earth Sciences*, 59(1), 100–113.
- Räämet A., Soomere T. 2011. Spatial variations in the wave climate change in the Baltic Sea. *Journal of Coastal Research*, Special Issue 64, 240–244.
- Räämet A., Soomere T., Zaitseva-Pärnaste I. 2010. Variations in extreme wave heights and wave directions in the north-eastern Baltic Sea. *Proceedings of the Estonian Academy of Sciences*, 59(2), 182–192.
- Räämet A., Suursaar Ü., Kullas T., Soomere T. 2009. Reconsidering uncertainties of wave conditions in the coastal areas of the northern Baltic Sea. *Journal of Coastal Research*, Special Issue 56, 257–261.
- Ranasinghe R., McLoughlin R., Short A., Symonds G. 2004. The Southern Oscillation Index, wave climate, and beach rotation. *Marine Geology*, 204, 273–287.
- Reimann T., Tsukamoto S., Harff J., Osadczuk K., Frechen M. 2011. Reconstruction of Holocene coastal foredune progradation using luminescence dating – An example from the Świna barrier (southern Baltic Sea, NW Poland). *Geomorphology*, 132(1–2), 1–16.
- Robertson W., Zhang K., Finkl C. W., Whitman D. 2008. Hydrodynamic and geologic influence of event-dependent depth of closure along the South Florida Atlantic coast. *Marine Geology*, 252, 156–165.
- Roland A., Ardhuin F. 2014. On the developments of spectral wave models: numerics and parameterizations for the coastal ocean. *Ocean Dynamics*, 64(6), 833–846.
- Rosentau A., Meyer M., Harff J., Dietrich R., Richter A. 2007. Relative sea level change in the Baltic Sea since the Littorina transgression. *Zeitschrift für Geologische Wissenschaften*, 35, 3–16.
- Ryabchuk D., Leont'yev I., Sergeev A., Nesterova E., Sukhacheva L., Zhamoida V. 2011. The morphology of sand spits and the genesis of longshore sand waves on the coast of the eastern Gulf of Finland. *Baltica*, 24(1), 13–24.
- Saks T., Kalvāns A., Zelčs V. 2007. Structure and micromorphology of glacial and non-glacial deposits in coastal bluffs at Sensala, Western Latvia. *Baltica*, 20, 19–27.
- Schmager G., Fröhle P., Schrader D., Weisse R., Müller-Navarra S. 2008. Sea State, Tides. In R. Feistel, G. Nausch, N. Wasmund, eds., *State and Evolution of the Baltic Sea, 1952–2005: A Detailed 50-Year Survey of Meteorology and Climate, Physics, Chemistry, Biology, and Marine Environment*. Hoboken: Wiley, 143–198.

- Schwarzer K., Diesing M., Larson M., Niedermeyer R., Schumacher W., Furmanczyk K. 2003. Coastline evolution at different time scales – examples from the Pomeranian Bight, southern Baltic Sea. *Marine Geology*, 194, 79–101.
- Sepp M., Jaagus J. 2011. Changes in the activity and tracks of Arctic cyclones. *Climatic Change*, 105, 577–595.
- Sooäär J., Jaagus J. 2007. Long-term variability and changes in the sea ice regime in the Baltic Sea near the Estonian coast. *Proceedings of the Estonian Academy of Sciences. Engineering*, 13(3), 189–200.
- Sepp M., Post P., Jaagus J. 2005. Long-term changes in the frequency of cyclones and their trajectories in Central and Northern Europe. *Nordic Hydrology*, 36(4–5), 297–309.
- Soomere T. 2005. Wind wave statistics in Tallinn Bay. *Boreal Environment Research*, 10, 103–118.
- Soomere T. 2008. Extremes and decadal variations of the northern Baltic Sea wave conditions. In E. Pelinovsky, C. Kharif, eds., *Extreme Ocean Waves*. Dordrecht, London: Springer, 139–157.
- Soomere T. 2013. Extending the observed Baltic Sea wave climate back to the 1940s. *Journal of Coastal Research*, Special Issue 65(2), 1969–1974.
- Soomere T., Healy T. 2011. On the Dynamics of “Almost Equilibrium” Beaches in Semi-sheltered Bays Along the Southern Coast of the Gulf of Finland. In J. Harff, S. Björck, P. Hoth, eds., *The Baltic Sea Basin*. Berlin, Heidelberg: Springer, 255–280.
- Soomere T., Keevallik S. 2001. Anisotropy of moderate and strong winds in the Baltic Proper. *Proceedings of the Estonian Academy of Sciences, Engineering*, 7, 35–49.
- Soomere T., Räämet A. 2011. Spatial patterns of the wave climate in the Baltic Proper and the Gulf of Finland. *Oceanologia*, 53(1-TI), 335–371.
- Soomere T., Räämet A. 2014. Decadal changes in the Baltic Sea wave heights. *Journal of Marine Systems*, 129, 86–95.
- Soomere T., Zaitseva I. 2007. Estimates of wave climate in the northern Baltic Proper derived from visual wave observations at Vislandi. *Proceedings of the Estonian Academy of Sciences. Engineering*, 13(1), 48–64.
- Soomere T., Kask A., Kask J., Healy T. 2008. Modelling of wave climate and sediment transport patterns at a tideless embayed beach, Pirita Beach, Estonia. *Journal of Marine Systems*, 74(S), S133–S146.
- Soomere T., Pindsoo K., Bishop S. R., Käär A., Valdmann A. 2013. Mapping wave set-up near a complex geometric urban coastline. *Natural Hazards and Earth System Sciences*, 13(11), 3049–3061.
- Soomere T., Weisse R., Behrens A. 2012. Wave climate in the Arkona Basin, the Baltic Sea. *Ocean Science*, 8, 287–300.
- Soomere T., Zaitseva-Pärnaste I., Räämet A., Kurennoy D. 2010. Spatio-temporal variations of wavefields in the Gulf of Finland. *Fundamental and Applied Hydrophysics*, 4(10), 90–101 (in Russian).

- Suursaar Ü. 2010. Waves, currents and sea level variations along the Letipea–Sillamäe coastal section of the southern Gulf of Finland. *Oceanologia*, 52 (3), 391–416.
- Suursaar Ü., Sooäär J. 2007. Decadal variations in mean and extreme sea level values along the Estonian coast of the Baltic Sea. *Tellus A*, 59, 249–260.
- Suursaar Ü., Jaagus J., Kont A., Ravis R., Tõnisson H. 2008. Field observations on hydrodynamic and coastal geomorphic processes off Harilaid Peninsula (Baltic Sea) in winter and spring 2006–2007. *Estuarine, Coastal and Shelf Science*, 80(1), 31–41.
- Tõnisson H., Orviku K., Lapinskis J., Gulbinskas S. 2013. The Baltic States: Estonia, Latvia and Lithuania. In E. Pranzini, A. Williams, eds., *Coastal Erosion and Protection in Europe*. Abingdon-New York: Routledge, Taylor and Francis, 47–80.
- Tõnisson H., Suursaar Ü., Orviku K., Jaagus J., Kont A., Willis D., Ravis R. 2011. Changes in coastal processes in relation to changes in large-scale atmospheric circulation, wave parameters and sea levels in Estonia. *Journal of Coastal Research*, Special Issue 64, 701–705.
- Tuomi L., Kahma K., Pettersson H. 2011. Wave hindcast statistics in the seasonally ice-covered Baltic Sea. *Boreal Environment Research*, 16, 451–472.
- Tuomi L., Pettersson H., Fortelius C., Tikka K., Björkqvist J.-V., Kahma K. K. 2014. Wave modelling in archipelagos. *Coastal Engineering*, 83, 205–220.
- Tuomi L., Pettersson H., Kahma K. 1999. Preliminary results from the WAM wave model forced by the mesoscale EUR-HIRLAM atmospheric model. *MERI – Report Series of the Finnish Institute of Marine Research*, 40, 19–23.
- Zaitseva-Pärnaste I., Soomere T., Tribštok O. 2011. Spatial variations in the wave climate change in the eastern part of the Baltic Sea. *Journal of Coastal Research*, Special Issue 64, 195–199.
- Zaitseva-Pärnaste I., Suursaar Ü., Kullas T., Lapimaa S., Soomere T. 2009. Seasonal and long-term variations of wave conditions in the northern Baltic Sea. *Journal of Coastal Research*, Special Issue 56, 277–281.
- Zeidler R. 1997. Climate change vulnerability and response strategies for the coastal zone of Poland. *Climatic Change*, 36, 151–173.
- Zeidler R. B., Wróblewski A., Miętus M., Dziadziuszko Z., Cyberski J. 1995. Wind, wave, and storm surge regime at the Polish Coast: Past, Present and Future. *Journal of Coastal Research*, Special Issue 22, 33–55.
- Zemlys P., Fröhle P., Davulienė L., Gulbinskas S. 2007. Nearshore evolution model for Palanga area: feasibility study of beach erosion management. *Geologija*, 57, 45–54.
- Zhamoida V., Ryabchuk D., Kropatchev Y., Kurennoy D., Boldyrev V., Sivkov V. 2009. Recent sedimentation processes in the coastal zone of the Curonian Spit (Kaliningrad region, Baltic Sea). *Zeitschrift der Deutschen Gesellschaft für Geowissenschaften*, 160(2), 143–157.
- Zhang W., Deng J., Harff J., Schneider R., Dudzinska-Nowak J. 2013. A coupled modeling scheme for longshore sediment transport of wave-dominated

- coasts – A case study from the southern Baltic Sea. *Coastal Engineering*, 72, 39–55.
- Zhang W., Harff J., Schneider R., Wu C. 2010. Development of a modelling methodology for simulation of long-term morphological evolution of the southern Baltic coast. *Ocean Dynamics*, 60(5), 1085–1114.
- Zhang W., Harff J., Schneider R., Meyer M., Zorita E., Hünicke B. 2014. Holocene morphogenesis at the southern Baltic Sea: Simulation of multi-scale processes and their interactions for the Darss–Zingst peninsula. *Journal of Marine Systems*, 129, 4–18.
- Žaromskis R., Gulbinskas S. 2010. Main patterns of coastal zone development of the Curonian Spit, Lithuania. *Baltica*, 23(2), 149–156.
- Ulsts V. 1998. *Latvian Coastal Zone of the Baltic Sea*. Riga: State Geological Survey of Latvia, 96 pp. (in Latvian).
- Ulsts V., Bulgakova J. 1998. *General Lithological and Geomorphological Map of Latvian Shore Zone – Baltic Sea and Gulf of Riga*. Riga: State Geological Survey of Latvia.
- [USACE] 2002. *Coastal Engineering Manual*. Manual No. 1110-2-1100. US Army Corps of Engineers (USACE), Washington, DC, Chapter III-3-2, (CD).
- van Rijn L. 1998. *Principles of Coastal morphology*. Amsterdam: AQUA Publications, 680 pp.
- Viška M., Soomere T. 2013. Long-term variations of simulated sediment transport along the eastern Baltic Sea coast as a possible indicator of climate change. In M. Reckermann, S. Köppen, eds., *7th Study Conference on BALTEX*, 10–14 June 2013, Borgholm, Island of Öland, Sweden; Conference Proceedings: Geesthacht, Germany. International BALTEX Secretariat Publication, 53, 99–100.
- Weisse R., von Storch H. 2010. *Marine Climate and Climate Change. Storms, Wind Waves and Storm Surges*. Berlin, Heidelberg: Springer, 220 pp.
- Woodroffe C. D. 2002. *Coasts: Form, Process and Evolution*. Cambridge: Cambridge University Press, 623 pp.

Acknowledgements

I would like to express my deepest gratitude to my supervisor academician Tarmo Soomere for guidance, patience, support and advise during my PhD study.

I am grateful to Dr. Andrus Räämet and Dr. Irina Nikolkina for providing modelled wave data.

I would like to thank my colleagues from the Laboratory of Wave Engineering for welcoming me in the team, particularly Maris Eelsalu, Andrea Giudici, Katri Pindsoo and Artem Rodin for supporting my research with useful advice.

Last but not least, I would like to thank my family for their patience and understanding during my work. My sincerest thanks go to my fiancé Viesturs Aigars for encouragement and enthusiasm that kept me going. Without his endless support this dissertation would not have been possible.

* * *

The studies were supported by DoRa scholarship funded from the European Social Fund.

Abstract

The thesis addresses the basic functional and structural properties of wave-driven alongshore sediment transport in the longest interconnected system of sedimentary coasts in the Baltic Sea basin. The area studied is located at the eastern coast of this water body and ranges from the Sambian (Samland) Peninsula to Pärnu Bay. This coastal region evolves under sediment deficit and contains extensive sections of erodible sediments that are vulnerable to strong waves and high water levels.

The wave-driven impact on this coastal stretch is analysed using the output of a high-resolution wind wave hindcast based on geostrophic winds and the Coastal Engineering Research Centre (CERC) wave energy flux model. Spatial variations in the closure depth of equilibrium beach profiles are established for the entire study area and linked to the zones of predominant erosion and accumulation. The largest closure depths (~7 m) are found at the NW coast of Latvia at the Western Estonian archipelago. A modified express formula is developed for the closure depth evaluation based on the annual mean significant wave height and accounting for the specific ratio of extreme to average wave heights in the Baltic Sea.

Structural features of alongshore transport are studied based on the net and bulk transport rates. Their values are largest in a short section of the Sambian Peninsula and along the NW Latvian (Courland) coast where net transport is up to 700 000 m³/yr. Transport is much weaker in the Gulf of Riga. It is shown that the classical counter-clockwise pattern of net transport along the eastern Baltic Sea coast contains several persistent divergence and convergence areas. Relatively persistent reversals of the net transport direction are to the south of Cape Akmenrags (Courland) and to the south of Klaipėda.

A persistent divergence point at Cape Akmenrags serves as a natural barrier for sediment transport and divides the study area into two almost independent compartments. The established qualitative transport patterns are almost insensitive to the implementation of wave transformation in the nearshore, interpretation of the wave data and reasonable variations in grain size. The best match with historical estimates of transport rates is obtained when the root mean square wave height is used to characterise the wave energy at breaking and the significant wave height is used to evaluate the group speed at breaking.

It is shown that the Curonian Spit is in an almost perfect equilibrium shape under the existing wave climate. Major changes in the course of coastal processes along this spit involve an increase in the total bulk sediment transport by about 20% during the simulated time interval. Net transport increased in the 1970s–1980s but decreased at the same rate from the mid-1990s onwards, suggesting a systematic change in wave direction. A rotation of the wave approach direction leads to an almost linear increase in net transport from its present almost zero value. The location of the most persistent convergence and divergence areas of net transport acceptably matches the granulometric composition of the nearshore seabed up to a few kilometres from the shoreline. The match is less evident for divergence areas.

Resümee

Doktoritöös käsitletakse tuulelainete poolt tekitatud pikiranda transpordi kvantitatiivseid ja struktuurseid omadusi. Vaatluse all on Läänemere pikim omavahel seotud setterandade süsteem piki mere idarannikut Sambia (Samlandi) poolsaarest Pärnu laheni. Seal domineerib setete defitsiit, mistõttu ulatuslikud rannalõigud kannatavad erosiooni all ning on tundlikud kõrgete lainete ja veeseisude suhtes.

Lainetuse mõju intensiivsuse ja lainete poolt käivitatud settetranspordi omaduste ning ruumilise muutlikkuse analüüs tugineb kogu Läänemere lainekliima kõrglahutusega numbrilisele rekonstruktsioonile 1970–2007. Lainetuse arvutustes on kasutatud modifitseeritud geostroofilisi tuuli. On arvutatud tasakaaluliste rannaprofiilide sulgemissügavuse ruumilised muutused uuringuala ja Eesti ranniku jaoks. Saadud hinnangud on seotud peamiste erosiooni ja akumulatsioonipiirkondadega Läti avatud rannikul. Suurimad sulgemissügavused (~7 m) on Läti looderannikul ja Lääne-Eesti saarte rannavetes. On tuletatud Läänemere ekstreemsete ja keskmiste lainekõrguste spetsiifilist suhet arvestav ekspressmeetod, mis võimaldab hinnata sulgemissügavust aasta keskmise lainekõrguse alusel.

Settetransporti käsitletakse Coastal Engineering Research Centre (CERC) lähemise raames: transport on võrdeline randa saabuva laineenergia vooga. Pikiranda transpordi struktuuri on analüüsitud tuginedes neto- ja brutotranspordi ruumilistele mustritele. Neto- ja brutotransport on suurimad Sambia poolsaare lääneosas ja Läti looderannikul, kus netotransport on kuni 700 000 m³ aastas. Transport on märksa tagasihoidlikum Liivi lahes. On näidatud, et klassikaline peamiselt vastupäeva liikuv settevool sisaldab mitmeid püsivaid divergentsi- ja konvergentsipiirkondi. Settetransport on sageli päripäeva Akmenragši neemest lõunas Kuramaa rannikul ja Klaipėdast lõunas Kura sääre rannikul.

Püsiv netotranspordi divergentsipiirkond Akmenragši neeme lähistel kujutab endast nähtamatut looduslikku tõket ning jagab kogu vaadeldava piirkonna kaheks peaaegu sõltumatuks setete süsteemiks. Kirjeldatud kvalitatiivsed jooned on invariantse mudeli selliste kesksete parameetrite suhtes nagu lainete refraktsiooni ja teravdumise arvutusskeem, lainekõrguse interpreteerimine CERC mudelis ja setete terasuuruse muutumine mõistlikes piirides. Parima kokkulangevuse vaatlusandmetega annab selline mudeli versioon, kus lainekõrgust murdlainete vööndi merepoolsel serval kirjeldab ruutkeskmise lainekõrgus, kuid murduma hakkavate lainete rühmakiirus arvutatakse olulise lainekõrguse kaudu.

On näidatud, et Kura sääre on praktiliselt perfektselt kohandunud olemasoleva lainekliimaga. Kuigi brutotransport piki Kura säärt suurenes ligikaudu 20% võrra aastail 1970–2007, kasvas netotransport vaid 1970ndail ja 1980ndail ning kahanes alates 1990ndate keskpaigast. Selline muutuste muster viitab lainelevi suuna süstemaatilistele muutustele. Saabuvate lainete suuna muutumine isegi vaid mõne kraadi võrra muudaks oluliselt Kura sääre praegust tasakaalu. Kõige püsivamate divergentsi- ja konvergentsipiirkondade lähistel paikneva merepõhja setete terasuurus peegeldab põhiosas demonstreeritud transpordi mustrit. Vastavus on suhteliselt hea konvergentsialade jaoks ning tagasihoidlikum divergentsialade puhul.

Appendix A: Curriculum Vitae

1. Personal data

Name	Maija Viška
Date and place of birth	23.07.1984, Riga, Latvia
Address	Akadeemia tee 21, 12618 Tallinn
Phone	(+372) 5592 8916; (+371) 2998 7112
e-mail	maija@ioc.ee

2. Education

Educational institution	Graduation year	Education (field of study / degree)
University of Latvia	2008	Environmental Science / MSc
University of Latvia	2006	Environmental Science / BSc

3. Language competence/skills

Language	Level
Latvian	native language
English	fluent
Russian	average
Estonian	basic skills

4. Special courses and further training

Period	Educational or other organisation
Mar. 2013	International Winter School <i>Remote sensing of Baltic Sea ice</i> , Finland
Sep. 2011	BalticWay Summer School <i>Preventive methods for coastal protection</i> , Lithuania
Jun. 2011 – Sep. 2011	Scientific visit to Institute of Coastal Research, Helmholtz-Zentrum Geesthacht, Germany, supported by the Alexander von Humboldt Foundation

5. Professional employment

Period	Organisation	Position
Sep. 2010 – to date	Institute of Cybernetics, Tallinn University of Technology	Technician
Dec. 2008 – to date	Latvian Institute of Aquatic Ecology	Scientific assistant

Aug. 2006 – Sep. 2008	Metrum Ltd	Photogrammetric engineer
Jan. 2006 – Jul. 2006	Intelligent systems Ltd	Cartographer

6. Research activity

6.1. Publications

Articles indexed by the Web of Science database (1.1):

Soomere T., **Viška M.** 2014. Simulated wave-driven sediment transport along the eastern coast of the Baltic Sea. *Journal of Marine Systems*, 129, 96–105.

Viška M., Soomere T. 2013. Simulated and observed reversals of wave-driven alongshore sediment transport at the eastern Baltic Sea coast. *Baltica*, 26(2), 145–156.

Peer-reviewed articles in other international journals (1.2) and collections (3.1):

Soomere T., **Viška M.**, Eelsalu M. 2013. Spatial variations of wave loads and closure depths along the coast of the eastern Baltic Sea. *Estonian Journal of Engineering*, 19(2), 93–109.

Soomere T., **Viška M.**, Lapinskis J., Räämet A. 2011. Linking wave loads with the intensity of erosion along the coasts of Latvia. *Estonian Journal of Engineering*, 17(4), 359–374.

Viška M., Soomere T. 2012. Hindcast of sediment flow along the Curonian Spit under different wave climates. In: *IEEE/OES Baltic 2012 International Symposium*, 8–11 May 2012, Klaipėda, Lithuania; Proceedings. IEEE, 7 pp.

Диденкулова И., **Вишка М.**, Куренной Д. 2011. Изменчивость берегового профиля под совместным воздействием судовых и ветровых волн. *Фундаментальная и прикладная гидрофизика: сб. науч. трудов. Санкт-Петербург: Наука*, 66–78.

Articles published in other conference proceedings (3.4):

Viška M., Soomere T. 2014. On sensitivity of wave-driven alongshore sediment transport patterns with respect to model setup and sediment properties. In: Witkowski A., Harff J., Reckermann M. (Eds.) *2nd International Conference on Climate Change - The environmental and socio-economic response in the Southern Baltic region*, 12–15 May 2014, Szczecin, Poland; Conference Proceedings: Geesthacht, Germany. International Baltic Earth Secretariat Publication, 2, 94–95.

Viška M., Soomere T. 2013. Long-term variations of simulated sediment transport along the eastern Baltic Sea coast as a possible indicator of climate change. In: Reckermann M., Köppen S. (Eds.) *7th Study Conference on BALTEX*, 10–14 June 2013, Borgholm, Island of Öland, Sweden; Conference Proceedings: Geesthacht, Germany. International BALTEX Secretariat Publication, 53, 99–100.

Abstracts of conference presentations (5.2):

Soomere T., **Viška M.** 2013. Retrieving the signal of climate change from numerically simulated sediment transport along the eastern Baltic Sea coast. In:

Chmiel M. et al. (Eds.) *Under the sea: Archaeology and palaeolandscapes. Final conference of COST Action TD0902 Submerged Prehistoric Archaeology and Landscapes of the Continental Shelf*, 23–27 September 2013, Szczecin, Poland; Book of Abstracts: Szczecin, 93.

Viška M., Soomere T. 2013. Spatio-temporal variations in the wave-driven alongshore sediment transport along the eastern Baltic Sea coast. In: *BSSC 9th Baltic Sea Science Congress: New Horizons for Baltic Sea Science*, 26–30 August 2013, Klaipeda, Lithuania, Abstract Book: Klaipeda. Coastal Research and Planning Institute of Klaipeda University (KU CORPI), 267.

Eelsalu M., Soomere T., **Viška M.** 2013. Closure depth along the north-eastern coast of the Baltic Sea. In: *9th Baltic Sea Science Congress: New Horizons for Baltic Sea Science*, 26–30 August 2013, Klaipeda, Lithuania, Abstract Book: Klaipeda. Coastal Research and Planning Institute of Klaipeda University (KU CORPI), 165.

Viška M., Soomere T. 2012. Hindcast of sediment flow along the Curonian Spit under different wave climates. In: *2012 IEEE/OES Baltic International Symposium "Ocean: Past, Present and Future. Climate Change Research, Ocean Observation & Advances Technologies for Regional Sustainability"*, 8–11 May 2012, Klaipeda, Lithuania, Presentation Abstracts: Klaipeda. Baltic Valley, 36.

Viška M., Soomere T. 2012. Decadal variations of simulated sediment transport patterns along the eastern coast of the Baltic Sea. In: Virtasalo J., Vallius H. (Eds.) *11th Colloquium on Baltic Sea Marine Geology*, 19–21 September 2012, Helsinki, Finland; Abstract Book, Espoo. Juvenes Print, Geological Survey of Finland; Guide 57, 98–99.

Soomere T., **Viška M.** 2012. On the stability of Curonian spit under changing wave climate. In: Virtasalo J., Vallius H. (Eds.) *11th Colloquium on Baltic Sea Marine Geology*, 19–21 September, Helsinki, Finland; Abstract Book, Espoo. Juvenes Print, Geological Survey of Finland; Guide 57, 76–77.

Viška M., Soomere T., Kartau K., Räämet A. 2011. Patterns of sediment transport along the Latvian and Estonian coasts along the Baltic Proper and the Gulf of Riga. In: *BSSC 8th Baltic Sea Science Congress*, 22–26 August 2011, St. Petersburg, Russia; Book of Abstract: St. Petersburg. Russian State Hydrometeorological University (RSHU), 91.

Didenkulova I., **Viška M.**, Kurennoy D. 2011. Change of the beach profile under the joint effect of ship and wind waves. In: *8th Baltic Sea Science Congress*, 22–26 August 2011, St. Petersburg, Russia, Book of Abstract: St. Petersburg. Russian State Hydrometeorological University (RSHU), 95.

Kartau K., **Viška M.**, Soomere T. 2011. Decadal variations of wave-driven sediment transport processes in the Gulf of Riga. In: *8th Baltic Sea Science Congress*, 22–26 August 2011, St. Petersburg, Russia, Book of Abstract: St. Petersburg. Russian State Hydrometeorological University (RSHU), 99.

Appendix B: Elulookirjeldus

1. Isikuandmed

Ees- ja perekonnanimi Maija Viška
Sünniaeg ja -koht 23.07.1984, Riia, Läti
Aadress Akadeemia tee 21, 12618 Tallinn
Telefon (+372) 5592 8916
 (+371) 2998 7112
e-mail maija@ioc.ee

2. Hariduskäik

Õppeasutus	Lõpetamise aeg	Haridus (eriala / kraad)
Läti Ülikool	2008	Keskkonnateaduste magister
Läti Ülikool	2006	Keskkonnateaduste bakalaureus

3. Keelteoskus

Keel	Tase
inglise	kõrgtase
läti	emakeel
vene	kesktase
eesti	algtase

4. Täiendõpe

Õppimise aeg	Täiendõppe läbiviija nimetus
Märts 2013	Rahvusvaheline suvekool <i>Remote sensing of Baltic Sea ice</i> , Tvärminne, Soome
September 2011	BalticWay suvekool <i>Preventiivsed meetodid keskkonna kaitseks</i> , Klaipeda, Leedu
Juuni–september 2011	Kolmekuuline visiit Ranniku-uuringute Instituuti Helmholtz-Zentrum Geesthacht, Saksamaa

5. Teenistuskäik

Töötamise aeg	Tööandja nimetus	Ametikoht
Sept. 2010 – tänaseni	Tallinna Tehnikaülikool, Küberneetika Instituut	tehnik
Dets. 2008 – tänaseni	Läti Veekogude Ökoloogia Instituut	teaduslik assistent
Aug. 2006 – sept. 2008	Metrum Ltd.	insener
Jan. 2007 – juuli 2006	Intelligent systems Ltd	kartograaf

6. Teadustegevus

Avaldatud teadusartiklite ja konverentsiteeside ning peetud konverentsiettekannete loetelu on toodud ingliskeelse CV juures.

Paper I

Soomere T., **Viška M.**, Lapinskis J., Räämet A. 2011. Linking wave loads with the intensity of erosion along the coasts of Latvia. *Estonian Journal of Engineering*, 17(4), 359–374.

Linking wave loads with the intensity of erosion along the coasts of Latvia

Tarmo Soomere^a, Maija Viška^a, Jānis Lapinskis^b and Andrus Räämet^a

^a Institute of Cybernetics at Tallinn University of Technology, Akadeemia tee 21, 12618 Tallinn, Estonia; soomere@cs.ioc.ee

^b Laboratory of Sea Coasts, University of Latvia, Alberta Str. 10, Riga, Latvia

Received 7 October 2011, in revised form 4 November 2011

Abstract. Numerically estimated wave properties and the associated closure depth along the eastern Baltic Sea coast from the Sambian (Samland) Peninsula up to Pärnu Bay in the Gulf of Riga are compared against the existing data about accumulation and erosion. Typical values of the closure depth are about 5–6 m (maximum 6.58 m) at the open Baltic Sea coast, 3–4 m in the Gulf of Riga and 2–2.5 m in semi-sheltered smaller bays. The areas of intense accumulation or erosion (especially the areas of their high variability) generally coincide with the sections, hosting high wave intensity, except for a few locations, dominated by anthropogenic impact. It is shown that the longshore variations in wave intensity (or closure depth) can be used to identify the location of major accumulation and erosion domains. The sections that host the largest change in the wave height along the coast reveal erosion or accumulation features, depending on the predominant wave approach direction.

Key words: coastal processes, wave modelling, erosion, accumulation, longshore transport, Baltic Sea, Gulf of Riga.

1. INTRODUCTION

The coasts of the Baltic Sea develop in relatively rare conditions of this almost non-tidal water body of relatively large dimensions [1], highly intermittent wave regime [2] and complicated patterns of vertical motions of the crust [3]. While large sections of the Baltic Sea coasts are bedrock-based and extremely stable, the southern and eastern coasts of this basin mostly consist of relatively soft and easily erodable sediment. Almost all these coasts suffer from sediment deficit [4–8] and are thus very sensitive to large hydrodynamic loads [7,9] and

especially to the sea level rise [10]. Their evolution typically has a step-like manner and episodes of rapid changes take place when high waves occur simultaneously with high water level [7,9].

Several studies have highlighted rapid erosion events at certain locations of the Baltic Sea in the recent past [7–9]. These events are usually associated with changes in the wave climate (potentially caused by the changes in cyclonic activity) [11,12] or with the associated changes to the duration of ice cover [7,8]. Some authors [7,13] even suggest that the increasing storminess (expressed as a statistically significant increasing trend of the number of storm days over the last half-century) and extreme storms in 2001–2005 have already caused extensive erosion and alteration of large sections of depositional coasts in the eastern Baltic Sea. The destruction of beaches owing to the more frequent occurrence of high water levels and intense waves, as well as owing to the lengthening of the ice-free period, may have already overridden the stable development of several sections of Baltic Sea coasts [7]. Another stress factor for the coast is a decrease in the time interval between strong storms. This decrease may destroy the normal recovery cycle of natural beaches: a subsequent storm may impact upon an already vulnerable beach profile [13].

The combination of changing storminess with ever increasing anthropogenic loads and rapid industrial development of several coastal sections has created an acute need for detailed studies into the reaction of the Baltic Sea coasts to the changing driving forces. The primary factor, shaping these almost tideless coasts, is the nearshore wave climate. Recent studies have established the basic properties of the Baltic Sea wave climatology for the open sea areas and for selected coastal sites using instrumental measurements [14], historical wave observations [15,16] and numerical simulations [17–19]. These studies have been linked with the properties of and potential changes to the coastal processes for limited coastal sections [13,20,21].

The existing studies into the evolution and future of the eastern Baltic Sea coasts have been mostly either descriptive [6–8,22] or focused on various scenarios of the water level rise [3,10,23–25] or on the role of combinations of storm surges and rough seas [4,7,8,26–28]. There are very few attempts to predict the long-term impact of wave-driven coastal processes on the evolution of coastal morphology [29]. For the relatively young eastern Baltic Sea coasts, especially for the comparatively straight sections of the Latvian coast, the basic process should be straightening [22]. For sandy coasts its intensity essentially depends on the magnitude of longshore littoral drift and, therefore, on the wave approach direction. In conditions of sediment deficit, its intensity apparently even more strongly depends on the ability of waves to erode partially protected coastal sections (e.g. formations of till or sandstone that frequently occur along the Lithuanian and Latvian coasts).

In this paper, we make an attempt to link the spatial variability in the long-term wave climate (specifically, the numerically estimated overall intensity of wave-driven coastal processes) in selected parts of the eastern Baltic Sea with the



Fig. 1. Scheme of the study area.

existing data about the long-term rate of coastal accumulation and erosion (that are systematically available along the coast of Latvia). For this purpose, we use the threshold for wave heights that are exceeded during 12 h a year and the closure depth (that also accounts for the wave periods). The study area covers the mostly sandy coastal section from the Sambian Peninsula to Kolka Cape and the south-western and eastern coasts of the Gulf of Riga, including a short section of Estonian coast up to Pärnu Bay (Fig. 1).

The paper is structured as follows. We start from a short overview of the wave and coastal data and a description of the method for the calculation of the closure depth from the wave properties in Section 2. Spatial variations in the wave properties and closure depth are discussed in Section 3. Section 4 is dedicated to the analysis of interrelations of closure depth and erosion and accumulation rates. The basic message from the analysis is formulated in Section 5.

2. METHOD AND DATA

The basic characteristic of the intensity of coastal processes is the amount of wave energy that reaches a particular coastal section during a selected time interval [30]. To a first approximation, the long-term average scalar wave energy flux directed to the shore can be used to quantify wave impact on the coast. This

quantity (which is decisive in studies into wave energy potential and properly characterizes the intensity of processes on coasts fully consisting of finer sediment), however, only partially and in many cases unsatisfactorily characterizes the processes on the coast. The reason is that the water level along the open parts of the eastern Baltic Sea coasts normally varies insignificantly and waves usually impact on a relatively narrow nearshore band [31]. The processes within this band are in many cases in approximate equilibrium [31] and do not reveal substantial changes to the local sediment budget even in areas of intense sediment transit. As mentioned above, events of rapid coastal evolution occur here infrequently, during events when rough seas are accompanied with high water level and when waves act on unprotected sediment or are powerful enough to erode sections that are partially protected (e.g. by boulders or by a cobble-pebble pavement).

Therefore, it is natural to associate the intensity of the straightening of the coasts (and, therefore, the major erosion and accumulation events) with the impact of the strongest wave storms that usually are accompanied by high water levels. It is not clear beforehand whether one can apply commonly used parameters of wave statistics such as the thresholds for the highest 5% or even 1% of significant wave heights (that are frequently used to estimate long-term changes to extreme wave conditions [18,32]) for this purpose. For example, wave situations that occur with a probability of 1% a year reflect wave storms with a total duration of about 3.5 days a year. Owing to the two-peak structure of the angular distribution of strong winds in the Baltic Proper [33] and large variations in the orientation of the coastal sections in question, a large part of rough seas is not necessarily accompanied with a high water level in the study area.

A more convenient measure to characterize the potential intensity of coastal processes is the threshold $H_{s,0.137}$ for significant wave height that occurs within 12 h a year, equivalently, the threshold for the roughest 0.137% of the wave conditions. The typical duration of the strongest wave storms in the Baltic Sea is close to this time interval. As breaking waves usually contribute to the water level in the nearshore, it is natural to assume that the highest water levels for a particular year generally occur during such storms. Storms, in which this threshold is exceeded, are also thought to maintain the shape of the coastal profile down to so-called closure depth (the largest depth where wind waves effectively keep a fixed-shape profile). This depth not only characterizes the overall intensity of wave impact for a particular coastal section but also serves as a key property of the beach [30,34] and a convenient basis for rapid estimates of sediment loss or gain [19,35,36]. This quantity also implicitly accounts for the wave periods in such storms and thus even better characterizes the impact of storm waves than solely the wave height. Differently from wave properties, the closure depth can be relatively easily measured in field conditions and compared with the theoretical estimates [34].

The data set of coastal monitoring for Latvia, unfortunately, only covers the changes to the shoreline and to the dry coast area. For this reason we employ an alternative estimate for the closure depth h^* based on long-term wave statistics.

The simplest estimates of h^* assume a linear relation between the (annual) average significant wave height H_{sa} and the closure depth (e.g. $h^* \approx 6.75H_{sa}$ [37]), which is not necessarily true in the complicated geometry of the Baltic Sea [20]. In order to account for this peculiarity, we employ a second-order (quadratic or parabolic) approximation to the closure depth [38] that explicitly accounts for the frequency of occurrence of rough wave conditions and the relevant wave period, and that has led to good results for semi-sheltered beaches in Estonia [20]:

$$h^* = 1.75H_{s,0.137} - 57.9 \frac{H_{s,0.137}^2}{gT_s^2}. \quad (1)$$

Here g is acceleration due to gravity and T_s is the typical peak period in such wave conditions. In reality, the closure depth gradually increases as in the course of time extremely strong storms (that are averaged out by using Eq. (1)) may shape the coastal profile to even larger depths [39]. As such storms usually cover the entire Baltic Proper and affect quite long sections of the coast, it is reasonable to assume that their impact leads to a more or less homogeneous increase in h^* along the entire study area. The presence of such a bias would affect the particular values of h^* but would not significantly change the pattern of its alongshore variations and, therefore, the link between the local wave intensity and the rate of erosion or accumulation.

The closure depth was calculated for each nearshore grid cell using numerically simulated wave properties along the eastern Baltic Sea coast. The time series of the significant wave height and peak period were extracted from the long-term simulations of wave fields for 1970–2007 with a temporal resolution of 1 h for the entire Baltic Sea using the third-generation spectral wave model WAM [40] driven by properly adjusted geostrophic winds. The regular rectangular model grid with a resolution of about 3×3 NM extends from $09^\circ 36'$ to $30^\circ 18'E$ and from $53^\circ 57'$ to $65^\circ 51'N$ [17]. The directional wave energy spectrum at each sea point was represented by 24 equally spaced directions. Differently from the standard configuration of the WAM model, an extended frequency range (42 frequencies with an increment of 1.1, up to about 2 Hz or wave periods down to 0.5 s) was used to ensure realistic wave growth rates in low wind conditions after calm situations.

The presence of ice was ignored. Doing so is generally acceptable for the southern part of the coastal section in question but may substantially overestimate the overall wave intensity in the Gulf of Riga. The estimates for the highest waves and for the closure depth, however, are much less affected by the presence of ice during some months. The windiest months are November–December in the northern Baltic Sea [41]. This is even more clearly evident in terms of wind speeds over 13.9 m/s (over 7 m/s on the Beaufort scale [42]). A shift of the most stormy period to January since about 1990 [42] is accompanied with a similar change in the ice-free period. Therefore, the strongest wave storms (that define the closure depth) occur before the ice formation. For the same

reason the highest percentiles of wave conditions and the average wave height over the ice-free period have no correlation with the length of the ice cover even in the Gulf of Finland [⁴³].

The nearshore wave properties (significant wave height H_s and peak period T_s) were commonly extracted for the grid points closest to the shoreline. If, however, the water depth at such points was less than the threshold $H_{s,0.137}$, the next offshore grid point was chosen. Doing so was necessary, for example, for three grid points in the vicinity of the Estonian-Latvian border near Ikla and Ainaži (Fig. 2). In order to account for the potential interannual variability in the wave conditions, we used two methods. Firstly, the closure depth was found as an average of a set of the relevant annual values for each of the 38 years of the simulation period. Secondly, it was estimated directly from the hourly time series of simulated wave heights. The results differed by a few mm.

The intensity of coastal processes is characterized in terms of the long-term rate of coastal erosion or accumulation, extracted from the data obtained from monitoring of coastal geological processes monitoring in Latvia. The monitoring network for this about 497 km long coast was started in 1987–1990, depending

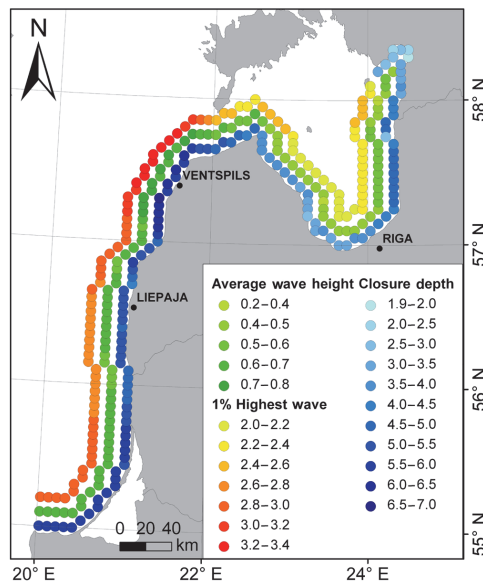


Fig. 2. Longshore variation of the average significant wave height, threshold for the highest 1% of significant wave height and the closure depth (colour scale, m) for wave conditions in 1970–2007. The closure depth is given for the centres of grid cell of the wave model, data from which are used in calculations.

on the particular coastal section. Starting from 1993–1994, the stationary network covers all the coastal area of Latvia [^{22,44}]. The monitoring system consists of two clusters of activities: firstly, the levelling of coastal cross-section profiles (usually from the waterline up to an area well beyond the reach of waves and aeolian transport) and, secondly, regular measurements of the recession of the upper part of the coastal bluff.

The beach and (fore)dune profiles cover the vicinity of the waterline (attached to the long-term mean water level, interpreted here as the zero level in the Baltic height system) and the subaerial transition zone. The latter is interpreted as the part of the shore, which is actively involved in the contemporary coastal processes such as wave- and wind-driven accumulation and erosion, including berms and active aeolian patterns such as foredunes and dunes, if present. The inland border of a profile was determined using the data on the intensity of vertical changes in the coastal terrain. As a rule, the areas in which the vertical changes exceeded 0.01 m/year were included into the data set. The profile length varies between 30 and 200 m, depending on the coastal section. The overall data set – about 400 profiles – is divided into groups of 20–50 that characterize particular coastal districts. The distance between profiles in each group is 200–800 m. The distance between the groups depends on the diversity of the coastal section and is 5–10 km on average. The location of each profile group has been chosen to represent the specific character of the local coastal system, with a goal to characterize as adequately as possible its sediment budget. The levelling is carried out once a year, usually in late summer and autumn when the low summer-season waves have restored the beach that might have been damaged during autumn and winter storms.

The levelling has been used in those coastal sections where the broad beach and the aeolian relief have been developed [⁴⁴]. In several sections the upper part of the coast consists of a narrow beach and a steep bluff or scarp. The sediment balance for such sections was calculated using about 2000 properly grouped scarp retreat stations, which allowed determining the distance between a fixed point inland and the steep coastal bluff and, consequently, the bluff retreat rate. The mapping of the retreating bluff has been done using partly the methodology for the research of coastal erosion in the rivers of Great Britain and Canada [^{45,46}]. The distance has been measured by a tape-line with a field accuracy of 0.1 m. The distance between the individual stations is about 10–50 m, that is, much shorter than the distance between profiles. In essence, the levelling allows for more detailed estimates of the sediment budget (both erosion and accumulation) in a particular coastal section whereas the measurements of the scarp give a picture of non-invertible processes.

The profiles and the results, characterizing the bluff retreat, were used to calculate the overall change to the sediment volume as follows:

$$V_i = \sum_{i=1}^N \frac{Q_i + Q_{i+1}}{2} L_i, \quad (2)$$

where V_i is the total volume in a particular coastal domain between the location of two profiles, $i = 1, \dots, N$, Q_i is the cross-sectional area of a single profile, L_i is the distance between the profiles or scarp retreat stations and the change to the sediment volume of two profiles is given in cubic metres per annum and per metre of the coastline.

3. SPATIAL VARIATIONS IN THE WAVE INTENSITY

The longshore variation in the simulated closure depth (Fig. 2) largely coincides with similar variations in the average significant wave height and the threshold for the 1% of highest wave conditions [47]. Only at some places (for example, near Kolka) it is much better correlated with the long-term average wave height. As expected, to some extent it follows the spatial variations of the long-term threshold for the 5% of highest wave conditions [47]. The relatively large values of the average closure depth are found along the western coast of the Kurzeme Peninsula (about 5.4 m). On average, the calmest is the western coast of the Gulf of Riga where the average closure depth is 3.5 m. The largest values of h^* for single calculation points, up to 6.58 m, are found along the western coast of the Kurzeme Peninsula between latitudes 57° and $57^\circ 30'$. To the south of this area the closure depth decreases to some extent and reaches a local minimum (4.35 m) in the neighbourhood of the border between Latvia and Lithuania. It increases again to values around 5.8 m further south along the Curonian Spit and Sambian Peninsula.

The closure depth is substantially smaller, in the range of 2.8–4.9 m along the western and eastern coasts of the Gulf of Riga, and well below 3 m in the interior of Pärnu Bay [36]. The smallness obviously reflects a relatively low wave intensity in this water body that is connected with the rest of the Baltic Sea via quite narrow and shallow straits. Interestingly, the closure depth reveals considerable variations along the Gulf of Riga, with an average of 3.5 m and a minimum of 2.8 m along its western coast, and clearly large values (4.3 m on average) along the eastern coast. This difference evidently reflects the anisotropic nature of wind fields in this region: the angular distribution of strong winds contains two peaks corresponding to SW and N–NW winds, respectively [33]. There is, in general, a good agreement between the longshore variations of the closure depth and the threshold for the 1% of the highest waves whereas the match of the closure depth and the average wave height is worse. A more detailed discussion of this match is presented below.

4. AREAS OF EROSION AND ACCRETION

It is of direct interest for applications and coastal zone management to see whether the numerically simulated estimates for the closure depth match the areas of intense erosion or accumulation. The relevant comparison is made based on the above-described coastal monitoring data.

A comparison of the spatial variations in the closure depth with the existing data about the rates of erosion and accumulation along the Latvian coast [6] shows that there is a certain general consistency between the two characteristics at large scales. Namely, both the erosion and accumulation rates are systematically larger in sections with large closure depths (equivalently, with a relatively large overall wave impact) (Fig. 3). This feature indicates that the coasts in question are, in general, in a rapid development phase. As substantial cross-shore sediment motion is unlikely here, the coasts are characterized by the motion of substantial amounts of sediment along the coast [22]. The length of eroding coastal sections considerably exceeds that for accumulating sections [6,22] (Figs 3, 4). Only very few sections are close to equilibrium (Fig. 5). For some areas (e.g., most of the eastern coast of the Gulf of Riga) no data exists [6,22].

This consistency is almost fully lost on the level of pointwise comparison of the closure depth with the erosion and accumulation rate (Fig. 4). This feature signifies that the key parameters governing this rate are the local properties of the coast (incl. the orientation of the coastline with respect to the predominant wave approach direction) rather than alongshore changes to the wave intensity.

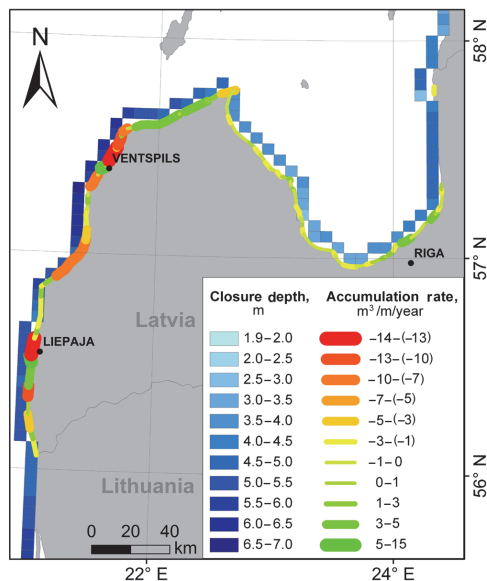


Fig. 3. Comparison of the closure depth for wave conditions in 1970–2007 with the accumulation rate along the Latvian coast for about 1990–2006 [6]. This rate is positive for accumulation areas and negative for erosion areas. There is very little data for the eastern coast of the Gulf of Riga to the north of the latitude 57°20'N.

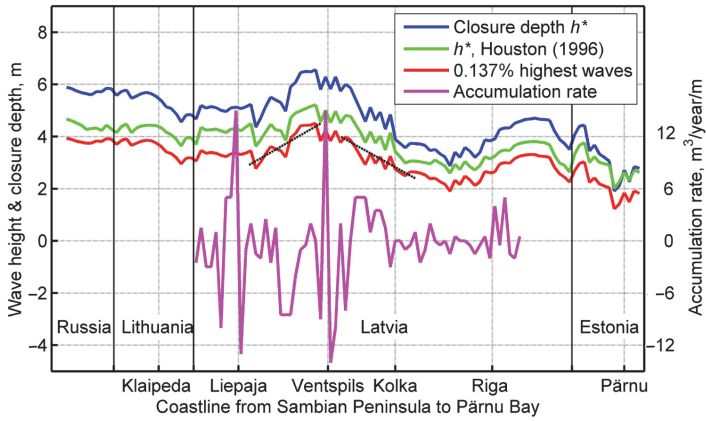


Fig. 4. Spatial variation of the threshold for the highest 0.137% significant wave height, the closure depth calculated from Eq. (1) and from the simplified relation $h^* \approx 6.75H_{sa}$ of Houston (1996) [37] and the erosion (negative values) and accumulation (positive values) rate along the eastern Baltic Sea from 20°E, 55°N on Sambian Peninsula (Fig. 1) up to Pärnu Bay with a step of about 3 NM (5.5 km). Short dashed lines reflect the mean slope of the longshore variation to the highest 0.137% of waves.

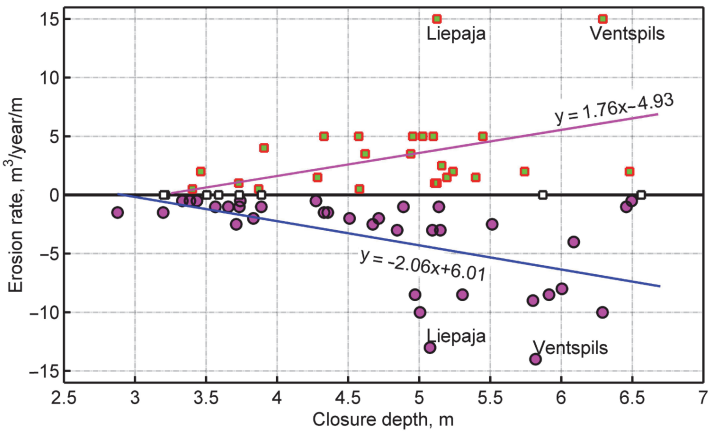


Fig. 5. The dependence of the erosion (magenta circles) and accumulation (green squares) rate on the closure depth along the Latvian coast. White squares correspond to the coastal sections with no changes in the sediment volume. The rates for the vicinity of Liepaja and Ventspils are strongly impacted by the harbour constructions.

The areas with the largest accumulation and erosion rates at calculation points 35–36 and 53–54 (Figs 3, 4) reflect the impact of large harbours at Liepaja and Ventspils. Their quays and breakwaters largely block the natural littoral drift and cause rapid accumulation to the south of these harbours and extensive erosion to the north of the latter. An area of relatively rapid accumulation on the western coast of Kurzeme Peninsula apparently is connected with a considerable change in the orientation of the coastline at 57°35'N and the related change in the approach angle of predominant waves. A similar accumulation to the east of Riga (River Daugava mouth) most likely reflects the river-induced sediment inflow.

There is only one mostly naturally developing longer coastal section in the study area at calculation points 43–51 where erosion predominates. Also, there is only one longer section at points 60–67 along the NW coast of the Kurzeme Peninsula where accumulation predominates. It is remarkable that these sections host the largest average longshore gradients for both the wave height and the closure depth. The section where both these quantities increase over a relatively long distance (between calculation points 44 and 48) is rapidly eroded while there is quite intense accumulation in a section between points 60 and 66. A sensible explanation to this property can be found from a qualitative analysis of the wave approach directions. Namely, waves created by N–NW winds approach the NW coast of the Kurzeme Peninsula almost shore-normal. Therefore, waves approaching from SW mostly govern the longshore transport here and make it move to the NE. As the intensity of waves gradually decreases in the same direction, the littoral flow also decreases. The resulting convergence of littoral flow becomes evident as sediment accumulation. An opposite situation where the wave activity increases along the coast in the direction of the littoral flow occurs at points 43–51. This intensification of wave impact (divergence of the related wave energy flux) becomes evident as a longer eroding section.

The described features are intuitively obvious when the magnitude of the longshore sediment flux is associated with the longshore component of the energy flux model [48]. Remarkably, they become evident here already on the level of longshore variations of the closure depth. In essence, this property means that the location of extensive domains of accumulation and erosion can be extracted already from the nature of longshore changes to the wave heights, provided the predominant wave approach direction is known.

Notice that the linear expression for the closure depth only coincides with the results of Eq. (1) in the interior of Pärnu Bay (Fig. 4). In this region the extreme wave heights are usually damped to some extent due to the joint effect of refraction and wave-bottom interaction, but these factors insignificantly affect the propagation of shorter waves under moderate wind conditions. Generally, the linear expression seems to underestimate the closure depth by about 20%.

There is effectively no correlation between the closure depth and the accumulation or erosion rate along the coastal section in question (Fig. 5). On the other hand, the variability of the erosion or accumulation rate clearly increases with the increase in the closure depth. Analysis of the interrelation of erosion and

closure depth separately for accumulation and erosion areas (Fig. 5) reveals an obvious relationship between the development of the coast and wave activity: the intensity of coastal changes (expressed as either the erosion or accumulation rate), clearly increases with the increase in the wave activity. The relevant correlation coefficients are, however, quite small ($r^2 = 0.29$ between the closure depth and erosion rate; $r^2 = 0.13$ between the closure depth and accumulation rate) and, formally, no statistically significant relationship can be identified. The difference between these coefficients is probably associated with the overall sediment deficit in the considered coastal section. In general, the described properties simply reflect the intuitively obvious fact that the overall intensity of coastal processes increases with the increase in the wave impact. It is also consistent with the observation that both the accumulation and erosion rates show greater changes and amplitudes in Baltic Proper than in the western part of the Gulf of Riga (Fig. 3).

5. DISCUSSION AND CONCLUSIONS

The described results not only confirm the intuitively obvious perception – that the overall intensity of coastal processes directly depends on the available wave energy – but also expand it towards better understanding of the spatial variation of the driving forces shaping the eastern Baltic Sea coasts. This variation, as expected, to large extent follows the similar variation in the threshold for 1% of the highest waves. This threshold (that can be easily extracted from contemporary wave reconstructions) eventually can be used as a basic indicator of the wave impact on coastal processes in this water body (although it usually contains several storm events that are not accompanied by high water level and thus have clearly lower impact on coastal processes compared with the strongest storms).

The numerically estimated closure depth for the coasts of the Baltic Proper considerably exceeds its value for the Gulf of Riga. While the largest average closure depth occurs along the western coast of the Kurzeme Peninsula (about 5.4 m), the calmest is the western coast of the Gulf of Riga where the average closure depth is 3.5 m. These values evidently are characteristic for the Baltic Proper and large sub-basins of the Baltic Sea, respectively, while in smaller semi-sheltered bays such as in Pärnu Bay or near Pirita Beach in Tallinn Bay [20] it typically is in the range from 2 to 2.5 m.

The intensity of coastal processes is usually thought to be a function of wave energy flux, a quantity that also depends on the wave period. The typical wave periods vary insignificantly in the Baltic Proper and reveal almost no temporal variation along its eastern coast [18]. It is, therefore, somewhat unexpected that the closure depth (and thus the intensity of coastal processes) shows noticeable deviations from the threshold $H_{s,0.137}$. An obvious source of these deviations is the potential variation in the water depth in the nearshore: a part of wave energy

may be redistributed and/or damped before it reaches the surf zone. A more subtle reason is the potential difference in peak wave periods, corresponding to very rough seas in different sea areas. While such a difference naturally exists between the Baltic Proper and the Gulf of Riga, recent research (that will be published elsewhere) has shown evidence about systematic difference in the peak periods in strong storms in southern and northern parts of the Baltic Sea. These deviations, therefore, basically signify the complexity of wave processes and their extensive spatio-temporal variations in the Baltic Sea and along its coasts.

The presented estimates are based exclusively on simulated wave heights and periods, and ignore the dependence of the longshore sediment flux on the wave approach direction. The performed analysis suggests that the longshore variations in wave height may still be useful for the approximate determination of the location of major accumulation and erosion domains. Namely, these coastal sections that host the largest average increase in the (average or extreme) wave height (or closure depth) along the coast in the direction of the littoral flow should reveal erosion features. Contrariwise, accumulation is expected to occur in sections where the wave height decreases along the coast in this direction. In other words, the location of extensive domains of accumulation and erosion can be extracted already from the analysis of the wave heights, provided the predominant wave approach direction is known.

The gradual shift in the directional distribution of winds in this area [⁴⁹] that apparently is accompanied by similar changes in the wave directions [²¹] may seriously affect the magnitude of coastal processes in the study area. These potential effects call for more detailed studies of the associated changes in the coastal processes, the identification of major changes in the littoral flow and their consequences to the evolution of the beaches. These aspects may be particularly important for beaches from the Curonian Spit to Kurzeme. Differently from Estonian beaches that are stabilized by the postglacial land uplift to some extent, these beaches of the central Baltic Proper are mostly maintained by littoral drift of sandy sediment from neighbouring coastal sections.

ACKNOWLEDGEMENTS

This study was performed in the framework of the BalticWay project, which is supported by the funding from the European Community's Seventh Framework Programme (FP/2007–2013) under grant agreement No. 217246, made with the joint Baltic Sea research and development programme BONUS. The research was partially supported by the Estonian Science Foundation (grant No. 7413) and targeted financing by the Estonian Ministry of Education and Research (grant SF0140007s11).

REFERENCES

1. Leppäranta, M. and Myrberg, K. *Physical Oceanography of the Baltic Sea*. Springer Praxis, Berlin, Heidelberg, 2009.
2. Soomere, T. Extremes and decadal variations of the northern Baltic Sea wave conditions. In *Extreme Ocean Waves* (Pelinovsky, E. and Kharif, C., eds). Springer, 2008, 139–157.
3. Harff, J., Lemke, W., Lampe, R., Luth, F., Lübke, H., Meyer, M., Tauber, F. and Schmolcke, U. The Baltic Sea coast-A model of interrelations among geosphere, climate, and anthroposphere. In *Coastline Changes: Interrelation of Climate and Geological Processes*. Geological Society of America Special Papers, 2007, **426**, 133–142.
4. Labuz, T. A. The West Pomerania coastal dunes – alert state of their development. *Zeitschrift der Deutschen Gesellschaft für Geowissenschaften*, 2009, **160**, 113–122.
5. Zaromskis, R. and Gulbinskas, S. Main patterns of coastal zone development of the Curonian Spit, Lithuania. *Baltica*, 2010, **23**, 149–156.
6. Eberhards, G. and Lapinskis, J. *Processes on the Latvian Coast of the Baltic Sea*. Atlas. University of Latvia, Riga, 2008.
7. Orviku, K., Jaagus, J., Kont, A., Ratas, U. and Rivis, R. Increasing activity of coastal processes associated with climate change in Estonia. *J. Coast. Res.*, 2003, **19**, 364–375.
8. Ryabchuk, D., Kolesov, A., Chubarenko, B., Spiridonov, M., Kurennoy, D. and Soomere, T. Coastal erosion processes in the eastern Gulf of Finland and their links with geological and hydrometeorological factors. *Boreal Environ. Res.*, 2011, **16** (Suppl. A), 117–137.
9. Eberhards, G., Lapinskis, J. and Saltupe, B. Hurricane Erwin 2005 coastal erosion in Latvia. *Baltica*, 2006, **19**, 10–19.
10. Leont'yev, I. O. Budget of sediments and forecast of long-term coastal changes. *Oceanology*, 2008, **48**, 428–437.
11. Suursaar, Ü., Jaagus, J., Kont, A., Rivis, R. and Tõnisson, H. Field observations on hydrodynamic and coastal geomorphic processes off Harilaid Peninsula (Baltic Sea) in winter and spring 2006–2007. *Estuar. Coast. Shelf Sci.*, 2008, **80**, 31–41.
12. Orviku, K., Suursaar, Ü., Tõnisson, H., Kullas, T., Rivis, R. and Kont, A. Coastal changes in Saaremaa Island, Estonia, caused by winter storms in 1999, 2001, 2005 and 2007. *J. Coast. Res.*, 2009, **25**, (SI 56), 1651–1655.
13. Tõnisson, H., Suursaar, Ü., Orviku, K., Jaagus, J., Kont, A., Willis, D. A. and Rivis, R. Changes in coastal processes in relation to changes in large-scale atmospheric circulation, wave parameters and sea levels in Estonia. *J. Coast. Res.*, 2011, **27**, (SI 64), 701–705.
14. Broman, B., Hammarklint, T., Rannat, K., Soomere, T. and Valdmann, A. Trends and extremes of wave fields in the north-eastern part of the Baltic Proper. *Oceanologia*, 2006, **48** (S), 165–184.
15. Soomere, T. and Zaitseva, I. Estimates of wave climate in the northern Baltic Proper derived from visual wave observations at Vilsandi. *Proc. Estonian Acad. Sci. Eng.*, 2007, **13**, 48–64.
16. Zaitseva-Pärmaste, I., Suursaar, Ü., Kullas, T., Lapimaa, S. and Soomere, T. Seasonal and long-term variations of wave conditions in the northern Baltic Sea. *J. Coast. Res.*, 2009, **25**, (SI 56), 277–281.
17. Räämet, A. and Soomere, T. The wave climate and its seasonal variability in the northeastern Baltic Sea. *Estonian J. Earth Sci.*, 2010, **59**, 100–113.
18. Soomere, T. and Räämet, A. Long-term spatial variations in the Baltic Sea wave fields. *Ocean Sci.*, 2011, **7**, 141–150.
19. Tuomi, L., Kahma, K. K. and Pettersson, H. Wave hindcast statistics in the seasonally ice-covered Baltic Sea. *Boreal Environ. Res.*, 2011, **16**, 1–22.
20. Soomere, T., Kask, A., Kask, J. and Healy, T. R. Modelling of wave climate and sediment transport patterns at a tideless embayed beach, Pirita Beach, Estonia. *J. Marine Syst.*, 2008, **74**, Suppl., S133–S146.

21. Kelpšaitė, L., Dailidienė, I. and Soomere, T. Changes in wave dynamics at the south-eastern coast of the Baltic Proper during 1993–2008. *Boreal Environ. Res.*, 2011, **16** (Suppl. A), 220–232.
22. Eberhards, G., Grīne, I., Lapinskis, J., Purgalis, I., Saltupe, B. and Torklere, A. Changes in Latvia's seacoast (1935–2007). *Baltica*, 2009, **22**, 11–22.
23. Johansson, M. M., Kahma, K. K., Boman, H. and Launiainen, J. Scenarios for sea level on the Finnish coast. *Boreal Environ. Res.*, 2004, **9**, 153–166.
24. Kont, A., Jaagus, J. and Aunap, R. Climate change scenarios and the effect of sea-level rise for Estonia. *Global Planet. Change*, 2003, **36**, 1–15.
25. Pruszek, Z. and Zawadzka, E. Potential implications of sea-level rise for Poland. *J. Coast. Res.*, 2008, **24**, 410–422.
26. Tõnisson, H., Orviku, K., Jaagus, J., Suursaar, Ü., Kont, A. and Rivas, R. Coastal damages on Saaremaa Island, Estonia, caused by the extreme storm and flooding on January 9, 2005. *J. Coast. Res.*, 2008, **24**, 602–614.
27. Suursaar, Ü. and Kullas, T. Decadal changes in wave climate and sea level regime: the main causes of the recent intensification of coastal geomorphic processes along the coasts of Western Estonia? In *Coastal Processes*. WIT Transactions on Ecology and the Environment, 2009, **126**, 105–116.
28. Hanson, H. and Larson, M. Implications of extreme waves and water levels in the southern Baltic Sea. *J. Hydraul. Res.*, 2009, **46**, 292–302.
29. Zhang, W. Y., Harff, J., Schneider, R. and Wu, C. Y. Development of a modelling methodology for simulation of long-term morphological evolution of the southern Baltic coast. *Ocean Dynam.*, 2010, **60**, 1085–1114.
30. Dean, R. G. and Dalrymple, R. A. *Coastal Processes with Engineering Applications*. Cambridge University Press, 2002.
31. Soomere, T. and Healy, T. R. On the dynamics of “almost equilibrium” beaches in semi-sheltered bays along the southern coast of the Gulf of Finland. In *The Baltic Sea Basin* (Harff, J., Björck, S. and Hoth, P., eds). Springer, Heidelberg, 2011, 255–279.
32. Suursaar, Ü. Waves, currents and sea level variations along the Letipea-Sillamäe coastal section of the southern Gulf of Finland. *Oceanologia*, 2010, **52**, 391–416.
33. Soomere, T. and Keevallik, S. Anisotropy of moderate and strong winds in the Baltic Proper. *Proc. Estonian Acad. Sci. Eng.*, 2001, **7**, 35–49.
34. Dean, R. G. Equilibrium beach profiles: characteristics and applications. *J. Coast. Res.*, 1991, **7**, 53–84.
35. Kask, A., Soomere, T., Healy, T. R. and Delpeche, N. Rapid estimates of sediment loss for “almost equilibrium” beaches. *J. Coast. Res.*, 2009, **25** (SI 56), 971–975.
36. Kartau, K., Soomere, T. and Tõnisson, H. Quantification of sediment loss from semi-sheltered beaches: a case study for Valgerand Beach, Pärnu Bay, the Baltic Sea. *J. Coast. Res.*, 2011, **27** (SI 64), 100–104.
37. Houston, J. R. Simplified Dean's method for beach-fill design. *J. Waterw. Port. C. Div.*, 1996, **122**, 143–146.
38. Birkemeier, W. A. Field data on seaward limit of profile change. *J. Waterw. Port. C. Div.*, 1985, **111**, 598–602.
39. Nicholls, R. J., Birkemeier, W. A. and Hallermeier, R. J. Application of the depth of closure concept. In *Proc. 25th International Conference on Coastal Engineering*. ASCE, Orlando, 1996, 3874–3887.
40. Komen, G. J., Cavaleri, L., Donelan, M., Hasselmann, K., Hasselmann, S. and Janssen, P. A. E. M. *Dynamics and Modelling of Ocean Waves*. Cambridge University Press, 1994.
41. Mietus, M. (coordinator). *The Climate of the Baltic Sea Basin*. Marine meteorology and related oceanographic activities. Report No. 41. World Meteorological Organization, Geneva, 1998.
42. Lehmann, A., Getzlaff, K. and Harlass, J. Detailed assessment of climate variability in the Baltic Sea area for the period 1958 to 2009. *Clim. Res.*, 2011, **46**, 185–196.

43. Soomere, T., Zaitseva-Pärnaste, I. and Räämet, A. Variations in wave conditions in Estonian coastal waters from weekly to decadal scales. *Boreal Environ. Res.*, 2011, **16** (Suppl. A), 175–190.
44. Eberhards, G. and Saltupe, B. Coastal processes monitoring in Latvia – experiment and practice. *Folia Geographica VII*. Geographical Society of Latvia, 1999, 1–10.
45. Hooke, J. M. Magnitude and distribution of rates of river bank. *J. Hydrol.*, 1979, **42**, 39–62.
46. Hudson, H. R. A field technique to directly measure river bank erosion. *Canadian J. Earth Sci.*, 1982, **19**, 381–383.
47. Räämet, A., Soomere, T. and Zaitseva-Pärnaste, I. Variations in extreme wave heights and wave directions in the north-eastern Baltic Sea. *Proc. Estonian Acad. Sci.*, 2010, **59**, 182–192.
48. Kamphuis, J. W. *Introduction to Coastal Engineering and Management*. World Scientific, Singapore, New Jersey, 2000.
49. Jaagus, J. Long-term changes in frequencies of wind directions on the western coast of Estonia. *Publications, Institute of Ecology at Tallinn University*, 2009, **11**, 11–24.

Lainekoormuse ja rannikuprotsesside intensiivsuse seosest Läänemere idarannikul

Tarmo Soomere, Maija Viška, Jānis Lapinskis ja Andrus Räämet

On analüüsitud sulgemissügavuse muutumist ja selle seost ranniku kulutuse ning kuhjumise kohta teadaolevate andmetega piki Läänemere idarannikut Sambia poolsaarest Riia lahe kirdeosani. Pinnalainete parameetrid on leitud WAM-mudeli abil lahutusvõimega 3 meremiili aastate 1970–2007 jaoks. Sulgemissügavus on Läänemere avaosa rannikul tavaliselt 5–6 m (maksimaalselt 6,58 m), Riia lahe rannikul 3–4 m ja Pärnu lahes 2–2,5 m. Kiire kuhjumine ja kulutus toimub üldiselt rannalõikudes, milles lainete intensiivsus ning sulgemissügavus on suhteliselt suured, välja arvatud vähesed inimtegevuse poolt oluliselt mõjutatud piirkonnad. On näidatud, et lainetuse intensiivsuse või sulgemissügavuse pikiranda gradiendi alusel saab määratleda peamisi kulutus- ja kuhjepiirkondi: lainekõrguse kasv piki settevoolu suunda viitab kulutusele ning selle kahanemine kuhjumisele.

Paper II

Soomere T., **Viška M.**, Eelsalu M. 2013. Spatial variations of wave loads and closure depths along the coast of the eastern Baltic Sea. *Estonian Journal of Engineering*, 19(2), 93–109.

Spatial variations of wave loads and closure depths along the coast of the eastern Baltic Sea

Tarmo Soomere^{a,b}, Maija Viška^a and Maris Eelsalu^a

^a Institute of Cybernetics at Tallinn University of Technology, Akadeemia tee 21, 12618 Tallinn, Estonia; soomere@cs.ioc.ee

^b Estonian Academy of Sciences, Kohtu 6, 10130 Tallinn, Estonia

Received 18 April 2013, in revised form 9 May 2013

Abstract. The closure depth is a key parameter in coastal processes as it characterizes the overall wave intensity in the nearshore and indicates the water depth down to which storm waves are able to maintain a universal shape of equilibrium coastal profiles. The properties and alongshore variations of the closure depth for the eastern Baltic Sea coast are evaluated at a coarse resolution (5.5 km) and for the vicinity of Tallinn Bay at a higher resolution (0.5 km). The study is based on numerical simulations of wind-generated wave fields. It is shown that, due to the small contribution of remote swell in the Baltic Sea, the typical ratio of wave heights in strongest storms and average wave heights is about 5.5, which departs considerably from that of open ocean coasts. A modification of the formula for the approximate calculation of the closure depth from the average wave height is derived. The estimates are based on four methods: from the wave heights of the strongest storms, from average wave heights based on a linear approximation, and using two versions of a second-order approximation. The greatest closure depth of up to 7.25 m was found to occur along the coast of the Baltic Proper near Hiiumaa, Saaremaa and the Kurzeme Peninsula. These areas also experience the largest wave intensities. Along other parts of the Baltic Proper coast the closure depth is typically 5–6 m, whereas in the Gulf of Riga and along the southern coast of the Gulf of Finland it is usually in the range of 3–4 m.

Key words: equilibrium beach profile, closure depth, wave modelling, Baltic Sea, Gulf of Finland, Gulf of Riga.

1. INTRODUCTION

A fascinating property of sedimentary coasts lining ocean basins, marginal seas and large lakes is that the basic shapes of their cross-sections (called coastal profiles below) are essentially identical, in spite of the fact that they are exposed to extremely different wave conditions and may have different sediment properties [1]. This uniform shape is continuously maintained by ocean swells

and wind-generated waves that give rise to persistent, so-called equilibrium beach profiles [2]. The existence of such a persistent shape was the core assumption of, for example, the Bruun's Rule [3]. This rule explains the relatively large changes in the location of the shoreline produced even by small changes in the mean sea level. Originally it predicted shoreline retreat, resulting from chronic sea level rise by applying the equilibrium profile concept. The Bruun's rule was subsequently extended to more complex cases such as variable heights of the berm [4], landward migration of barrier beaches [5], and the presence of offshore bars [6].

A breakthrough in the understanding of the appearance of such profiles was achieved about three decades ago when it became evident that equilibrium profiles could be described in terms of a simple power law

$$h(y) = Ay^b, \quad (1)$$

that expresses the water depth $h(y)$ along such profiles in terms of the distance y from the waterline whereas the profile scale factor A depends on the grain size of the bottom sediments. The exponent b can vary over quite a large range. The most widely used version of Eq. (1) is the Dean's equilibrium beach profile (EBP) with $b = 2/3$ that corresponds to the uniform wave energy dissipation per unit water volume in the surf zone [1]. For Dutch dune profiles, for example, $b = 0.78$ provides a better fit [7], and a range of $b = 0.73 - 1.1$ appears to be more suitable for Israeli beaches [8]. Values of the exponent b larger than 1 correspond to convex profiles and are relatively rare. For example, for Pikakari Beach in Tallinn Bay, the Baltic Sea, "non-reflecting" beach profiles with $b = 4/3$ may exist under the combined effect of irregular wind-wave fields and regular groups of longer-period waves, generated by high-speed ferries [9]. Although the power laws, characterizing coastal profiles, are not able to replicate many details of realistic nearshore profiles such as the presence of sand bars, the techniques that rely on this concept are extremely useful for solving a number of practical and theoretical problems of beach evolution and coastal zone management [1].

Another basic parameter of an EBP is the closure depth h_c , which is defined as the maximum depth at which breaking waves effectively adjust the nearshore profile [10,11]. Seawards of the closure depth, storm waves may occasionally move bottom sediments but are not able to maintain a specific profile.

Most applications of profiles, described by Eq. (1), assume that $b = 2/3$. The width W and the mean slope $\tan \theta = h_c/W$ of the profile are used as additional parameters [12] for applications of the Bruun's Rule along any particular coastal section to characterize the potential effects of sea-level change as well as for the application of the inverse Bruun's Rule to determine the amount of sediment, eroded or accreted in the course of the shoreline changes [13,14]. The parameters can be easily determined if two other fundamental quantities are known: the typical grain size (that determines parameter A) and the closure depth h_c . The mean slope of an EBP is simply the ratio of the closure depth h_c to the width W

of the profile. The width is usually treated as the distance from the coast to the point at which the water depth corresponds to the closure depth. It does not include the subaerial part of the beach profile. For the profile, described by Eq. (1), the width and the mean slope of the beach can be expressed as

$$W = (h_c/A)^{3/2}, \quad \tan \theta = h_c/W = \frac{A^{3/2}}{h_c^{1/2}}. \quad (2)$$

All the listed parameters may vary along a beach and should therefore be treated as functions $A(x)$, $h_c(x)$ and $W(x)$ of the distance x along the shoreline.

A basic simplification, provided by the theory of EBPs, is that the parameter A and the closure depth are considered to be almost independent of each other and that they can be derived from completely different arguments. While parameter A depends on the typical grain size of the sediment, the closure depth is mostly a function of the local wave climate. The determination of the former is thus possible via granulometric analysis of bottom sediment, whereas the latter can be estimated either from repeated profiling or approximated from numerical modelling.

The closure depth h_c is generally defined as the depth where repeated survey profiles pinch out to a common line [15]. The instantaneous coastal profiles along macrotidal open ocean coasts frequently differ from the theoretical power law because the location of the surf zone may vary substantially over a tidal cycle and the width of the EBP is not always uniquely defined. Also, very severe storms tend to extend the EBP towards the offshore [16]. Additional problems arise in the case of subsiding coasts where the EBP may be masked by flooded coastal features, and in the case of Arctic coasts where the presence of ice may modify the evolution of a coast [17]. For these reasons several authors have suggested to evaluate the closure depth on the basis of certain properties of the local wave climate. The underlying assumption is that the closure depth basically depends on the roughest wave conditions that persist for a reasonable time [11]. Another frequently used assumption is that the ratio of certain measures, characterizing the roughest waves, and the mean wave height varies insignificantly [16], which is correct, for example, for wave systems having a Pierson–Moskowitz spectrum.

The simplest but still widely used (essentially linear) approximation for the closure depth, based on these assumptions, is [16,18,19]

$$h_c \cong q_1 H_{0.137\%} \cong q_2 H_{\text{mean}}, \quad (3)$$

where H_{mean} is the annual mean significant wave height, $H_{0.137\%}$ is the threshold of the significant wave height that occurs for 12 h a year (that is, the wave height that is exceeded with a probability of 0.137%; originally it was meant to represent a storm in which such wave heights persisted for 12 subsequent hours), $q_1 = 1.5$ [16] (often a value of $q_1 = 1.57$ is used [11,12]) and $q_2 = 6.75$.

Equation (3) assumes a specific constant ratio of the annual mean H_{mean} and a higher percentile of the significant wave height, namely $H_{0.137\%} \cong 4.5 H_{\text{mean}}$ [19].

This ratio is established for wave fields with a Pierson–Moskowitz spectrum. It matches the observed wave statistics along the US coasts [19] but does not necessarily hold for semi-enclosed seas where remote swell is almost absent and the wave height is mainly governed by local storms. A specific feature of the wave climate in the Baltic Sea is that the average wave conditions are relatively mild but very rough seas may occur episodically in long-lasting severe storms [20–22]. Waves generated by such storms are much higher than one would expect from the mean wave conditions. The main reason for this feature is that the complicated geometry of the Baltic Sea and its subbasins rarely matches perfectly with the wind field in terms of favourable wave generation. Moreover, the strongest storms in the Baltic Proper and in the Gulf of Finland approach from directions from which winds in general are rather infrequent [23,24]. As a result, simplified estimates, based on the annual mean wave parameters, may lead to considerable errors in estimations of the closure depth [25,26].

The purpose of the present paper is twofold. Firstly, the ratio of extreme and average wave properties along the eastern Baltic Sea coast are analysed with the aim of establishing the extension of spatial variations of this ratio and to explore the possibilities of using simplified methods for the evaluation of the closure depth along this coast. For the eastern Baltic Sea coast as a whole this analysis is performed at a relatively coarse resolution (about 5.5 km). A much finer resolution (about 500 m) is applied for the analysis of the situation in the vicinity of Tallinn Bay, which is a typical example of the deeply indented bays, characterizing the southern coast of the Gulf of Finland. Secondly, typical values for the closure depths of the sections of the eastern Baltic Sea coast, exposed to the predominant waves, are determined to establish the range of variation of the relevant wave loads. This depth not only serves as a key property of the beach profile but also directly characterizes the overall intensity of wave impact for a particular coastal section (and thus the potential of coastal erosion) and implicitly indicates the relative level of wave energy resources for the different coastal stretches. For this purpose, adequate values of the parameter q_2 in Eq. (3) are estimated for the Baltic Sea conditions and the closure depth is calculated from second-order approximations, in this way expanding the observations, previously described in [26], to the entire coastline of Estonia. This analysis is also performed at a higher resolution for an urban area around Tallinn which is characterized by a complex coastal geometry.

2. PHYSICAL SETTING AND COMPUTATIONAL METHODS

Starting at the Sambian Peninsula in the southeast (20°E, 55°N), the study area covers the entire nearshore of Lithuania, Latvia and Estonia with about 5.5 km long coastal sections. The study area extends to the eastern part of the Gulf of Finland, to Kurgolovo in Russia (28°E, 59°51'N). The coastline of the Baltic Proper and the Gulf of Finland (about 950 km) is divided into 154 sections and the nearshore of the Gulf of Riga (about 450 km) into 68 sections. Wave

statistics and closure depths were calculated for each of these 222 sections (Fig. 1). In order to avoid the potential distortion of wave fields in nearshore areas with complex geometry, the grid cells of the wave model (see below) were chosen at water depths ranging from 7 to 48 m, with an average of 18 m. This restriction means that several grid cells used in this study differ from the cells used in a previous analysis [14,26]. The differences are minor along the coast of Lithuania and the Baltic Proper coast of Latvia but substantial in the eastern part of the Gulf of Riga where Pärnu Bay was omitted in our analysis.

The dataset, generated for these nearshore cells, adequately characterizes the wave loads along relatively straight coastlines such as the coast of Lithuania and Latvia, and part of Estonian coast in the Gulf of Riga as well as Narva Bay. Along the rest of the Estonian coast the situation, regarding wave properties, is essentially different. Straight shoreline sections typically occur here at spatial scales of about 1 km and less and can therefore not be resolved by the 5.5 km spatial resolution. As an example, the variability of wave loads and closure



Fig. 1. Grid cells of the wave model used to evaluate nearshore wave statistics and closure depths for relatively straight coastal sections and at locations open to the offshore. The box indicates the detailed study area in the vicinity of Tallinn Bay.

depths were calculated at a higher resolution for the wave-dominated micro-tidal coastline of Tallinn Bay and adjacent small bays (Fig. 2), where straight coastal stretches extend for only a few hundreds of metres and up to a kilometre or two, but at larger scales are interrupted by peninsulas and headlands, separating individual bays that are deeply indented into the mainland. This is a relatively young coast, which is still actively in the process of straightening [27]. In addition, the bays open into a variety of directions so that they are individually impacted by storms approaching from different angles.

To match the difference in resolution of the regional eastern Baltic Sea coast and the Tallinn Bay area, two sets of numerically simulated wave data were generated. For the analysis of wave loads and closure depths along the former coastline, hourly time series were extracted from numerical simulations of the Baltic Sea wave fields, performed for 1970–2007, using the third-generation spectral wave model WAM [28]. The model was run for a regular rectangular grid that covers the entire Baltic Sea with a spatial resolution of 3' along latitude and 6' along longitude (about 3 × 3 nm) [29]. The bathymetry of the model was based on data from [30], which has a resolution of 1' along latitude and 2' along longitude.

The wave model was forced with wind data corresponding to an elevation of 10 m above the sea surface, constructed from the Swedish Meteorological and Hydrological Institute (SMHI) geostrophic wind database. This data set has a spatial and temporal resolution of 1° × 1° and 3 h, respectively (6 h before

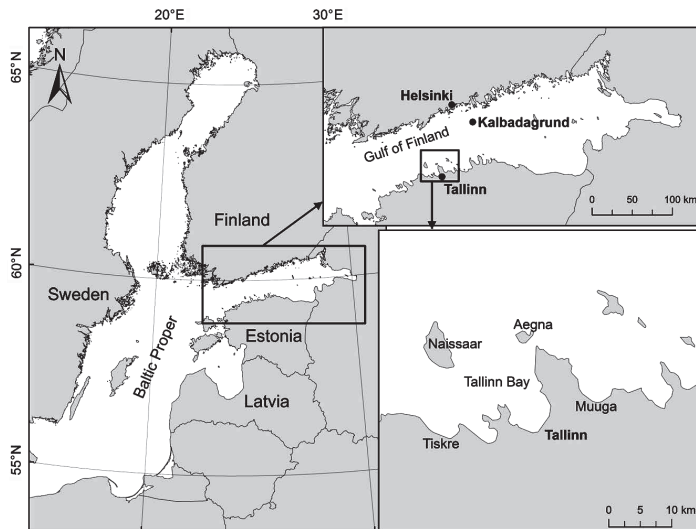


Fig. 2. Computational areas of the triple-nested wave model, applied to the Tallinn Bay area and the location of the wind measurement site at Kalbadagrund.

September 1977). The geostrophic wind speed was multiplied by 0.6 and the wind direction was turned counter-clockwise by 15° [31]. This approximation of the vertical structure of wind properties is frequently used in the Baltic Sea region. Although it completely ignores stability aspects of the atmospheric stratification, it leads to an acceptable reproduction of circulation patterns [32]. The use of an extended frequency range of wave harmonics (42 frequency bins with an increment of 1.1) down to wave periods of about 0.5 s ensures realistic wave growth rates under weak winds after calm periods and an adequate reproduction of high-frequency part of the wave fields [20,22]. Thus, at each grid cell, 600 spectrum components were calculated (24 evenly spaced directions with a directional resolution of 15° and 42 frequencies ranging from 0.042 to 2.08 Hz).

The accuracy and reliability of wave calculations, using this approach, are discussed in a number of recent papers [31,33]. They demonstrate that the simulated wave properties satisfactorily replicate the time series of measured wave data [33] and also reproduce the statistical properties of the wave fields at several observation sites quite well [31]. The presence of sea ice is ignored in the calculations. Although this is generally acceptable for the southern part of the Baltic Proper, it may substantially overestimate the wave load in the northern Baltic, especially in the Gulf of Riga and the Gulf of Finland. However, as the strongest storms usually occur before the ice cover is formed, this approximation is evidently still adequate for the estimation of the closure depth and extreme wave loads.

Wave properties in the vicinity of Tallinn Bay were calculated with a spatial resolution of about 470 m using a triple-nested version of the WAM model for the years of 1981–2012. Additionally to the coarse model (with a spatial step of about 5.5 km) run for the entire Baltic Sea (Fig. 2), a medium-resolution model was run for the Gulf of Finland with a grid step of about 1.8 km. The bathymetry of the models is based on data from [30]. Finally, a high-resolution model with a grid step of about 470 m ($1/4'$ along latitude and $1/2'$ along longitude), which resolves the major local topographic and bathymetric features, was run for the Tallinn Bay area (Fig. 3). The standard frequency range of the WAM model (from 0.042 to 0.41 Hz, 25 frequencies) was employed for stronger winds. It was extended to 2.08 Hz (42 frequencies) for wind speeds ≤ 10 m/s to better represent the wave growth under weak wind and short fetch conditions.

All three models in the hierarchy were forced with a spatially homogeneous wind field that matches the wind, measured in fully marine conditions not affected by the land. Such a wind measurement site is located at Kalbådagrund, a caisson lighthouse in the central part of the Gulf of Finland (Fig. 2, $59^\circ 59'N$, $25^\circ 36'E$). Here, wind speed and direction are recorded at a height of 32 m above mean sea level. To reduce the recorded wind speed to the reference height of 10 m, height correction factors of 0.91 for neutral, 0.94 for unstable and 0.71 for stable stratifications have been employed in earlier studies [34]. As a first approximation, a factor 0.85 was used in the present case, which is similar to that used in [20].



Fig. 3. Grid cells of the fine model used for the evaluation of wave properties in the nearshore of Tallinn Bay. Graphics by K. Pindsoo.

The nearshore wave time series along this coastal stretch in the vicinity of Tallinn Bay were estimated using a simplified scheme for long-term wave hindcasting, in which calculations of the sea state were reduced to an analysis of a cluster of wave field maps, precomputed from single-point wind data. This method produces adequate results in the study area where wave fields rapidly become saturated and have a relatively short memory (normally no longer than 12 h) of wind history [20]. This feature makes it possible to split the wave calculations into a number of short independent sections of 3–12 h. As a first approximation, it was assumed that an instant wave field in Tallinn Bay is a function of a short section of the wind dynamics and that the contribution of remote wind conditions in the open Baltic Sea to the local wave field in Tallinn Bay is insignificant. For Tallinn Bay, these assumptions are correct for about 99.5% of all cases [20]. As waves are relatively short in the Baltic Sea [21] and usually even shorter in its semi-enclosed sub-basins [22], the wave model using the innermost grid allows a satisfactory description of wave properties in the coastal zone down to depths of about 5 m and as close to the coast as about 200–300 m [20].

3. RESULTS

3.1. Longshore variations of wave properties

Basic wave properties (mean wave height and various quantiles of wave heights) vary substantially along the eastern Baltic Sea coast (Fig. 4). The overall

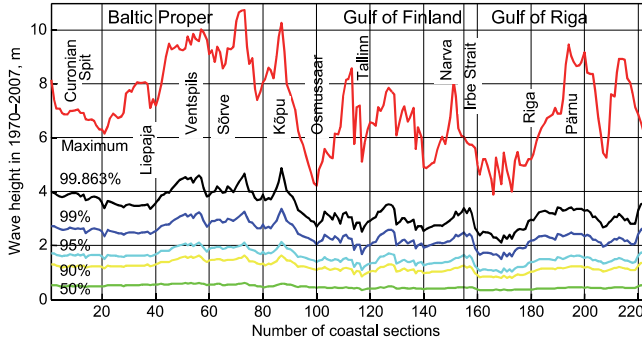


Fig. 4. Modelled significant wave height (overall maximum over the years of simulation and thresholds for various quantiles) in the nearshore of the eastern Baltic Proper, the Gulf of Finland and the Gulf of Riga for the period 1970–2007. The numbers of grid points are given in Fig. 1.

wave height maximum for the entire study area was computed as 10.7 m, which exceeds the maxima of 9.6–9.7 m estimated for offshore conditions in the open Baltic Sea under extreme storms [^{35,36}] by about 10%. Nevertheless, the individual maxima for selected nearshore locations may still be realistic due to wave energy focusing, caused by refraction in certain domains [^{37,38}]. The maximum significant wave heights of >8 m, computed for the Gulf of Finland and for the Gulf of Riga, appear to be overestimates, even though single waves with a height of around 10 m have been reported in older literature from the southern part of the Gulf of Riga during extreme north-northwesterly storms. The number of such wave conditions, however, is very small; for example, in the eastern Gulf of Riga such wave heights have been recorded during a single storm only. The threshold for wave heights, occurring with a frequency of 0.1%, is well below 4 m for the Gulf of Riga, varies between 4 and 5 m in the nearshore of the Baltic Proper, and is around 3 m in the Gulf of Finland.

The ratio of the maximum and mean wave height (interpreted as either the arithmetic mean of all hourly values of the wave height or, alternatively, as the median wave height $H_{50\%}$) also varies substantially along the coastline. The minimum and maximum values differ by a factor of 2 (Fig. 5). The ratio of the 99.863th percentile, $H_{0.137\%}$, and the mean wave height, H_{mean} (Fig. 5), however, varies much less. Almost its values lie in a relatively narrow range from 5 to 6, with an overall mean of 5.54. Although the maximum value of $H_{0.137\%}/H_{\text{mean}}$ is 6.38, it exceeds 6 in only 13 out of the 222 coastal sections. The minimum value is 4.84 with only 5 values lying below 5. This result suggests that the use of Eq. (3) for the calculation of the closure depth, based on the annual mean wave height, is definitely not justified in the Baltic Sea conditions. This equation, on average, underestimates the closure depth by about 20%. However, as demonstrated below, the use of the 99.863th percentile for this purpose is still adequate.

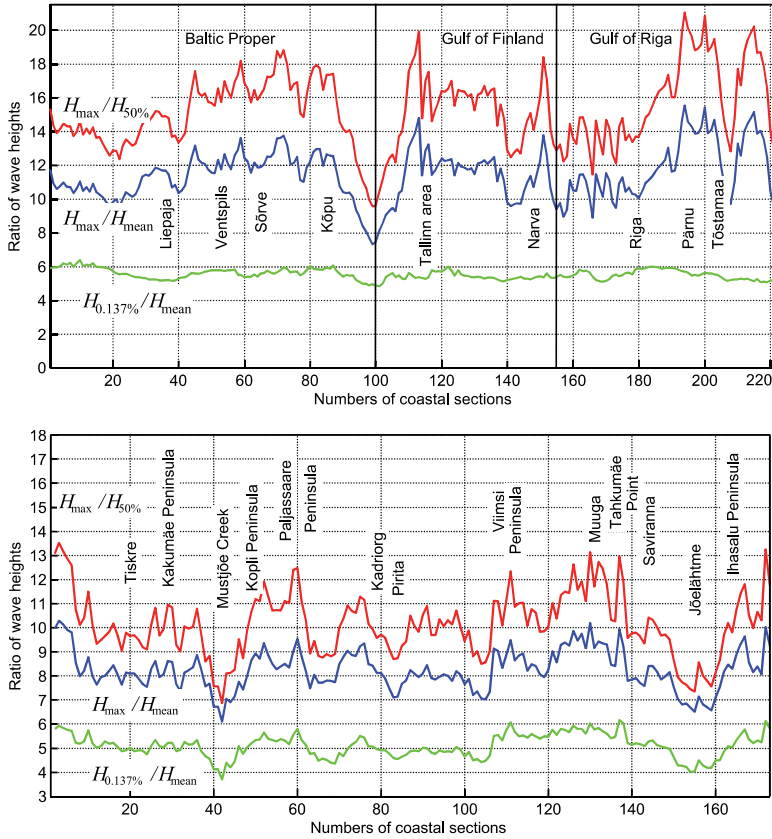


Fig. 5. The ratio of maximum and average significant wave height along the eastern Baltic Sea coast and the Gulf of Riga in the period 1970–2007 (upper panel; numbers of grid points in Fig. 1) and for the Tallinn Bay area in the period 1981–2012 (lower panel, numbers of grid points in Fig. 3). Here $H_{50\%}$ stands for the median wave height.

Figure 5 also demonstrates that there is no obvious relationship between the geometry or orientation of the coastline and the values of the ratio $H_{0.137\%}/H_{\text{mean}}$. This ratio is close to 6 along almost straight coastal stretches such as the entire Curonian Spit or the vicinity of Ventspils, and also to the east of Tallinn in the Gulf of Finland or near Riga. This ratio exhibits minimum values at the entrance to the Gulf of Finland and near Liepāja, the two areas having radically different orientations, besides being exposed to greatly different wave conditions. This observation suggests that a first approximation to the closure depth in the Baltic Sea conditions can be found by using the relationship

$$h_c^B \cong 1.5H_{0.137\%} \cong 8.25H_{\text{mean}}. \quad (3')$$

The alongshore variation of the ratio $H_{0.137\%}/H_{\text{mean}}$ is even larger along the coastal stretch around Tallinn with its complicated geometry (Fig. 5). The ratio of the maximum wave height and the 99.9th percentile (not shown) varies by about 20% in the study area (1.42–1.78). This level of variation signals that, in this region, the distributions of occurrence of different very large wave heights may have quite different properties for different sections. This conjecture is further supported by the behaviour of the ratio $H_{0.137\%}/H_{\text{mean}}$. It varies from about 3.7 to 6.1 whereas its average over the entire coastal stretch around Tallinn is about 5. Somewhat surprisingly, this value is by about 10% smaller than the one for the entire eastern Baltic Sea coast calculated using the wave data from grid points located slightly farther offshore. A potential reason for this difference may be a relatively larger influence of remote swell in the nearshore of the deeply indented bays. Because such swells are almost totally absent in the Baltic Proper, even these comparatively low levels may increase the annual mean wave height and thereby adjust the rate in question.

3.2. Closure depth

The estimates of the closure depth were calculated from the modified Eq. (3') with $q_2 = 8.25$ and from the second-order (so-called parabolic) approximations that describe the closure depth as a quadratic function of the wave height and that also involve the wave period [^{11,12}]:

$$h_c = p_1 H_{0.137\%} - p_2 \frac{H_{0.137\%}^2}{gT_s^2}. \quad (4)$$

In Eq. (4), g is the gravity acceleration. In the original version of this approximation [^{11,12}], $p_1 = 2.28$, $p_2 = 68.5$ and T_s is the typical peak period that corresponds to the largest significant wave height that occurs for 12 h a year. This expression is known to somewhat overestimate the closure depth but is still often used in coastal engineering as a conservative estimate in the design of beach refill. Another version of parameters in Eq. (4) with values of $p_1 = 1.75$ and $p_2 = 57.9$ [^{16,19}] matches the average values of closure depth quite well and also the estimates derived using Eq. (3). These expressions give more realistic results for semi-sheltered domains of the Baltic Sea [^{14,25}]. The use of even higher-order approximations is evidently not justified as the concept of closure depth is an approximation in itself.

The calculations were performed using two different approaches. Firstly, the values of $H_{0.137\%}$ and the corresponding typical periods and the closure depth for each section were evaluated separately for every year in the period 1970–2007. The closure depth was then estimated as an average of the annual values. Secondly, all these quantities were evaluated directly from the entire dataset comprising 333 096 hourly values of wave time series. Consistently with the concept of gradual increase in the width of the EBP [¹⁶], the results based on the

sequence of annual values were slightly smaller than those obtained directly from the entire time series. The difference between the results for individual coastal sections was surprisingly small, being less than 4% for single sections and about 2.5% on average. This suggests that the overall storminess level remained fairly constant during the entire simulation period.

The calculations with three of the four applied methods produced almost the same results (Fig. 6), whereas Eq. (4) with $p_1 = 2.28$ and $p_2 = 68.5$ gave some-

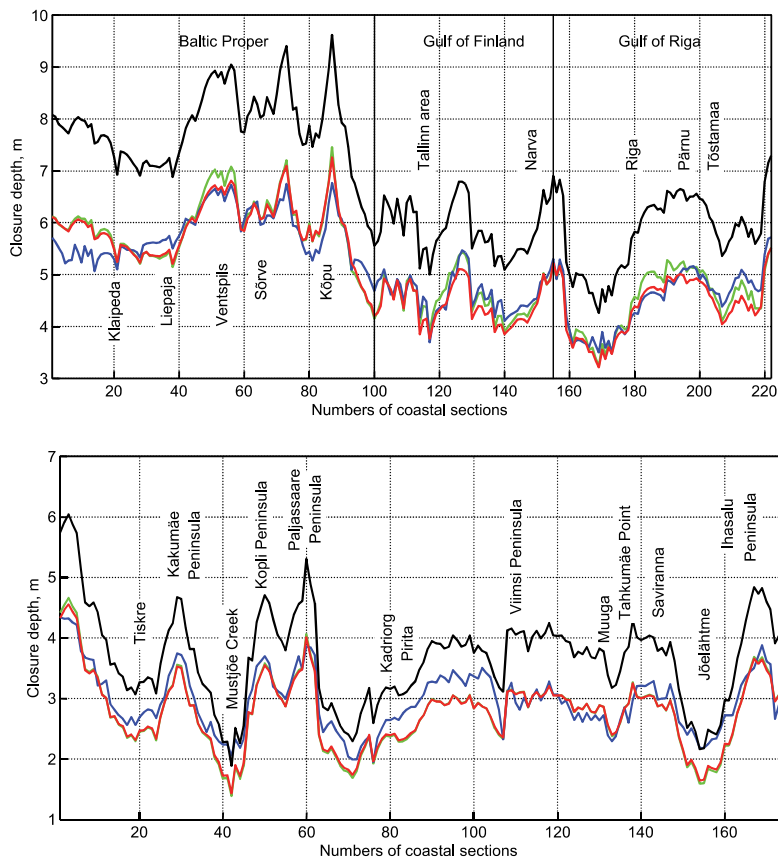


Fig. 6. Closure depths along the coasts of the Baltic Proper, the Gulf of Finland and the Gulf of Riga (upper panel), and in the Tallinn Bay area (lower panel) calculated using Eq. (3') with $q_1 = 1.5$ (green) and $q_2 = 8.25$ (red), and Eq. (4) with $p_1 = 1.75$ and $p_2 = 57.9$ (blue), and $p_1 = 2.28$ and $p_2 = 68.5$ (black). The quantity $H_{0.137\%}$ was calculated over the entire time interval of wave simulations for 1970–2007 (upper panel) and for 1981–2012 (lower panel).

what larger values. As expected, the closure depth is largest (up to 7.25 m) in regions that are fully open to the predominant south-westerly winds in the Baltic Proper and where the overall wave intensity is the largest in the entire Baltic Proper. These areas are the west coasts of the islands of Hiiumaa and Saaremaa, and north-northwest coast of the Kurzeme Peninsula. The coasts of the Baltic Proper all have a closure depth >5 m, whereas almost the entire coastline of the Gulf of Finland and the Gulf of Riga (except for a very few locations) has a closure depth well below 5 m (Fig. 7). This difference is consistent with the well-known difference in the properties of wave climate in these three domains.

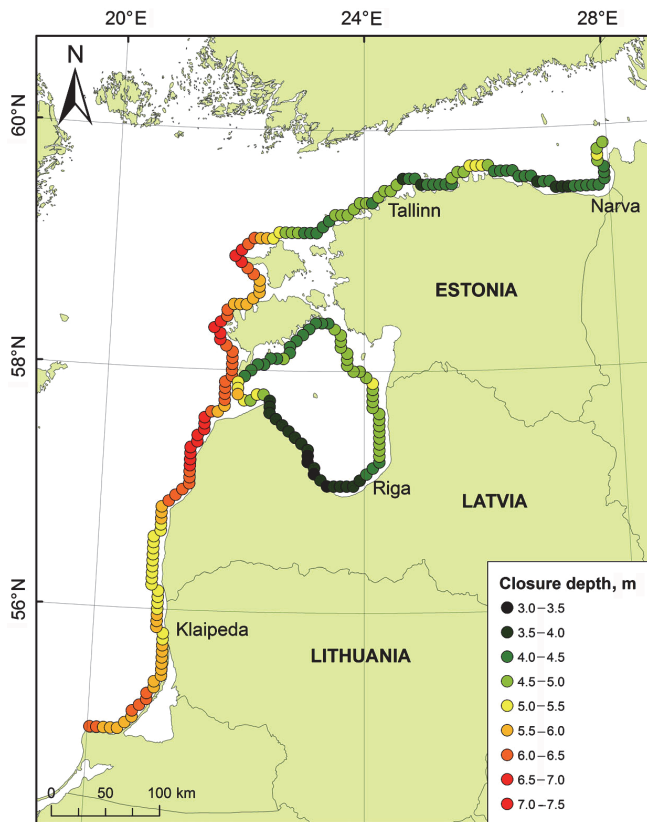


Fig. 7. Comparison of closure depths at the coasts of the Baltic Proper, Gulf of Finland and Gulf of Riga calculated using Eq. (4) with $p_1 = 1.75$ and $p_2 = 57.9$. The quantity $H_{0.137\%}$ has been calculated over the entire time interval 1970–2007.

As expected, the closure depth is clearly smaller in the Tallinn Bay area. Because the wave properties for this area were calculated not only with a much finer resolution but also at grid points located relatively close to the coast, the wave model was able to account for most of the wave transformation and decay in the nearshore. For this reason the closure depth even for the most open sections in this domain is smaller than the corresponding values estimated using the coarse model. Typical values of the closure depth in this region are in the range of 2.5–3.5 m, which is about 1 m smaller than the estimates using the coarse model. In several bayheads the closure depth drops to 1.5 m, whereas it reaches over 4 m along a number of headlands.

Apart from the very strong alongshore variability of the closure depths in this region, an interesting feature is that the values calculated using Eq. (4) with $p_1 = 1.75$, $p_2 = 57.9$ deviate in some places from the estimates derived using the simpler expressions (3) and (3'), but match the values obtained using Eq. (4) with $p_1 = 2.28$, $p_2 = 68.5$. Such areas are characterized by exceptionally low $H_{0.137\%}/H_{\text{mean}}$ ratios (cf. Fig. 5). These values, however, are in the range of 4–4.5 and thus only slightly smaller than the typical values for the open ocean coasts. This feature once more highlights the intrinsic difference of the Baltic Sea wave climate from that in many other parts of the world oceans and stresses the point that the generic approximations and relationships derived from the wave properties along open ocean coasts may fail in the Baltic Sea conditions.

4. DISCUSSION AND CONCLUSIONS

The results reveal a substantial difference in the wave statistics for open ocean coasts and for the coasts of semi-sheltered basins. While in both coastal settings the ratio between certain higher quantiles of wave heights and the average wave height varies insignificantly, this ratio ($H_{0.137\%}/H_{\text{mean}} \cong 4.5$ for open ocean coasts) is much larger (approximately 5.5) along the eastern Baltic Sea coasts. This difference is evidently related to the proportion of remote swell in the particular coastal stretch. Along ocean coasts, relatively low-amplitude swell is known to substantially contribute to the total wave energy and its flux [³⁹], whereas extreme wave heights are mostly governed by severe local storms. The absence of this remote component of wave energy is the most plausible explanation for the observation that the mean wave energy levels along the coasts of sheltered seas are much lower in comparison to those associated with extremely large wave heights of open ocean coasts. This observation is implicitly supported by a clearly lower ratio of the extreme and average wave heights in the Tallinn Bay area. This area is sheltered from the predominant south-westerly winds but is frequently affected by low swells generated in the Baltic Proper. This component to the wave activity increases the mean wave height and leads to a certain decrease in the ratio in question; particularly in bays that are even more sheltered.

An important consequence of the analysis is that the simple equations for the evaluation of the closure depth, based on the average wave height and derived for

open ocean conditions, have to be modified for the use in semi-sheltered regions. In areas where remote swell is virtually absent (such as the Baltic Proper), a suitable expression for the closure depth is $h_c^B \cong 1.5H_{0,137\%} \cong 8.25H_{\text{mean}}$. This expression may need further modification for certain sub-basins that experience an appreciable level of remote swells such as the Gulf of Finland that is widely open to the Baltic Proper. This peculiarity, however, does not modify the role of the highest waves in shaping the coastal profile and Eq. (3) in terms of $H_{0,137\%}$ is evidently applicable to all coastal regions, even if it reflects extreme wave properties for several shorter storms.

The alongshore distribution of closure depths in the three basins, considered here, basically corresponds to similar variations in extreme wave heights. The largest closure depths of up to 7.25 m along the Baltic Proper occur in areas experiencing the largest wave intensities, whereas much smaller closure depths (usually well below 5 m) are found in the Gulf of Riga and along the southern coast of the Gulf of Finland. In more sheltered bays the closure depth may be even smaller (about 2 m).

ACKNOWLEDGEMENTS

This study was a part of the project “Science-based forecast and quantification of risks to properly and timely react to hazards impacting Estonian mainland, air space, water bodies and coasts” (TERIKVANT), supported by the European Union (European Regional Development Fund, ERDF) and managed by the Estonian Research Council within the framework of the Environmental Technology R&D Programme KESTA. The research was partially supported by the targeted financing of the Estonian Ministry of Education and Research (grant SF0140007s11), by the Estonian Science Foundation (grant No. 9125), and through support of the ERDF to the Centre of Excellence in Non-linear Studies CENS. The authors are deeply grateful to Andrus Räämet for providing the simulated wave data and to Prof. Dr. Burghard W. Flemming for numerous suggestions towards improving the manuscript.

REFERENCES

1. Dean, R. G. and Dalrymple, R. A. *Coastal Processes with Engineering Applications*. Cambridge University Press, Cambridge, 2002.
2. Dean, R. G. Equilibrium beach profiles: characteristics and applications. *J. Coast. Res.*, 1991, 7, 53–84.
3. Bruun, P. Sea level rise as a cause of erosion. *J. Waterw. Harb. Div.* – ASCE, Vancouver, 1962, **88**, 117–133.
4. Edelman, T. Dune erosion during storm conditions. In *Proc. 13th International Conference on Coastal Engineering*. ASCE, Vancouver, 1972, 1305–1312.
5. Dean, R. G. and Maurmeyer, E. M. Models for beach profile response. In *CRC Handbook of Coastal Processes and Erosion* (Komar, P. D., ed.). CRC Press, Boca Raton, 1983, 151–166.

6. Dean, R. G., Healy, T. R. and Dommerholt, A. A “blind-folded” test of equilibrium beach profile concepts with New Zealand data. *Marine Geol.*, 1993, **109**, 253–266.
7. Stetzel, H. J. *Cross-shore Transport During Storm Surges*. Delft Hydraulics, Delft, The Netherlands, Publ. No. 476, 1993.
8. Kit, E. and Pelinovsky, E. Dynamical models for cross-shore transport and equilibrium bottom profiles. *J. Waterw. Port Coast. Ocean Eng.*, 1998, **124**, 138–146.
9. Didenkulova, I. and Soomere, T. Formation of two-section cross-shore profile under joint influence of random short waves and groups of long waves. *Marine Geol.*, 2011, **289**, 29–33.
10. Hallermeier, R. J. Uses for a calculated limit depth to beach erosion. In *Proc. 16th International Conference on Coastal Engineering*. ASCE, Hamburg, 1978, 1493–1512.
11. Hallermeier, R. J. A profile zonation for seasonal sand beaches from wave climate. *Coast. Eng.*, 1981, **4**, 253–277.
12. *Coastal Engineering Manual*. Manual No. 1110-2-1100. US Army Corps of Engineers, Washington, DC, Chapter III-3-2, 2002 (CD).
13. Kask, A., Soomere, T., Healy, T. R. and Delpêche, N. Rapid estimates of sediment loss for “almost equilibrium” beaches. *J. Coast. Res.*, 2009, Special Issue 56, 971–975.
14. Kartau, K., Soomere, T. and Tõnisson, H. Quantification of sediment loss from semi-sheltered beaches: a case study for Valgerand Beach, Pärnu Bay, the Baltic Sea. *J. Coast. Res.*, 2011, Special Issue 64, 100–104.
15. Kraus, N. C. Engineering approaches to cross-shore sediment processes. In (*Proc. Short Course On) Design and Reliability of Coastal Structures* (Lamberti, A., ed.), attached to 23rd International Conference on Coastal Engineering, Venice, 1992, 175–209.
16. Birkemeier, W. A. Field data on seaward limit of profile change. *J. Waterw. Port. Coast. Ocean Eng.*, 1985, **111**, 598–602.
17. Are, F. and Reimnitz, E. The A and m coefficients in the Bruun/Dean Equilibrium Profile equation seen from the Arctic. *J. Coast. Res.*, 2008, **24**, 243–249.
18. Nicholls, R. J., Birkemeier, W. A. and Hallermeier, R. J. Application of the depth of closure concept. In *Proc. 25th International Conference on Coastal Engineering*. ASCE, Orlando, 1996, 3874–3887.
19. Houston, J. R. Simplified Dean’s method for beach-fill design. *J. Waterw. Port. Coast. Ocean Eng.*, 1996, **122**, 143–146.
20. Soomere, T. Wind wave statistics in Tallinn Bay. *Boreal Environ. Res.*, 2005, **10**, 103–118.
21. Broman, B., Hammarklint, T., Rannat, K., Soomere, T. and Valdmann, A. Trends and extremes of wave fields in the north-eastern part of the Baltic Proper. *Oceanologia*, 2006, **48(S)**, 165–184.
22. Soomere, T., Weisse, R. and Behrens, A. Wave climate in the Arkona Basin, the Baltic Sea. *Ocean Sci.*, 2012, **8**, 287–300.
23. Soomere, T. Extreme wind speeds and spatially uniform wind events in the Baltic Proper. *Proc. Estonian Acad. Sci. Eng.*, 2001, **7**, 195–211.
24. Soomere, T. and Keevallik, S. Directional and extreme wind properties in the Gulf of Finland. *Proc. Estonian Acad. Sci. Eng.*, 2003, **9**, 73–90.
25. Soomere, T., Kask, A., Kask, J. and Healy, H. Modelling of wave climate and sediment transport patterns at a tideless embayed beach, Piritä Beach, Estonia. *J. Mar. Syst.*, 2008, **74**, Suppl., S133–S146.
26. Soomere, T., Viška, M., Lapinskis, J. and Räämet, A. Linking wave loads with the intensity of coastal processes along the eastern Baltic Sea coasts. *Estonian J. Eng.*, 2011, **17**, 359–374.
27. Raukas, A. and Hyvärinen, H. (eds). *Geology of the Gulf of Finland*. Valgus, Tallinn, 1992 (in Russian).
28. Komen, G. J., Cavaleri, L., Donelan, M., Hasselmann, K., Hasselmann, S. and Janssen, P. A. E. M. *Dynamics and Modelling of Ocean Waves*. Cambridge University Press, Cambridge, 1994.
29. Räämet, A. and Soomere, T. The wave climate and its seasonal variability in the northeastern Baltic Sea. *Estonian J. Earth Sci.*, 2010, **59**, 100–113.

30. Seifert, T., Tauber, F. and Kayser, B. A high resolution spherical grid topography of the Baltic Sea, 2nd ed. Baltic Sea Science Congress, Stockholm, 2001, Poster #147. www.io-warnemuende.de/iowtopo
31. Soomere, T. and Räämet, A. Spatial patterns of the wave climate in the Baltic Proper and the Gulf of Finland. *Oceanologia*, 2011, **53**(1-T1), 335–371.
32. Myrberg, K., Ryabchenko, V., Isaev, A., Vankevich, R., Andrejev, O., Bendtsen, J., Erichsen, A., Funkquist, L., Inkala, A., Neelov, I. et al. Validation of three-dimensional hydrodynamic models in the Gulf of Finland based on a statistical analysis of a six-model ensemble. *Boreal Environ. Res.*, 2010, **15**, 453–479.
33. Räämet, A., Suursaar, Ü., Kullas, T. and Soomere, T. Reconsidering uncertainties of wave conditions in the coastal areas of the northern Baltic Sea. *J. Coast. Res.*, 2009, Special Issue 56, 257–261.
34. Launiainen, J. and Laurila, T. Marine wind characteristics in the northern Baltic Sea, *Finnish Mar. Res.*, 1984, **250**, 5–86.
35. Soomere, T., Behrens, A., Tuomi, L. and Nielsen, J. W. Wave conditions in the Baltic Proper and in the Gulf of Finland during windstorm Gudrun. *Nat. Hazard. Earth Syst. Sci.*, 2008, **8**, 37–46.
36. Tuomi, L., Kahma, K. K. and Pettersson, H. Wave hindcast statistics in the seasonally ice-covered Baltic Sea. *Boreal Environ. Res.*, 2011, **16**, 451–472.
37. Soomere, T. Anisotropy of wind and wave regimes in the Baltic Proper. *J. Sea Res.*, 2003, **49**, 305–316.
38. Babanin, A. V., Hsu, T.-W., Roland, A., Ou, S.-H., Doong, D.-J. and Kao, C. C. Spectral wave modelling of Typhoon Krosa. *Nat. Hazard. Earth Syst. Sci.*, 2011, **11**, 501–511.
39. Arinaga, R. A. and Cheung, K. F. Atlas of global wave energy from 10 years of reanalysis and hindcast data. *Renew. Energy*, 2013, **39**, 49–64.

Lainekoormuste ja sulgemissügavuste muutlikkus Läänemere idarannikul

Tarmo Soomere, Maija Viška ja Maris Eelsalu

Sulgemissügavus iseloomustab lainetuse intensiivsust rannikuvööndis ja kirjeldab, millise sügavuseni kujundavad tormilained tasakaalulise rannaprofiili. Selle parameetri väärtused on leitud aastaiks 1970–2007 rekonstrueeritud tormilainete omaduste alusel lahutusvõimega 5,5 km piki kogu Läänemere idarannikut Sambia poolsaarest Soome lahe idaosani ja Liivi lahes nelja erineva meetodika abil. Sulgemissügavused Tallinna lahe ümbruses on leitud aastaiks 1981–2012 rekonstrueeritud lainetuse omaduste alusel lahutusvõimega 500 m. On näidatud, et kõrgeimate lainete (mida iseloomustab aastas keskmiselt 12 tunni jooksul esinev oluline lainekõrgus) ja keskmiste lainekõrguste suhe nimetatud rannikaladel on ligikaudu 5,5, mis ületab selle suhte väärtuse avaookeani rannikutel enam kui 20% võrra. Erinevus on tingitud ummiklainete väikesest osakaalust Läänemere lainetuses. On tuletatud sulgemissügavuse arvutusvalemi Läänemere tingimuste jaoks sobiv modifikatsioon. Suurimad sulgemissügavused (kuni 7,25 m) paiknevad Läänemere avaosa põhjapoolses sektoris Hiiumaa, Saaremaa ja Kuramaa rannikualal. Läänemere avaosa teistes rannikuloikudes on sulgemissügavus üldiselt vahemikus 5–6 m, Soome ja Liivi lahes 3–4 m.

Paper III

Soomere T., **Viška M.** 2014. Simulated wave-driven sediment transport along the eastern coast of the Baltic Sea. *Journal of Marine Systems*, 129, 96–105.



Simulated wave-driven sediment transport along the eastern coast of the Baltic Sea

Tarmo Soomere^{a,b}, Maija Viška^{a,*}

^a Institute of Cybernetics at Tallinn University of Technology, Akadeemia tee 21, 12618 Tallinn, Estonia

^b Estonian Academy of Sciences, Kohtu 6, 10130 Tallinn, Estonia

ARTICLE INFO

Article history:

Received 29 November 2011

Received in revised form 4 September 2012

Accepted 5 February 2013

Available online 15 February 2013

Keywords:

Coastal zone management

Alongshore sediment transport

Wave hindcasting

Wave climate

Baltic Sea

Curonian Spit

Akmenrags Cape

ABSTRACT

Alongshore variations in sediment transport along the eastern Baltic Sea coast from the Sambian (Samland) Peninsula up to Pärnu Bay in the Gulf of Riga are analysed using long-term (1970–2007) simulations of the nearshore wave climate and the Coastal Engineering Research Centre (CERC) wave energy flux model applied to about 5.5 km long beach sectors. The local rate of bulk transport is the largest along a short section of the Sambian Peninsula and along the north-western part of the Latvian coast. The net transport has an overall counter-clockwise nature but contains a number of local temporary reversals. The alongshore sediment flux has several divergence and convergence points. One of the divergence points at the Akmenrags Cape divides the sedimentary system of the eastern coast of the Baltic Proper into two almost completely separated compartments in the simulated wave climate. Cyclic relocation of a highly persistent convergence point over the entire Curonian Spit suggests that this landform is in almost perfect dynamical equilibrium in the simulated approximation of the contemporary wave climate.

© 2013 Elsevier B.V. All rights reserved.

1. Introduction

The coasts of the Baltic Sea can be divided into two large categories. Bedrock-based, frequently skären type predominates along its northern coast, starting from the vicinity of Saint Petersburg and extending over the entire Bothnian Sea and the Gulf of Bothnia down to the south-eastern (SE) part of Sweden. Sedimentary coasts predominate along the southern and eastern coasts of this water body, from the southern tip of Sweden over Denmark, Germany, Poland and the Baltic states. Most of the coasts of Estonia are heavily fragmented by numerous islands, peninsulas and bays deeply cut into the mainland. This fragmentation confines alongshore sediment transport into relatively small almost disconnected compartments (Soomere and Healy, 2011).

The longest connected domain of sedimentary coasts of the Baltic Sea, the focus of the current study, stretches from the Sambian Peninsula to the east and north-east (NE), and extends up to the eastern coast of the Gulf of Riga (Fig. 1). This section is generally thought to represent a large, more or less continuous sedimentary system (Žaromskis and Gulbinskas, 2010). An idealised view is that sediment is mostly transported counter-clockwise along both the SE coast of the Baltic Proper (Gudelis et al., 1977; Knaps, 1966) and the southern and eastern coast of the Gulf of Riga, with a discontinuity and/or partial discharge at the Kolka Cape (Žaromskis and Gulbinskas, 2010). As typical for the Baltic Sea, sediment transport along this section is not necessarily continuous (Knaps, 1982). While the Curonian Spit is a sandy landform, large parts

of underwater slope in Latvia are covered with boulders, pebbles and coarse sand washed out of till. Only a few parts of the Latvian nearshore host large amounts of fine sediment, for example, coasts of Irbe Strait, southern part of the Gulf of Riga and a short coastal section to the SE of Kolka Cape (Ulsts, 1998).

During the existence of the Baltic Sea in its contemporary shape, this coastal domain has undergone remarkable changes. The sediment volume eroded from the Sambian Peninsula has been partially transported to the east and NE, and created the Curonian Spit (Žaromskis and Gulbinskas, 2010). The Lithuanian and Latvian coasts further to the north of the Curonian Spit have been markedly straightened by prolonged marine erosion and deposition (Eberhards, 2003; Eberhards et al., 2006; Gudelis, 1967; Knaps, 1966; Ulsts, 1998). The changes are less marked in the Gulf of Riga but still substantial even in relatively sheltered areas such as Pärnu Bay (Kartau et al., 2011). As a result, most of the domain in question consists of two main types of coasts: cliffed abrasional parts, with more or less clearly defined scarp or bluff in usually relatively soft cliffs, and gently sloping, generally advancing depositional coasts (Eberhards, 2003; Eberhards et al., 2006; Gudelis, 1967).

Almost all these coasts develop under overall sediment deficit (Eberhards and Lapinskis, 2008; Kartau et al., 2011; Žaromskis and Gulbinskas, 2010) and weak uplift of the crust superimposed with climatically controlled sea level rise (Harff and Meyer, 2011). They are thus very sensitive to changes in the hydrodynamic loads (Eberhards et al., 2006) and especially to the sea level rise. Even sections that usually show accumulation features such as the Curonian Spit may be heavily damaged in certain storms (Žaromskis and Gulbinskas, 2010). Large parts of the Latvian coast are estimated in terms of risk of erosion as either “very vulnerable” or “vulnerable”. Such risk of erosion is most common

* Corresponding author. Tel.: +372 6204178; fax: +372 6204151.
E-mail address: maija@ioc.ee (M. Viška).

along both the Baltic Proper coast (69%) and the coast of the Gulf of Riga (66%) (Eberhards, 2003; Eberhards et al., 2006).

The major factor shaping the coasts in the almost tideless Baltic Sea (Leppäranta and Myrberg, 2009) is the wave activity. Although currents do play a role in the transport of fine material in the offshore, in this paper we focus on sediment transport processes in the surf and swash zone governed by wave activity. In this light it is natural that rapid erosion events at certain locations in the recent past (Eberhards et al., 2006; Orviku et al., 2003) are associated with a combination of changes to the wave climate and with a decrease in the length of the ice season (Orviku et al., 2003; Ryabchuk et al., 2011; Tönisson et al., 2011). Although there may exist extensive interannual and considerable decadal-scale variations in the (annual mean) wave height at certain locations (Soomere and Räämet, 2011), no long-term changes to the spatially averaged annual mean wave height have been identified in the entire Baltic Sea (Broman et al., 2006; Soomere et al., 2012; Zaitseva-Pärmaste et al., 2011). A specific feature of the Baltic Sea is that changes in the nearshore wave climate are not necessarily associated with an alteration of the wave height. For example, owing to a relatively small size of the basin, a systematic change in the trajectories of cyclones crossing the sea (Sepp et al., 2005) may become evident as a change in the wave approach direction. The latter change may substantially impact not only the magnitude but even the direction of the wave-driven littoral flow. Moreover, the wind climate of the northern Baltic Proper has a two-peak directional structure. The most frequent are south-western (SW) winds whereas somewhat less frequent north-northwestern (NNW) winds may be even stronger (Soomere and Keevallik, 2001). The distribution of wave approach directions matches this pattern (Räämet et al., 2010). Owing to the specific orientation of a part of the coastline in question, even a relatively minor change in the proportion of these two peaks may substantially change the resulting net littoral flow.

There exist very few theoretical estimates of the direction of wave- and current-driven littoral flow in this area. To a certain extent, the predominant direction of littoral flow can be estimated based on the similar direction of local wind-driven nearshore currents. The strongest currents among these near the Latvian coast are created by northerly and westerly winds (Eberhards, 2003). The data from a hydrometeorological station near Ventspils shows that in 1980–2000 the predominant winds were from the SW, west and south. These winds produce alongshore water movement to the north. The associated wave fields apparently create littoral flow in the same direction (Eberhards, 2003).

Recent studies have established the basic properties of the Baltic Sea wave climate for the open sea and for selected coastal sites using instrumental measurements (Broman et al., 2006; Soomere et al., 2012), historical wave observations (Zaitseva-Pärmaste et al., 2009, 2011) and numerical simulations (Soomere and Räämet, 2011; Suursaar, 2010; Suursaar et al., 2008). These studies have been linked with the potential changes to the coastal processes for limited coastal sections (Hanson and Larson, 2009; Kelpšaitė et al., 2009, 2011; Tönisson et al., 2011). An attempt to link the alongshore changes to the overall wave intensity with the major erosion and accumulation regions is described in (Soomere et al., 2011). Several efforts made towards predicting the long-term impact of wave-driven coastal processes on the evolution of coastal morphology are presented in (Zhang et al., 2010) for a neighbouring section of the southern Baltic Sea.

There have also been attempts to use different mathematical methods (incl. the Coastal Engineering Research Council (CERC) method employed in this paper) for estimates of sediment transport along the eastern Baltic Sea coast. Calculations for a few locations along the coast suggest that this transport is mostly to the north or NE but may be reversed near Pape (close to the Lithuanian–Latvian border) where that net sediment flow seems to be mostly directed to the south (Ulsts, 1998). Observations, however, clearly signify that the appearance of sand ridges at this location have features

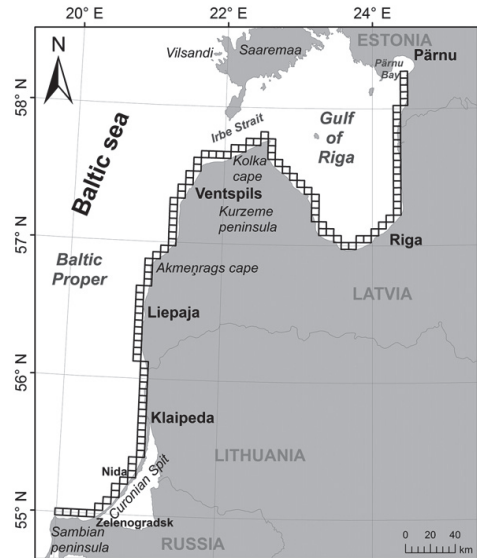


Fig. 1. Study area and the location of calculation points of the wave model on the eastern coast of the Baltic Sea.

characteristic to sediment transport to the north (Ulsts, 1998). Another set of calculations for about 25 points from the Sambian Peninsula to the Kolka Cape (Eberhards, 2003) shows a more realistic pattern of alongshore variations in the littoral flow but still has too low resolution for making definite conclusions about its details. Several more detailed modelling attempts have been undertaken for limited coastal sections (e.g. the vicinity of Palanga, Lithuania) (Zemlys et al., 2007).

In this paper, we make an attempt to systematically analyse the alongshore variations in the wave-driven sediment transport and the associated net littoral flow. The focus is on decadal changes to these quantities along the eastern Baltic Sea coast from the Sambian (Samland) Peninsula up to Pärnu Bay in the Gulf of Riga (Fig. 1). The main goal is to identify sections in which the net transport systematically increases or decreases along the direction of the littoral flow. These areas can be associated with major erosion and accumulation domains, respectively. To a first approximation, we ignore both cross-shore and alongshore variations in the sediment properties and concentrate exclusively on potential erosion and accumulation patterns created by alongshore changes in the wave properties. This approach is justified in a longer perspective: it opens a way for predictions of changes to such areas in the future wind climate irrespectively of short-term and/or local changes to the sediment properties. This goal also makes it possible to use a generic energy flux model for the calculation of the alongshore transport: in this context the exact transport rate is immaterial and the necessary information is extracted from its alongshore variations.

We start with a short overview of the numerically simulated wave data, a description of the method for the calculation of the alongshore sediment transport and a justification of the analysis of alongshore variations in this quantity in Section 2. Results of calculations of alongshore variations in the bulk transport (equivalently, variations in areas with potentially high activity of coastal processes) and net transport are discussed in Sections 3 and 4, respectively. Section 5 focuses on the analysis of divergence and convergence regions of the net littoral flow, with a goal to identify potential areas of fastest accumulation and erosion. The basic messages are formulated in Section 6.

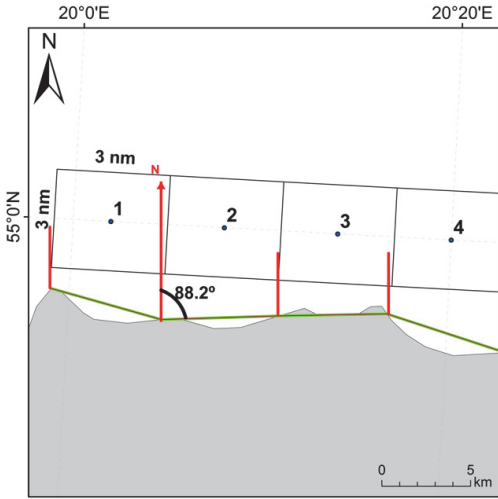


Fig. 2. Approximation of the coast with a piecewise straight line (green lines) at the westernmost points of the study area. The orientation of this approximate line is used in calculations of the alongshore sediment fluxes.

2. Methods and data

The south-eastern and eastern Baltic Sea coast from the Sambian (Samland) Peninsula up to Pärnu Bay is divided into 110 approximately 3 nautical miles (about 5.5 km) long sectors. Their length mimics the spatial resolution of the wave model (Fig. 2). The location of the sectors follows the location of the wave model grid points closest to the shoreline. The coastline within each sector is approximated by a straight line following the general orientation of the coast. Doing so is equivalent to replacing the actual coastline by a piecewise straight line. The intensity of wave-driven alongshore sediment transport is assumed to be constant in each sector. The parameters of each section of the approximate coastline were managed using the geospatial processing program ArcMap.

The instantaneous magnitude of wave-driven alongshore sediment transport is estimated in terms of its potential rate Q_t (USACE, 2002), expressed in cubic metres per each metre of coastline per unit of time [$m^3/m/s$] for each coastal section. Following the temporal resolution of the numerically simulated wave data, the calculations are made

for 1 h long time intervals. The sign (chosen so that the motion from the left to the right hand of the person looking to the sea is positive) and magnitude of the potential transport rate at a given time instant show the direction and intensity of sediment transport, respectively. An estimate of net transport (residual sediment motion in some direction, that is, the amount of sediment that has been finally moved by waves alongshore, equivalent to an estimate of the magnitude of littoral flow) over a certain time interval $[t_0, t_1]$ can be obtained by integrating Q_t over $[t_0, t_1]$. The net transport with positive sign means, therefore, that sediments are transported counter-clockwise along the coastline and with negative sign is marked the opposite movement of the sediments. A measure of bulk transport (the amount of sediment moved back and forth) is obtained similarly, by integrating $|Q_t|$ over $[t_0, t_1]$. The ratio of the net and bulk potential transport characterises the intensity of transit of sediments through the sector in question compared to the back-and-forth motions.

The calculation scheme follows the one used in (Soomere et al., 2008) for a short section of Pirita Beach at the northern coast of Estonia. We employ the commonly used measure of wave-driven alongshore transport—the potential immersed weight transport rate (USACE, 2002)

$$I_t = (\rho_s - \rho)g(1-p)Q_t \tag{1}$$

that accounts for porosity p and specific weight of coastal sediment. Here ρ_s and ρ are the densities of sediment particles and sea water, respectively, $g = 9.81 \text{ m/s}^2$ is the acceleration due to gravity and p is the porosity coefficient. The quantity I_t has the dimension of energy flux (wave power) and thus can be consistently related to the wave parameters. The widely used CERC method to calculate the potential transport rate from the parameters of nearshore waves (USACE, 2002) is based on the assumption that I_t is simply proportional to the rate of beaching of the alongshore component of wave energy flux P_t per unit of length of the coastline:

$$I_t = KP_t \tag{2}$$

where K is a nondimensional coefficient. If the wave propagation direction makes an angle α with the normal to the coast, the alongshore component of the energy flux is $P_y = E c_g \sin \alpha$ (E is the wave energy and c_g is the group speed) and the rate of its beaching per unit of the coastline is

$$P_t = E c_g \sin \alpha \cos \alpha \tag{3}$$

Since the majority of sediment transport occurs in the surf zone, energy and group velocity in Eq. (3) are usually chosen to characterise

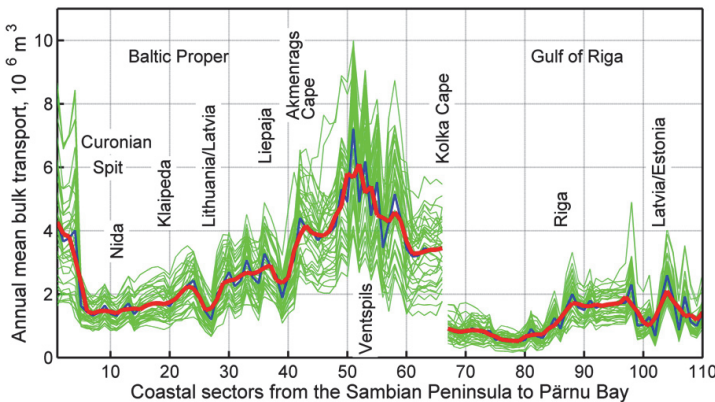


Fig. 3. Bulk potential sediment transport at the eastern Baltic Sea coast from the Sambian Peninsula to Pärnu Bay. Thin green lines indicate the bulk transport for single years, blue line — pointwise averaged bulk transport for 1970–2007 and bold red line — the values at the blue line smoothed over three subsequent coastal sectors.

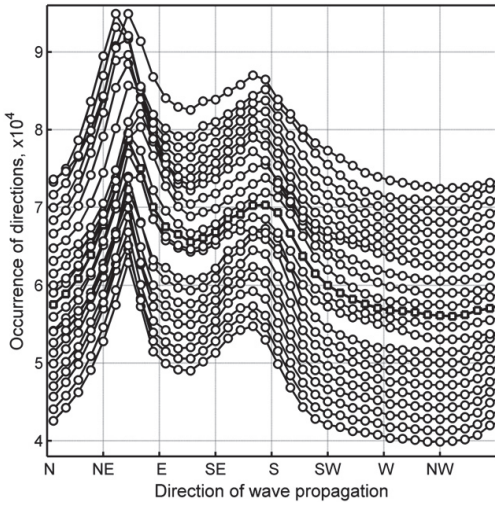


Fig. 4. Frequency of occurrence of simulated wave propagation directions at coastal sections 30–52 along the Latvian coast from the Lithuanian border up to Ventspils in 1970–2007. The vertical scale corresponds to the data for section 30. The subsequent sections are shifted upwards by 150 with respect to each other for better readability. The data for section 41 (Akmenrags Cape) is indicated using bold squares.

the wave properties at the seaward border of the surf zone. At this location waves can be reasonably well described as shallow-water waves; thus,

$$E_b = \frac{\rho g H_b^2}{8}, \quad c_{gb} = \sqrt{g d_b} = \sqrt{\frac{g H_b}{\kappa}}, \quad (4)$$

$$Q_t = \frac{K \rho \sqrt{g}}{16(\rho_s - \rho)(1 - p)\sqrt{\kappa}} H_b^2 \sqrt{H_b} \sin 2\alpha_b, \quad (5)$$

where H_b is the wave height at breaking, $\kappa = H_b/d_b$ is the breaking index, d_b is the breaking depth and α_b is the angle between the wave crests and the isobaths at the breaking. The porosity is set to $p = 0.4$. The dependence of the coefficient K on the wave properties is accounted for using the following empirical expression (USACE, 2002, part III-1):

$$K = 0.05 + 2.6 \sin^2 2\alpha_b + 0.007 u_{mb}/w_f, \quad (6)$$

where $u_{mb} = \kappa \sqrt{g d_b}/2$ is the maximum orbital velocity in breaking waves within the linear wave theory and $w_f = 1.6 \sqrt{g d_{50}(\rho_s - \rho)/\rho}$ is an approximation of the fall velocity in the surf zone. The potential transport rate insignificantly depends on the variations in the coastal sediment texture in the Baltic Sea conditions (Soomere et al., 2008). For reasons explained in the Introduction, we ignore these variations. In calculations we used two values: $d_{50} = 0.063$ mm (corresponding to the finest sand) and $d_{50} = 0.17$ mm. The latter value roughly corresponds to the data from Pärnu Bay (Kartau et al., 2011), the Lithuanian coast (Zemlys et al., 2007) and the Curonian Spit (Zhamoïda et al., 2009). The overall bulk transport rate for $d_{50} = 0.17$ mm is about 90% from the one for $d_{50} = 0.063$ mm. Below we only present the results for the choice $d_{50} = 0.17$ mm.

The calculations of the alongshore sediment flux rely on numerically simulated wave parameters. The time series of wave height, period and direction are estimated hourly using the third-generation spectral wave model WAM (Komen et al., 1994). The model is run for the entire Baltic Sea basin (from 09°36' E to 30°18' E and from 53°57' N to 65°51' N) with a spatial resolution of 3' along latitudes and 6' along longitudes (about 3 × 3 nautical miles) and directional resolution of 15° (24 equally spaced directions for wave propagation) for 38 years (1970–2007) (Räämet and Soomere, 2010). The frequency range of wave harmonics (42 frequencies with an increment of 1.1, accounting for wave periods down to 0.5 s) ensures realistic wave growth rates in low wind conditions after calm situations. The presence of ice was ignored. Doing so is generally acceptable for the southern part of the coastal section in question but may substantially overestimate the overall wave intensity Gulf of Riga. The accuracy and reliability of the wave calculations are discussed in a number of recent papers; see (Soomere and Räämet, 2011) and references therein. In particular, the use of the simulated wave data set led to reasonable results for sediment budget for the northern coast of Pärnu Bay (Kartau et al., 2011).

The key issue in surface wave hindcasts, particularly in the context of coastal processes where the rate of wave energy beaching may be as high as $H^{2.5}$ (where H is the wave height) and the wave propagation direction is equally important, is the proper choice of wind information. The estimates of long-term (> 1 year) changes to coastal processes are only reliable if the wind data set is maximally homogeneous in time. The potential local inaccuracies in the wind (and wave) representation are less critical in this context as they are expected to be smoothed out when averaging the transport over relative long time intervals. For this reason we prefer to use surface winds derived from geostrophic wind data. The wind data for the wave model (near-surface wind at 10 m level) was constructed from the Swedish Meteorological and Hydrological Institute (SMHI) geostrophic wind database with a spatial and

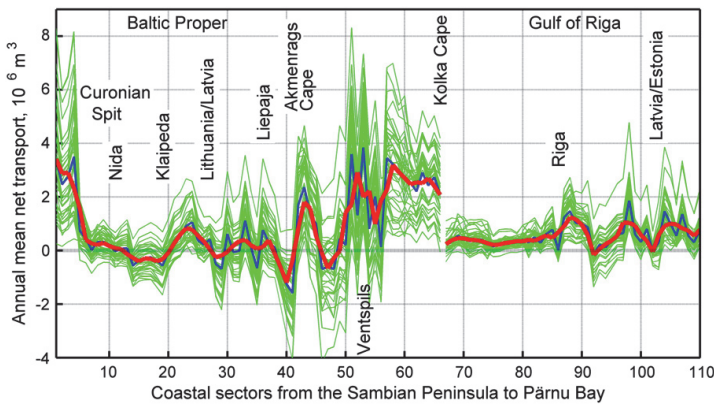


Fig. 5. Net potential sediment transport at the eastern Baltic Sea coast from the Sambian Peninsula to Pärnu Bay. Notations are the same as for Fig. 3.

temporal resolution of $1^\circ \times 1^\circ$ and 3 h, respectively (6 h before September 1977). The geostrophic wind speed was multiplied by 0.6 and the wind direction was turned counter-clockwise by 15° (Räämet and Soomere, 2010).

The basic wave properties (significant wave height H_s , peak period T_p and mean wave propagation direction) are hindcast at the centre of the closest grid points to the shore (Fig. 2). These properties and the resulting potential sediment transport were assumed to be constant within the hourly intervals. The modifications to the wave properties during the propagation from the centre of the grid point to the surf zone are estimated using linear wave theory and the assumption that the wave energy is concentrated in monochromatic plane waves with the period equal to the peak period and the direction of propagation equal to the hindcast mean propagation direction. Given the uncertainties in the wind data and wave hindcast, more exact calculations of transport properties based on the full wave spectrum or exact estimates of wave energy loss owing to wave-bottom interactions are not reasonable.

We use a rough estimate of wave shoaling by choosing the breaking index $\kappa=1$ and assuming that the breaking wave height H_b is simply equal to the modelled wave height. This simplified approach is suitable for our task as we are basically interested in spatial variations in the alongshore transport and inaccuracies in the estimates of the changes to the wave height in the nearshore are largely the same along the coast. The situation is different for the refraction. Its rate substantially depends on the initial approach angle of waves, which may largely vary along the coast. The change in the wave propagation direction is calculated using the Snell's law $\sin \theta/c_f = \text{const}$, where θ is the local angle between the wave crests and the isobaths and c_f is wave celerity (phase velocity). An application of this law requires an approximate solution to the dispersion relation, which is a transcendental equation for the wave number $k=2\pi/L$ or the wave length L

$$c_f = \frac{\omega}{k} = \frac{\sqrt{gk \tanh(kh)}}{k} = \sqrt{\frac{g \tanh(2\pi h/L)}{2\pi/L}} \quad (7)$$

A solution with an error not exceeding 1.7% is (Dean and Dalrymple, 2002, p. 90):

$$L = L_0 \left\{ \tanh \left[\left(2\pi \sqrt{\frac{h}{gT^2}} \right)^{3/2} \right] \right\}^{2/3} \quad (8)$$

where $L_0 = gT^2/(2\pi)$ is the length of waves with period T in deep water.

Both the discussed measures of transport express the volume of sediments carried through a cross-section of the beach in ideal conditions (that is, assuming unlimited amount of sand along the entire coast and ignoring all human interventions and coastal engineering structures) within a unit of time and thus drastically overestimate the actual transport rate along the Baltic Sea coast for most sections of the coast. The difference is particularly large in sections where the sediment layer is not continuous or has a limited thickness. The results are only conditionally applicable for stony coasts. For this reason we shall analyse not the sediment transport rate itself but the variations of the potential transport rate along the coast and in time. These variations carry key information about how probable is accumulation or erosion within a particular coastal sector and/or how the overall properties of alongshore sediment flux have changed over decades.

3. Bulk potential alongshore transport

The hindcast bulk sediment transport along the eastern Baltic Sea coast from the Sambian Peninsula to the entrance into Pärnu Bay (Fig. 3) reveals the existence of several sections with different transport properties. There are several sharp local variations in the transport rate evidently connected with the particular choice of the representation of

the local geometry of the coastline. The reasonably smoothed (over three adjacent coastal sectors called simply points below) bulk transport rate changes relatively smoothly along the entire coast of the Baltic Proper. A discontinuity occurs because of the abrupt turn of the coastline at the Kolka Cape.

The simulated intensity of bulk transport is the largest, up to $6 \times 10^6 \text{ m}^3/\text{year}$ in average and up to $10 \times 10^6 \text{ m}^3/\text{year}$ in single years, along the NW part of the Latvian coastline, to the north of the Akmenrags Cape. A short section of transport of almost the same intensity exists at the westernmost border of the study area on the Sambian Peninsula. The transport rate is much lower, around $10^6 \text{ m}^3/\text{year}$ in the Gulf of Riga, with somewhat larger values up to $2 \times 10^6 \text{ m}^3/\text{year}$ along the eastern coast of this water body.

Fig. 3 signifies that two coastal sections apparently host clearly higher intensity of coastal processes: the section of the Sambian Peninsula adjacent to the Curonian Spit and the NW coast of Latvia. The largest local variations in the bulk transport rate occur in the westernmost part of the Curonian Spit (sector 5 in Fig. 3 where the transport rate drastically decreases over a few km) and around the Akmenrags Cape (near sector 41), to the north of which the transport rate rapidly increases. A comparable increase occurs slightly to the south of Ventspils (near sector 50) while further to the northeast of this point the bulk transport decreases to some extent.

The difference in the long-term wave heights between these areas and the rest of the coastline of the Baltic Proper is fairly minor (Räämet and Soomere, 2010). Therefore, the variations in the intensity of bulk transport stem from the gradual change in the wave approach angle along this segment of the shore (Fig. 1). This change is mainly caused by variations in the coastline orientation. Its orientation changes by more than 60° along the section of the Latvian coast from the Lithuanian border up to Ventspils. The location of the main and secondary maxima of the distributions of the frequency of occurrence of wave propagation directions (to the north-northeast and south-southeast, respectively) vary much less, no more than by ± 1 frequency bin ($\pm 15^\circ$) for the main maximum and within just one frequency bin for the secondary maximum (Fig. 4).

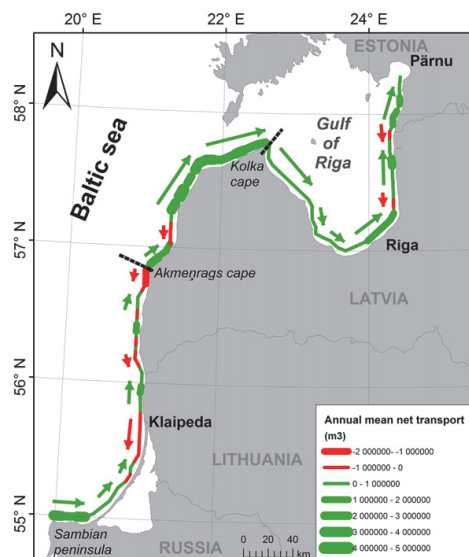


Fig. 6. Simulated annual mean net potential transport rate along the study area for 1970–2007.

Areas with a more or less constant bulk transport rate are the Curonian Spit, the western coast of the Gulf of Riga and the Latvian section of the eastern coast of this gulf. A large part of the difference between the intensity of bulk transport at the eastern and western coasts of the Gulf of Riga comes from the fact that waves driven by the most frequent (SW) winds propagate offshore from the western coast.

The interannual variability of the bulk transport rate at particular sectors is reasonable. Its extreme pointwise values are roughly twice as large as the long-term mean while the minimum levels are about a half of the long-term ones. The level of interannual variability is roughly the same for the coasts of the Baltic Proper and the Gulf of Riga.

4. Simulated net potential alongshore transport

The intensity of net alongshore transport is a quantity with sign. Additionally to the (scalar) wave energy, it also accounts for the balance of wave energy flux approaching a particular coastal sector from different directions of the normal to the coast. The overall appearance of the pointwise net sediment transport (Fig. 5) first confirms the well known fact that the sediment transport is largely directed to the east, NE or north along the open Baltic Sea coast and counter-clockwise along the western, southern, and eastern coasts of the Gulf of Riga (Eberhards et al., 2009; Pruszek, 2004; Žaromskis and Gulbinskas, 2010). The annual mean values of this transport vary in a much larger range than those for the bulk transport: from values close to zero up to about 3×10^6 m³/year for the long-term average and up to 8×10^6 m³/year for single years. The locations for the most intense net transport are the same as those hosting strong bulk transport: the Sambian Peninsula and a coastal section to the NE of the Akmenrags Cape.

The simulated values of net transport may be, as discussed above, severely overestimated for sectors that have limited amount of sand (cf. Fröhle and Dimke, 2008). They are, however, realistic for predominantly sandy sectors. For example, according to historical estimates of R. Knaps based on the amount of dredging at large ports in Latvia (Liepaja and Ventspils), the average capacity of alongshore transport has been in the range of $(0.5\text{--}1) \times 10^6$ m³/year (Eberhards, 2003). Our estimate of the long-term average rate is about 0.86×10^6 for the sections along the Baltic Proper, 0.4×10^6 at Liepaja and about 2×10^6 at Ventspils. Similar transport rates at Liepaja and at Ventspils have been also evident in 1990–2004 (Eberhards et al., 2009; Fig. 9).

The direction of net transport is highly variable along the coast of the Baltic Proper. Not surprisingly, there are several sections in which the annual mean transport rate has been positive (directed counter-

clockwise along the coast) over all the 38 years. These are the region of the Sambian Peninsula and a short section of the NW coast of Latvia (Fig. 5) that host also the most intense bulk transport rates. Several smaller sections hosting exclusively transport to the north are located along the eastern coast of the Gulf of Riga. The net transport, albeit relatively weak, is almost completely to the south along the SW coast of the Gulf of Riga (cf. Eberhards et al., 2009). In all other sectors the net transport direction has been variable.

The simulated patterns of net transport reveal, as expected, much more detailed structure than similar historical estimates constructed based on a limited amount of data (Eberhards, 2003; Ulst, 1998). All these estimates demonstrate a high capacity of littoral flow to the north or NE along the NW coast of the Kurzeme Peninsula and a much less capacity in the vicinity of Liepaja (see also Eberhards et al., 2009). The estimates for the magnitude and even direction of this flow (Fig. 6), differ, however for most of the Curonian Spit, the area between Klaipeda and the Akmenrags Cape, and for certain sections of the eastern coast of the Gulf of Riga. According to the historical estimates of R. Knaps, littoral flow along the Lithuanian and Latvian coasts of the Baltic Proper was always directed to the north, with possible interruptions at Klaipeda Strait and in the vicinity of the large ports. The same structure is evident in early simulations based on a few data points (Eberhards, 2003).

Most probably, part of the listed differences stem from a different spatial resolution of the simulations. An extensive section of southwards littoral flow along the eastern coast of the Gulf of Riga on historical maps of R. Knaps, however, suggests that quite large changes to the structure of net transport may have occurred owing to local changes in the wind climate in the recent past. The evidence about such changes in the wave climate (incl. the wave approach directions) along certain sections of the NE Baltic Sea coast is fragmented (Räämet et al., 2010; Soomere and Räämet, 2011; Suursaar, 2010). Also, their spatial extension is not clear. Another reason for discrepancies in the Gulf of Riga is that the wave model was run without taking into account the ice cover in winters. This may lead to considerable difference between the simulated and actual wave climates during winters. While this might not be so important for the southern Baltic Proper, this could explain part of the differences compared to the previously published analysis in the Gulf of Riga.

The pointwise rate of the net and bulk transport (Fig. 7) additionally characterises the persistence of the transport direction in different sections of the study area. The annual mean transport has been always to the east along the Sambian Peninsula although in some years the net flux is only about 10% of the bulk transport. The coasts of the Curonian Spit, Lithuania and Latvia, up to Ventspils are mostly characterised by

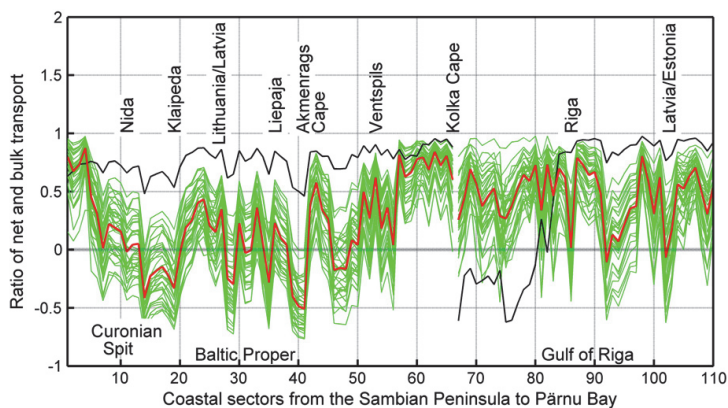


Fig. 7. The ratio of net and bulk potential sediment transport at the eastern Baltic Sea coast in single years (thin green line) and in average over 1970–2007 (bold red line). Solid black line indicates the ratio for 1984 when the transport to the north predominates in the entire study area.

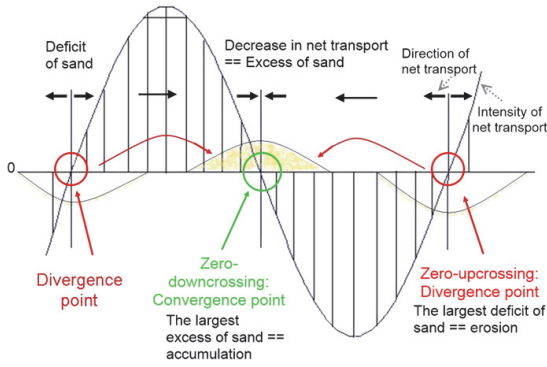


Fig. 8. The relationship between the intensity (sinusoidal line) and direction (horizontal arrows) of alongshore net transport and likely accumulation/erosion areas.

high variability of the net transport. There are, however, a few short sections (e.g. at both sides of the Akmenrags Cape) where the transport has been almost unidirectional. The sections around Ventpils may reveal different transport directions for different years. The transport is highly unidirectional along the NW coast of the Kurzeme Peninsula. Somewhat surprisingly, the ratio in question is quite moderate along the SE coast of the Gulf of Riga, probably owing to strong impact of relatively infrequent N–NW winds.

The transport may be almost unidirectional in single years. For example, in 1984 more than 50% of the sediment brought into motion was carried to the north along the coasts of the Baltic Proper and the Gulf of Riga. Although bulk sediment transport over the entire study

area was at a long-term average level in this year, the net transport was almost three times as large as its average value.

5. Divergence and convergence of net alongshore transport

The mutual location of lines characterising net transport along the study area within single years in Figs. 5 and 7 suggests that the sections hosting the reversal of the overall counter-clockwise pattern as well as the locations of large alongshore gradients in the net sediment flux are quite stable over many years. This property makes it possible to estimate the typical areas for (long-term) erosion and accumulation based on the alongshore variations in the net sediment transport. For example, if the net transport intensity increases along the direction of the littoral flow, then waves tend to carry away more sediment from such sectors than arrives from remote areas. Such beach sectors (in which the net transport diverges) generally suffer from sediment deficit and their erosion is highly probable (Fig. 8). Contrariwise, if the magnitude of sediment flux decreases along its net direction, waves bring to each such sector (in which the flux converges) more sediment than is carried away and eventually accumulation will occur (cf. Hanson and Larson, 2009). The intensity of erosion or accumulation depends on the rate of alongshore changes in the sediment flux, equivalently, on the slope of the relevant line in Fig. 8. Another key quantity is the above-discussed ratio of the local rates of net and bulk transport. For each coastal sector it characterises to some extent how vulnerable a section is with respect to changes at a particular side of this sector.

The most probable and systematic (albeit not necessarily the most intense) accumulation and erosion areas can be associated with the zero-crossings of the alongshore distribution of the net potential transport. For the coordinate system used in Fig. 8 the zero-downcrossing points indicate the convergence (accumulation)

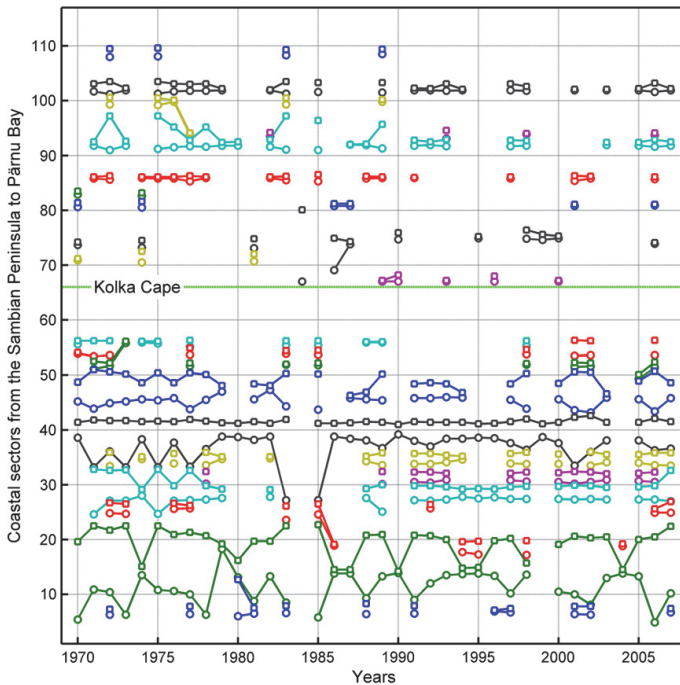


Fig. 9. Numerically simulated location of zero-crossing points in the net potential sediment transport along the study area in 1970–2007: circles – convergence points; squares – divergence points.

areas and zero-upcrossing points show the divergence (potential erosion) areas.

Fig. 5 demonstrates that the locations of zero-crossings of the net transport may considerably vary in different years. A particularly interesting aspect is the range of changes of these locations. The relevant intervals cover the areas where intense accumulation or erosion may occur in a particular wind climate and for the existing configuration of the coastline. Fig. 9 presents spatio-temporal dynamics of the set of the zero-crossing points along the study area. The points are calculated based on the alongshore distribution of the net sediment transport for each year (green lines in Fig. 5). As in Fig. 3, there is a discontinuity at the Kolka Cape. Most of the persistent divergence and convergence points are situated at the coast of the Baltic Proper while similar points along the coasts of the Gulf of Riga are evident only in certain years.

Within the simulation period, the sediment transport was exceptional in the years 1984 and 2004. It was mostly unidirectional to the north in 1984 and to the south in 2004. These two years were not exceptional in terms of annual mean wave parameters (such as the wave height or the distribution of wave approach directions) at Lithuanian observation sites (Zaitseva-Pärnaste et al., 2011). Remarkably, the annual mean wave height was exceptionally low at Vilsandi for these two years: it reached the lowest values for the periods of 1954–1995 and 1995–2008, respectively (Zaitseva-Pärnaste et al., 2011).

Interestingly, some zero-crossing points keep their location over many years (Fig. 9) while other similar points exert large shifts along the coast (Fig. 10). The extent of relocation indicates the range of the likely erosion or accumulation area associated with the long-term sediment transport. The largest amplitude of such repositioning has the convergence point in the region of the Curonian Spit. Over years, its location has varied from the western end of the spit at Zelenogradsk up to the northern tip of the spit at the Klaipeda Strait. This point moves along the entire spit cyclically, every three to five years (Fig. 11). Remarkably, the range of its variations exactly coincides with the extension of this spit. A natural consequence of such a character of variations is that the entire Curonian spit regularly receives some sand under the simulated wave climate although its certain sections may suffer from erosion (Gilbert, 2008; Zhamoida et al., 2009). In other words, the presented results suggest that the Curonian Spit is in almost perfect equilibrium under the simulated contemporary wave climate. This conjecture is not fully unexpected because the spit has been created over a few 1000s of years. An adjacent divergence point, usually located near Klaipeda, occasionally affects the northern part of the spit, which still is mostly stable and predominantly experiences accumulation (Žaromskis and Gulbinskas, 2010). Its regular impact is consistent with the observations that the coastal sections at and to the north of Klaipeda regularly suffer from sediment deficit (Gilbert, 2008).

Two zero-crossing points (one convergence and one divergence point) between Klaipeda and Liepaja have very limited range of relocations. Their presence apparently results from the local changes to the orientation of the coastline. As they are evident only in selected years, their role in the large-scale sediment transport pattern evidently is minor. The presence of another convergence point in the vicinity of Liepaja may be associated with the evident local straightening of the coastline in this region, a process that apparently played a role in the formation of the Liepaja Lake from a former coastal lagoon. This lake was formed in the Littorina Sea period. Between the lake and sea several barriers and other accumulation forms of Littorina Sea are still evident. The coastal area separating the lake from the Baltic Proper also contains contemporary (fore)dune ridges over Littorina Sea period landforms. The sea shore near the Liepaja Lake shows features of naturally restoring foredune and accretion with slowly growing foredunes (Ulsts, 1998).

Two other zero-crossing points to the north of the Akmenrags Cape are also present in selected years, apparently depending on short-time variations in the wind patterns.

The zero-crossing points at the coasts of the Gulf of Riga are only evident in a few years whereas their presence has decreased in the recent

past. This tendency may indicate certain changes to the wave climate in this region where the locally generated waves govern the evolution of the coasts and where possible changes to the wind and wave direction (noticed in the Estonian mainland (Jaagus, 2009; Jaagus and Kull, 2011) and in NE Estonia (Räämet et al., 2010) to the north of the study area, and in the southern Baltic Sea (Lehmann et al., 2011) to the south of the study area) have a stronger impact on the coastal processes than in the Baltic Proper. In particular, the changes to the frequency of appearance of the points in question show that the wave climate may have exerted appreciable changes since the 1970s.

Even more interesting is the question whether or not more or less stable points of divergence exist in the study area. The net transport from such points (or from short sections around such points) is almost always directed so that sediments are not carried through such sections. In other words, such points serve as a sort of invisible barrier for sediment transport.

Figs. 9 and 10 demonstrate that the location of the divergence point near the Akmenrags Cape almost does not change. This point is clearly evident in almost all years (except 1984 when none of the usual zero-crossing points was evident and 2004 when only a couple of such points were present). Although sediment may pass such a sector during certain exceptional time intervals, such points generally serve as major natural barriers for the sediment flow. Consequently, this divergence point apparently divides the Latvian coast of the Baltic Proper into two almost completely disconnected sediment compartments. This feature evidently stems from match of the change in the overall orientation of the coastline by about 15° at the Akmenrags Cape with the specific two-peak structure of predominant winds in the northern Baltic Proper and may change in other wind and wave climates.

6. Conclusions and discussion

The performed analysis first confirms several well-known properties of net sediment flux along the eastern Baltic Sea coast such as the mostly counter-clockwise and largely unidirectional transport of available

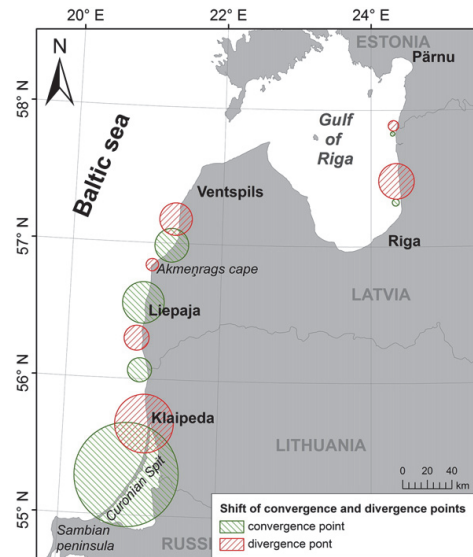


Fig. 10. The range of relocation of persistent zero-crossing points in the net potential sediment transport along the study area in 1970–2007. The range for convergence areas indicates the likely accumulation domain and the range for divergence areas the likely erosion domain. The diameter of the circles indicates the maximum excursion of the zero-crossing points in 1970–2007.

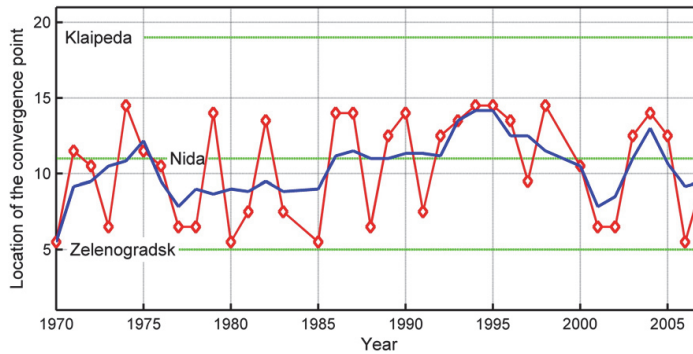


Fig. 11. Relocation of the major convergence point of the net potential sediment flux (red rhombi) and its three-year moving average (solid blue line) along the Curonian Spit in 1970–2007. Thin green horizontal lines indicate the location of the western (Zelenogradsk) and northern (Klaipeda) ends of the spit and the position of Nida on the spit.

sediment along the entire domain from the Sambian Peninsula up to Pärnu Bay. Also, the location of the apparent major erosion areas such as the Sambian Peninsula and accumulation regions such as the vicinity of the Kolka Cape, and high variations in the intensity of both net and bulk sediment transport along the eastern coast of the Baltic Proper match well the existing observational evidence. The simulated potential net transport intensity is largely overestimated for stony coastal sections but close to realistic values of transport for mostly sandy areas. The numerically simulated areas of systematic erosion and accumulation also generally match the observed processes.

The calculations showed some further light to these properties of sediment transport that are invariant with respect to the exact magnitude of transport. Local variations in the orientation of the coastline result in a high interannual variability of the net transport. The transport apparently may be reversed in selected years along most of the Latvian coast of the Baltic Proper and also along the eastern coast of the Gulf of Riga. The transport (in terms of annual average) is almost continuously unidirectional only along short sections of the Sambian Peninsula and the NW coast of the Kurzeme Peninsula where both bulk and net transport intensity are the largest. The described features suggest that the entire study area is currently in the straightening process. A major discontinuity in the sediment flow at the Kolka Cape is consistent with the rapid accumulation in this region.

The spatial pattern of the simulated net transport contain several persistent divergence and convergence areas that separate regions with oppositely directed net sediment flux and correspond to the most likely erosion and accumulation regions. One such highly persistent accumulation region moves cyclically over the entire Curonian Spit. This peculiarity suggests that this landform is almost in equilibrium under the numerical representation of the existing wind climate. A highly persistent area of divergence of net transport and thus a likely erosion domain exists at the Akmenrags Cape. Its presence suggests that sediments usually do not pass this cape. Consequently, it is likely that the eastern coast of the Baltic Proper hosts two almost separated sedimentary compartments in the contemporary wave climate.

Finally, our simulations expose that the numerically evaluated sediment transport rates, in average, up to a few times exceed the transport rates estimated from local observations. A part of the difference is related with the presence of limited amount of mobile sediments in many coastal sections. The CERC model (and some other models using the same principles such as GENESIS) drastically overestimates the bulk and net transport rates in such areas (Fröhle and Dimke, 2008) and generally cannot be used for morphodynamical projections. For this reason we have only analysed the parameters and features (sections with the most intense transport, direction of the net transport, divergence and convergence points) that are invariant with respect to the magnitude

of transport rates and that are governed by the alongshore variations in these rates. Another reason for discrepancies, especially in the Gulf of Riga, is that the presence of sea ice was ignored. This may lead to considerable differences between our simulated and actual wave climate during winters.

The presence of winter ice and the scarcity of mobile sediment in some coastal sections obviously affect the intensity of alongshore transport. While more comprehensive accounting for these factors may add certain details to the presented picture, it is not likely that the established basic patterns would change. Still, the systematic deviation of the numerically evaluated and observed transport rates even in mostly sandy areas of the eastern Baltic Sea calls for a study towards identification of the source of deviations and towards the development of more adequate sediment transport models for the Baltic Sea conditions.

Acknowledgements

The research was supported by the targeted financing by the Estonian Ministry of Education and Research (grant SF0140007s11), Estonian Science Foundation (grant No 9125) and the European Union via a support to the Estonian Centre of Excellence CENS from the European Regional Development Fund and by the DoRa international PhD studentships for M.Viška. The authors are deeply grateful to Alexander von Humboldt Foundation for granting the research stay in the Institute for Coastal Research, Geesthacht, in June–September 2011.

References

- Broman, B., Hammarklint, T., Rannat, K., Soomere, T., Valdmann, A., 2006. Trends and extremes of wave fields in the north-eastern part of the Baltic Proper. *Oceanologia* 48, 165–184 (S).
- Dean, R.G., Dalrymple, R.A., 2002. *Coastal processes with engineering applications*. Cambridge University Press, Cambridge (475 pp.).
- Eberhards, G., 2003. The sea coast of Latvia. University of Latvia, Riga (in Latvian).
- Eberhards, G., Lapinskis, J., 2008. Processes on the Latvian coast of the Baltic Sea. *Atlas*. University of Latvia, Riga (64 pp.).
- Eberhards, G., Lapinskis, J., Saldupe, B., 2006. Hurricane Erwin 2005 coastal erosion in Latvia. *Baltica* 19 (1), 10–19.
- Eberhards, G., Grīne, I., Lapinskis, J., Purgalis, I., Saldupe, B., Torklere, A., 2009. Changes in Latvia's seacoast (1935–2007). *Baltica* 22 (1), 11–22.
- Fröhle, P., Dimke, S., 2008. Analysis of Potential Long Shore Sediment Transport at the Coast of Mecklenburg-Vorpommern. In: Zanke, U., Roland, A., Sängler, N., Wiesemann, J.U., Dahlem, G. (Eds.), *Proc. Chinese-German Joint Symposium on Hydraulic and Ocean Engineering*, Darmstadt, Germany, August 24–30, 2008. University of Darmstadt, pp. 161–164.
- Gilbert, G. (Ed.), 2008. State of the coast of the South-East Baltic: an indicators-based approach to evaluating sustainable development in the coastal zone of the South East Baltic Sea. P.P. Shirshov Institute of Oceanology, Atlantic Branch, Kaliningrad (164 pp.).
- Gudelis, V., 1967. The morphogenetic types of Baltic Sea coasts. *Baltica* 3, 123–145 (in Russian).

- Gudelis, V., Kirlyš, V., Močiėkienė, S., 1977. Littoral drift regime and dynamics along the eastern coast of the Baltic Sea in the off-shore zone of the Curonian Spit according to the data of 1956–1974. *Trans. Lith. Acad. Sci. B* 4 (101), 123–128 (in Russian).
- Hanson, H., Larson, M., 2009. Implications of extreme waves and water levels in the southern Baltic Sea. *J. Hydraul. Res.* 46 (2), 292–302.
- Harff, J., Meyer, M., 2011. Coastlines of the Baltic Sea – zones of competing between geological processes and a changing climate: examples from the southern Baltic. In: Harff, J., Björck, S., Hoth, P. (Eds.), *The Baltic Sea Basin. Central and Eastern European Development Studies*. Springer, Heidelberg, pp. 149–164.
- Jaagus, J., 2009. Long-term Changes in Frequencies of Wind Directions on the Western Coast of Estonia. In: Kont, A., Tõnisson, H. (Eds.), *Climate change impact on Estonian coasts*, Publication 11/2009. Institute of Ecology, Tallinn University, pp. 11–24 (in Estonian).
- Jaagus, J., Kull, A., 2011. Changes in surface wind directions in Estonia during 1966–2008 and their relationships with large-scale atmospheric circulation. *Estonian J. Earth Sci.* 60 (4), 220–231.
- Kartau, K., Soomere, T., Tõnisson, H., 2011. Quantification of sediment loss from semi-sheltered beaches: a case study for Valgerand Beach, Pärnu Bay, the Baltic Sea. *J. Coast. R. Spec. Issue* 64, 100–104.
- Kelpšaitė, L., Parnell, K.E., Soomere, T., 2009. Energy pollution: the relative influence of wind-wave and vessel-wave energy in Tallinn Bay, the Baltic Sea. *J. Coast. R. Spec. Issue* 56, 812–816.
- Kelpšaitė, L., Dailidiene, I., Soomere, T., 2011. Changes in wave dynamics at the south-eastern coast of the Baltic Proper during 1993–2008. *Boreal Environ. Res.* 16 (Suppl. A), 220–232.
- Knaps, R.J., 1966. Sediment transport near the coasts of the Eastern Baltic. Development of sea shores under the conditions of oscillations of the Earth's crust, Valgus, Tallinn, pp. 21–29 (in Russian).
- Knaps, R., 1982. Effects of shoreline unevenness on sediment drift along the shore. *Baltica* 7, 195–202 (in Russian).
- Komen, G.J., Cavaleri, L., Donelan, M., Hasselmann, K., Hasselmann, S., Janssen, P.A.E.M., 1994. *Dynamics and modelling of ocean waves*. Cambridge University Press, Cambridge (532 pp.).
- Lehmann, A., Getzlaff, K., Harlass, J., 2011. Detailed assessment of climate variability in the Baltic Sea area for the period 1958 to 2009. *Clim. Res.* 46 (2), 185–196.
- Leppäranta, M., Myrberg, K., 2009. *Physical oceanography of the Baltic Sea*. Springer Praxis, Berlin, Heidelberg (378 pp.).
- Orviku, K., Jaagus, J., Kont, A., Ratas, U., Rivis, R., 2003. Increasing activity of coastal processes associated with climate change in Estonia. *J. Coast. Res.* 19 (2), 364–375.
- Pruszk, Z., 2004. Polish coast – two cases of human impact. *Baltica* 17 (1), 34–40.
- Räämet, A., Soomere, T., 2010. The wave climate and its seasonal variability in the northeastern Baltic Sea. *Estonian J. Earth Sci.* 59 (1), 100–113.
- Räämet, A., Soomere, T., Zaitseva-Pärnaste, I., 2010. Variations in extreme wave heights and wave directions in the north-eastern Baltic Sea. *Proc. Estonian Acad. Sci.* 59 (2), 182–192.
- Ryabchuk, D., Kolesov, A., Chubarenko, B., Spiridonov, M., Kurennoy, D., Soomere, T., 2011. Coastal erosion processes in the eastern Gulf of Finland and their links with geological and hydrometeorological factors. *Boreal Environ. Res.* 16 (Suppl. A), 117–137.
- Sepp, M., Post, P., Jaagus, J., 2005. Long-term changes in the frequency of cyclones and their trajectories in Central and Northern Europe. *Nord. Hydrol.* 36 (4–5), 297–309.
- Soomere, T., Healy, T.R., 2011. On the dynamics of “almost equilibrium” beaches in semi-sheltered bays along the southern coast of the Gulf of Finland. In: Harff, J., Björck, S., Hoth, P. (Eds.), *The Baltic Sea basin. Central and Eastern European Development Studies*. Springer, Heidelberg, pp. 255–279.
- Soomere, T., Keevallik, S., 2001. Anisotropy of moderate and strong winds in the Baltic Proper. *Proc. Estonian Acad. Sci. Eng.* 7 (1), 35–49.
- Soomere, T., Räämet, A., 2011. Spatial patterns of the wave climate in the Baltic Proper and the Gulf of Finland. *Oceanologia* 53 (1–II), 335–371.
- Soomere, T., Kask, A., Kask, J., Healy, T.R., 2008. Modelling of wave climate and sediment transport patterns at a tideless embayed beach, Pirita Beach, Estonia. *J. Mar. Syst.* 74, S133–S146 (S).
- Soomere, T., Viška, M., Lapinskis, J., Räämet, A., 2011. Linking wave loads with the intensity of erosion along the coasts of Latvia. *Estonian J. Eng.* 17 (4), 359–374.
- Soomere, T., Weisse, R., Behrens, A., 2012. Wave climatology in the Arkona Basin, the Baltic Sea. *Ocean Sci.* 8 (2), 287–300.
- Suursaar, Ü., 2010. Waves, currents and sea level variations along the Letipea-Sillamäe coastal section of the southern Gulf of Finland. *Oceanologia* 52 (3), 391–416.
- Suursaar, Ü., Jaagus, J., Kont, A., Rivis, R., Tõnisson, H., 2008. Field observations on hydrodynamic and coastal geomorphic processes off Harilaid Peninsula (Baltic Sea) in winter and spring 2006–2007. *Estuar. Coastal Shelf Sci.* 80 (1), 31–41.
- Tõnisson, H., Suursaar, Ü., Orviku, K., Jaagus, J., Kont, A., Willis, D.A., Rivis, R., 2011. Changes in coastal processes in relation to changes in large-scale atmospheric circulation, wave parameters and sea levels in Estonia. *J. Coast. Res. Spec. Issue* 64, 701–705.
- Ulsts, V., 1998. *Latvian Coastal Zone of the Baltic Sea*. Riga (96 pp., in Latvian).
- USACE, 2002. *Coastal Engineering Manual*. Department of the Army. U.S. Army Corps of Engineers (Manual No. 1110-2-1100).
- Zaitseva-Pärnaste, I., Suursaar, Ü., Kullas, T., Lapimaa, S., Soomere, T., 2009. Seasonal and long-term variations of wave conditions in the northern Baltic Sea. *J. Coast. Res. Spec. Issue* 56, 277–281.
- Zaitseva-Pärnaste, I., Soomere, T., Tribštok, O., 2011. Spatial variations in the wave climate change in the eastern part of the Baltic Sea. *J. Coast. Res. Spec. Issue* 64, 195–199.
- Žaromskis, R., Gulbinskas, S., 2010. Main patterns of coastal zone development of the Curonian Spit, Lithuania. *Baltica* 23 (2), 149–156.
- Zemlyš, P., Fröhle, P., Gulbinskas, S., Davulienė, L., 2007. Near-shore evolution model for Palanga area: feasibility study of beach erosion management. *Geologija* 57, 45–54.
- Zhamoïda, V., Ryabchuk, D.V., Kropatchev, Y.P., Kurennoy, D., Boldyrev, V.L., Sivkov, V.V., 2009. Recent sedimentation processes in the coastal zone of the Curonian Spit (Kaliningrad region, Baltic Sea). *Z. Dtsch. Gesell. Geowiss.* 160 (2), 143–157.
- Zhang, W.Y., Harff, J., Schneider, R., Wu, C.Y., 2010. Development of a modelling methodology for simulation of long-term morphological evolution of the southern Baltic coast. *Ocean Dyn.* 60 (5), 1085–1114.

Paper IV

Viška M., Soomere T. 2013. Simulated and observed reversals of wave-driven alongshore sediment transport at the eastern Baltic Sea coast. *Baltica*, 26(2), 145–156.

**Simulated and observed reversals of wave-driven alongshore sediment transport at the eastern Baltic Sea coast***Maija Viška, Tarmo Soomere*

Viška, M., Soomere, T. 2013. Simulated and observed reversals of wave-driven alongshore sediment transport at the eastern Baltic Sea coast. *Baltica*, 26 (2), 145–156. Vilnius. ISSN 0067-3064.

Manuscript submitted 21 August 2013 / Accepted 21 November 2013 / Published online 11 December 2013
© Baltica 2013

Abstract This paper aims to analyse the sensitivity of patterns of numerically simulated potential sediment transport along the eastern Baltic Sea coast. The study area extends from the Sambian (Samland) Peninsula to Pärnu Bay in the Gulf of Riga. The magnitudes of net and bulk transport depend largely on how the shoaling and refraction of the waves are resolved. The qualitative patterns of net and bulk sediment transport are almost insensitive with respect to the details of wave transformation in the nearshore and with respect to grain size. The overall counter-clockwise transport along the study area contains two persistent reversals along the coast of the Baltic Sea proper and two frequently recurring reversals along the eastern margin of the Gulf of Riga. Individual years with normal levels of wind speed may host completely different patterns of sediment transport. The location of the most persistent convergence and divergence areas of the net transport acceptably matches the granulometric composition of the nearshore seabed up to a few km from the shoreline.

Keywords • *Alongshore sediment transport* • *Coastal processes* • *CERC model* • *Geological composition of the nearshore* • *Baltic Sea* • *Gulf of Riga*

✉ *Maija Viška, Tarmo Soomere (soomere@cs.ioc.ee), Institute of Cybernetics at Tallinn University of Technology, Akadeemia tee 21, EE-12618 Tallinn, Estonia.*

INTRODUCTION

The study area – the eastern coast of the Baltic Sea, from the Sambian (Samland) Peninsula in Kaliningrad District, Russia, to Pärnu Bay in Estonia – is an example of a sequence of partially connected sedimentary compartments (Knaps 1966; Eberhards 2003). Single sediment grains may be, theoretically, transported to distance of about 700 km along this stretch. It is usually described in a generalized manner as a more or less continuous sedimentary system (Žaromskis, Gulbinskas 2010) in which the sediment is transported counter-clockwise (Knaps 1966; Gudelis *et al.* 1977; Eberhards *et al.* 2009) and where the basic process is the straightening of the coastline (Knaps 1966; Gudelis 1967; Ulsts 1998; Eberhards 2003).

Early estimates of the magnitude and direction of the wave-driven alongshore sediment flux in the eastern Baltic Sea were obtained using an improved

Munch-Petersen formula (Munch-Petersen 1936; Knaps 1938, 1965) and upgraded in later years (Ulsts 1998; Lapinskas 2010). The results commonly match the historical observations of sediment transport. The simulated long-term net sediment transport is generally counter-clockwise, from the south to the north along the Lithuanian and Latvian coasts until the Kolka Cape and further counter-clockwise in the Gulf of Riga.

In a closer view, however, this picture has a number of interesting and nontrivial features. Both the nature and typical grain size of sediments change considerably over this stretch (Ulsts 1998; Kalnina *et al.* 2000; Saks *et al.* 2007). The Curonian Spit is entirely sandy. The western Courland (Kurzeme) coasts often consist of gravel with pebbles and boulders, or of sand and gravel with some pebbles. In the contrary, the coasts of the Gulf of Riga mostly consist of mixed sediments and have much finer-grained sand.

The intensity of erosion and accumulation along the study area addressed in many studies, in particular, based on the analysis of shoreline changes (Gudelis *et al.* 1977; Eberhards, Lapinskis 2008; Eberhards *et al.* 2009; Kartau *et al.* 2011, among others). The sediment transport, coastal processes in general and erosion in particular are usually more intense along the open Baltic Sea coast than in the Gulf of Riga. The local deviations of the littoral flow from the above-described general pattern have been analysed using both observational (Gilbert 2008; Eberhards *et al.* 2009; Zhamoida *et al.* 2009) and numerically simulated data sets (Ulsts 1998; Zemlys *et al.* 2007; Viška, Soomere 2012; Soomere, Viška 2013). The alongshore transport is the most intense along the north-eastern coast of the Courland Peninsula and in the western part of the Sambian Peninsula.

Several eminent headlands like the Akmenrags Cape (Stone Cape in some sources), Ovisrags Cape or Kolka Cape may serve as natural barriers for the alongshore sediment flow (Eberhards 2003). A part of sediment brought into motion by waves may be transported away from the coast at these capes and headlands (Eberhards 2003). The direction of the alongshore net transport, however, may be variable, at least within single years. Numerical simulations signal the presence of an end station of the transport at the Kolka Cape, a major divergence area of net transport in the vicinity of the Akmenrags Cape and a pair of convergence and divergence areas near Klaipėda (Soomere, Viška 2013; U. Bethers, pers. comm. 2013). This means that several segments may host clockwise net transport (called reversals below) on both the coasts of the Baltic Proper and the eastern Gulf of Riga, and that the sedimentary systems along the Baltic Proper may be only partially connected. The situation is different along the Curonian Spit. It hosts a highly mobile convergence area that literally “feeds” with sand different parts of the spit in different years and keeps the entire landform in an almost perfect equilibrium (Viška, Soomere 2012).

It is natural to expect that the described features of the simulated alongshore transport become evident in the composition of the nearshore and coastal sediments. The relevant comparisons have only been performed near large harbours where the coastal engineering structures have stopped the littoral flow or where extensive dredging has been necessary to maintain the required depth of the fairway and harbour basins (Eberhards 2003; Eberhards *et al.* 2009). Such comparisons are not straightforward as the seabed in the nearshore may consist of sand masses formed in the past or may reflect morphological structures (tombolo, salient) formed owing to certain local features. Moreover, the comparisons have to cover a long enough time interval in order to eliminate the impact of local features such as the formation and gradual relocation of sand bars. Their dynamics often resembles interspersed periods of

erosion (during the formation of a sand bar) and accumulation (when a sand bar approaches the waterline) (Ulsts 1998). Also, the availability of mobile sediments is limited in many sections of the coast.

It is thus not surprising that numerical estimates of the potential alongshore transport (e.g., Viška, Soomere 2012) by several times exceed the observed transport intensity. An obvious reason for this mismatch is the use of the significant wave height to characterise the energy flux of beaching waves in the version of the CERC (Coastal Engineering Research Centre) model that was tuned for the root mean square wave height (Soomere, Viška 2013). While designed to compensate for a systematic under-estimation of the modelled wave heights (Räämet, Soomere 2010), doing so led to severe over-prediction of the alongshore transport rate.

The implications of the inability of numerical wave models to properly represent the directional structure of approaching waves (cf. Räämet *et al.* 2010) and the use of simplified approximations for wave refraction and shoaling on the simulated transport rate are less clear. As the details of the nearshore bathymetry are usually poorly known, they are commonly ignored (e.g., Zemlys *et al.* 2007) and the isobaths of the shallow-water region are assumed to be parallel to the coast. It is also customary to assume that the incidence angle of open-ocean waves at the breaker line is small and that the joint impact of refraction and shoaling can be evaluated using an implicit expression (Dean, Dalrymple 1991). The study area, however, hosts a substantial amount of wave fields that propagate almost along the coast. Their refraction is accompanied by a considerable decrease in the wave height. This feature motivated to employ a simplified scheme for the shoaling-driven changes and to resolve the refraction process in detail (Viška, Soomere 2012; Soomere, Viška 2013). For larger incidence angles this scheme may overestimate both the breaking-wave height and the approach angle at the breaker line.

It is likely that the described reasons of the mismatch between the simulated and observed sediment transport rates do not substantially modify the qualitative features of transport. In particular, they apparently do not affect the pattern of convergence and divergence areas of sediment flux. In this paper, authors address the problem of stability of various qualitative features of numerically simulated potential sediment transport along the eastern Baltic Sea coast using the CERC approach. The focus is on the impact of above-discussed aspects that were either ignored in the previous research or only approximately accounted for. First of all, the joint impact of refraction and shoaling of waves along their propagation from the grid cells of the wave model until the breaker line is accurately resolved based on the linear wave theory. Doing so makes it possible to adequately represent the impact of waves that approach the study area under large incidence angles. Further, the calculations are repeated

with several values of the typical grain size and using different specifications of the modelled wave height.

These efforts demonstrate that the qualitative patterns of the alongshore sediment transport are stable with respect to changes in the model and its input data. It is thus likely that these patterns become evident in the composition of nearshore sediments. The coastline of most of the study area has considerably advanced towards the sea since the Litorina Sea (Eberhards *et al.* 2009), therefore, the composition of nearshore (at least down to the closure depth and to some extent offshore) is largely governed by the wave-driven sediment relocation. The seabed sediments should thus mirror not only the overall intensity of coastal processes (Soomere *et al.* 2013b) but also the general pattern of sediment motions. For example, the vicinity of the major divergence areas of sediment flux the seabed should be almost void of finer sediment whereas frequent convergence areas are eventually characterized by abundance of sand and silt. In other words, the geological composition of the nearshore may provide an implicit means to evaluate the adequacy of numerical simulations. The final part of the paper focuses on the comparison of the established pattern of alongshore transport and the geological composition of seabed.

MATERIAL AND METHODS

Similarly to (Viška, Soomere 2012; Soomere, Viška 2013), the calculations rely on the hourly time series of wave properties evaluated using the third-generation spectral wave model WAM (Komen *et al.* 1994) and adjusted geostrophic winds. The wave model was run for the entire Baltic Sea with a spatial resolution of about three nautical miles for 1970–2007 (Räämet, Soomere 2010). The presence of ice was ignored. Doing so is generally acceptable for the southern part of the study area but may substantially overestimate the impact of waves in the Gulf of Riga. The long-term average significant wave height is underestimated by about 15% by Räämet, Soomere (2010). The reader is referred to (Soomere, Räämet 2011) for a more detailed discussion of the existing simulations of the Baltic Sea wave climate.

The study area is divided into 110 about 5.5–7 km long sections (Fig. 1) that match the locations of grid cells of the wave model. The alongshore transport is calculated using the CERC approach from the wave height and approach direction at the breaker line. These quantities are evaluated from the modelled time series of significant wave height, peak period and mean direction. The joint impact of shoaling and refraction on the wave height and direction from the grid cell until the breaker line is evaluated using standard assumptions of the linear wave theory. The numerically reconstructed wave field is assumed to be monochromatic, the wave height h_0 at a grid cell equal to the modelled significant wave height h_{s0} or root mean square wave height h_{rms0} , the period T equal to the modelled peak

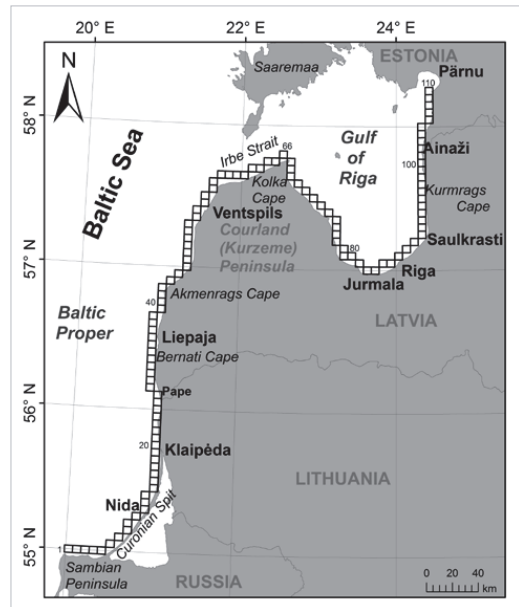


Fig. 1 Scheme of calculation points of the wave model and corresponding coastal sections along the study area. Compiled by M. Viška.

period, and the wave direction matching the modelled mean direction. We also assume that the depth isolines are straight and parallel to the average orientation of the coastline within each coastal section. Wave reflection, whitewater, interactions with seabed and nonlinear interactions within the wave field are ignored. Under these assumptions the wave height h_b at the breaker line is (Dean, Dalrymple 1991)

$$h_b = h_0 \left(\frac{c_{g0} \cos \theta_0}{c_{gb} \cos \theta_b} \right)^{1/2} \quad (1),$$

where c_g is the group speed and θ is the approach angle of waves and subscripts 0 and b represent wave properties at a model grid cell and at the breaker line, respectively.

The changes to the wave direction follow Snell's law $\sin \theta / c_f = \text{const}$ and thus $\sin \theta_b = \sin \theta_0 c_{f0} / c_{fb}$, where c_f is the phase speed (celerity) and the meaning of subscripts has been explained above. The phase and group speed at a model grid cell are found from the finite-depth dispersion relation $\omega = \sqrt{gk_0 \tanh k_0 d_0}$ where $\omega = 2\pi / T$ is the angular frequency, $g = 9.81 \text{ m s}^{-2}$ is the acceleration due to gravity, k_0 is the wave number and d_0 is the water depth at the wave model cell.

The calculation of the breaking-wave height h_b relies on the concept of breaking index $\gamma_b = h_b / d_b$, where d_b is the water depth at the breaker line. There is no consensus about the common value of the breaking index. For monochromatic waves approaching strongly

reflecting beaches it may reach values ~ 1.5 whereas for almost horizontal bed it is $0.55\text{--}0.6$ (Nelson 1994; Massel 1996). For irregular waves in the surf zone the ratio h_b/d_b may be much smaller, even in the range of $0.2\text{--}0.5$ (Lentz, Raubenheimer 1999). The coasts in the study area are mostly sedimentary, with gently sloping profiles resembling Dean's equilibrium profile. As we are interested in the location of the seaward border of the surf zone, the use of a constant value $\gamma_b = 0.8$ is justified (USACE 2002; Dean, Dalrymple 1991, 2002).

As breaking waves are long waves, their group speed c_{gb} and phase speed c_b are equal: $c_{gb} = \sqrt{gd_b} = \sqrt{gh_b/\gamma_b}$. Substituting these expressions into Eq. (1) leads to the following algebraic equation of 6th order for the breaking-wave height h_b (Soomere *et al.* 2013a):

$$F(h_b) = h_b^6 \frac{g^2 \sin^2 \theta_0}{\gamma_b^2 c_{f0}^2} - h_b^5 \frac{g}{\gamma_b} + h_b^4 c_{g0}^2 (1 - \sin^2 \theta_0) = 0. \quad (2)$$

The leading term of Eq. (2) vanishes for incident waves with $\theta_0 = 0$. Such waves only experience shoaling under the described set of assumptions and their breaking height is $h_b = (h_0^4 c_{g0}^2 \gamma_b / g)^{1/3}$ (Komar, Gaughan 1972; Dean, Dalrymple 1991). This expression is often used for almost incident waves for which $\cos \theta_b \approx 1$ and $\sin^2 \theta_b \approx 0$ (Dalrymple *et al.* 1977; Dean, Dalrymple 1991, p. 115).

As the Baltic Sea waves often approach the coast under quite large angles (Viška, Soomere 2012), we solve the full equation (2). It has only three non-zero coefficients. Its leading term and the constant term have the same sign whereas the coefficient at h_b^5 has the opposite sign. Therefore, the polynomial $F(h_b)$ has exactly one minimum at $\tilde{h} = 5\gamma_b c_{f0}^2 / 6g \sin^2 \theta_0$. Consequently, Eq. (2) has two different real solutions if this minimum corresponds to a negative value of $F(\tilde{h})$, a double real solution if $F(\tilde{h}) = 0$ and no real solutions if $F(\tilde{h}) > 0$. The latter case probably means that the modelled waves are already breaking (cf. Soomere *et al.* 2013a).

The solution that represents the breaking-wave height can be identified by considering the case $\theta_0 \rightarrow 90^\circ$. For such angles, the constant term of Eq. (2) is very small, the smaller real solution tends to zero and the larger real solution approaches a constant value $\tilde{h} = \gamma_b c_{f0}^2 / g$. For typical Baltic Sea wave fields, this value substantially exceeds the possible wave heights and the smaller real solution represents the breaking-wave height.

The intensity of wave-driven alongshore sediment transport is estimated in terms of the potential immersed weight transport rate (called simply transport rate below) $I_t = (\rho_s - \rho)g(1-p)Q_t$ (USACE 2002). We use $\rho_s = 2650 \text{ kg m}^{-3}$ and $\rho = 1015 \text{ kg m}^{-3}$ for the densities of sediment (sand) particles and sea water, respectively, and $p = 0.4$ for the

porosity coefficient. According to the CERC method $I_t = KP_t$, where $P_t = Ec_{gb} \sin \theta_b \cos \theta_b$ is the rate of beaching of the alongshore component of wave energy flux Ec_g at the breaker line and E is the wave energy. Following (USACE, 2002), we use the expression $K = 0.05 + 2.6 \sin^2 2\theta_b + 0.007 u_{mb} w_f$ for the coefficient K designed for the use of the root mean square wave height (USACE 2002, III-2). Here $u_{mb} = (h_b/2)\sqrt{g/d_b} = \sqrt{g\gamma_b h_b}/2$ is the maximum orbital velocity according to the linear wave theory and $w_f = 1.6\sqrt{gd_{50}(\rho_s - \rho)}/\rho$. An appreciable approximation for the typical grain size of sand in the study area is $d_{50} = 0.17 \text{ mm}$ (Zemlys *et al.* 2007; Zhamoida *et al.* 2009; Kartau *et al.* 2011). The resulting hourly transport rates are used to evaluate annual means of the bulk and net (positive for counter-clockwise drift) transport for each coastal section (cf. Viška, Soomere 2012; Soomere, Viška 2013).

SIMULATED SEDIMENT TRANSPORT

The significant wave height of a monochromatic wave train coincides with the root mean square height of such a train and thus is applicable for the CERC formula in case of regular swells. This approach is obviously incorrect for wind seas. The contemporary definition of significant wave height is $h_s = 4\sigma$, where σ is the standard deviation of the water surface elevation. The energy of a wind sea equals to the energy of a sinusoidal wave train with the root mean square wave height $h_{rms} = 2\sqrt{2}\sigma = h_s/\sqrt{2}$ of the wind sea; equivalently, $E = (1/8)\rho gh_{rms}^2 = (1/16)\rho gh_s^2$.

There is no consensus on how to quantify the breaker line for a wind sea as waves of different heights start to break at different depths. A conservative estimate for the water depth at the breaker line is $d_b = h_{rmsb}/\gamma_b$, where h_{rmsb} is the root mean square wave height at breaking.

For almost incident waves it is acceptable to ignore the leading term in Eq. (2) (Dalrymple *et al.* 1977; Dean, Dalrymple 1991). The coefficient K only weakly depends on the (particular specification of the) wave height. Therefore, to a first approximation, a change in the specification of the height of such waves reduces to an introduction of a linear coefficient in the CERC formula. For example a replacement of the root mean square wave height by the significant wave height results an increase in the sediment transport by $2\sqrt{2} \approx 2.83$ times. This property is reflected by the difference in the (constant) coefficient $K_c = 0.39$ for the significant wave height and $K_c = 0.92$ for the root mean square wave height in the earlier research (USACE 2002, III-2). Importantly, in spite of a substantial change to the magnitude of the transport rate, such a replacement affects neither the direction of the transport nor the qualitative pattern of its alongshore variations. Consequently, the pattern of divergence and convergence areas of net transport driven by almost incident waves is invariant with respect to the choice of the wave height in the CERC formula.

This feature is not necessarily valid for waves with larger incidence angles, for which refraction additionally modifies the transport rate. The use of h_{rms} instead of h_s means that the constant term in Eq. (2) decreases and the graph of the polynomial F is shifted downwards in (h, F) -coordinates. Therefore, for any incidence angle $0 < \theta_0 < 90^\circ$ we have $h_{rmsb} < h_{sb}$. The relative weight of the constant term and the difference between h_{rmsb} and h_{sb} decrease with the increase in θ_0 .

Recalculation of the net and bulk transport rates using the exact solution of Eq. (2) leads to a certain decrease in the long-term average of both these quantities (Fig. 2, 3, Table 1). A closer inspection (not

shown) reveals that the transport driven by waves approaching the coast under large angles ($\theta_0 > 30^\circ$) was considerably overestimated in (Soomere, Viška 2013). The transport by waves with $\theta_0 < 30^\circ$ was usually slightly underestimated as shoaling often led to a considerable increase in the wave height.

The qualitative patterns of annual average net and bulk transport (Fig. 3) calculated using Eq. (2) almost exactly coincide with those evaluated by Soomere, Viška (2013) using a simplified approach for shoaling. The open coast of Baltic Sea hosts much higher bulk transport than the Gulf of Riga. The most intense transport takes place along the Sambian Peninsula and in

the north-western Courland Peninsula (that host almost 50% of the entire net transport in the study area). The biggest spatial variability in the calculated transport rates is also on the north-western coast of Latvia. The match of the areas of larger and smaller transport is almost perfect for the bulk transport except for a short segment of the western part of the Curonian Spit. Interestingly, local variations in the transport along the study area are generally smaller for the calculations based on Eq. (2) than in (Soomere, Viška, 2013). This feature evidently reflects more adequate estimates of the impact of waves approaching under large angles by Eq. (2) and signals that such waves provided extremely large (and often overestimated) contributions to both net and bulk transport in (Soomere, Viška 2013).

The use of solutions of Eq. (2) instead of the simplified approach of Soomere, Viška (2013) generally leads to a certain decrease (by a few per cent along the coast of the Baltic Proper and about 10% in the Gulf of Riga) in the annual and long-term average bulk

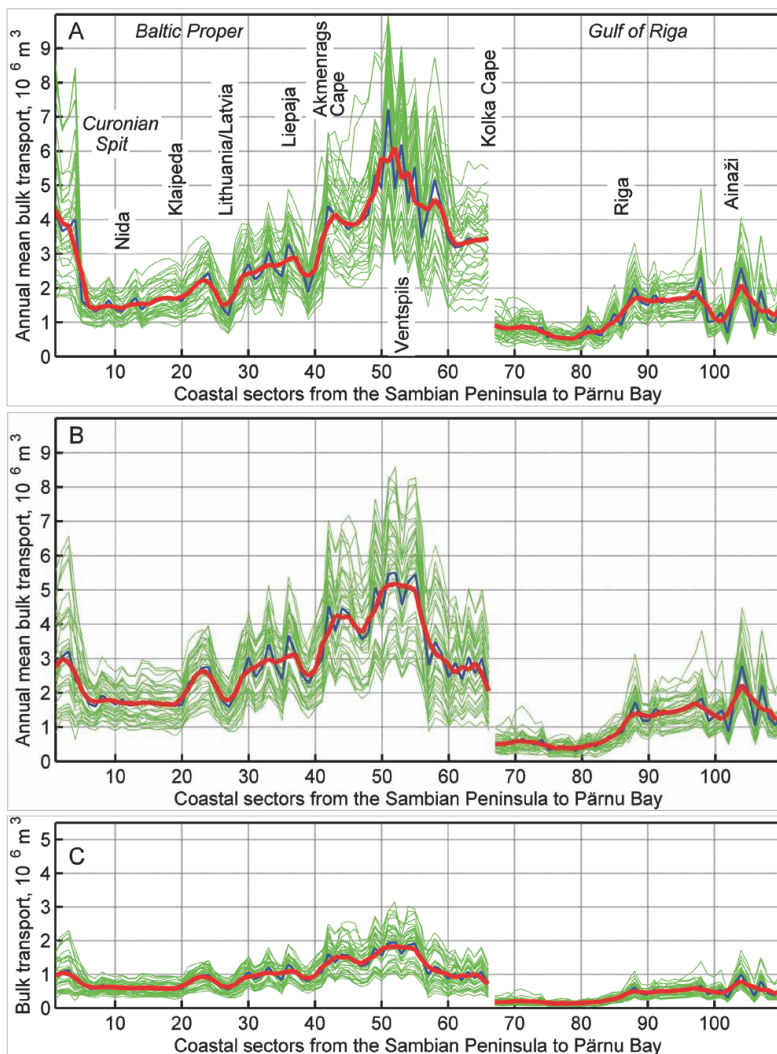


Fig. 2 A. Simulated potential bulk transport in the study area for $d_{50} = 0.17$ mm, using significant wave height as input for the CERC formula and a simplified representation of shoaling (Soomere, Viška 2013). Green: single years, blue: average for 1970–2007; red: moving average of the blue line over three subsequent coastal sections. B. The same as panel A but using the full solution of Eq. (2). C. The same as panel B but using root mean square wave height as input for the CERC formula. Compiled by T. Soomere.

transport. The changes are the largest in the sections hosting the most intense transport. These sections evidently have the largest proportion of waves approaching under large incidence angles. Some parts of the study area, for example, the western part of the Curonian Spit, reveal an increase in the bulk transport when the solutions to Eq. (2) are employed. The decrease in the net transport is more systematic, about 10% on average.

The match of the rates of net transport calculated in (Soomere, Viška 2013) and using Eq. (2) is less exact (Fig. 3). The segments of its large and small absolute values fully coincide but its alongshore variations calculated using Eq. (2) exhibit less frequent zero-crossings (divergence and convergence areas). For example, the reversal Ventspils (Soomere, Viška 2013) is present only in a few years in the calculations employing Eq. (2). Another similar reversal to the north of the border between Latvia and Lithuania is also present less frequently. Both short segments of southwards transport on the eastern coast of the Gulf of Riga also become evident in selected years and are not present in the long-term mean.

The changes associated with the variations in the typical grain size are even smaller, about 6–8% for both the bulk and net transport (Table 1). Importantly, no qualitative changes are found in the patterns of the net and bulk transport for different grain sizes (Fig. 3).

The magnitude of the simulated transport is extremely sensitive with respect to the input wave data. The use of root mean square wave height as the input for the CERC formula (incl. the expression for the group speed) leads, similarly to the case of almost-incident waves, to a radical decrease in the wave-driven transport by about 2.8 times (Fig. 2, 3, Table 1). The potential net transport becomes considerably (by about 30–40%, Fig. 4) smaller in this case than the transport estimated from the field data. For example, the simulated net transport along the north-western coast of the Courland Peninsula ($500\text{--}700 \times 10^3 \text{ m}^3 \text{ a}^{-1}$) is about 70% of the estimate $750\text{--}1000 \times 10^3 \text{ m}^3 \text{ a}^{-1}$ by Eberhards (2003).

A large part of this difference may stem from the interpretation of the location of the breaker line. For regular swells (that are common for the open ocean coast) it is natural to interpret the breaker line as the location where most of the crests start to break and to associate it with the breaking depth h_{rmsb} for the root mean square wave height. The largest waves in a typical wind sea (that is common for the Baltic Sea) are better described by the significant wave height. Their breaking (and the associated intense motion of bottom sediments) starts at deeper locations characterized by the breaking depth for the waves with the significant wave height h_{sb} . As the CERC formula expresses the sediment transport in the entire surf zone, it is natural to assume that it relies on the energy flux supplied at the line where relatively large waves often break,

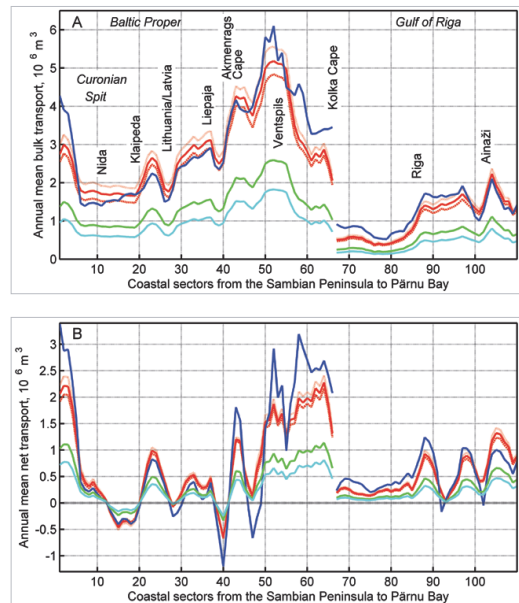


Fig. 3 Simulated potential bulk transport (A) and net transport (B). All lines indicate the moving average over three subsequent coastal sections, calculated as an average over all years 1970–2007. Blue: $d_{50} = 0.17$ mm, simplified representation of shoaling, significant wave height as input for the CERC formula (Soomere, Viška 2013). Other colours correspond to the use of solutions of Eq. (2). Red lines: significant wave height as input for the CERC formula; dotted line (upper): $d_{50} = 0.063$ mm, solid line (middle): $d_{50} = 0.17$ mm, dashed line (lower): $d_{50} = 1.0$ mm. Green: $d_{50} = 0.17$ mm; root mean square wave height as input for the wave energy but group velocity at the breaker line estimated based on the significant wave height. Cyan: $d_{50} = 0.17$ mm, root mean square wave height as input for the CERC formula. Compiled by T. Soomere.

that is, at the depth of h_{sb}/γ_b . Calculations using the “mixed” specification of the wave height (h_{sb} for the wave energy and h_{rmsb} for the group speed at the breaking line) led to a reasonable match of the simulated and observed transport rates (Fig. 4).

SENSITIVITY OF THE CONVERGENCE AND DIVERGENCE AREAS

The entire pattern of the simulated net transport reflects the well-known overall counter-clockwise sediment flux. Differently from the earlier research, it contains two short but relatively persistent reversals (Fig. 4). These reversals can be characterized using the associated areas of divergence and convergence of the transport (Soomere, Viška 2013). Four such areas (divergence near Klaipėda and at the Akmenrags Cape, convergence at the Curonian Spit and to the north of Liepaja) appear at the same locations in all calculations (Fig. 4). Several less persistent divergence and convergence areas (Soomere, Viška 2013) are represented in Fig. 4 as segments that have almost

Table 1 Annual average bulk and net transport (in 10^3 m^3 , both annual mean of net transport and the mean of its absolute values) along the eastern coast of the Baltic Proper and in the Gulf of Riga for different variations of the calculation scheme and interpretation of the input wave height in the CERC formula. The case $d_{50} = 0.17$ and accounting for only refraction corresponds to the data presented in Soomere and Viška (2013).

Properties of the run			Net, Baltic Proper		Net, Gulf of Riga		Bulk	
d_{50} , mm	Use of Eq. (2)	Wave height	mean	Abs (mean)	mean	Abs (mean)	Baltic Proper	Gulf of Riga
0.063	yes	h_s	840	1020	528	542	3102	1144
0.17	no	h_s	864	1167	555	565	2983	1198
0.17	yes	h_s	783	955	496	509	2870	1064
1.0	yes	h_s	730	895	467	478	2658	991
0.17	yes	h_{rms}	277	338	175	180	1011	375

zero long-term net transport. Between such areas occasionally short-term reversals may occur. While some of such short-term reversals correspond to local minima of the bulk transport, one reversal to the north of Riga hosts intense bulk transport.

One persistent reversal area is located in the northern part of the Curonian Spit between Nida and Klaipėda. Its borders vary considerably in different years (Fig. 5) whereas in single years it may be replaced by a northwards sediment flux. Its northern border (a

divergence area next to Klaipėda) thus probably does not serve as a robust barrier for the sediment motion to the north. Such an ‘intermittent’ transport regime seems to be an intrinsic part of the dynamical equilibrium of the spit (Viška, Soomere, 2012). The overall appearance of the reversal indicates that in the long-term perspective the divergence area around Klaipėda suffers from sediment deficit.

A relatively short but persistent reversal of sediment transport is located between Liepāja and the Akmen-

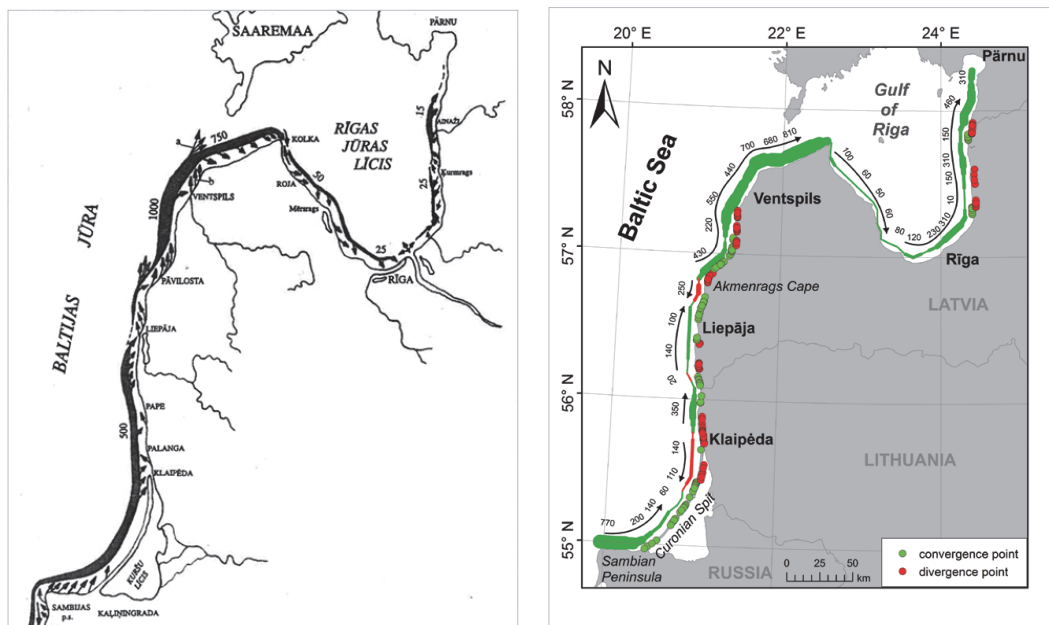


Fig. 4 Direction (arrows) and magnitude (numbers at arrows, in 1000 m^3) of net sediment transport: left – original scheme by R. Knaps, amended by V. Ulsts (1998); right – simulated potential net sediment transport using $d_{50} = 0.17$ mm, Eq. (2) and root mean square wave height as the input to the CERC formula. Compiled by M. Viška.

rags Cape. Its length considerably varies in time, from about 15 up to 50 km. The convergence area at its southern border substantially moves in different years (Fig. 5). The most interesting feature is the highly persistent divergence area at the Akmenrags Cape. Its location varies only by about ± 5 km from its average position. It is evident during all the simulated years except for the quite unusual year 1984 (Soomere, Viška 2013).

The divergence and convergence areas and the related reversals are much less persistent in the Gulf of Riga. No such areas seem to exist at its western coast except possibly in a few single years. The long-term sediment flux almost vanishes or is reversed at two locations at the eastern coast of the gulf – near Saulkrasti and at the border between Latvia and Estonia (Fig. 3). The simulated net sediment transport shows quite frequently occurring short reversals at both sites. In selected years, the reversal near Saulkrasti may extend to several tens of km. This matches the results of Knaps (1965) where this reversal covers more than 30 km. It occasionally starts from the Kurmrags Cape and extends approximately to almost Saulkrasti. The vicinity of this cape suffers from erosion: a seamount that was originally located on the top of a coastal sandstone scarp is now at the waterline.

Another area of divergence is often (during about a half of years) located near Ainaži. The associated reversal is quite short, normally <15 km. Knaps (1965) identified here no reversal and concluded that the long-term average sediment flow is to the north. Eberhards (2003) discussed the situation at this site in the light of

silting of the nearshore. A set of underwater sandbars are visible to the south of Ainaži on orthophotos made in 1982. Their position and appearance signals the alongshore sediment flux to the south. A similar pattern can be seen also in orthophotos taken in 2007. Therefore, the simulated data for this region for 1970–2007 likely reflect the correct average direction of sediment flow to the south, despite the fact that some of previous calculations and observations showed an uninterrupted average flux to the north.

Although the described pattern of net transport (incl. its reversals) seems to be stable, it may undergo substantial changes in single years. For example, in 1984 the annual average transport was directed to the north. While such a pattern was only slightly unusual for the coast of the Baltic Proper, it was exceptional in the Gulf of Riga: the simulated sediment transport along its western coast was entirely to the north (Soomere, Viška 2013). This hindcast matches the observational evidence that large sediment volumes were transported to the north this year. Ulsts (1998) found a significant sediment movement to the north between Roja Harbour (on the western coast of the Gulf of Riga) and the Kolka Cape. Together with intense sediment supply along the western coast of the Courland Peninsula, this process resulted in the formation of a temporary spit to the east of the Kolka Cape.

THE COMPOSITION OF THE NEARSHORE SEABED

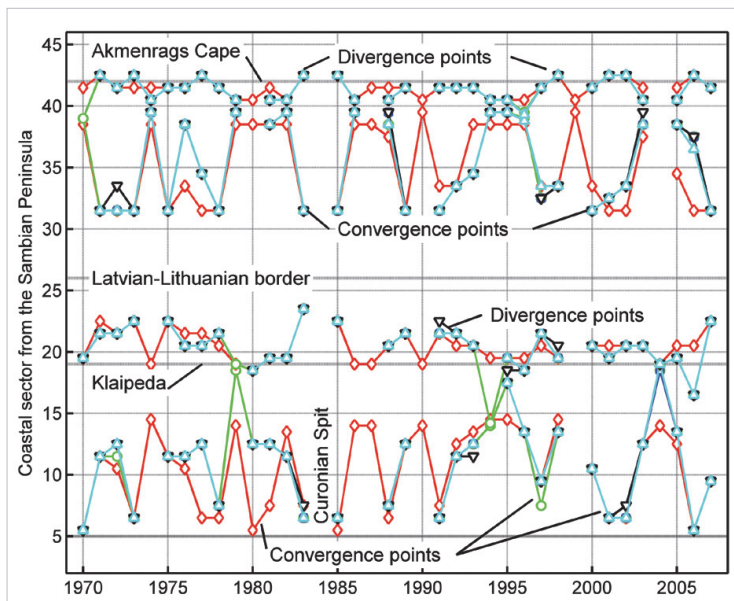


Fig. 5 Location of persistent divergence and convergence areas on the eastern Baltic Proper coast. Red: $d_{50} = 0.17$ mm, simplified representation of shoaling (Soomere, Viška 2013). Other colours correspond to the use of solutions of Eq. (2). Green: $d_{50} = 1.0$ mm, blue $d_{50} = 0.17$ mm, black $d_{50} = 0.063$ mm, all using significant wave height as the input to the CERC formula; cyan: $d_{50} = 0.17$ mm, root mean square wave height as the input for the CERC formula. Compiled by M. Viška and T. Soomere.

The presented results confirm that the overall counter-clockwise pattern of net sediment transport along the eastern Baltic Sea coast and in the Gulf of Riga is modulated by several persistent reversals. The four most persistent divergence and convergence areas are almost insensitive with respect to the variations in the sediment transport model, the typical grain size and even with respect to the interpretation of the wave height. This invariance suggests that they have been present for a long time and, most probably, have exerted a certain impact on the sediment structure in the adjacent nearshore. We use for comparisons of this pattern and the geological composition of the study area a composite map of nearshore bottom sediments (Fig. 6). It is compiled using data from (Bottom... 1996; Ulsts, Bulgakova 1998; Bitinas *et al.* 2004) using three different systems to denote various sediment classes that do not fully overlap.

The Curonian Spit entirely consists of fine sand. It is thus natural that its nearshore is sandy whereas finer sand is found further offshore. A very narrow fine-grained sediment strip is mostly present in the vicinity of the waterline along the Courland coast starting from the Latvian–Lithuanian border and extends until the Irbe Strait. This strip simply reflects the tendency for some sand to gather around the waterline even if there is a general deficit of finer sediment. Thus, its presence cannot be associated with the locations of divergence or convergence areas. For this reason, we focus on the geological composition of a somewhat wider underwater area.

To the north of Klaipėda only the immediate nearshore contains a sandy strip. In more offshore locations till interspersed with some sand predominates until Palanga. The area where till predominates almost exactly matches the region in which divergence of the sediment flux may occur. The sandy strip widens to the north of Palanga, approximately in the area where a relatively persistent convergence area is frequently located (Fig. 4). It drastically diminishes at the border between Latvia and Lithuania where the net sediment transport is often reversed. In this segment gravel with pebbles and boulders covers the nearshore and extends almost to the waterline. A frequent divergence area is, however, located somewhat to the north of the section where gravel with pebbles and boulders predominate until the waterline (Fig. 4). Therefore, there is no perfect match of this divergence area with the geological composition of the nearshore although the sandy strip is relatively wide in this area.

A divergence area frequently occurs at and to the south of the Bernati Cape. This area is mostly characterized by a low sedimentary coast that was inactive before the middle of the 20th century. It started to suffer from erosion in 1954. The length of the eroding section reached about 3–4 km in 1993. The average coastline retreat was 13 m in years 1991–1993 (Ulsts 1998). Particularly strong erosion has occurred at this cape during the last quarter of the 20th century, possibly because of the changes in the main wave approach direction and hence an increase in the sediment transport rate (Eberhardts 2003). This conjecture matches a major change in the air-flow direction since 1988 in the northern Baltic Sea (Soomere, Räämet 2013).

A larger coastal segment that often hosts a convergence area is located in the vicinity of Liepāja (Fig. 4). Consistently with this observation, there is an area of fine-grained sand at Liepāja. The sandy area is, however, narrow and occasionally discontinuous to the north of this city. This mismatch evidently reflects the impact of Liepāja Harbour. Its constructions disrupt the natural sediment transport and cause a deficit of sediments to the north of Liepāja where mostly gravel with pebbles and boulders occur on the seabed.

Consistently with the appearance of a persistent divergence area (Fig. 4), the nearshore of the Akmenrags Cape contains almost no fine sediments (Fig. 6) although the beach itself is sandy and occasionally

contains growing foredunes. A sandy or silty strip of appreciable width reappears at a distance of a few km to the north of this cape (Fig. 6). It extends over the entire segment where the simulations indicate a frequent convergence area (Fig. 4). A headland between this segment and Ventspils contains much less sand and at places consists of gravel, pebbles and boulders, again consistently with an occasional presence of a divergence area (Fig. 4).

The simulations suggest that almost unidirectional (on the annual average) sediment transport to the north-east occurs from Ventspils to the Kolka Cape. No clearly distinguishable convergence or divergence areas exist along this stretch. The upper layer of the seabed is mostly sandy or silty, signalling intense transport in this section. Starting from the Irbe Strait a fine-grained sand strip in the nearshore becomes wider and reaches a maximum width near the Kolka Cape (Fig. 6). The intense sediment transport along the western coast of the Courland Peninsula to the entrance of the Gulf of Riga has caused an extensive growth of the Kolka Cape to the north-east and deposition of large volumes of sand in its vicinity in the past (Ulsts 1998; Eberhardts 2003). A part of this sand is transported further into the interior of the Gulf of Riga. The flux of sand to the south-east of the Kolka Cape is relatively weak (because of a limited fetch for waves approaching from the north-west) but almost unidirectional (except for the unusual year 1984 as discussed above). Its intensity generally increases along the coast until Jurmala. Near this city, the coastline turns and the sediment is further driven by waves excited by south-western winds. Interestingly, no persistent convergence area exists near the River Daugava mouth, possibly because of the joint impact of waves excited by south-western and north-north-western winds (Ulsts 1998). These two wave systems together cause intense transport back and forth between Jurmala and Saulkrasti.

The sandy strip in the nearshore becomes narrower to the north-east of Riga but is continuous until Saulkrasti where an appreciably persistent convergence area exists (Fig. 4). Its interplay with an often occurring divergence area (located just to the north of Saulkrasti) may be the reason why the nearshore of Saulkrasti is sandy but boulders and rock predominate to the north of this city until Tuja. Another pair of divergence and convergence areas is located at Ainaži. Although they appear only in selected years (Soomere, Viška, 2013), it is still characteristic that a relatively wide spot of nearshore sand is located exactly where Fig. 4 shows a small convergence area.

The presented comparison confirms that all major simulated convergence areas (Fig. 4) have an appreciable match with relatively wide nearshore areas covered with silt or sand (Fig. 6). The match of the nearshore sediment composition with divergence areas is less evident but is still typical that such areas mostly contain coarse sediment – gravel, pebbles, boulders or even pre-Quaternary rock.

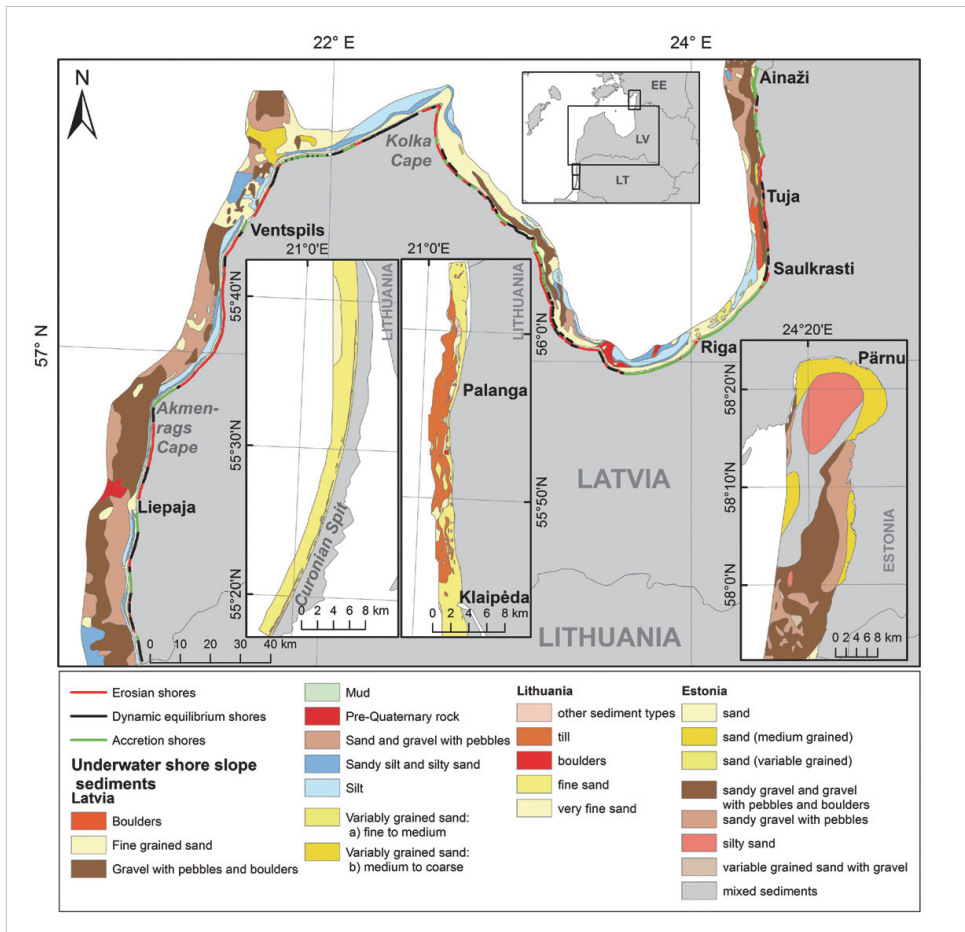


Fig. 6 Geological composition of the nearshore of the study area. Note that different countries use different specifications of sediment types. Compiled by M. Viška.

DISCUSSION

The results of numerical simulations confirm the existence of the well-known generally counter-clockwise pattern of net sediment transport along the study area. This pattern involves an end station at the Kolka Cape, two persistent reversals along the coast of the Baltic Proper and two frequently occurring reversals on the eastern coast of the Gulf of Riga. As expected, its qualitative appearance is stable with respect to the details of the calculation scheme of the alongshore transport and input conditions such as the typical grain size and the particular interpretation of the wave height.

It is well known that the use of the CERC formula is associated with relatively large uncertainties in the resulting magnitude of sediment transport (USACE 2002). The results presented above call for a re-evaluation of its certain parts for the specific conditions of the Baltic Sea. Low levels of remote swells in this water body have been shown to impact the validity of commonly used expressions for the closure depth. The formulas designed for the open ocean coasts work properly in semi-enclosed bayheads where the proportion of remote swells is comparable to that on the open ocean coasts (Soomere *et al.* 2013b). Our results suggest that it may be reasonable to apply in the CERC formula the group speed of breaking waves using the significant wave height at the Baltic Sea coasts (where the wind seas predominate).

An important task of this research was to identify observational support to the presence of reversals of the net transport. It is natural to associate persistent convergence areas with abundance and/or accumulation of sand. In the contrary, divergence areas may be associated with a deficit of sand and erosion regions.

As the location of such areas may substantially vary in different years, their match with the composition of the coast and the nearshore is not necessarily straightforward. In addition, their impact not necessarily becomes evident in segments affected by other processes, for example, intense dynamics of sand bars that serve as a buffer for changes in the nearshore (Weishar *et al.* 1991). Their cyclic relocation may easily override the impact of, for example, a divergence area for many years. The presented comparison suggests that there is an acceptable match between the location of major convergence and divergence areas and the geological structure of the seabed to a distance of a few km from the waterline. The match is less evident for divergence areas but it is still typical that such areas contain coarse sediments.

The presented analysis suggests that long-term changes in the study area may be substantially modulated by decadal variability in the wind and wave climate. The situation at the Bernati Cape (where erosion started from the mid-1950s and was relatively intensive in the 1990s) or near Aināzi (where the analysis of processes during different time intervals may give controversial results) vividly exemplifies the importance of the long-term view. An important message, albeit not new in the coastal science, is that a long interval, at least several tens of years of observations or simulations, is often necessary in order to obtain an adequate representation of the nature of processes. Given the extensive natural variability of the processes in the study area, it is not surprising that the analyses based on different averaging periods may lead to substantially different conclusions and seeming discrepancies between the results of different authors.

Finally, the simulations also revealed that the long-term transport patterns may show radically different nature during single years with quite usual wind speeds and wave heights but with unusual wave approach directions. Namely, truly exceptional years (such as 1984) in terms of a completely different pattern of sediment transport may occur in the study area in the existing wave climate. This feature calls for further studies into these properties of the climate of semi-enclosed seas that substantially affect wave-driven sediment transport patterns such as changing wind directions (Jaagus, Kull 2011), combinations of high water level and wave storms (Orviku *et al.* 2003) or changes to the ice cover (Ryabchuk *et al.* 2011).

CONCLUSIONS

The overall counter-clockwise pattern of net sediment transport along the eastern Baltic Sea coast and in the Gulf of Riga contains two persistent reversals on the coast of the Baltic Proper and two frequently occurring reversals on the eastern coast of the Gulf of Riga. This pattern is stable with respect to the particular modelling scheme of the alongshore transport, the typical grain

size and even with respect of the interpretation of the wave height.

The established pattern may show radically different nature during single years with unusual direction of wave storms. An acceptable match exists between the location of major convergence and divergence areas of sediment flux and the geological structure of the nearshore seabed.

Acknowledgements

Authors highly appreciate supportive comments of Dr. Loreta Kelpšaitė (Klaipėda) and Prof. Vitalijs Zelčs (Riga) on the original submission. The study was a part of the project “Science-based forecast and quantification of risks to properly and timely react to hazards impacting Estonian mainland, air space, water bodies and coasts” (TERIKVANT), supported by the European Regional Development Fund (ERDF) within the framework of the Environmental Technology R&D Programme KESTA. The research was supported by the Estonian Ministry of Education and Research (targeted financing No. SF0140007s11), Estonian Science Foundation (grant No. 9125) and European Union (via a support to the Estonian Centre of Excellence CENS from the ERDF and by the DoRa international PhD studentship for M. Viška).

References

- Bitinas, A., Aleksa, P., Damušytė, A., Gulbinskas, S., Jarmalavičius, D., Kuzavinis, M., Minkėvičius, V., Pupienis, D., Trimonis, E., Šečkus, R., Žaromskis, R., Žilinskas, G., 2004. *Geological atlas of Lithuanian Baltic sea coast*. Lithuanian Geological Survey, Vilnius, 94 pp.
- Bottom sediments of the Gulf of Riga*. Geological Survey of Latvia, 1996, 53 pp.
- Dalrymple, R. A., Eubanks, R. A., Birkemeier, W. A., 1977. Wave-induced circulation in shallow basins. *Journal of the Waterways, Ports, Coastal and Ocean Division-ASCE* 103, 117–135.
- Dean, R. G., Dalrymple, R. A., 1991. *Water wave mechanics for engineers and scientists*. World Scientific, 353 pp.
- Dean, R. G., Dalrymple, R. A., 2002. *Coastal processes with engineering applications*. Cambridge University Press, Cambridge, 475 pp.
- Eberhards, G., 2003. *The sea coast of Latvia*. University of Latvia, Riga. [In Latvian].
- Eberhards, G., Lapinskis, J., 2008. *Processes on the Latvian coast of the Baltic Sea. Atlas*. University of Latvia, Riga, 64 pp.
- Eberhards, G., Grīne, I., Lapinskis, J., Purgalis, I., Saltupe, B., Torklere, A., 2009. Changes in Latvia's seacoast (1935–2007). *Baltica* 22 (1), 11–22.
- Gilbert, G. (Ed.), 2008. *State of the coast of the South-East Baltic: an indicators-based approach to evaluating sustainable development in the coastal zone of the South East Baltic Sea*. P.P. Shirshov Institute of Oceanology, Atlantic Branch, Kaliningrad, 164 pp.
- Gudelis, V., 1967. The morphogenetic types of Baltic Sea coasts. *Baltica* 3, 123–145. [In Russian].
- Gudelis, V., Kirlyš, V., Močiekienė, S., 1977. Littoral drift regime and dynamics along the eastern coast of the Baltic Sea in the off-shore zone of the Curonian Spit according to the data of 1956–1974. *Transactions of the Lithuanian Academy of Sciences B 4 (101)*, 123–128. [In Russian].

- Jaagus, J., Kull, A., 2011. Changes in surface wind directions in Estonia during 1966–2008 and their relationships with large-scale atmospheric circulation, *Estonian Journal of Earth Sciences* 60 (4), 220–231. <http://dx.doi.org/10.3176/earth.2011.4.03>
- Kalniņa, L., Dreimanis, A., Mūrniece, S., 2000. Palynology and lithostratigraphy of Late Elsterian to Early Saalian aquatic sediments in the Ziemeļu–Jūrkalne area, western Latvia. *Quaternary International* 68–71, 87–109.
- Kartau, K., Soomere, T., Tõnisson, H., 2011. Quantification of sediment loss from semi-sheltered beaches: a case study for Valgerand Beach, Pärnu Bay, the Baltic Sea. *Journal of Coastal Research, Special Issue* 64, 100–104.
- Knaps, R., 1938. Prüfung der Formel von prof. Munch-Petersen über Materialwanderung an der lettischen Küste. *VI Baltische Hydrologische Konferenz, Bericht*, Berlin, 60–103.
- Knaps, R., 1965. *Перемещение наносов у берегов восточной Балтики [Sediment transport along the eastern Baltic Sea coasts]*. Latgidroprom, Riga, 57 pp. [In Russian].
- Knaps, R. J., 1966. Sediment transport near the coasts of the Eastern Baltic. In Development of sea shores under the conditions of oscillations of the Earth's crust, Valgus, Tallinn, 21–29. [In Russian].
- Komar, P. D., Gaughan, M. K., 1972. Airy wave theory and breaker wave height prediction. In Proceedings of the 13th Conference on Coastal Engineering, July 10–14, Vancouver 1972, ASCE, New York, 405–418.
- Komen, G. J., Cavaleri, L., Donelan, M., Hasselmann, K., Hasselmann, S., Janssen, P. A. E. M., 1994. *Dynamics and modelling of ocean waves*. Cambridge University Press, Cambridge, 532 pp.
- Massel, S. R., 1996. On the largest wave height in water of constant depth. *Ocean Engineering* 23, 553–573. [http://dx.doi.org/10.1016/0029-8018\(95\)00049-6](http://dx.doi.org/10.1016/0029-8018(95)00049-6)
- Lentz, S., Raubenheimer, B., 1999. Field observations of wave setup. *Journal of Geophysical Research – Oceans* 104 (C11), 25867–25875.
- Lapinskis, J., 2010. *Dynamics of the Kurzeme coast of the Baltic Proper*. Doctoral Thesis, University of Latvia, Riga. [In Latvian].
- Munch-Petersen, T., 1936. Über Materialwanderung an Meeresküsten. *V Hydrologische konferenz der Baltischen Staaten*, Helsinki, 67.
- Nelson, R. C., 1994. Depth limited design wave heights in very flat regions. *Coastal Engineering* 23, 43–59. [http://dx.doi.org/10.1016/0378-3839\(94\)90014-0](http://dx.doi.org/10.1016/0378-3839(94)90014-0)
- Orviku, K., Jaagus, J., Kont, A., Ratas, U., Ravis, R., 2003. Increasing activity of coastal processes associated with climate change in Estonia. *Journal of Coastal Research* 19, 364–375.
- Ryabchuk, D., Kolesov, A., Chubarenko, B., Spiridonov, M., Kurennoy, D., Soomere, T., 2011. Coastal erosion processes in the eastern Gulf of Finland and their links with geological and hydrometeorological factors. *Boreal Environment Research* 16 (Suppl. A), 117–137.
- Räämet, A., Soomere, T., 2010. The wave climate and its seasonal variability in the northeastern Baltic Sea. *Estonian Journal of Earth Sciences* 59 (1), 100–113.
- Räämet, A., Soomere, T., Zaitseva-Pärnaste, I., 2010. Variations in extreme wave heights and wave directions in the north-eastern Baltic Sea. *Proceedings of the Estonian Academy of Sciences* 59 (2), 182–192. <http://dx.doi.org/10.3176/proc.2010.2.18>
- Saks, T., Kalvāns, A., Zelčs, V., 2007. Structure and micro-morphology of glacial and non-glacial deposits in coastal bluffs at Sēnsala, Western Latvia. *Baltica* 20, 19–27.
- Soomere, T., Pindsoo, K., Bishop, S. R., Käär, A., Valdmann, A., 2013a. Mapping wave set-up near a complex geometric urban coastline. *Natural Hazards and Earth System Sciences* 13 (11), 3049–3061. <http://dx.doi.org/10.5194/nhess-13-3049-2013>
- Soomere, T., Räämet, A., 2011. Spatial patterns of the wave climate in the Baltic Proper and the Gulf of Finland. *Oceanologia* 53 (1-TI), 335–371. <http://dx.doi.org/10.5697/oc.53-1-TI.335>
- Soomere, T., Räämet, A., 2013 [2014]. Decadal changes in the Baltic Sea wave heights, *Journal of Marine Systems* 129, 86–95. <http://dx.doi.org/10.1016/j.jmarsys.2013.03.009>
- Soomere, T., Viška, M., 2013 [2014]. Simulated wave-driven sediment transport along the eastern coast of the Baltic Sea. *Journal of Marine Systems* 129, 96–106. <http://dx.doi.org/10.1016/j.jmarsys.2013.02.001> [ScienceDirect, retrieved on 29 Nov. 2013].
- Soomere, T., Viška, M., Eelsalu, M., 2013b. Spatial variations of wave loads and closure depth along the eastern Baltic Sea coast, *Estonian Journal of Engineering* 19 (2), 93–109. <http://dx.doi.org/10.3176/eng.2013.2.01>
- Ulsts, V., 1998. *Latvian coastal zone of the Baltic Sea*. Riga, 96 pp. [In Latvian].
- Ulsts, V., Bulgakova, J., 1998. *General lithological and geomorphological map of Latvian shore zone – Baltic Sea and Gulf of Riga*. State Geological Survey of Latvia, Riga, maps.
- [USACE], 2002. *Coastal Engineering Manual*. Department of the Army. U.S. Army Corps of Engineers. Manual No. 1110-2-1100.
- Viška, M., Soomere, T., 2012. Hindcast of sediment flow along the Curonian Spit under different wave climates. In Proceedings of the IEEE/OES Baltic 2012 International Symposium “Ocean: Past, Present and Future. Climate Change Research, Ocean Observation & Advanced Technologies for Regional Sustainability,” May 8–11, Klaipėda, Lithuania. IEEE Conference Publications, 7 pp., doi 10.1109/BALTIC.2012.6249195
- Weishar, L., Tiffney, W., DeKimpe, J., Fields, M., 1991. Shoreline response to offshore shoals and storms. Low Beach, Nantucket MA. In O. T. Magoon, H. Converse, V. Tippie, L. T. Tobin, D. Clark (eds), Seventh Symposium on Coastal and Ocean Management (Coastal Zone '91), July 8-12, 1992, Long Beach, California, United States, New York, NY, American Society of Civil Engineers, 2435–2449.
- Zemlys, P., Fröhle, P., Gulbinskas, S., Davulienė, L., 2007. Near-shore evolution model for Palanga area: feasibility study of beach erosion management. *Geologija* 57, 45–54.
- Zhamoida, V., Ryabchuk, D. V., Kropatchev, Y. P., Kurennoy, D., Boldyrev, V. L., Sivkov, V. V., 2009. Recent sedimentation processes in the coastal zone of the Curonian Spit (Kaliningrad region, Baltic Sea). *Zeitschrift der Deutschen Gesellschaft für Geowissenschaften* 160 (2), 143–157. <http://dx.doi.org/10.1127/1860-1804/2009/0160-0143>
- Žaromskis, R., Gulbinskas, S., 2010. Main patterns of coastal zone development of the Curonian Spit, Lithuania. *Baltica* 23 (2), 149–156.

Paper V

Viška M., Soomere, T. 2012. Hindcast of sediment flow along the Curonian Spit under different wave climates. In: *IEEE/OES Baltic 2012 International Symposium*, May 8–11, 2012, Klaipeda, Lithuania, Proceedings. IEEE, 7 pp., doi: 10.1109/BALTIC.2012.6249195

Hindcast of sediment flow along the Curonian Spit under different wave climates

M. Viška and T. Soomere

Wave Engineering Laboratory

Institute of Cybernetics at Tallinn University of Technology

Akadeemia tee 21, 12618 Tallinn, Estonia

Abstract- We analyze wave-driven longshore sediment transport along the Curonian Spit, a narrow about 98 km long sandy peninsula at the south-eastern coast of the Baltic Sea. The bulk and net longshore sediment transport in existing and in a selection of future wave climates is calculated using the CERC formula for about 3 nautical miles long sections. The calculations are based on numerically simulated long-term time series of wave properties along the beach evaluated using adjusted geostrophic winds for 1970–2007. Changes to the wave climate are simulated by means of systematic rotation of the contemporary wave approach direction clockwise and counterclockwise. The spit is in an almost perfectly equilibrium shape under the existing wave climate. Systematic rotation of the wave approach direction leads to an almost linear increase in the net transport rate from its present almost zero value whereas the bulk transport rate would insignificantly change. A rotation by more than 10° results in complete disappearance of convergence points of sediment flow along the spit and apparently to substantial coastal damage.

I. INTRODUCTION

The southern and eastern Baltic Sea coasts mostly consist of relatively soft and easy erodable sediment [1]. Their evolution in the changing climate, in particular, under gradual water level rise [2], apparent increase in storminess [3] and shortening of the ice cover length [4] is of great concern of the coastal nations along the entire coast [5],[6],[7]. According to some authors, a combination of these factors may already have overridden the mostly stable development of the eastern Baltic Sea coasts [4],[7]. Under the largest pressure are coastal landforms that develop under direct impact of waves such as coastal bluffs, dunes and especially sandy spits.

The focus of the current study is on Curonian Spit (Fig. 1), a narrow sandy peninsula that has been formed relatively recently, during a few millennia, through intense wave-driven sand drift from the Sambian Peninsula [8]. Its presence is a remarkable example of the process of straightening of marine coasts by prolonged erosion and deposition in the Baltic Sea region [1],[9],[10],[11]. Today it is a 98 km long sandy landform at the south-eastern coast of the Baltic Sea. It stretches from the Sambian Peninsula in Kaliningrad district (Russia) until Klaipeda in Lithuania and separates the Curonian Lagoon from the Baltic Proper. This 0.4–4 km wide structure is exceptionally fragile. It is under continuous impact of natural forces, predominantly of wind and waves, and virtually all its sections (even these that usually show accumulation features) may be heavily damaged in certain storms [8].

Recent studies have indicated that the Curonian Spit is generally stable in the existing wave climate [12]. All its sections frequently serve as convergence points of the longshore sediment transport in certain years [12] and are thus regularly filled by sand owing to natural processes. The highly curved shape of this landform suggests that this stability may be lost for certain changes in wave approach direction. While secular changes in the wave direction are only a few degrees at the open ocean coasts [13],[14],[15], rotation of the most frequent wave approach direction by 90° degrees over a half-century has been documented in the Gulf of Finland [16]

In this paper we examine the stability of the Curonian Spit with respect to a certain rotation in the overall wave approach direction. Such a process may easily occur in the Baltic Sea owing to a shift in the trajectories of storm cyclones [17],[18]. It may become evident as a systematic change in the wind directions [19]. While an increase in the wave heights or a shortening of the ice cover usually enhances the existing processes, a change in the wave approach direction has a potential to alter even the qualitative appearance of coastal

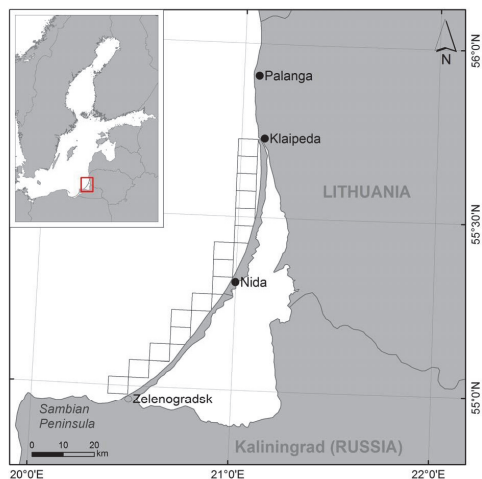


Figure 1. Location scheme of the Curonian Spit in the south-eastern part of the Baltic Sea. Boxes represent the 15 grid cells used in the calculations of sediment flux and the associated coastal sections. Filled dots show the locations of wave observation sites in Lithuania.

processes (e.g. the direction of littoral flow or a regular rotation of shorter beaches [20]). While such a reaction usually does not destroy the beaches that are supported from both sides by rocky headlands, a similar rotation may lead to substantial changes to long and narrow spits that do not have such supporting structures.

It is natural to assume that narrow, slowly developing spits are have an almost equilibrium shape. Such equilibrium may simply express a balance of longshore drift in coastal sections with abundance of sand. It is well known that virtually all sections of the eastern Baltic Sea coast, including the Curonian Spit, are mostly shaped by waves and suffer from sediment deficit [1],[8],[11]. In such conditions and under strong wave impact a landform can only evolve in a stable manner if the wave action keeps it in an almost equilibrium state.

This assumption was further quantified in [12] using the concept of divergence and convergence points of sediment flow. A divergence point is a likely erosion area from where sediment is transported away from this area, to both sides. Contrarily, a convergence point is likely an accretion domain where sediment is brought from both sides. Simulations of sediment transport demonstrated that a clear convergence point of sediment flow is always located somewhere along the spit. In different years 1970–2007 this point moves along the entire spit so that all sectors, in average, are filled by sand at a certain year. The location of this accretion zone was substantially shifted every three to five years [12]. Therefore, sediment brought to the Curonian Spit is moved along the spit cyclically, providing sand to virtually each its section after certain time intervals under the existing wave climate [12] although some places may at times suffer from erosion. These results show that Curonian Spit apparently is in almost equilibrium shape under the contemporary wave climate. This assumption is supported by the conjecture that damages to its beaches are usually local and associated with extreme wave storms [8].

An indirect measure of the closeness of such a wave-shaped landform to an equilibrium shape is the ratio of net and bulk longshore sediment transport. In this paper we examine the current status of longshore transport at the Curonian Spit under the existing wave climate. We first quantify the potential sediment transport rate using the Coastal Engineering Research Council (CERC) method and simulated wave time series for 38 years. Further on, we examine the stability of the spit with respect to small changes (a rotation by a few degrees) in the directional structure of the wave climate. The purpose of this exercise is to see how far the spit currently is from an equilibrium stage (defined as a shape from which the long-term integral net transport along the spit vanishes) and which sort of changes in the typical wave approach direction would be favorable for its stability and which changes would likely adversely impact its development.

II. WAVE CLIMATE AT THE CURONIAN SPIT

Information about the wave climate at the Curonian Spit is available from long-term numerical simulations [21],[22] and

visual observations performed from the coast [23],[24],[25]. Three visual observation sites exist at the Lithuanian Baltic Sea coast: Nida, Palanga and Klaipeda. The distance between these sites is less than 50 km and it is not unexpected that many observed wave properties (especially seasonal and long-term course as well as different empirical probability distributions) largely coincide [25].

The main properties of the wave climate at Nida (Fig. 1), which is the most representative for wave properties along the Curonian Spit, are typical for the coastal areas of the Baltic Proper. Observations at Nida have been made since 1956 [25]. The wave climate is generally quite mild, with the long-term mean significant wave height (below called simply wave height) approximately 0.9–1 m in the open sea [21],[22] and 0.7 m in the nearshore [25]. More than 50% of wave fields have wave heights below 0.5 m [25]. Still, extremely severe storms with wave heights close to 10 m may occur in this part of the Baltic Sea [30]. The most frequent peak periods are 3–5 s. The wave fields exhibit strong seasonal and interannual variability, which is typical for the Baltic Sea. The waves are highest (monthly average over 0.8 m) at Nida from September till January and the lowest (monthly average as low as 0.5 m) in May. The annual mean wave height ranges between 0.4 and over 1 m in 1956–2008. A drastic wave height decrease occurred at Nida for 1990–1995 and a gradual increase was observed starting from about 1996 [25].

As wave approach directions are recorded with a directional resolution of 45° at Nida, we describe the directional structure of wave fields based on the results of numerical experiments [22] that are also used below for the calculation of alongshore drift. We use hourly time series of wave properties calculated in high resolution (about 3×3 nautical miles (nm)) for the entire Baltic Sea over 38 years (1970–2007) by the third-generation spectral wave model WAM [26] driven by adjusted geostrophic winds in idealized ice-free conditions [22]. The regular rectangular grid (11545 sea points) extends from $09^\circ 36' E$ to $30^\circ 18' E$ and from $53^\circ 57' N$ to $65^\circ 51' N$. The wave energy spectrum at each sea point was represented by 24 equally spaced directions and 42 frequencies with an increment of 1.1. An extended frequency range up to about 2 Hz (wave periods down to 0.5 s) was used to ensure realistic wave growth rates in low wind conditions after calm situations that are frequent in this basin [27]. The results of the simulations were extensively verified against the existing instrumental wave measurements in the northern Baltic Proper and visual wave observations along the Estonian coast in [22],[28].

The empirical distribution of wave propagation directions has two peaks for each sector of the Curonian spit (Fig. 2). These peaks are clearly separated for the northern part of the spit where waves mostly approach to sector from west-southwest (WSW) to north-northwest (NNW). The peak corresponding to wave propagation to east-northeast is more pronounced for the northern part of the spit and corresponds to waves approaching from WSW. The secondary peak at south-southeast reflects a relatively large portion of waves

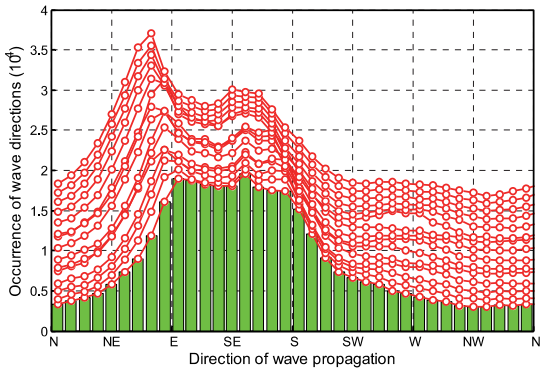


Figure 2. Wave propagation directions at different sections of the Curonian Spit. The bars correspond to the southernmost part of the spit. The distributions for subsequent sections along the spit from south to north (Fig. 1) are vertically shifted by 0.1 units of the vertical axis.

approaching from NNW. These peaks have almost equal heights at the southernmost part of the spit. The nearshore of the relevant coastal sections is to some extent sheltered from waves approaching from southwest by the Sambian Peninsula (Fig. 1). As a result, waves approach from a wide sector (from west to north) with an almost equal frequency. This structure of the “wave rose” simply reflects the two-peak nature of the directional structure of predominant winds [29]. The highly anisotropic, two-peak structure is even more pronounced for moderate and strong winds [30] and, therefore, in terms of wave-induced longshore transport.

The described directional structure of the wave approach directions suggests that the two predominant wave systems may have created a sort of dynamical equilibrium for the spit in the form of alternating-direction sediment flow events. This assumption may be examined by estimating the ratio of bulk and net transport along the entire spit. If the bulk transport by an order of magnitude extends the net transport, then different storms may move large amounts of sediments along the spit but the sediment is usually not carried away from the spit.

III. METHODS AND DATA

The Curonian Spit was divided into fifteen approximately 3 nautical miles (about 5.5 km) long sectors. These sectors match the wave model grid points that are closest to coastline. The coastline in each sector is approximated by a straight line that follows the orientation of coast. The alongshore wave-driven sediment transport intensity is assumed to be constant in each sector. The potential wave-driven sediment transport is evaluated using the CERC (Coastal Engineering Research Council) model [31]. As mentioned above, we use hourly time series of wave properties at each sector calculated for 1970–2007 using the 3rd generation wave model WAM with a spatial resolution of 3 nm driven by adjusted geostrophic winds [22]. From the variety of output information of the WAM model we

use the significant wave height, peak period and mean wave direction.

A. CERC Model

Wave-driven longshore sediment transport is commonly estimated in terms of its potential rate Q_t [31] using the CERC method. This rate expresses the volume of sediments carried through a coastal section in cubic meters per each meter of coastline per unit of time in idealized conditions such as a relatively straight coastline and sufficient amount of sediment. These conditions are not necessarily fulfilled along the eastern Baltic Sea coast and the potential transport rate usually exceeds the actual values of transport by an order of magnitude. The quantities used in this study (the overall transport direction, major divergence and convergence points of littoral flow, ratio of net and bulk transport etc.) almost entirely depend on the difference of the transport (either potential or realistic) in adjacent coastal sections and are, therefore, invariant with respect to the particular way of the evaluation of the transport rate.

The potential immersed weight transport rate I_t is equivalent to the potential longshore transport rate [31]:

$$I_t = (\rho_s - \rho)g(1-p)Q_t. \quad (1)$$

The rate I_t accounts for sediment porosity and specific weight of sediment components. Here ρ_s and ρ are the densities of sediment particles and sea water, respectively, $g = 9.81 \text{ m/s}^2$ is the acceleration due to gravity and p is the porosity coefficient. The CERC method is based on assumption that $I_t = KP_t$ is proportional to the beaching rate of the longshore wave energy flux (wave power) per unit of length of the coastline P_t . Here K is a nondimensional (CERC) coefficient. If the wave propagation direction makes an angle α with the normal to the coast, the shoreward component of the energy flux is $P_t = Ec_g \cos \alpha$ (E is the wave energy and c_g is the group speed) and the rate of its beaching per unit of the coastline is

$$P_t = Ec_g \sin \alpha \cos \alpha. \quad (2)$$

Since the majority of sediment transport occurs in the surf zone, energy and group velocity in Eq. (2) are usually evaluated at the seaward border of the surf zone. At this location waves can be reasonably well described as long waves; thus,

$$E_b = \frac{\rho g H_b^2}{8}, \quad c_{gb} = \sqrt{g d_b} = \sqrt{\frac{g H_b}{\kappa}}, \quad (3)$$

$$Q_t = \frac{K \rho \sqrt{g}}{16(\rho_s - \rho)(1-p)\sqrt{\kappa}} H_b^2 \sqrt{H_b} \sin 2\alpha_b, \quad (4)$$

where H_b is the wave height at breaking, $\kappa = H_b/d_b$ is the breaking index, d_b is the breaking depth and α_b is the angle between the wave crests and the isobaths at the breaking. The potential transport rate insignificantly depends on the variations in the coastal sediment texture in the Baltic Sea conditions [32]. For this reason, we ignore longshore variations in sand properties along the Curonian Spit and use a constant value $d_{50} = 0.063 \text{ mm}$ for the median size of sand

grains. The dependence of the coefficient K on the wave properties is accounted for using the following empirical expression ([31], part III-1):

$$K = 0.05 + 2.6 \sin^2 2\alpha_b + 0.007 u_{mb} / w_f, \quad (5)$$

where $u_{mb} = \kappa \sqrt{gd_b} / 2$ is the maximum orbital velocity in breaking waves within the linear wave theory and $w_f = 1.6 \sqrt{gd_{50}(\rho_s - \rho)} / \rho$ is an approximation of fall velocity in the surf zone.

Calculations are made with a temporal resolution of 1 hour, following simulated wave data. A measure of bulk transport over a certain time interval $[t_0, t_1]$ is obtained by integrating $|I_t|$ over $[t_0, t_1]$ and net transport by integrating I_t over $[t_0, t_1]$. Net transport is the residual sediment motion in some direction and bulk transport is the total amount of sediment brought into motion (moved in any direction, back and forth alongshore) by waves. The sign of net transport indicates the direction of sediment movement for a person looking to the sea. With positive sign (to the right for this person) sediments follow the predominant counterclockwise flow direction from south-west to north-east along the Curonian Spit and negative sign stands for the opposite direction.

B. Snell's Law, Wave Shoaling and Breaking

The wave shoaling was evaluated in a simplified manner by choosing the breaking index $\kappa = 1$. This choice is equivalent to the assumption that the increase in wave height in the shoaling process is balanced by partial damping of wave energy owing to nearshore processes such as wave-bottom interaction, whitecapping and refraction. In this approximation, $d_b = H_b$ and the breaking wave height is equal to the modeled wave height at the centers of each grid cells. These centers are mostly located at a depth of about 20 m and at a distance of about 3 km from the coastline (Fig. 1).

The change in the wave propagation direction over this distance (up to the seaward border of the surf zone) was calculated using the Snell's law $\sin \theta / c_f = \text{const}$, where θ was the local angle between the wave crests and the isobaths and c_f is wave celerity (phase velocity). It was assumed that the entire wave energy of a wave field was concentrated in the component with the period equal to the mean period and propagation direction equal to the mean propagation direction. An application of the Snell's law required an approximate solution to the dispersion relation. It is a transcendental equation for the wave number $k = 2\pi/L$ or the wave length L

$$c_f = \frac{\omega}{k} = \frac{\sqrt{gk \tanh(kh)}}{k} = \frac{\sqrt{g \tanh(2\pi h/L)}}{2\pi/L}, \quad (7)$$

where h is the local water depth. A solution with an error not exceeding 1.7 % is ([33], p. 90):

$$L = L_0 \left\{ \tanh \left[\left(2\pi \sqrt{\frac{h}{gT^2}} \right)^{3/2} \right] \right\}^{2/3}, \quad (8)$$

where $L_0 = gT^2 / (2\pi)$ is the length of waves with period T in deep water.

C. Changes in Wave Direction

Potential changes in the directional structure of the wave climate were simulated in a simplified manner, by means of rotation of all wave approach directions provided by the WAM wave model by a constant angle. Doing so reflects to some extent possible systematic changes to the trajectories of cyclones: a shift of a trajectory more to the north becomes evident in the wave properties at a particular location of the Curonian Spit as a clockwise rotated pattern of the resulting wave fields. Similarly, a shift of a trajectory to the south usually implies a counterclockwise rotation of the observed wave patterns.

For relatively small shifts it is reasonable to assume that the wind strength and cyclone size change insignificantly. Therefore, comparatively small changes in the wave direction apparently are not accompanied by substantial changes in the wave height and period. This viewpoint is to some extent supported by the observation that the wave directions in certain parts of European coasts have undergone clear changes while there is virtually no change in the heights of the North Atlantic wave fields [13].

Following this idea, the wave approach direction of each hourly value of the entire 38-year long series of simulated wave properties was rotated by a certain amount whereas the wave height and period were not modified. The rotation was performed from 1° till 20° with a step of 1° to both directions. The resulting time series was applied as new input data for calculating longshore sediment transport.

IV. RESULTS

A. Bulk and Net Transport

The overall bulk potential transport rate integrated over the entire Curonian Spit (Fig. 3, 15 sectors) is about $2.6 \times 10^7 \text{ m}^3$, that is, about $1.7 \times 10^6 \text{ m}^3$ at each sector. As mentioned above, this measure is calculated under idealized conditions and apparently overestimates the actual transport rate by an order of magnitude. It exhibits extensive interannual variability: its extreme pointwise values are roughly twice as large as the long-term mean while the minimum levels are about a half of the long-term ones (Fig. 3). This quantity exhibits a weak increasing (but not statistically significant) trend. However, its course reveals clear, almost periodical cycles with a typical time scale about 8–10 years and amplitudes close to about 1/4 of the long-term average of this measure of transport. As no cyclic course is evident in the long-term behavior in the wind speed [34], the decadal variations in question apparently are associated with changes to wave propagation directions.

The total net potential transport integrated over the entire Curonian Spit fluctuates around zero and exhibits very small absolute values, usually a few percent of the bulk transport for the particular year (Fig. 4). Therefore, in the existing wave climate the long-term net sediment transport has no preferred

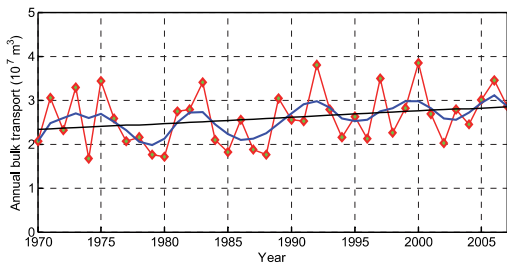


Figure 3. Annual mean bulk sediment transport along the entire Curonian Spit (red) its five-year average (blue) and linear trend (black line).

direction. Moreover, its almost zero long-term average $-1.7 \times 10^5 \text{ m}^3$ (which is less than 1% from the corresponding value of the bulk transport) suggests that the Curonian Spit is in an almost equilibrium state.

The relative variability of the overall potential net transport is much larger than the similar variability of the bulk transport. In single years net transport forms up to 50% of the bulk transport. This feature confirms that during certain shorter periods extensive redistribution of sediment may occur. Interestingly, the long-term variations in the net potential transport only partially follow those for the bulk transport. The temporal course of the net transport also shows a clear presence of a signal with a typical scale of about 10 years. The long-term course of this measure has a different nature. The net transport increased in the 1970s and 1980s and decreased at essentially the same rate since the mid-1990s.

The discussed particularly small ratio of the overall net and bulk transport suggests that even a small change in the wind properties may lead to a substantial misbalance in the sediment transport.

B. Ratio of Bulk and Net Transport

As discussed above, the closeness of the shape of the Curonian Spit to an equilibrium landform can be to some extent characterized by the ratio of the net and bulk transport (both integrated over the entire Curonian Spit and for a longer time interval). This quantity is very small, below 0.01 for the numerically simulated contemporary wave climate in 1970–2007. For relatively small rotations the bulk transport changes

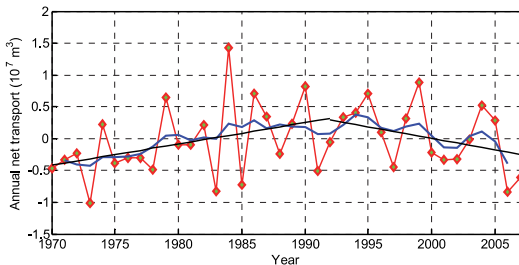


Figure 4. Annual mean net sediment transport along the entire Curonian Spit (red) its five-year average (blue) and trendlines for 1970–1993 and 1993–2007.

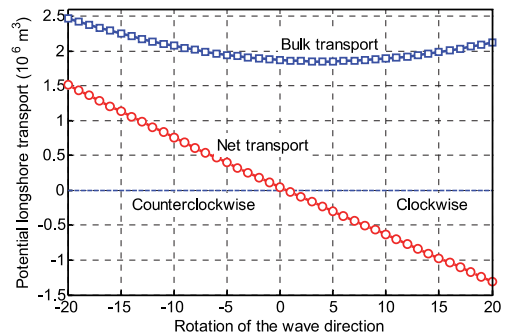


Figure 5. Annual mean bulk and net transport per a single coastal section of the Curonian Spit for rotated wave climates..

insignificantly (Fig. 5), by about 20% from its values for rotations up to 20° . Interestingly, its maximum corresponds to clockwise rotation by 5° , that is, to the case when the cyclones would be shifted to the north.

The model suggests that the net transport over the entire Curonian Spit would change almost linearly with respect to the rotation angle. It is remarkable that the current wave climate corresponds to the almost exact crossing point of the relevant line and the x -axis. This feature confirms that the current shape of the Curonian spit perfectly matches the existing wave climate and that any substantial changes to the wave approach direction may substantially increase the intensity of coastal processes in this domain.

The ratio of the net and bulk transport is almost zero for the existing wave climate (Fig. 6). Its absolute values increase rapidly and almost linearly for wave climates rotated to any direction and reach the level of about 0.1 (which would apparently quite strong residual sediment transport) already for rotations by $2\text{--}3^\circ$.

C. Loss of Convergence Zones

An increase in the net transport and even in the ratio of net and bulk transport not necessarily means that the entire landform would suffer from strong erosion. As discussed above and in [12], an interesting feature of the Curonian Spit is that a clear convergence point of sediment flow is always located somewhere along the spit. This peculiarity means that

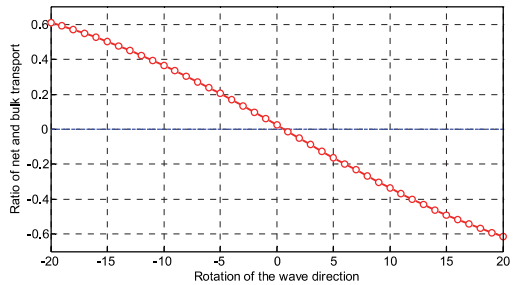


Figure 6. Ratio of the mean bulk and net transport over the entire Curonian Spit for rotated wave climates

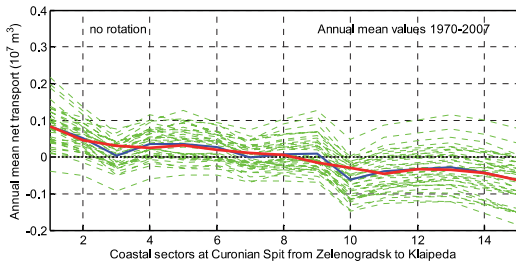


Figure 7. Annual net transport for single years (green) and long-term average (blue, red) for different sections of the Curonian Spit for the existing wave climates.

all sectors, in average, are filled by sand at a certain year. If this feature persists for rotated wave climates, it is likely that the spit might be slightly reshaped but it will not lose large amounts of sediment.

The strongest convergence point of alongshore sediment flux is the point where the pointwise net sediment transport has a zero-downcrossing along the direction of sediment flux [12]: transport from both sides is directed to this point that is filled by sediment for some time. Under the existing wave climate there typically exists one such point that moves along the spit for different years (Fig. 7). Its formal “average” (zero-downcrossing of the average red line) location is close to the center of the spit. Another convergence point in the eastern part of the spit appears occasionally and apparently plays a smaller role in the long-term evolution of the spit.

With a clockwise rotation of the wave climate, the long-term average location of the major convergence point first moves to the eastern end of the spit already for a rotation by 5° (Fig. 8)

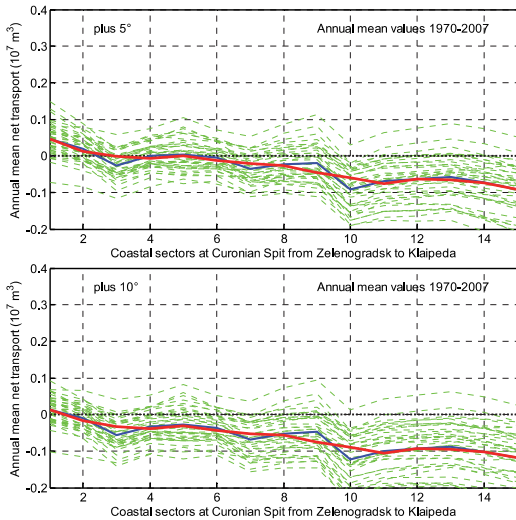


Figure 8. Annual net transport for single years (green) and long-term average (blue, red) for Curonian Spit for clockwise rotation of the wave climate by 5° (upper panel) and 10° (lower panel).

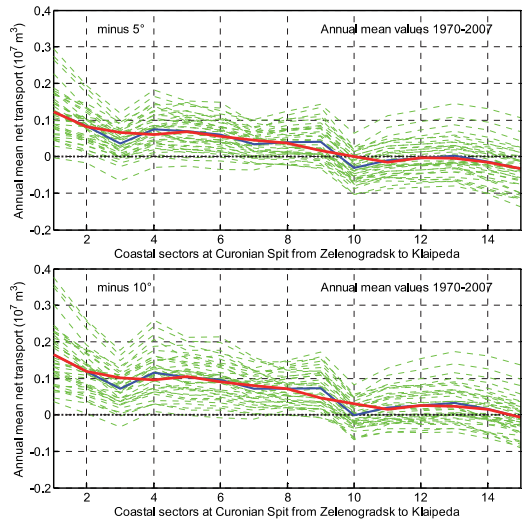


Figure 9. Annual net transport for single years (green) and long-term average (blue, red) for Curonian Spit for counterclockwise rotation of the wave climate by 5° (upper panel) and 10° (lower panel)

and disappears for most of the years if the wave system would be rotated by 10°. Although this point appears at single years, it is likely that quite strong net sediment flux to the east in most of years would cause rapid erosion of several unprotected sections of the beach because there would be no compensating sediment flux across Klaipeda Strait.

For counterclockwise rotation, the major convergence point is shifted to the northern end of the spit and reaches the Klaipeda region for a rotation of 10° (Fig. 9). Differently from the above-discussed clockwise rotation, strong transport to the north will apparently dominate in virtually all years in the entire eastern section of the spit. This not necessarily means a full destruction of the spit as the sediment transport may be compensated by material eroded from the Sambian Peninsula.

V. CONCLUSIONS AND DISCUSSION

The performed analysis confirms the intuitively obvious premise that the shape of the Curonian Spit matches well the existing wind climate. Although substantial amounts of sediment may be transported in either direction along the spit in different years under the two-peak distribution of wave approach directions, in long-term run there is very low net sediment transport. In other words, in natural conditions the local erosion patterns evidently are reversible and the damaged coastal sections apparently will naturally recover to a large extent.

The simple model in use signifies a remarkable balance of different events of wave-driven alongshore transport over longer time intervals. In a way, this is not unexpected as the spit has been shaped by the existing wave climate and apparently would have had another shape if the wave climate in the past would have been different. Therefore, an important

conjecture from this balance is that the wave climate has likely been very much the same over a longer time interval in the past. The duration of the presence of this (contemporary) wave climate can be roughly estimated from the actual rate of net and bulk transport.

An important warning message is that even a small rotation of the wave climate, equivalently, a secular shift in the trajectories of cyclones from their present location, could strongly adversely impact the further development of the Curonian Spit. The simple model in use suggests that major changes or damages might occur even if the rotation is as small as a few degrees. Substantial damages are likely if the rotation will exceed about 10° clockwise as virtually no sediment enters the system from the north. Although even larger changes in the wind and wave directions have been reported for the Baltic Sea basin [16],[19] and for the Atlantic Ocean [13], it is very likely that such changes are reversible and over no drastic changes would occur over longer time intervals.

ACKNOWLEDGMENT

The research was supported by the targeted financing by the Estonian Ministry of Education and Research (grant SF0140007s11) and Estonian Science Foundation (grant No 9125). Maija Viška is supported by the framework of international PhD studentships (DoRa) in Estonia. We thank Dr. Andrus Räämet for providing the simulated wave data.

REFERENCES

- [1] V. Gudelis, "The morphogenetic types of Baltic Sea coasts," *Baltica*, vol. 3, pp. 123–145, 1967, [В. Гуделис, "Морфогенетические типы берегов Балтийского моря," *Балтика* 3, с. 123-145.].
- [2] I. Dailidienė, L. Davulienė, A. Stankevičius, and K. Myrberg, "Sea level variability at the Lithuanian coast of the Baltic Sea," *Boreal Environ. Res.*, vol. 11, pp. 109–121, 2006.
- [3] H. Alexandersson, T. Schmith, K. Iden, and H. Tuomenvirta, "Long-term variations of the storm climate over NW Europe," *Global Atmos. Ocean Syst.*, vol. 6, pp. 97–120, 1998.
- [4] K. Orviku, J. Jaagus, A. Kont, U. Ratas, R. Rivis, "Increasing activity of coastal processes associated with climate change in Estonia," *J. Coast. Res.*, vol. 19, pp. 364–375, 2003.
- [5] R.B. Zeidler, "Climate change vulnerability and response strategies for the coastal zone of Poland," *Climatic Change*, vol. 36, pp. 151–173, 1997.
- [6] G. Eberhards, J. Lapinskis, and B. Saltupe, "Hurricane Erwin 2005 coastal erosion in Latvia," *Baltica*, vol. 19, pp. 10–19, 2006.
- [7] D. Ryabchuk, I. Leontyev, A. Sergeev, E. Nesterova, L. Sukhacheva, and V. Zhamoida, "The morphology of sand spits and the genesis of long-shore sand waves on the coast of the eastern Gulf of Finland," *Baltica*, vol. 24, pp. 13–24, 2011.
- [8] R. Žaromskis and S. Gulbinskas, "Main patterns of coastal zone development of the Curonian Spit, Lithuania," *Baltica*, vol. 23, pp. 149–156, 2010.
- [9] V. Ulsts, *Latvian Coastal Zone of the Baltic Sea*. Riga, 1998, p. 96 [V. Ulsts, "Baltijas jūras Latvijas krasta zona," Riga, 1998, 96 lpp.].
- [10] R.J. Knaps, "Sediment transport near the coasts of the Eastern Baltic," in *Development of Sea Shores Under the Conditions of Oscillations of the Earth's Crust*. Tallinn: Valgus, 1966, pp. 21–29 [Р.Я. Кнапс "Движение наносов у берегов Восточной Балтики. Развитие морских берегов в условиях колебательных движений земной коры," Валгус, Таллинн, 1966, с. 21-29].
- [11] G. Eberhards, *The Sea Coast of Latvia*. Riga: University of Latvia, 2003, pp. 127–178 [G. Eberhards "Latvijas jūras krasti," Latvijas Universitāte, Riga, 2003, 127-178 lpp.].
- [12] T. Soomere and M. Viška, "Simulated sediment transport along the eastern coast of the Baltic Sea", unpublished; submitted *Journal of Marine Systems*, 2012
- [13] G. Dodet, X. Bertin, and R. Taborda, "Wave climate variability in the North-East Atlantic Ocean over the last six decades," *Ocean Modelling*, vol. 31, pp. 120–131, 2010.
- [14] W.C. Dragani, P.B. Martin, C.G. Simonato, and M.I. Campos, "Are wind wave heights increasing in south-eastern South American continental shelf between 32 degrees S and 40 degrees S?" *Cont. Shelf Res.*, vol. 30, pp. 481–490, 2010.
- [15] M.A. Hemer, J.A. Church, and J.R. Hunter, "Variability and trends in the directional wave climate of the Southern Hemisphere," *Int. J. Climatol.*, vol. 30, 2010, pp. 475–491, 2010.
- [16] A. Räämet, T. Soomere, and I. Zaitseva-Pärmaste, "Variations in extreme wave heights and wave directions in the north-eastern Baltic Sea," *Proc. Estonian Acad. Sci.*, vol. 59, pp. 182–192, 2010.
- [17] A. Lehmann, K. Getzlaff, and J. Harlaß, "Detailed assessment of climate variability in the Baltic Sea area for the period 1958 to 2009," *Clim. Res.*, vol. 46, pp. 185–196, 2011.
- [18] M. Sepp and J. Jaagus, "Changes in the activity and tracks of Arctic cyclones," *Clim. Change*, vol. 105, pp. 577–595, 2011.
- [19] J. Jaagus and A. Kull, "Changes in surface wind directions in Estonia during 1966–2008 and their relationships with large-scale atmospheric circulation," *Estonian J. Earth Sci.*, vol. 60, pp. 220–231, 2011.
- [20] R. Ranasinghe, R. McLoughlin, A. Short, and G. Symonds, "The Southern Oscillation Index, wave climate, and beach rotation," *Mar. Geol.*, vol. 204, pp. 273–287, 2004.
- [21] G. Schmager, P. Fröhle, D. Schrader, R. Weisse, and S. Müller-Navarra, "Sea State, Tides," in *State and Evolution of the Baltic Sea 1952–2005*, R. Feistel, G. Nausch, and N. Wasmund, Eds. Hoboken, NJ: Wiley, 2008, pp. 143–198.
- [22] A. Räämet and T. Soomere, "The wave climate and its seasonal variability in the northeastern Baltic Sea," *Estonian J. Earth Sci.*, vol. 59, pp. 100–113, 2010.
- [23] L. Kelpšaitė, H. Herrmann, and T. Soomere, "Wave regime differences along the eastern coast of the Baltic Proper," *Proc. Estonian Acad. Sci.*, vol. 57, pp. 225–231, 2008.
- [24] L. Kelpšaitė, I. Dailidienė, and T. Soomere, "Changes in wave dynamics at the south-eastern coast of the Baltic Proper during 1993–2008," *Boreal Environ. Res.* 16, Suppl. A, pp. 220–232, 2011.
- [25] I. Zaitseva-Pärmaste, T. Soomere, and O. Tribštok, "Spatial variations in the wave climate change in the eastern part of the Baltic Sea," *J. Coast. Res.*, Special Issue 64, pp. 195–199, 2011.
- [26] G.J. Komen, L. Cavaleri, M. Donelan, K. Hasselmann, S. Hasselmann, and P.A.E.M. Janssen, *Dynamics and modelling of ocean waves*. Cambridge: Cambridge University Press, 1994, p. 532.
- [27] T. Soomere, "Wind wave statistics in Tallinn Bay," *Boreal Environ. Res.*, vol. 10, pp. 103–118, 2005.
- [28] T. Soomere and A. Räämet, "Spatial patterns of the wave climate in the Baltic Proper and the Gulf of Finland," *Oceanologia*, vol. 53 (1-TI), pp. 335–371, 2011.
- [29] T. Soomere, "Anisotropy of wind and wave regimes in the Baltic Proper," *J. Sea Res.* vol. 49, pp. 305–316, 2003.
- [30] T. Soomere and S. Keevallik, "Anisotropy of moderate and strong winds in the Baltic Proper," *Proc. Estonian Acad. Sci. Eng.*, vol. 7, pp. 35–49, 2001.
- [31] *Coastal Engineering Manual*, Department of the Army, U.S. Army Corps of Engineers: Manual No. 1110-2-1100, 2002.
- [32] T. Soomere, A. Kask, J. Kask, and T.R. Healy, "Modelling of wave climate and sediment transport patterns at a tideless embayed beach, Piritas Beach, Estonia," *J. Marine Syst.*, vol. 74, S133–S146, 2008.
- [33] R.G. Dean and R.A. Dalrymple, *Coastal Processes with Engineering Applications*. Cambridge: Cambridge University Press, 2002, p. 90.
- [34] A. Räämet and T. Soomere, "Spatial variations in the wave climate change in the Baltic Sea," *J. Coast. Res.*, Special Issue 64, pp. 240–244, 2011.

**DISSERTATIONS DEFENDED AT
TALLINN UNIVERSITY OF TECHNOLOGY ON
CIVIL ENGINEERING**

1. **Heino Mölder.** Cycle of Investigations to Improve the Efficiency and Reliability of Activated Sludge Process in Sewage Treatment Plants. 1992.
2. **Stellian Grabko.** Structure and Properties of Oil-Shale Portland Cement Concrete. 1993.
3. **Kent Arvidsson.** Analysis of Interacting Systems of Shear Walls, Coupled Shear Walls and Frames in Multi-Storey Buildings. 1996.
4. **Andrus Aavik.** Methodical Basis for the Evaluation of Pavement Structural Strength in Estonian Pavement Management System (EPMS). 2003.
5. **Priit Vilba.** Unstiffened Welded Thin-Walled Metal Girder under Uniform Loading. 2003.
6. **Irene Lill.** Evaluation of Labour Management Strategies in Construction. 2004.
7. **Juhan Idnurm.** Discrete Analysis of Cable-Supported Bridges. 2004.
8. **Arvo Iital.** Monitoring of Surface Water Quality in Small Agricultural Watersheds. Methodology and Optimization of Monitoring Network. 2005.
9. **Liis Sipelgas.** Application of Satellite Data for Monitoring the Marine Environment. 2006.
10. **Ott Koppel.** Infrastruktuuri arvestus vertikaalselt integreeritud raudtee-ettevõtja korral: hinnakujunduse aspekt (Eesti peamise raudtee-ettevõtja näitel). 2006.
11. **Targo Kalamees.** Hygrothermal Criteria for Design and Simulation of Buildings. 2006.
12. **Raido Puust.** Probabilistic Leak Detection in Pipe Networks Using the SCEM-UA Algorithm. 2007.
13. **Sergei Zub.** Combined Treatment of Sulfate-Rich Molasses Wastewater from Yeast Industry. Technology Optimization. 2007.
14. **Alvina Reihan.** Analysis of Long-Term River Runoff Trends and Climate Change Impact on Water Resources in Estonia. 2008.
15. **Ain Valdmann.** On the Coastal Zone Management of the City of Tallinn under Natural and Anthropogenic Pressure. 2008.
16. **Ira Didenkulova.** Long Wave Dynamics in the Coastal Zone. 2008.
17. **Alvar Toode.** DHW Consumption, Consumption Profiles and Their Influence on Dimensioning of a District Heating Network. 2008.
18. **Annely Kuu.** Biological Diversity of Agricultural Soils in Estonia. 2008.

19. **Andres Tolli.** Hiina konteinerveod läbi Eesti Venemaale ja Hiinasse tagasisaadetavate tühjade konteinerite arvu vähendamise võimalused. 2008.
20. **Heiki Onton.** Investigation of the Causes of Deterioration of Old Reinforced Concrete Constructions and Possibilities of Their Restoration. 2008.
21. **Harri Moora.** Life Cycle Assessment as a Decision Support Tool for System optimisation – the Case of Waste Management in Estonia. 2009.
22. **Andres Kask.** Lithohydrodynamic Processes in the Tallinn Bay Area. 2009.
23. **Loreta Kelpšaitė.** Changing Properties of Wind Waves and Vessel Wakes on the Eastern Coast of the Baltic Sea. 2009.
24. **Dmitry Kurennoy.** Analysis of the Properties of Fast Ferry Wakes in the Context of Coastal Management. 2009.
25. **Egon Kivi.** Structural Behavior of Cable-Stayed Suspension Bridge Structure. 2009.
26. **Madis Ratassepp.** Wave Scattering at Discontinuities in Plates and Pipes. 2010.
27. **Tiia Pedusaar.** Management of Lake Ülemiste, a Drinking Water Reservoir. 2010.
28. **Karin Pachel.** Water Resources, Sustainable Use and Integrated Management in Estonia. 2010.
29. **Andrus Räämet.** Spatio-Temporal Variability of the Baltic Sea Wave Fields. 2010.
30. **Alar Just.** Structural Fire Design of Timber Frame Assemblies Insulated by Glass Wool and Covered by Gypsum Plasterboards. 2010.
31. **Toomas Liiv.** Experimental Analysis of Boundary Layer Dynamics in Plunging Breaking Wave. 2011.
32. **Martti Kiisa.** Discrete Analysis of Single-Pylon Suspension Bridges. 2011.
33. **Ivar Annus.** Development of Accelerating Pipe Flow Starting from Rest. 2011.
34. **Emlyn D.Q. Witt.** Risk Transfer and Construction Project Delivery Efficiency – Implications for Public Private Partnerships. 2012.
35. **Oxana Kurkina.** Nonlinear Dynamics of Internal Gravity Waves in Shallow Seas. 2012.
36. **Allan Hani.** Investigation of Energy Efficiency in Buildings and HVAC Systems. 2012.
37. **Tiina Hain.** Characteristics of Portland Cements for Sulfate and Weather Resistant Concrete. 2012.
38. **Dmitri Loginov.** Autonomous Design Systems (ADS) in HVAC Field. Synergetics-Based Approach. 2012.
39. **Kati Kõrbe Kaare.** Performance Measurement for the Road Network: Conceptual Approach and Technologies for Estonia. 2013.

40. **Viktorija Voronova**. Assessment of Environmental Impacts of Landfilling and Alternatives for Management of Municipal Solid Waste. 2013.
41. **Joonas Vaabel**. Hydraulic Power Capacity of Water Supply Systems. 2013.
42. **Inga Zaitseva-Pärnaste**. Wave Climate and its Decadal Changes in the Baltic Sea Derived from Visual Observations. 2013.
43. **Bert Viikmäe**. Optimising Fairways in the Gulf of Finland Using Patterns of Surface Currents. 2014.
44. **Raili Niine**. Population Equivalence Based Discharge Criteria of Wastewater Treatment Plants in Estonia. 2014.
45. **Marika Eik**. Orientation of Short Steel Fibres in Concrete: Measuring and Modelling. 2014.